

CHAPTER XV

DECLASSIFIED

EFFECT OF OPERATING CONDITIONS AND DESIGN ON AFTERBURNER PERFORMANCE

By Bruce T. Lundin, David S. Gabriel, and William A. Fleming

INTRODUCTION

X67-87775

Afterburners for turbojet engines have, within the past decade, found increasing application in service aircraft. Practically all engines manufactured today are equipped with some form of afterburner, and its use has increased from what was originally a short-period thrust-augmentation application to an essential feature of the turbojet propulsion system for flight at supersonic speeds.

The design of these afterburners has been based on extensive research and development effort in expanded laboratory facilities by both the NACA and the American engine industry. Most of the work of the engine industry, however, has either not been published or is not generally available owing to its proprietary nature. Consequently, the main bulk of research information available for summary and discussion is of NACA origin. However, because industrial afterburner development has closely followed NACA research, the omission is more one of technical detail than method or concept.

One principal difficulty encountered in summarizing the work in this field is that sufficient knowledge does not yet exist to rationally or directly integrate the available background of basic combustion principles into combustor design. A further difficulty is that most of the experimental investigations that have been conducted were directed chiefly toward the development of specific afterburners for various engines rather than to the accumulation of systematic data. This work has, nonetheless, provided not only substantial improvements in the performance of afterburners but also a large fund of experimental data and an extensive background of experience in the field. Consequently, it is the purpose of the present chapter to summarize the many, and frequently unrelated, experimental investigations that have been conducted rather than to formulate a set of design rules. In the treatment of this material an effort has been made, however, to convey to the reader the "know-how" acquired by research engineers in the course of afterburner studies.

The material presented is divided into the following topics:

- (1) Experimental procedures
- (2) Burner-inlet diffusers
- (3) Ignition, starting, and transient performance
- (4) Fuel-injection systems
- (5) Flameholder design
- (6) Combustion space
- (7) Effect of operating variables on performance
- (8) Combustion instability (screech)
- (9) Effects of diluents on performance

CC-38 back

Each topic is treated somewhat independently, although interacting considerations are discussed where known or important. Numerous references are listed for the convenience of those who may desire more detailed treatment than is possible herein.

No attempt is made to describe the details of the apparatus and test procedures used, although they are available in many of the references. The general range of afterburner operating conditions discussed comprise burner-inlet velocities from 400 to 600 feet per second, burner-inlet pressures from 500 to 3500 pounds per square foot absolute, inlet temperatures of approximately 1700° R, and afterburner fuel-air ratios from about 0.03 to about 0.08. Most of the data were obtained with afterburners operating on full-scale engines in either an altitude test chamber or an altitude wind tunnel. Some data were also obtained from static-test-stand engine setups and from full-scale afterburners connected to a preheater and an air-supply duct.

EXPERIMENTAL PROCEDURES

The blower-rig setup was provided with a preheater and an annular burner-inlet diffuser to simulate turbine-outlet conditions and was connected to central laboratory combustion-air and exhaust equipment. A choked, fixed-area exhaust nozzle that discharged into an exhaust plenum chamber was provided at the afterburner outlet. The full-scale turbojet engines used for most of the investigations were installed either in an altitude wind tunnel or in an altitude test chamber; some data were also obtained from static sea-level test stands. All engines were installed on thrust-measuring platforms.

In the engine installations, the principal independent operating variables were afterburner fuel-air ratio and inlet pressure. Variations in fuel-air ratio required simultaneous variation in exhaust-nozzle area by use of either a variable-geometry nozzle or a series of fixed nozzles in order to maintain constant turbine-inlet temperature; control of afterburner-inlet pressure was obtained by varying the simulated altitude of engine operation. Variations in afterburner-inlet velocity could be made independently of other operating variables only by changes in afterburner diameter. Afterburner-inlet temperature was established by engine operating requirements, and was not an independent variable of operation. Because the blower-rig setup was divorced from engine operating requirements, changes in inlet velocity could be made at constant values of inlet pressure and of fuel-air ratio by variations of the exhaust-nozzle area.

The type of fuel used in the various investigations was determined primarily by availability or, in the case of specific engine development programs, by military requirements. Most of the early experiments were therefore conducted with gasoline or kerosene, and later experiments with JP-3 or JP-4 fuel. Only a few experiments have been conducted in which a given afterburner was operated on more than one type of fuel. Specific data on the effect of fuel type are therefore not available. Except for differences in spontaneous ignition characteristics, as discussed later, however, no large effect of fuel type within the range used has become apparent in the general course of the work.

When the afterburner on the engine setups was equipped with a fixed-area exhaust nozzle, the afterburner-outlet temperature was determined by two methods. One is based on flow continuity through the nozzle throat and the other on momentum, or jet thrust, considerations. With the flow-continuity method, the actual measurements required to compute exhaust temperature are nozzle-outlet total pressure, effective nozzle flow area, and total gas flow; with the momentum method they are

nozzle-outlet total pressure, jet thrust, and total gas flow. With proper instrumentation and by use of appropriate gas properties and nozzle coefficients, satisfactory agreement between the two methods is usually obtained. When the afterburner was equipped with a variable-area exhaust nozzle, the outlet temperature was usually computed only by the momentum method because of the uncertainty of the effective nozzle flow area under all conditions of operation. In the blower-rig setup, the burner thrust was not measured, and outlet temperature was therefore computed only by the flow-continuity method.

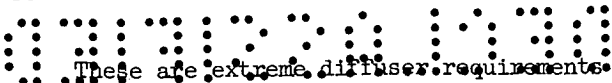
The combustion efficiency of an afterburner has been computed on at least four different bases in the various references cited. These four definitions of combustion efficiency are: (1) ratio of actual enthalpy rise to heat input in the fuel, (2) ratio of the ideal fuel flow for the actual temperature rise to the actual fuel flow, (3) ratio of the actual temperature rise to the ideal temperature rise for the fuel flow, and (4) ratio of actual enthalpy rise to ideal enthalpy rise based on the corresponding temperature rises. At fuel-air ratios above stoichiometric, methods (3) and (4) give values of efficiency appreciably greater than those computed by methods (1) and (2); at lower fuel-air ratios, all four methods substantially agree. The data presented herein from different sources are, however, either for fuel-air ratios at which the differences in efficiency are only 3 or 4 percent or the results from any one investigation, or within any one figure, are consistent within themselves. It was therefore considered unnecessary, for the purpose of this summary report, to reduce all efficiency data to a common basis. Because of the differences in efficiency calculations, however, and because different types of afterburners in various states of development were used, the results presented herein should not be compared from one unrelated figure to another.

For all calculations, the fuel-flow to the afterburner was taken to be the sum of the fuel directly injected into the afterburner and the unburned fuel entering the afterburner because of incomplete combustion in the primary engine combustor. The afterburner is thus made liable for unburned primary-combustor fuel. The afterburner fuel-air ratio is defined as the ratio of this weight of fuel to the weight of unburned air from the primary engine combustor (or preheater).

AFTERBURNER-INLET DIFFUSERS

The aerodynamic characteristics of the diffuser between the turbine exhaust and the afterburner inlet have an important influence on the performance of the afterburner. These characteristics, in conjunction with those of the turbine, determine both the velocity distribution and the mass-flow distribution entering the afterburner. The effectiveness of the diffuser in reducing gas velocity below the turbine-discharge value is important, because high burner-inlet velocities have a detrimental effect on afterburner performance. The mass-flow distribution determines the required fuel-flow distribution and, hence, the design of the fuel-injection system. In addition, diffuser pressure losses have a first-order effect on thrust.

Turbine-exhaust gases are discharged from the turbine into the annular inlet of the afterburner diffuser at average axial Mach numbers from 0.4 to 0.8, and at flow directions that may be axial or as much as 40° from the axial, depending on the turbine design. To provide satisfactory velocities at the afterburner inlet, the diffuser is usually required to have an area ratio between 1.5 and 2.0. Space and weight considerations usually dictate maximum diffuser length less than twice the afterburner diameter.



These are extreme diffuser requirements and in most cases they lie outside the realm of known diffuser-design techniques. It is not surprising that large pressure and velocity gradients usually exist at the outlet of afterburner diffusers, or that an appreciable loss in total pressure occurs in the diffuser.

Effect of Diffuser-Outlet Velocity on Afterburner Performance


No precise criteria are known that relate the performance of an afterburner to the magnitude of the velocity gradient at the burner inlet. Experience has shown, however, that afterburner performance is sensitive to magnitude of the velocity of the gases flowing around the flameholders, deteriorating as the gas velocity near the flameholders increases. A typical example from reference 1 of the effect of velocity on the performance of a highly developed afterburner is shown in figure 158. The afterburner was about $4\frac{1}{2}$ feet long and had a conventional V-gutter flameholder and conventional fuel-system components. As shown in figure 158(a), the inlet velocity at the center of the burner was low (typical of most afterburner diffusers) compared with the velocity in the region of the flameholders. When the average velocity through the afterburner was about 380 feet per second, the velocity near the flameholders was approximately 440 feet per second. As the average velocity increased, the velocity in the center of the burner remained about the same but the velocity near the flameholders increased. At an average velocity of 675 feet per second, the velocity near the flameholders was as high as 800 feet per second.

The combustion efficiency, as shown in figure 158(b), decreased considerably as the average inlet velocity increased. At a burner-inlet pressure of 570 pounds per square foot the efficiency decreased from about 0.88 at an average inlet velocity of 380 feet per second to about 0.60 at an average inlet velocity of 680 feet per second. It is apparent that, in this burner, the velocity in the region of the flameholders may not exceed 450 to 500 feet per second if combustion efficiencies of 0.85 or higher are to be maintained at low burner-inlet pressures; to maintain efficiencies of 0.8, local velocities should not exceed about 600 feet per second. At high afterburner-inlet pressures, the performance is considerably less sensitive to velocity. As shown in the figure, at a burner-inlet pressure of about 1100 pounds per square foot, combustion efficiencies above 0.80 may be obtained with local velocities of about 750 feet per second, corresponding in this case to an average velocity of about 675 feet per second.

Similar trends have been found in other investigations. For example, in one afterburner development (ref. 2) in which the velocity in the region of the flameholder was about 700 feet per second, combustion efficiencies above 0.72 could not be obtained at low burner-inlet pressures, even though a relatively long burner length was used and extensive development effort was expended on the flameholder and fuel system.

A qualitative measure of the merit of an afterburner-inlet diffuser is, therefore, the magnitude of the gas velocities it provides in the region of the flameholder. For an afterburner about $4\frac{1}{2}$ feet long that is to operate at low inlet pressures, the diffuser should provide velocities in the region of the flameholder that do not exceed 500 to 600 feet per second. For high inlet pressures, local velocities as high as 750 feet may be acceptable.

In the absence of a rigorous method of diffuser design, two general types of diffuser have been developed. One is a long diffuser having a gradually increasing



flow area, and the other is a short diffuser in which the inner body ends abruptly at some convenient length. With the short diffuser, the blunt end of the inner body can serve as part of the flameholding surface. With long diffusers, the average velocity of the gases entering the burner is low, but some combustion length is sacrificed (for a given over-all afterburner length); with short diffusers, combustion length is greater but gas velocities are higher. It is evident that one of the parameters of primary importance in determining the effect of diffuser performance on afterburner performance is the diffuser length. Other design features of interest are the shape of the diffuser inner body and the type of control devices, such as vortex generators, or vanes, that may be added to improve performance.

Effect of Diffuser Length

The effects of diffuser length on diffuser-outlet velocity profiles and pressure losses are reported in reference 3, which presents the performance of the series of four diffusers represented in figure 159. Diffuser length varied from less than 0.1 diameter to 1.05 diameter; all had an outlet-inlet area ratio of 1.92. Accompanying the variation in length was a variation in the shape of the inner body that, as will be discussed in a subsequent paragraph, probably had little effect on performance. The diffusers were tested in a duct that imposed a diffuser-inlet velocity distribution approximating fully developed pipe flow. This velocity distribution is an approximate simulation of the diffuser-inlet velocity conditions in some engines.

Velocity profile at the diffuser outlet and the pressure loss for the four diffusers are shown in figure 160. As discussed in reference 3, because of the errors inherent in measuring total pressures in highly turbulent streams, the values of pressure drop presented should be considered qualitative and indicative of relative losses only. Pressure loss data for diffuser 4 have no intrinsic significance, inasmuch as the diffuser consists simply of a sudden expansion. As diffuser length was increased the loss in total pressure increased but the velocity profile improved.

With diffuser 3 (fig. 160(b)), the velocity in the region in which flameholders would be located was above 0.8 of the diffuser-inlet velocity. If diffuser 3 were to be used with an afterburner, the average burner-inlet velocity could not exceed approximately 400 feet per second (corresponding to a diffuser-inlet velocity of about 700 ft/sec), if velocities in the flameholder region are to be maintained below the 500 to 600 feet per second required for good high-altitude performance. Increasing the length-diameter ratio from 0.51 (diffuser 3) to 1.05 (diffuser 1) would permit an increase in average burner-inlet velocity to approximately 470 feet per second without exceeding velocities of 500 to 600 feet per second in the flameholder region. The average burner-inlet velocity requirement for most modern engines is generally between 450 and 550 feet per second. It is apparent that although the increase in length from 0.51 to 1.05 diameters considerably improves the performance of this series, a length-diameter ratio of 1.0 (at an area ratio of 1.92) is not great enough to assure efficient burner operation at high altitudes for all modern engines.

Data are not available to show directly the effect on velocity profile of increasing the length of the 1.92-area-ratio diffusers beyond the 1.05 length-diameter ratio. In figure 161 the performance of the three diffusers shown in figure 160 is plotted as the ratio of the average burner-inlet velocity to the approximate velocity of the gases flowing through the portion of the burner inlet in which flameholders would be located, against the length-diameter ratio. The improvement in this velocity ratio as diffuser length increases is evident. Extrapolation of these data indicates that a diffuser length-diameter ratio of about 1.5 would permit the

use of average burner inlet velocities of about 500 feet per second. Figure 161 also presents data for two diffusers having greater values of length-diameter ratio. One, with an area ratio of 1.5, has a length-diameter ratio of 2.35; the other, with an area ratio of 1.3, has a length-diameter ratio of 1.85. An improvement in velocity ratio is evident for the longer, lower area-ratio diffusers as compared with the 1.92-area-ratio diffusers. Although a direct quantitative comparison of the data for the five diffusers can not be made because of differences in diffuser-inlet conditions, the improvement undoubtedly is the combined results from both the increase in length and the decrease in area ratio. Sufficient data are not available to separate the two effects. It appears, however, that with reasonably uniform diffuser-inlet conditions, maldistribution of velocity at the burner inlet will limit the average velocity that may be tolerated without large performance losses only for installations in which the length-diameter ratio is less than about 2, and the area ratio is greater than $\frac{1}{2}$.

Diffusers with Truncated Inner Bodies

In many diffusers, the flow separates from the inner body several inches upstream of the diffuser outlet. Such flow separation occurred, for example, in diffusers 2 and 3 (fig. 159). In such cases, the presence of an inner body downstream of the separation point probably has no effect on diffuser performance. The diffuser inner body could therefore have been cut off at the separation point, thus providing a reduction in over-all length without altering the performance. If, however, the inner body is cut off appreciably upstream of the separation point, an effect of length on performance would be expected. Performance of some diffusers altered in this manner is presented in reference 4; the data are summarized in figure 162. This figure presents the pressure losses and the diffuser-outlet velocity profile for truncated diffusers of two lengths and of two inner-body angles (or diffuser area ratio) for a given length.

Increasing the length-diameter ratio from 0.35 to 0.5 resulted in a significant improvement in velocity profile and a reduction in total-pressure losses of over 50 percent. Performance of the two diffusers having a length-diameter ratio of 0.5 was not affected by the small difference in outlet-to-inlet area ratio.

As previously discussed, cutting off the diffuser before the separation point results in an increase in velocity at the diffuser outlet compared with a diffuser that extends to the separation point. The ratio of average burner-inlet velocity to local velocity in the flameholder region for the two longest cut-off diffusers of figure 162 is approximately 0.7. Such diffusers could therefore be used in afterburners with average inlet velocities of about 390 feet per second without sacrifice in altitude performance or increase in burner length. Although the velocity ratio of 0.7 is about the same as that presented in figure 161 for a 1.92-area-ratio diffuser with a length-diameter ratio of 0.51, no generality is implied by the results because of differences in area ratio and diffuser-inlet conditions.

Effect of Inner-Body Shape

As discussed previously, it was assumed in the investigation of diffuser length that the shape of the inner body has a negligible effect on diffuser performance. The validity of this assumption is supported by the results of previously unpublished NACA tests, shown in figures 163 and 164. Figure 163 shows the configurations and axial area variation of two diffusers with different inner bodies that were tested in an afterburning engine. The rate of change of flow area with length was

CLOSED

greatly different for the two inner bodies up to a length of about 34 inches. The velocity distribution was measured at the 34-inch station. As shown in figure 164, the velocity profiles were very nearly the same with the two inner bodies. These results indicate that inner-body shape (for a constant diffuser length) has only a minor effect on diffuser-outlet velocity profile. The data also showed pressure losses for the two diffusers were very nearly the same.

Flow-Control Devices

Of the numerous flow-control devices that have been used in flow passages, only vortex generators have been comprehensively investigated in diffusers suitable for afterburner inlets. Brief investigations have, however, also been made of annular vanes and annular shrouds or splitter ducts.

Vortex generators. - References 3, 5, 6, and 7, discuss tests in which vortex generators were used to energize the boundary layer along the inner cone (and in some cases along the outer shell as well). Their action is to delay flow separation, and thereby permit the use of slightly shorter diffusers without loss in performance or slightly improve performance for the same diffuser length. It has been found that differences in diffuser-inlet velocity profile, diffuser length, inlet whirl, and diffuser shape all influence the optimum vortex generator configuration. In general, it has been found that effective vortex generators must be placed several chord lengths upstream of the diffuser separation point and must be long enough radially to extend through the boundary layer into the free stream. For diffusers 2 or 3 feet in diameter, from 20 to 40 equally spaced vortex generators are required. Chord length was between 1 and 3 inches and angle of attack was between 13° and 15° in most tests. Within this range, the effectiveness of the vortex generators was not sensitive to chord length or angle of attack. The optimum values of axial location and vortex generator span must be determined experimentally for each configuration.

Typical effects of vortex generators on diffuser performance are shown in figure 165. Outlet-velocity distributions are given for diffusers 1 and 3 of figures 159 and 160. The vortex generator configurations used in these tests were considered to be approximately optimum on the basis of preceding investigations. Twenty-four vortex generators were installed 1 inch upstream of the confluence of the cylindrical section of the diffuser inlet section and the curved portion of the inner body. Each was an NACA 0012 untwisted airfoil of 3-inch chord and 1/2-inch span with the chord skewed 15° to the axis of the diffuser. Alternate vortex generators were skewed to the left, and the intermediate ones skewed to the right. With both long and short diffusers, the vortex generators improve the velocity profile only slightly. The effect of vortex generators on pressure drop has also been found to be very small.

Annular vanes. - Cascades of annular vanes are suggested in reference 8 as a device to improve velocity distribution in diffusers. A brief investigation of annular vanes for afterburner diffusers is reported in reference 6. Three configurations investigated and their outlet-velocity distributions are shown in figure 166. In configuration A, a cascade of five annular vanes was installed, with a blunt inner cone. The vanes were simple, slightly cambered, sheet metal hoops with rounded leading edges. Successive vanes had slightly different angles of attack as suggested in reference 8. As shown in figure 166, the outlet-velocity profile with this configuration was fairly uniform, neglecting small gradients caused by wakes off the vanes. The pressure loss of configuration A was very high, however, (7 percent of diffuser-inlet total pressure). Configuration B had a longer inner cone, with vortex generators attached and no annular vanes. Although the pressure

loss was only about two-thirds that of diffuser A, the velocity profile was poor with a large separated region in the center of the burner. The vortex generators were removed from configuration B, and the two upstream vanes of diffuser A were installed to form configuration C. Both pressure loss and velocity profile were about the same for configuration C as for configuration B.

On the basis of these preliminary tests, annular cascades are effective in preventing large gradients in burner-inlet velocity, but only at the expense of large pressure losses. Additional development may produce a more favorable combination of inner body and vanes.

Splitter shrouds. - The use of splitter shrouds to divide the diffuser into two concentric annular passages was briefly investigated in reference 9. The short diffuser represented in figure 167 was tested with and without a splitter shroud surrounding the inner body. The splitter produced a lower velocity in the outer 4 inches of the diffuser outlet, but velocity in the center of the annulus was increased to an undesirably high value. With the splitter, diffuser pressure loss was slightly higher.

These results have been generally confirmed by tests in other types of diffusers. The use of the splitter reduces the velocity in one passage, but the reduction is usually accompanied by an increase in velocity in the other passage to undesirably high values. Although the data available are by no means conclusive, splitter shrouds seem to be of doubtful advantage.

Effects of Whirl on Diffuser and Afterburner Performance

Depending on engine design and to some extent on engine operating conditions, the direction of flow at the turbine outlet (diffuser inlet) may be as much as 20° to 30° from axial. Typically, as the flow progresses through the diffuser the angle of whirl increases, with the greatest increase occurring near the center body. As a result, a diffuser-inlet whirl angle of about 20° may result in an average diffuser-outlet (afterburner-inlet) whirl angle as high as 40° or 50° with local whirl angles near the center body as high as 70° or 80° (ref. 3). The effects of this whirl on afterburner and diffuser performance have been investigated in reference 10, and some typical results are reviewed in the subsequent paragraphs.

Effects of whirl on afterburner performance. - In figure 168, the effects of whirling flow on the combustion efficiency of the typical afterburner of reference 10 are shown. The whirl angles at the diffuser outlet (without straightening vanes) were greater than 30° (fig. 168(a)) over most of the flow passage. Performance of the afterburner with this large whirl and with most of the whirl eliminated by straightening vanes is compared in figure 168(b). It is evident that whirl has no significant effect on afterburner combustion efficiency. Similar results were obtained over a range of altitudes between 30,000 and 50,000 feet. Because changes in whirl angle result in changes in velocity and mass flow distribution at the afterburner inlet, it was necessary to revise the fuel distribution to obtain an optimum distribution when the whirl angle was changed. The afterburner was otherwise unchanged for the comparative tests.

Although whirl angle has little effect on combustion efficiency, large whirl angles can lead to operational problems. In burners with a large amount of whirl and with fuel injection ahead of inner-body support struts, flame may seat in the wakes from these struts and cause warping and buckling of the diffuser parts. To avoid these operational difficulties, it seems advisable to reduce whirl at the burner inlet. Experience indicates that whirl angles at the burner inlet up to approximately 20° may be tolerated without operational difficulty.

Flow-straightening vanes. - Airfoil-shaped flow-straightening vanes have been installed at the turbine discharge in several investigations to reduce whirl. Some of the vanes were fabricated from sheet metal and some were cast. Typical effects of straightening vanes on the diffuser-inlet whirl angle are shown in figure 169. Without straightening vanes whirl angle in excess of 20° (corresponding to diffuser-outlet whirl angles of approximately 40°) occurred over most of the passage. With straightening vanes, the whirl angle was 10° or less. Similar results have been obtained in other investigations (see fig. 168(a)).

The shape of the straightening vanes used is illustrated in figure 170. The vanes, designed to produce axial discharge, have the leading edge skewed to the diffuser axis at the approximate whirl angle. This inlet angle varies radially to match the local whirl angle, and chord length is greatest in the region of greatest whirl. Maximum effectiveness is obtained with vanes spanning the full passage. A ratio of vane spacing to vane chord of about $3/4$ has provided satisfactory performance in several designs.

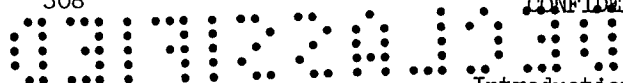
The presence of vanes in the high-velocity gas stream at the turbine discharge has been found to approximately double the pressure loss in the diffuser-vane combination. However, the reduction in whirl caused by the vanes reduces the resultant velocity over the flameholder (by reduction of the tangential component) and thereby reduces the flameholder pressure loss. As a consequence, it has been found that in most installations the over-all afterburner pressure losses are approximately the same with and without straightening vanes.

Summary

Typical afterburner-inlet diffusers produce varying degrees of nonuniformity in the velocity profile at the burner inlet, with high velocities near the outer wall in the region of the flameholder and lower velocities in the center of the burner. Because the gas velocity at the flameholder is usually limited by combustion considerations, the allowable average burner-inlet velocity, and hence the burner diameter, is largely a function of the uniformity of this velocity profile. One of the most significant design variables affecting the outlet-velocity distribution is diffuser length. Although data are not available to provide detailed design rules, several investigations have demonstrated that increasing diffuser length results in a more uniform velocity profile although with some increase in pressure loss. The shape of the diffuser inner body has no appreciable effect on its performance. Vortex generators provide small improvements in diffuser velocity profile, but other flow-control devices such as annular vanes and splitter ducts have not been successfully applied. Afterburner-inlet whirl has a negligible effect on combustion efficiency but may lead to burning in the wakes of support struts and attendant overheating and warping of adjacent parts of the diffuser. Turbine-outlet whirl may be reduced to acceptable values by relatively simple straightening vanes.

IGNITION, STARTING, AND TRANSIENT PERFORMANCE

The afterburner starting cycle includes three steps: (1) introduction of the fuel, (2) ignition of the fuel, and (3) control of exhaust-nozzle area to obtain steady-state afterburner operation. The ignition phase of afterburner starting has been investigated in somewhat greater detail than the other two phases because of the need for repeated starts during afterburner investigations in altitude facilities.



Introduction of Fuel

A significant portion of the time required to start an afterburner after the control lever is advanced to the afterburning position is consumed in accelerating the fuel pump and filling the afterburner fuel lines and manifold. The time required to fill the fuel piping and manifolds is obviously directly proportional to the volume of the piping that must be filled at each start and inversely proportional to the fuel-flow rate set by the starting control. The time required to accelerate the conventional turbine-driven fuel pump usually does not exceed 1 second at any flight condition. Likewise, the time required to fill the afterburner fuel piping at low altitudes where the fuel-flow rates are high is also very short. At high-altitude conditions, however, the time required to fill a given volume of fuel piping becomes quite significant because of the reduced fuel-flow rate.

The effect of this set, or starting, fuel-flow rate on the time required to reach operating manifold pressure is shown in figure 171. Data are presented for a 6000-pound sea-level-thrust engine (ref. 11) and for a 10,000-pound-thrust engine. The afterburner fuel systems of the two engines were similar and utilized air-turbine-driven fuel pumps, with the turbine driven by compressor bleed air. The volume of piping that had to be filled prior to each start (neglecting any residual fuel downstream of the fuel shut-off valve) was approximately 135 cubic inches for the 6000-pound-thrust engine and 200 cubic inches for the 10,000-pound-thrust engine.

In figure 171, the time required to reach the operating manifold pressure is plotted against the ratio of the fuel-system volume to the starting fuel-flow rate. Data are presented for several flight conditions, which define a single curve. The time required to fill the fuel systems varied from 2 to 9 seconds, with the longer times occurring at the higher altitude conditions, where the flow rates were lowest. Agreement of the two sets of data indicates that the time required to accelerate the fuel pump to delivery speed was about the same for both systems. Measurements on the 10,000-pound-thrust engine showed that about 1 second of the total time was required to accelerate the pump from rest. These data thus indicate that to avoid delays in filling the fuel system before the afterburner can be ignited, it is important to keep to a minimum the volume of fuel piping that must be filled prior to each afterburner start.

Ignition

Three general methods of igniting afterburner fuel have been used: (1) spark ignition, (2) spontaneous ignition, and (3) hot-streak ignition. Some of the early research on these methods of ignition is summarized in reference 12. The spark ignition method utilizes a spark plug to ignite a combustible mixture provided within a sheltered region of the burner. Spontaneous ignition is obtained in an afterburner when the pressure, temperature, velocity, and fuel-air ratio conditions within the burner are such that the fuel-air mixture ignites without addition of energy from an outside agency. In the hot-streak method, afterburner ignition is obtained by momentarily increasing the fuel-air ratio in one of the primary engine combustors to about twice the normal operating value. This momentary excess of fuel produces a streak of flame that extends through the turbine and into the afterburner and thus provides the ignition source for the afterburner fuel.

Spark ignition. - Most of the early afterburners utilized a spark-ignition system (ref. 13 and an unavailable NACA publication). The spark plug was generally installed in a sheltered region at the downstream end of the afterburner diffuser inner body, as illustrated in figure 172. Experience with this type of system

SECRET

indicated that ignition could seldom be initiated at altitudes above about 30,000 feet, and the systems were not particularly reliable at lower altitudes.

Three factors contribute to the poor reliability of the spark ignition method. One factor is breakdown of the electrical insulation in the region of high gas temperature, which causes a short circuit in the ignition lead. A second factor is melting or burning of the electrodes during afterburner operation, which prevents reignition of the burner. A third factor often preventing ignition is that the spark is either improperly located or releases too little energy to initiate ignition. The ignition systems used provided a spark energy of only about 0.02 joule per spark at a repetition rate of several hundred sparks per second. Although higher spark energies, such as those provided by the capacitor-type systems discussed in chapter III of reference 14, would be expected to improve the ability of the spark to effect ignition, no good solution to the problems of electrode insulation breakdown or electrode burning has been obtained. Because other methods of afterburner ignition held promise of being more reliable, further development of a spark system for afterburner ignition was discontinued.

Spontaneous ignition. - Methods of spontaneously igniting the afterburner fuel have also been investigated to determine the applicability and degree of effectiveness of this method. Although this method of ignition was seldom employed in gasoline-fueled afterburners without an explosive light-off, the conversion to kerosene and later to JP-3 and JP-4 fuels sufficiently lowered the spontaneous-ignition temperature of the fuel to provide satisfactory spontaneous-ignition characteristics in some afterburners. The spontaneous-ignition temperature of several fuels is indicated by the following values from chapter III of reference 14.

Fuel	Spontaneous-ignition temperature, °F
Grade 100/130 aviation gasoline	844
Kerosene	480
JP-3 fuel	484
JP-4 fuel	484

These temperatures were measured in a static system and are much lower than the temperatures required for ignition in afterburners. Nevertheless they should indicate the relative ease with which different types of fuels can be spontaneously ignited under afterburner conditions. Although the above fuels ignited spontaneously in some afterburners, in other afterburner configurations spontaneous ignition could not be obtained at turbine-outlet temperatures up to current maximum values of 1700° to 1750° R.

There are no consistent results available to indicate the specific differences in afterburner design that result in some burners' being readily ignitable spontaneously while others are not. It is, in fact, concluded in chapter III of reference 14 that the effects of various design or operating variables on spontaneous ignition (designated therein as ignition by hot gases) are incompletely understood. However, it has been observed in various afterburner experiments that relatively minor alterations in radial fuel distribution may have marked effects on the spontaneous-ignition characteristics. In general, it is believed that the two afterburner design factors having a major influence on the ability to obtain

ignition in this manner are the fuel-air-ratio distribution and the velocity profile within the burner. Fuel-air ratios that are somewhat richer than stoichiometric in a sheltered zone, with low velocities in and near such a zone, are believed to promote spontaneous ignition.

Spontaneous ignition has been obtained at burner-inlet pressures as low as about 500 pounds per square foot absolute; both burner-inlet pressure and burner-inlet temperature have been found to exert a pronounced effect on ignition limits (ref. 15). The effects of inlet pressure and temperature on the limits of spontaneous ignition with JP-3 in one afterburner configuration are shown in figure 173. Each data point on this figure represents a single afterburner start; the fuel-air-ratio value is that at which ignition occurred as the afterburner fuel flow was gradually raised. Each curve thus represents a boundary between the ignition and no-ignition regions at a given pressure. The region to the left of each curve represents the fuel-air ratios at which spontaneous ignition could not be obtained. At a burner-inlet pressure of about 1500 pounds per square foot absolute, the inlet temperature had no effect on the fuel-air ratio required for successful ignition, but at lower pressures, large increases in fuel-air ratio were required to obtain spontaneous ignition as the burner-inlet temperature was reduced. Similarly, these data show that for a given fuel-air ratio a reduction in burner-inlet pressure required a large increase in burner-inlet temperature for spontaneous ignition to occur. Spontaneous ignition of this afterburner was unobtainable at a burner-inlet pressure of 500 pounds per square foot.

The effect of burner-inlet pressure on the fuel-air ratio required to obtain spontaneous ignition for several other afterburner configurations is illustrated in figure 174. As in the previous figure, each data point represents a single afterburner start as afterburner fuel flow was being increased. These data also indicate that higher fuel-air ratios are required to obtain spontaneous ignition as the burner-inlet pressure is reduced. It should also be noted that there are appreciable differences in the required fuel-air ratio among the several configurations. The poor reproducibility of spontaneous-ignition limits is indicated by the wide band of fuel-air ratio over which ignition occurred in the several configurations.

The effect of altitude on the time required for spontaneous ignition to occur after the preset fuel manifold pressure is reached differs greatly among various afterburners. In one installation, the time required for spontaneous ignition increased from about 4 seconds at an altitude of 15,000 feet to 40 seconds at an altitude of 45,000 feet (unpublished NACA data). In contrast to this result, another quite similar afterburner (ref. 11) exhibited little effect of altitude on spontaneous ignition time, with the time for ignition varying between 4 and 8 seconds at altitudes between 30,000 and 50,000 feet.

These data, as well as related experience on other afterburners, indicate that the ability of an afterburner to ignite spontaneously cannot be predicted, nor can any practical modifications necessary to provide reliable spontaneous ignition in any given afterburner be specified. Therefore, spontaneous ignition, although it may be fortuitously obtained in some afterburners, is not a method that can be generally relied upon.

Hot-streak ignition. - Because of its high degree of reliability and simplicity, the hot-streak ignition method has received widespread application in research afterburners. The earliest hot-streak ignition systems provided supplemental fuel through one of the main engine fuel nozzles. The system was operated manually to supply the excess flow at the discretion of the operator for a period of about 1 second. This method of injection was subsequently modified to isolate the hot-streak fuel from the engine fuel manifold and thereby simplify the installation.

CONFIDENTIAL 311

This later system utilized a fuel-injection orifice located about one-half of the distance down the combustor from the main fuel nozzle, as shown in figure 175. Details of a typical hot-streak injector installation are shown in figure 176(a). For can-type combustors, the injector is designed to approximately double the fuel-air ratio of the combustor in which it is located. In annular-type combustors, the injector is designed to provide a similar increase in local fuel-air ratio and thus handles a flow of 10 to 15 percent of the main engine fuel flow. A large number of afterburners utilizing this type of system have been consistently ignited at altitudes up to 50,000 or 55,000 feet, which correspond to burner-inlet pressures down to about 500 pounds per square foot absolute (refs. 11 and 12). The system has been used with equal success on engines having one-, two-, or three-stage turbines. In each case it has been found that once the fuel-air ratio in the afterburner has reached a combustible level, the hot-streak fuel need be injected for only $1/2$ to 1 second to ignite the afterburner.

To explore the effect of the hot-streak-injector location on the ignition limits, the effectiveness of several hot-streak injectors located immediately upstream of the turbine nozzle was investigated and compared with that of the more conventional upstream location. Details of the turbine-inlet injector installation are shown in figure 176(b). This injector was also designed to double the fuel-air ratio in one combustor can. The time required before a burst from the hot-streak system would ignite the afterburner using both types of hot-streak injectors is compared in figure 177 for altitudes of 30,000 to 50,000 feet. Also included for comparison is the time required to ignite this afterburner spontaneously. The time required for ignition is defined as the period between the time at which full afterburner fuel manifold pressure was obtained after a throttle burst and (1) the time at which the burner ignited spontaneously, or (2) the time at which a $1/2$ to 1 second burst of hot-streak fuel flow would provide ignition. Minimum ignition times for several preset fuel-air ratios are plotted in the figure. Minimum time for the hot-streak systems was determined by progressively reducing the time between the throttle burst and actuation of the hot-streak ignitor until ignition could no longer be obtained from the burst of hot-streak fuel flow.

In general, the data of figure 177 indicate a relatively minor effect of either afterburner fuel-air ratio or altitude on the time for hot-streak ignition, with about 1 or 2 seconds being required in most cases. At the lower altitudes, ignition occurred slightly sooner with the turbine-inlet fuel injector than with the upstream injector, but at an altitude of 50,000 feet the turbine-inlet injector failed to provide ignition because of the absence of flame through the turbine. Increasing the injector flow two- to threefold did not improve the ignition characteristics of the turbine-inlet injector. Furthermore, when the turbine-inlet injector flow was reduced by one-half or more, afterburner ignition was unobtainable at any altitude investigated.

Failure of the turbine-inlet injector to provide flame through the turbine at high altitude was attributed to insufficient time for the fuel to ignite before entering the turbine. This premise was borne out by the fact that moving the turbine-inlet injector 3 inches farther upstream resulted in ignition characteristics comparable to those observed with the upstream injector.

Although the improvements in ignition that have been described and which result from proper installation of the ignition system are considered to apply to most afterburners, the ignition times shown in figure 177 do not apply to all afterburner designs. In some afterburners subjected to extensive ignition tests, hot-streak ignition has occurred during the process of filling the fuel manifolds so that the ignition time, as defined herein, was essentially zero.

Because the time required to fill the fuel piping and obtain a combustible mixture in the afterburner following a throttle burst varies with altitude and varies from engine to engine, a single burst of hot-streak fuel for a period of $1/2$ to 1 second would have to be very accurately scheduled to provide reliable ignition at all flight conditions. However, continuous injection of hot-streak fuel for periods much longer than $1/2$ to 1 second would, in all probability, overheat the turbine stator. Therefore, to provide reliable afterburner ignition without endangering turbine life, the hot-streak ignition system should be designed to provide intermittent bursts of fuel for periods of $1/2$ to 1 second from the time the throttle burst occurs until the control senses that the afterburner has ignited. Of course, it is important that the control system be designed so that in the event of failure the hot-streak fuel cannot be continuously injected into the engine.

Hundreds of afterburner starts with the hot-streak ignition system injecting fuel into an engine combustor for periods up to 1 second have resulted in no apparent effect on the turbine rotor blades or on the stator blades located in the path of the hot-streak flame. The absence of any rotor or stator blade deterioration attributable to the hot streak indicates that although the gas temperature may suddenly rise as much as 1000°R , the increase in metal temperature is much less because of the thermal capacity of the turbine blades. To support and explain these practical observations, transient metal temperatures were measured at the stator-blade leading edge in a single-stage turbine assembly as large step increases were made in engine fuel flow. The actual response in stator-blade metal temperature to the sudden changes in gas temperature can be characterized by a time constant. Typical values of this time constant, defined as the time to reach 63 percent of the final value in response to a step input, are shown in figure 178; the data cover a range of turbine-inlet pressures from 3000 to 12,500 pounds per square foot absolute. These pressures correspond to an altitude variation from 7000 to 45,000 feet at a Mach number of 0.8 for the engine used.

The significance of these time constants is illustrated by the computed values of stator-blade temperature rise shown in figure 179. These values were computed using the time constants of figure 178, with the assumption that the engine was operating at an average turbine-inlet temperature of 2000°R and that the temperature in the path of the hot-streak flame increased in a stepwise fashion to 3000°R for periods of $1/2$ to 1 second. The values of blade-temperature rise thus calculated are seen to be considerably less than the sudden rise in gas temperature in the path of the hot streak.

The turbine rotor-blade temperatures are, of course, affected to a much lesser extent by the hot-streak flame than are the stator blades. This insensitivity of the rotor blades to the hot streak is due to the speed with which the rapidly rotating blades pass through the local hot region.

The foregoing discussion of the hot-streak ignition system indicates that, with proper installation, the system is a simple and reliable method of initiating afterburner ignition.

Turbine-outlet hot-streak ignition. - In view of the requirement that the pre-turbine hot-streak fuel be injected for only short intervals to avoid overheating the turbine, and in view of the possibility that accidental prolongation of the injection period would cause turbine-stator failure, the feasibility of obtaining dependable ignition with a hot-streak ignitor located immediately downstream of the turbine was investigated on one engine. Three hot-streak fuel-injector configurations were investigated. Details of these injectors are shown in figure 180. The principal difference among the fuel injectors was the size, location, and number of fuel orifices. One injector consisted of a straight tube with seven orifices

DECLASSIFIED
CONFIDENTIAL 313

directed toward the turbine; another injector consisted of a bent tube pointed toward the turbine with four orifices in the end of the tube, and the third injector was a similar tube with the end left open to the full inner diameter of the tube. The afterburner on which these injectors were evaluated was of conventional design with a double V-gutter flameholder, having relatively uniform values of fuel-air-ratio distribution and velocity profile upstream of the flameholder.

Afterburner ignition limits of the three turbine-outlet hot-streak fuel injectors are compared in figure 181, which also indicates ignition limits with the conventional preturbine hot streak. Each data point represents an attempt to ignite the afterburner. All starting attempts were made at a turbine-outlet temperature of 1710° R. Although the ignitor fuel-air ratio does not represent the fuel-air ratio in the region of the fuel injector, it serves to generalize the ignitor fuel flows for all altitudes as a fraction of the engine air flow.

The three turbine-outlet hot-streak injectors were equally effective, although they were inferior to the preturbine hot-streak system. With the turbine-outlet injector, the maximum altitude for dependable ignition was between 50,000 and 55,000 feet. In comparison, the preturbine hot-streak system ignited this afterburner at altitudes up to 60,000 feet, which was the operating limit of the afterburner.

Stabilization of Operation

The greater part of the time consumed in the afterburner starting sequence occurs while the control is stabilizing engine conditions immediately following ignition. This fact is illustrated by the investigation of reference 11 (and unpublished NACA data), in which a production-type electronic control and a continuously variable exhaust nozzle were used on an engine. An example of how the control and engine variables are affected by the starting cycle is illustrated by a typical oscillograph trace in figure 182. There is a 6- or 7-second interval between advance of the throttle and ignition, followed by 7 or 8 seconds of oscillatory operation of the engine afterburner before steady-state conditions are reached. The oscillations are caused by an interaction of the various loops of the control, in conjunction with the dynamic behavior of the engine. In this particular control system, engine speed is controlled by primary engine fuel flow, and turbine-outlet temperature is controlled by exhaust-nozzle area.

The following sequence of events occurs in the engine afterburner and the control during ignition and stabilization of operation: the fuel-air mixture in the afterburner ignites while the exhaust nozzle is in a closed or nonafterburning position, because the exhaust nozzle restricts flow, the pressure in the afterburner increases, raising the pressure level throughout the engine and tending to decrease the engine speed; to maintain engine speed constant, the speed control increases the primary engine fuel flow; this increase in engine fuel flow, along with the increase in pressure level at the turbine outlet, tends to drive the turbine-outlet temperature over the limiting value; this over-temperature condition then causes the exhaust-nozzle control to open the exhaust nozzle; because the temperature-error signal is usually large, the nozzle starts to open very rapidly, which decreases the pressure level in the afterburner; this decrease in afterburner pressure tends to make the engine overspeed, which causes the control to reduce the engine fuel flow, both the increase in nozzle area and the decrease in engine fuel flow cause the turbine-outlet temperature to decrease rapidly and thus reduce the temperature-error signal to the control. The signal reduction causes the control to stop the nozzle opening and, in some cases, actually to start closing the nozzle before the required area is obtained; the turbine-outlet temperature is driven over the limit and the cycle is again repeated but with diminishing magnitude. The cycling is

continued until the proper nozzle area is reached. Amplitude of the oscillations may be reduced by changing the constants of the control system, but such a modification would make the control action slower.

The period of oscillation depends on the time constant of the engine and on the control-system constants. Because the engine time constant (rotor inertia divided by change in torque for a given change in engine speed) increases with altitude, the period of each oscillation and thus the time to reach equilibrium is greater at altitude. This increase in duration of the oscillations with altitude is shown in figure 183, for both hot-streak and spontaneous ignition. With hot-streak ignition, the duration of the oscillations increased from about 7 to 17 seconds, as the altitude was increased from 30,000 to 50,000 feet. The duration of the unsteady operation was about 2 seconds longer with spontaneous ignition than with hot-streak ignition at altitudes of 30,000 to 40,000 feet and was as much as 30 seconds longer at an altitude of 50,000 feet. The greater length of time required for the control to stabilize engine operation following spontaneous ignition is due to the more violent manner in which the fuel is ignited. The high fuel-air ratios required to obtain spontaneous ignition, particularly at high altitude, are probably the main contributors to the violent ignition of the fuel.

Complete Starting Sequence

The time required for each phase of the starting sequence and the total time consumed from throttle burst to stabilized afterburner operation at three altitudes and for both spontaneous and hot-streak ignition are summarized in figure 184. The time required for the complete starting sequence with hot-streak ignition increased from $11\frac{1}{2}$ to 27 seconds as the altitude increased from 30,000 to 50,000 feet. The same altitude variation increased the total starting time with spontaneous ignition from $16\frac{1}{2}$ to 60 seconds.

Of the total time for starting, the time required to obtain preset fuel manifold pressure amounted to only about 2 seconds at an altitude of 30,000 feet, although as long as 8 seconds were required at an altitude of 50,000 feet. After the manifold pressure reached the preset value, only 1 to 2 seconds were required to obtain ignition with the hot-streak system, as compared to 4 to 6 seconds for spontaneous ignition. Although ignition times significantly shorter than that provided by the hot-streak system cannot be expected, reductions in the time required to obtain a preset fuel manifold pressure would be obtainable by reducing the volume of the fuel lines that must be filled prior to each afterburner start.

As mentioned previously, the greatest portion of the starting time at each altitude is consumed in reaching equilibrium following ignition. Although the length of this stabilizing period is significant, it should be noted that the afterburner provides a substantial thrust increase shortly after ignition occurs. During the time that afterburner operation is becoming stabilized, the thrust will be oscillatory and may periodically equal or even exceed the final stabilized value. Because the hot-streak system provided smoother ignition than did spontaneous ignition, particularly at high altitudes, the oscillation was less severe with the hot-streak system; consequently the time required to stabilize operation was appreciably shorter at all altitudes.

CONFIDENTIAL 315

Summary

The complete starting cycle of an afterburner consists of filling the fuel pipes and manifolds with fuel, igniting the fuel, and establishing equilibrium engine-afterburner operation. Ignition of the fuel by means of a spark plug has proven to be unreliable; and spontaneous ignition, while successful and consistent in some afterburners, cannot be considered a generally reliable method. Hot-streak ignition, which produces a torch of flame into the afterburner by momentarily augmenting the fuel flow to a primary combustor, has been very successful in many types of afterburners. The time required to obtain ignition by this method varies from 1 to 3 seconds. The greatest length of time in the complete starting cycle is involved in establishing equilibrium operation of the engine-afterburner combination following ignition of the fuel. With a representative current control system, the time required for the exhaust-nozzle area, the primary engine fuel flow, and other engine variables to complete their oscillatory behavior and reach their final steady-state values increased from 11 to 27 seconds as the altitude was increased from 30,000 to 50,000 feet.

FUEL-INJECTION SYSTEMS

The primary function of the fuel-injection systems of an afterburner is to provide the proper distribution of fuel and air within the burner and adequate preparation of this fuel-air mixture for combustion. Proper distribution requires that the fuel be introduced into the gas stream at the correct locations, dependent upon the mass distribution of the turbine-discharge gases and the flameholder-area distribution. Adequate fuel preparation comprises thorough mixing of the fuel with the turbine-discharge gases, and vaporization of the mixture before it reaches the flameholder location, where combustion occurs. The basic processes involved in this union of fuel and air have been discussed in chapter I and II of reference 14.

Fuel-Spray Bars and Their Installation

The type of fuel-injection systems used almost exclusively at the Lewis laboratory and that has received widespread industrial acceptance is that of radial spray bars. These bars are located some distance upstream of the flameholder, usually within the turbine-discharge diffuser. The use of a relatively large number of spray bars, each with several fuel-injection orifices, provides the multiplicity of fuel-injection locations that is necessary for good dispersion of fuel across the gas stream. A distinct research advantage of spray-bar systems is that they can be easily removed for inspection and readily altered in both orifice number and orifice location.

A photograph of a typical fuel-spray bar is presented in figure 185. These spray bars are fabricated from commercial stainless-steel tubing; they are closed at the end and equipped with some means of attachment to the shell of the burner or burner-inlet diffuser. The inside diameter of the spray bar is usually between 1/8 and 1/4 inch; the bars are frequently left round, although in many installations they have been flattened somewhat, as shown in the photograph, to form a more streamlined cross section. The fuel orifices are simply holes drilled through the wall of the tubing at appropriate locations.

As illustrated in figure 186, the spray bars are evenly spaced circumferentially in a single plane across the burner or diffuser. They are usually cantilevered from their point of attachment on the inner or the outer shell; additional structural support is seldom necessary. For simplicity, all the spray bars are usually connected to a single manifold.

In the following presentation, the distribution of fuel-air ratio upstream of the flameholder under burner conditions is discussed for various afterburners. This discussion presents (1) the types of radial and circumferential fuel-air-ratio distribution afforded by various injection systems, and (2) the effects of fuel-air-ratio distribution on the over-all performance of the afterburner. Attention is also given to the degree to which the actual fuel-air-ratio distribution may be predicted from consideration of the injection-system design and the mass-flow profile of turbine exhaust gases. The accuracy of such predictions is not only pertinent to design, but the predictions are useful in evaluating the effects of fuel-air distribution on performance when actual measurements are not available. The effects of fuel mixing length, orifice size, injection pressure, and direction of fuel injection on afterburner performance are also summarized.

Radial Fuel-Air-Ratio Distribution in Afterburner

Measurements of the fuel-air ratio across the gas stream immediately upstream of the flameholder under burning conditions have been of considerable aid to afterburner research and development. These measurements have been obtained with the NACA mixture analyzer described in detail in reference 16.

Effect of spray-bar design on distribution. - A typical effect of a change in location of the fuel-injection orifices in a matched set of spray bars on the radial fuel-air distribution is shown in figure 187. These data, obtained from a full-scale afterburner installed on a blower rig (ref. 17), represent the fuel-air distributions measured 22.5 inches downstream of the fuel-spray bars. The fuel was injected in a transverse direction from 24 spray bars; this number, as will be illustrated subsequently, provides about the same distribution at all circumferential locations. Sketches of the spray bars, approximately to scale, are included in the figure to show the locations of the fuel-injection orifices.

With the six-orifice spray bar, the fuel-air ratio varied from approximately 0.070 near the center of the burner to less than half this value near the outer shell of the burner. By addition of two orifices near the outer shell of the burner to form the eight-orifice bar, the fuel-air ratio was made nearly the same all the way across the burner. The addition of a pair of orifices to the spray bar thus altered the fuel-air-ratio distribution from a 2 to 1 variation across the burner to an essentially uniform distribution.

Similar data on the effect of orifice location on fuel distribution are shown in figure 188 for a full-scale afterburner operating on a turbojet engine. A 16-orifice spray bar, with orifices spaced as shown in the sketch, provided the somewhat uneven fuel-air-ratio distribution shown by the solid curve. To increase the fuel-air ratio near the outer shell of the burner, a second set of spray bars was used that incorporated a closer spacing of fuel orifices near the outer shell. This spray bar, shown in the left portion of the figure, produced the fuel-air-ratio distribution indicated by the dashed curve. Although the fuel-air-ratio distribution obtained with this spray bar was slightly low in the mid-radial location, the fuel-air ratio near the outer shell was substantially increased.

Comparison of measured and calculated distribution. - The data of figures 187 and 188 show that changes in the location of the fuel-injection orifices produce, in at least a qualitative manner, the expected changes in actual fuel-air-ratio distribution. To determine the accuracy with which such changes may be quantitatively predicted, calculations of radial fuel-air-ratio distribution were made that were based on the radial location of the fuel orifices and the measured mass-flow profile of the turbine exhaust gases at the spray-bar location. These calculations were

thus based on a simple radial proportionment of fuel and air, neglecting such effects as inertial separation of the fuel and the air and diffusion of fuel vapor beyond the stream tube of air passing each orifice.

In figure 189, the results of such a calculation for the two fuel systems represented in figure 187 are compared with the measured fuel-air-ratio distribution. Although the minor variations of fuel-air-ratio distribution across the radius for each separate fuel system are not closely predicted, the general trends and the differences between the two fuel systems are predicted with fair accuracy. For both the uniform distribution of the eight-orifice bar and the decidedly nonuniform distribution produced by the six-orifice bar, the calculated fuel-air ratio is within 0.013 of the measured distribution.

Further evidence that these simple calculations of fuel-air-ratio distribution will predict general trends but not minor, or detailed, variations is presented in figure 190. The measured distributions of this figure are those previously presented in figure 188. Again, the calculated distributions agree with the measured distributions with regard to both general trend and level; the quantitative agreement is within about 0.018. Further inspection of these data, as well as other data not presented herein, shows that the measured fuel-air ratio is generally greater than the calculated values in the outer one-third of the burner. This rather general characteristic is attributed to a centrifugal separation of the fuel and air in passing through the annular diffuser, with the fuel tending to follow the initial axial direction of gas flow and the gases following more closely the curved walls of the diffuser inner cone.

From the foregoing, it may be concluded that the gross or principal effects of changes in spray-bar design on the resulting radial fuel-air-ratio distribution under burning conditions may be predicted with satisfactory accuracy from very simple considerations of the radial proportionment of the fuel and air. More detailed considerations of fuel vaporization and turbulent diffusion such as discussed in reference 18 therefore do not appear necessary for general afterburner development. In practice, a fuel-injection system for an afterburner is usually developed in two successive steps. First, the spray bar is designed to give the desired distribution on the basis of simple calculation of radial fuel and gas distribution, utilizing for this calculation the actual, and usually nonuniform, mass-flow profile at the spray-bar location. Detailed alterations to the spray bar are then made on the basis of measurements of the actual fuel-air-ratio distribution. The radial fuel distribution delivered by a spray bar may, of course, be altered by changing the location of the fuel orifices, the relative size of the orifices, or by a combination of both. As discussed in reference 17, it has been found that changing the radial location of the fuel orifices produces somewhat more predictable results than does changing the orifice size.

Effect of Radial Fuel-Air-Ratio Distribution on Performance

The effect of distribution of fuel-air ratio on the combustion performance of afterburners has been noted by many investigators over the past 4 or 5 years. This research was, until recently, conducted without the aid of actual measurements of the fuel-air-ratio distribution existing within the burner. It was generally observed, however, that fuel systems which would be expected on the basis of their design to provide most uniform distribution provided the highest combustion efficiency at high over-all fuel-air ratios, and hence provided highest maximum exhaust-gas temperatures. Some early work reported in both reference 19 and in the summary report of reference 12 indicated that progressive alterations to the fuel injectors made to obtain a more homogeneous mixture of fuel and air raised the peak combustion

efficiency and shifted the region of peak efficiency to higher over-all fuel-air ratios. Reference 12 also observed that the attainment of such "homogeneous" mixtures requires that the radial fuel distribution be tailored for each engine because of variations in turbine-outlet mass-flow profiles from one engine to another.

Spray-bar fuel-injection system. - Data that show the effect of a change in the radial distribution of fuel-air ratio on combustion efficiency and exhaust-gas temperature are presented in figures 191 and 192, respectively. A sketch illustrating the radial distribution of fuel-air ratio for one point of operation of each fuel system is included in the figures. The over-all fuel-air ratio at which each of these radial distributions was measured is indicated by the leader from the sketch. From considerations of the spray-bar design (as discussed later) and the constancy of the mass-flow profile of the gases as discussed in reference 17, it is believed that the radial distribution for each system stays about the same throughout the fuel-air-ratio range presented. The two fuel systems used for the data of these figures are those previously illustrated in figures 187 and 189, herein; they are described in greater detail as fuel-system configurations 1 and 3 in reference 17.

For fuel-air ratios higher than about 0.035, the uniform fuel-air-ratio distribution produced higher values of combustion efficiency and exhaust-gas temperature; for lower fuel-air ratios, the nonuniform fuel-air-ratio distribution gave slightly higher values. The nonuniform distribution also resulted in a slightly lower lean blow-out limit, as indicated by the small cross-hatched regions in the figure. This somewhat better combustor performance at low fuel-air ratios with the nonuniform distribution is due to the existence of localized regions within the burner in which the fuel-air ratio is high enough for good combustion, even at the low over-all values of fuel-air ratio. These locally rich regions are also the cause of the reduction in combustion efficiency at higher fuel-air ratios, because the local fuel-air mixture becomes greater than stoichiometric and thus too rich to burn completely. It is evident from these data, as well as from many other similar observations, that a uniform fuel-air-ratio distribution is desirable except for an afterburner intended primarily for very low temperature-rise operation.

Concentric manifold fuel system. - Data from another series of tests with a full-scale engine in which the radial distribution of fuel injection was varied is presented in figure 193. In this afterburner, fuel was injected from three concentric manifolds, each incorporating a large number of simple fuel orifices. The three manifolds were so connected to separate fuel throttles that the radial distribution of fuel could be varied during operation. A more complete description of this fuel system as well as the complete afterburner may be found in reference 6. Although the fuel-air-ratio distribution was not measured during the tests, the distribution provided by one method of operation relative to another was computed on the basis of the number and the location of fuel-injection orifices in operation, the distribution are illustrated by the sketches in the upper part of the figure. While no claims can be made for quantitative accuracy of fuel-air-ratio distribution, it is apparent that systems A, B, and C provided progressively more uniform radial distributions of fuel.

The combustion efficiencies concomitant with the three different fuel systems are shown in the lower part of the figure. Although the peak efficiency has the same value for all three systems, the fuel-air ratio at which peak efficiency occurred shifted to progressively higher values of over-all fuel-air ratio as the fuel distribution became more uniform. These data illustrate the desirability of a multiple, or at least, a dual orifice system if efficient operation is required over a wide range of fuel-air ratios. Such a dual orifice system, which could provide a nonuniform (locally rich) fuel distribution for low-temperature operation and a uniform mixture for high temperature, is mentioned in reference 12 also. Dual

systems have not been put into actual use in full-scale afterburners because their primary requirement is usually that of high thrust output; they have, however, found effective application to ram-jet combustors where efficient operation over a wide range of conditions is required (refs. 20 to 22).

Locally rich fuel injection. - A particularly striking, though extreme, example of the good combustion performance that may be obtained at low values of fuel-air ratio with a nonuniform fuel-air-ratio distribution is shown in figure 194. The fuel-injection system used in this afterburner consisted of 12 radial spray bars, each having four fuel orifices. At an over-all fuel-air ratio of 0.055, the local fuel-air ratio (fig. 194(a)) varied from about 0.02 to 0.11 across the radius of the burner, with the rich region located near the position of the single-ring flameholder. The combustion efficiency of this burner is shown in figure 194(b); the performance of the burner with the uniform distribution of figure 191 is included for comparison. As previously noted, operation with the uniform fuel distribution produced a peak efficiency at a fuel-air ratio of about 0.05 and a lean blow-out limit of about 0.03. With the very nonuniform fuel-air-ratio distribution, on the other hand, lean blow-out did not occur until an over-all fuel-air ratio of 0.004 was reached. Although the combustion efficiency decreased rapidly as the fuel-air ratio was increased, efficiencies approaching 100 percent were measured at the lowest fuel-air ratios.

Summary. - A summary of the manner in which afterburner fuel-air ratio for peak combustion efficiency varies with the degree of uniformity of radial fuel-air-ratio distribution is presented in figure 195. The abscissa of this figure is the integral across the burner of the absolute value of the difference between the local and the average fuel-air ratio, divided by the average fuel-air ratio. A value of zero thus indicates perfect uniformity of fuel-air-ratio distribution, and a value of 0.5, for example, means that the mean deviation of local fuel-air ratios from the average value is 50 percent of the average.

Included in figure 195 are all available data from tests in which the fuel-air-ratio distribution was systematically varied and the fuel-air ratio for peak combustion efficiency was observed. Data from references 17 and 23 are based on actual measurements of fuel-air-ratio distribution within the burner, while that from references 6 and 19 are, in the absence of actual measurements, based upon the arrangement of fuel-injection orifices across the burner flow passage. The greater degree of nonuniformity of distribution indicated by the fuel-injector design compared to the actual measurements is a result of the spreading and softening of the distribution between the point of fuel injection and the flameholder.

For both types of data, a rapid decrease in the fuel-air ratio at which peak efficiency occurs is apparent as the fuel-air-ratio distribution becomes less uniform. In order to have a peak combustion efficiency at a fuel-air ratio between 0.055 and 0.06, or to provide maximum temperature rise and thrust augmentation, the mean deviation in local fuel-air ratio should be no greater than 10 percent of the average value.

Circumferential Distribution of Fuel-Air Ratio in Burner

Just as the radial fuel-air-ratio distribution in an afterburner is determined by the number and location of the fuel orifices in each radial spray bar (if such a fuel system is used), so will the circumferential distribution be affected by the spacing between the spray bars and the amount of crossflow penetration of the fuel jet into the gas stream. The spacing between spray bars is, of course, determined directly by the number of bars used and the burner diameter, while the jet penetration is a function of orifice size, gas velocity, fuel-jet velocity, and other

properties affecting the vaporization rate of the fuel. These various factors are not independent but are, instead, closely interrelated. In the following discussion, the effect of the number of spray bars on both the circumferential fuel-air-ratio distribution and the burner performance is first examined at various gas velocities for a given orifice size. The effects of changing the orifice diameter are then presented for two gas velocities and different numbers of bars. Although data covering complete ranges of all the pertinent variables are not available, a review of the available data permits certain general conclusions to be drawn.

Although radial nonuniformity in distribution of fuel-air ratio may be desirable in those applications where efficient operation at low temperature rise is desired, it is logical to assume that the circumferential distribution should always be fairly uniform because of the circumferential symmetry of the flameholders in general use. It remains, therefore, to determine the type of fuel system required to give a sufficiently uniform circumferential distribution of fuel-air ratio at various gas velocities.

Effect of number of spray bars on fuel-air-ratio distribution. - The circumferential distributions of fuel-air ratio provided by 12 and by 24 radial spray bars are compared in figure 196. All spray bars were the same, with eight fuel orifices of 0.030-inch diameter in each. The gas velocity for these tests was between 500 and 600 feet per second; fuel was injected in a radial plane. The burner diameter was approximately 26 inches. A measure of the circumferential distribution of fuel-air ratio is provided in this figure by comparing the fuel-air ratios along two radii some 15 inches downstream from the spray bars; one radius was directly aft of a spray bar, and the other in a plane midway between adjacent spray bars. As indicated in the upper part of the figure, the radial fuel-air-ratio distribution is about the same for both radii when 24 spray bars were used, this result indicating a circumferentially uniform distribution. When 12 spray bars were used, however, the fuel-air ratio along the two radii differed by more than 2 to 1 over most of the area of the burner. As would be expected, the difference was greatest near the outer shell of the burner, where the spray bars were farther apart, and almost disappeared at the center of the burner. Thus, with 12 spray bars in this afterburner, there existed a combined radial and circumferential distortion in fuel-air-ratio distribution.

It should be noted that the poorer circumferential distribution of fuel with the 12 spray bars existed in spite of the higher fuel-injection pressures associated with the smaller number of fuel orifices. This result is contrary to what would be expected for nonvaporizing liquid jets, inasmuch as the correlation of reference 24 for liquid jets indicates that the higher injection pressures should have essentially offset the greater spacing between the bars for the conditions of this test; therefore, vaporization of the fuel had a significant influence on the circumferential fuel distribution. As might be expected, however, the jet penetrations generally indicated by the data of figure 196 are somewhat greater than would have been predicted from the data of reference 25 for air jets. Although more exact quantitative comparisons are not possible, it is apparent that the penetration characteristics of fuel jets in afterburners are between those of liquid jets and air jets, with the specific characteristics depending on the various factors that influence the vaporization rate of the fuel.

Effect of number of spray bars on performance. - The effects of the nonuniform circumferential fuel-air-ratio distribution illustrated in figure 196 on the combustion efficiency of the afterburner are presented in figure 197. Although the effects of this nonuniformity do not appear to be as large as those resulting from a radial nonuniformity, the combustion efficiency is 7 or 8 percentage points higher with the 24-spray-bar fuel system than with the 12-spray-bar system over most of the range of fuel-air ratio.

The data of figure 197 were obtained at a burner-inlet velocity of 500 to 600 feet per second; they indicate that, for these conditions, the higher fuel-injection pressures associated with the smaller number of spray bars did not provide sufficient penetration to give a uniform fuel distribution. It might be expected, however, that the fuel penetration across the gas stream would be greater at a lower gas velocity and the effect of the number of fuel-spray bars on the performance of the afterburner would be less. That this is actually the case is illustrated in figure 198, where the combustion efficiency at a burner-inlet velocity of 380 to 480 feet per second is shown to be the same for both 12 and 24 spray bars. For comparison, the combustion efficiency obtained at these lower gas velocities with the fuel-air-ratio distribution nonuniform in a radial direction, as obtained for the six-orifice spray bars of figure 187, is included as the dashed curve. In this case, the combustion efficiency decreased very rapidly with increasing fuel-air ratio, as previously discussed. Therefore, while low gas velocities permit the number of spray bars used to be reduced because of greater fuel penetration across the gas stream, the fuel orifices must be located radially to give good coverage across the burner if good performance is desired at high over-all fuel-air ratios.

Effect of orifice size on performance. - The results presented in the preceding section are for an orifice diameter of 0.030 inch. As was mentioned, a reduction in orifice diameter may increase the rate of fuel vaporization sufficiently to decrease the jet penetration and thereby have an adverse affect on burner performance. This effect would be reduced, of course, if a large number of spray bars were used. Data from reference 17 comparing the combustion efficiency with 0.030- and 0.020-inch-diameter fuel orifices are presented in figure 199; 24 spray bars were used in a 26-inch-diameter afterburner. It is apparent that in this case the jet penetration was not reduced enough by the reduction in fuel-orifice size to affect the performance appreciably. This result was, furthermore, obtained at the relatively high gas velocity of 500 to 600 feet per second.

If the spacing between spray bars is similar to that provided by 24 bars in a 26-inch-diameter burner, orifice diameters as small as 0.020 inch may, therefore, be used even at high gas velocities. If, on the other hand, only 12 spray bars are used, an orifice diameter of 0.020 inch does not appear to be large enough to provide good fuel distribution, even at gas velocities no higher than 400 feet per second. This conclusion is based on a comparison of figure 198 with 200, which is replotted from the data of reference 25. As indicated in figure 200, the spray-bar system for these data comprised 12 long spray bars, each having 8 orifices, and 12 shorter spray bars with 6 orifices per bar. The performance obtained when all 24 spray bars were used is compared with that obtained when only the 12 long spray bars were used. Although an exact comparison between the data of figures 198 and 200 is not possible because different afterburners were used, values of gas velocity, burner-inlet pressure, and burner diameter were about the same. The principal difference is that 0.020-inch orifices were used for the data of figure 200 as compared to the 0.030-inch orifices for the data of figure 198.

Contrary to the satisfactory performance indicated in figure 198 for the 12 spray bars having 0.030-inch orifices, the performance shown in figure 200 for 0.020-inch orifices was appreciably reduced when the number of spray bars was decreased from 24 to 12. Not only was the maximum gas temperature reduced from 3400° to 3000° R, but the combustion efficiency at the condition of maximum temperature was also about 20 percentage points lower. Although the fuel-injection pressure at stoichiometric fuel-air ratio was increased from 25 to 75 pounds per square inch for the smaller number of spray bars, the fuel penetration with the small orifices was obviously inadequate to overcome the wider spacing between the bars.

To recapitulate, the use of as few as 12 spray bars in a 26-inch-diameter afterburner provided good performance only when the gas velocity was relatively low (380 to 480 ft/sec) and the fuel orifices were as much as 0.030 inch in diameter. The performance of the 12-bar system was inferior to that of the 24-bar system at high gas velocities with 0.030-inch orifices, and at low gas velocities with 0.020-inch orifices. A spray-bar spacing corresponding to 24 spray bars in a 26-inch-diameter burner provided good performance at high gas velocities (500 to 600 ft/sec) with either 0.020- or 0.030-inch diameter orifices. Other combinations of orifice diameter and number of spray bars within these limits should, of course, be possible.

Effect of ratio of orifice size to spray-bar diameter. - The foregoing discussion indicates the possibility of reducing the number of spray bars somewhat if the jet penetration is increased by increasing the orifice diameter. Early fuel vaporization is apparently less with the larger orifices, and the penetration characteristics approach those of a purely liquid jet. (As discussed later, large axial mixing distances permit adequate fuel preparation for combustion.) If the fuel orifice becomes too large relative to the internal diameter of the spray bar, however, the static pressure within the bar and the effective flow area of the several orifices will vary. The effect of this ratio of orifice area to spray-bar area on the proportion of fuel delivered by each orifice is reproduced from the data of reference 17 in figure 201. Plotted against the ratio of total fuel-orifice area to spray-bar flow area is the ratio of fuel-flow through each orifice relative to that through the number 1 orifice (at the shank of the spray bar). For each value of total orifice area, all orifices were the same size. As this ratio of total orifice area to spray-bar area increases, the fuel orifices located toward the tip of the spray bar deliver proportionally greater amounts of the total fuel-flow. This variation in fuel delivery is a result of the higher static pressure within the bar at the tip and the higher relative flow coefficient of the tip orifices. Although the effects of these variations are probably negligible for area ratios of less than 0.5, the tip orifices deliver as much as 50 percent more fuel than the shank orifices for an area ratio of 1.0.

As discussed in reference 17, other factors affecting the amount of fuel delivered by each orifice are the length-diameter ratio of the orifice and the method of drilling the hole. Orifices having small length-diameter ratios, with the hole drilled undersize and reamed to final size, produced the greatest uniformity of flow from one orifice to another. Orifices produced in this manner have flow coefficients in the range of 0.5 to 0.6, based on the fuel pressure in the spray bar.

Effect of direction of fuel injection. - The data presented so far on fuel-injection systems were obtained with the fuel injected in a transverse direction, that is, across the gas stream. It might be expected that this direction of injection would be somewhat better than an upstream or downstream direction, simply because it would provide a better fuel coverage of the gas stream. This premise is substantiated in figure 202(a), which compares the combustion efficiencies obtained when fuel was injected alternatively in a transverse, upstream, or downstream direction from an otherwise identical system. Although the effect of the direction of fuel injection is not large at low fuel-air ratios, the combustion efficiency at the higher fuel-air ratios is considerably higher when fuel is injected in a transverse direction than when injected either upstream or downstream. It should be noted that this rather significant effect of the direction of fuel injection was obtained with a fuel-mixing distance of 29.5 inches; if a shorter fuel-mixing distance had been used, the effects might have been even greater.

A further comparison of the combustion efficiency of an afterburner with upstream and with downstream injection is presented in figure 202(b). In this burner, three concentric fuel manifolds were used; in one case fuel was injected in a downstream direction from all three manifolds, and in the other case the direction of injection of two of the manifolds was reversed. At the higher burner-inlet pressure, the effect of this change in direction of fuel injection was not large, but performance at the pressure of 620 pounds per square foot absolute was considerably better with upstream injection, particularly at the high fuel-air ratios. The very small fuel-mixing distance used in this afterburner (1.5 inches) probably accounts for this rather large effect of changing from a downstream to an upstream direction in this case.

Effect of fuel-mixing distance on performance. - There are few data indicating the isolated effect of change in the fuel-mixing distance (the distance between the fuel injector and the flameholder). Theoretical analyses of the evaporation of fuel sprays summarized in chapter I of reference 14 are not applicable, and experimental results are quite meager. Also, little work has been done on the subject of the mixing of fuel sprays with air (chapter II of ref. 14). It has been a matter of almost universal experience in full-scale afterburner research, however, that relatively large mixing distances (approaching 2 ft) are required for satisfactory performance, particularly at low burner-inlet pressures. The summary report of reference 12, for example, indicates an appreciable improvement in high-altitude performance of an afterburner when the fuel-mixing length was increased from $17\frac{1}{2}$ to $25\frac{1}{2}$ inches. The improvement in performance of one series of afterburners relative to that of another series described in reference 26 is also largely attributed to an increase in fuel-mixing distance. Although there is probably some basis for the viewpoint that large mixing distances tend to aggravate the problem of combustion instability, all available experience with afterburners of many types indicates that the combustion performance at high altitude will not be satisfactory with mixing distances of only a few inches. The fuel-mixing distances of all known afterburners that have what might be considered satisfactory high-altitude performance have been of the order of 20 inches or more.

Summary

The distribution of fuel-air ratio across the burner in both a radial and a circumferential direction has an important influence on both the combustion efficiency and on the fuel-air ratio at which maximum efficiency occurs. In general, uniform mixtures are required for high efficiencies at high fuel-air ratios, and nonuniform, or locally rich regions, are necessary for good efficiency at low fuel-air ratios. The required orientation of a nonuniform fuel-air-ratio distribution is related to the arrangement or type of flameholder. The radial fuel-air-ratio distribution provided by a fuel-injection system can be predicted with satisfactory accuracy by simple considerations of the radial proportionment of the injected fuel and gas flow. The uniformity of the circumferential pattern of fuel-air ratio will depend on both the spacing of the radial fuel-spray bars and the penetration characteristics of the fuel jet across the gas stream. The penetration characteristics of fuel jets in afterburners appear to be between those of pure liquid jets and air jets, with the relative position depending on the various factors that influence the rate of fuel vaporization. Highest combustion efficiency at high fuel-air ratios is obtained with fuel injection in a transverse direction to the gas stream and with mixing distances of at least 12 to 15 inches between the point of injection and the flameholder.

FLAMEHOLDER DESIGN

As in most of the various aspects of combustor design, knowledge of flameholder design principles has been accumulated empirically. The first experiments with afterburners showed that various bluff bodies in the air stream successfully anchored flame and provided a source for further propagation of combustion throughout the burner. Following these early results, numerous experiments have been performed to explore the size, shape, and arrangement of bluff-body flameholders with the objective of obtaining high combustion efficiency, high altitude limits, and low pressure drop. Because these experiments were necessarily carried out simultaneously with experiments to improve the design of other parts of afterburners, such as fuel-injection systems and inlet diffusers, the relations among the results of tests on different afterburners are obscure in many cases. Wherever possible, however, the results presented herein are selected from experiments that covered a range of pertinent burner designs. In this manner, the degree of generality of the results is revealed. Although types of flameholders other than bluff bodies (such as pilots and cans) may have considerable merit, the absence of information about them makes it necessary to limit the present discussion to bluff-body flameholders. Basic aspects of flow and combustion around flameholders may be found in chapters II and III of reference 14.

The flameholders that will be discussed are all formed of annular rings, or gutters, constructed in a manner similar to that shown in figure 203. The flameholders are usually attached to the wall of the burner with several streamlined struts. Although several methods of fabrication have been employed, the most satisfactory method from the standpoint of durability and ease of manufacture has usually been to weld sheets of Inconel about 1/8 of an inch thick into the shape required (in this case a V) and smooth off the weld on the external surfaces by grinding. Radial interconnecting gutters are similarly formed and attached by welding.

Effects of Cross-Sectional Shape

In references 27 and 28, a theory is advanced to explain the nature of stabilization of flames on gutters. According to the theory, hot gases from the burning boundaries of the fuel-air mixture surrounding the wake from a bluff body are recirculated upstream and enter the relatively cool boundary near the body. These hot gases increase the temperature of the mixture and carry ignition sources into the mixture. By this process, ignition of fresh mixture is initiated, and a continuous process of ignition is maintained.

Isothermal wake flow. - An experimental evaluation of the effect of cross-sectional shape on the recirculation characteristics of bluff bodies in isothermal flow is given in reference 29. "Bluffness" of a body is considered to be qualitatively proportional to the sum of the angles between the body's trailing edges and its axis of symmetry. It was reasoned that the recirculation characteristics of a bluff body were directly related to vortex strength (ratio of tangential velocity to vortex radius) and to shedding frequency of the vortices formed in the wake. Bluff bodies of twelve shapes were investigated; with the aid of hot-wire and flow-visualization techniques, the strength and shedding frequency of the vortices were determined. Some of the principal results are shown in figure 204.

In figure 204, the ratio of vortex strength to approaching gas velocity is plotted against the ratio of shedding frequency to gas velocity for five representative shapes. The various shapes investigated are shown in the sketches in the symbol key. The flameholders were circumferentially symmetrical except for the V-gutter flameholder with the vortex generators installed on the upstream splitter plate. The vortex generators of this flameholder were essentially small vanes

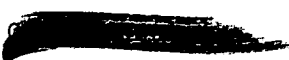
installed on both the inner and outer surfaces of the splitter vane or projecting cylinder. The vanes were inclined at an angle of about 16° to the axis of the burner and were about $3/4$ inch high and 1.2 inches in chord. The gutter width of each flameholder at the open end was $3/4$ inch. In figure 204, the general trend of increasing strength and decreasing frequency with increased bluntness of the flameholder is apparent. The changes in vortex strength and frequency are large.

3925
Combustion efficiency. - To determine the possible relation of these isothermal-wake characteristics to combustion performance, tests were made in a simulated afterburner facility to evaluate combustion efficiency, stability limits, and pressure-loss characteristics of flameholders with cross-sectional shapes similar to those tested in cold flow. The results of this investigation are reported in reference 1 and additional tests of two shapes are reported in reference 30. Typical results are shown in figure 205, where combustion efficiency is plotted against afterburner-inlet pressure. The two upper curves represent typical data selected from reference 1 and the two lower curves are from the afterburner study of reference 30. Although the efficiency levels of the two afterburners differed by about 25 percent (because of differences in flameholder size, fuel distribution, burner length, and burner-inlet velocity), the changes in efficiency with change in flameholder cross-sectional shape are about the same for both. In both afterburners, combustion efficiency was 2 to 20 percentage points lower with the U-shape gutter than with the V-shape gutter. For both burners, the difference in efficiency was greater at the lower inlet pressures.

In figure 206, the afterburner combustion efficiency is plotted as a function of afterburner-inlet velocity and pressure for various shapes of flameholder gutters. Parts (a) to (c) of this figure are for a fuel-air ratio of 0.047, and parts (d) to (f) for a fuel-air ratio of 0.067. Data are shown for ten flameholder cross-sectional shapes. The general trend of decreasing combustion efficiency with increasing afterburner velocity or decreasing inlet pressure is consistent for all shapes investigated, but scatter of the data obscures any general effect of shape on performance.

To aid in comparing the efficiencies of the various flameholders, the arithmetical average difference between the efficiency observed with the V-shape flameholder and with each of the other shapes was calculated; these differences in efficiency are plotted in the bar graphs of figure 207. Included in the calculations are a large number of data points that cover values of fuel-air ratio between 0.02 and 0.08, burner-inlet velocity between 400 and 700 feet per second, and burner-inlet pressure between 500 and 1200 pounds per square foot. Because insufficient data are available to isolate the effects of these variables, the observed values of efficiency at all operating conditions for a given flameholder were averaged together. In view of the trend of decreasing efficiency difference with increasing pressure shown in figure 205, the over-all average differences shown in figure 207 are probably conservative for low pressures and extreme for high pressures.

The results of figure 207 show that the U-shape flameholder is inferior to the flameholders of other shapes by amounts varying from 4 to 10 percent. Among the several shapes with highest efficiency, differences of only 2 or 3 percent were obtained. Below the bar for each flameholder shape is given the corresponding value of cold-flow vortex strength from reference 29. There is no apparent correlation between combustion efficiency and cold-flow vortex strength. It is evident from these results that although the U-shape gutter is inferior to gutters of most other shapes (particularly at low pressures), only small differences in combustion efficiency are obtained by using flameholders with cross-sectional shapes other than the V-shape.



Blow-out limits. - The effect of cross-sectional shape on operable fuel-air-ratio range is shown for several typical shapes in figure 208. Data from references 1 and 30 are included. The effect of gutter shape on the lean and the rich fuel-air-ratio limits is small (0.005 to 0.01). The principal effect of shape appears to be that the minimum pressure for stable combustion is from 50 to 200 pounds per square foot higher for the U-shape flameholder than for the other shapes investigated.

Pressure loss. - The effect of flameholder shape on total-pressure loss between burner inlet and outlet (excluding pressure losses in the diffuser) is shown in figure 209. Without burning (temperature ratio of 1.0), the pressure loss is from 1 to 2 percent of the burner-inlet pressure. With the exception of the flameholder with knife edges mounted on the sides of the gutter (square symbols), the pressure losses are the same with the various flameholders within ± 1 percent over the range of burner-temperature ratio investigated. Data for pressure drop with the U-shape gutter are available from reference 1 only for the nonburning condition, and are shown for the temperature ratio of 1.0 in figure 209. During cold flow, the pressure drop for the U-shape gutter is approximately the same as for the V-gutter. Data from reference 30 indicate, however, that during burning the pressure-loss ratio is 0.01 to 0.02 less with the U-shape flameholder than with a V-gutter flameholder of the same size ($22\frac{1}{2}$ -percent blockage).

In summary, the experimental investigations have shown that afterburner combustion efficiency may vary as much as 10 percent with flameholder cross-sectional shape. Of the various shapes investigated, the U-shape flameholder was inferior in both stability limit and combustion efficiency to all others. Combustion efficiency and stability limits of several shapes were comparable to the V-shape flameholder. Pressure losses for most of the shapes were approximately the same.

Effects of Gutter Width, Number of Gutters, and

Blockage on Combustion Performance

The size and arrangement of flameholders is one of the dominant factors affecting afterburner performance. The best arrangement of flameholders is a function of the factors of environment in which the flameholder must operate such as velocity and fuel-air-ratio distribution at the flameholder and type of wall-cooling system used. It is evident, therefore, that a single optimum location (axial and radial spacing) of flameholders does not exist for all possible environmental conditions. Some general trends and qualitative indications of best location are, however, discussed in a subsequent section. In this section the effects of gutter width, number of gutters, and blockage will be shown for a wide range of environmental conditions; general trends that are to a large degree independent of environment are discussed. All the results are for unstaggered flameholders.

Gutter width. - Some effects of gutter width are illustrated in figure 210. It is, of course, impossible in any experiment to isolate the individual effects of gutter width, gutter diameter, number of gutters, and percent blockage. The effects shown in figure 210 may, therefore, be influenced to some degree by variables other than gutter width and number of gutters. An attempt was made in each test to minimize the extraneous effects. In most cases, the flameholders were located in regions of nearly uniform afterburner-inlet velocity to avoid large effects of small changes in gutter diameter. Particular emphasis was placed on providing a uniform fuel-air-ratio distribution at the flameholder location.

3925

In figure 210(a), some results from reference 20 are shown. Combustion efficiency at a fuel-air ratio of 0.04 is plotted against burner-inlet pressure for two flameholders, each having two rings and the same blockage but with gutter widths of 2 and 1.6 inches. The 2-inch-wide gutter produced a combustion efficiency two to five points lower than the 1.6-inch gutter. Tests in the same afterburner showed that with 1/2-inch-wide gutters combustion could not be maintained at all pressure levels below approximately 1000 pounds per square foot absolute. The data shown in figure 210(b), taken from unpublished NACA tests, are contrary to the width trend indicated in figure 210(a). For this afterburner, a flameholder with a 2-inch-wide gutter had a combustion efficiency 2 to 6 percentage points higher than a flameholder with a $1\frac{5}{8}$ -inch-wide gutter. In figure 210(c), the results from reference 31 are shown for two flameholders each having three V-gutter rings. The $1\frac{1}{2}$ -inch-wide gutter had 48-percent blockage, and the $3/4$ -inch-wide gutter had 29-percent blockage. At inlet pressures near 1000 pounds per square foot absolute, the differences in gutter width and blockage had no appreciable effect on combustion efficiency. At lower pressures, the flameholder with narrower gutters and less blocked area produced a combustion efficiency as much as 5 percentage points less than the wide flameholder. Observation of the flame during the tests showed that at pressures less than 800 pounds per square foot absolute the flame was partially blown out with the $3/4$ -inch gutter, whereas the flame with the $1\frac{1}{2}$ -inch gutter was steady and complete. It is thus indicated that the reduction in efficiency at low pressures was due to the narrow gutters rather than the smaller blocked area.

Although there are inconsistencies in the data, it appears that increases in gutter width above $1\frac{1}{2}$ inches have no large effect on combustion efficiency. Reduction in gutter width from $1\frac{1}{2}$ inches to $3/4$ inch has no large effect on combustion efficiency, but may cause instability of the flame at low pressures. Gutter widths of $1/2$ inch did not support combustion at inlet pressures less than 1000 pounds per square foot absolute. These results were obtained with several afterburners and are apparently independent of burner-inlet velocity over the range between 450 and 620 feet per second. Because all of the burners investigated were 4 feet or more in length, the applicability of the results to shorter afterburners is not known.

Blow-out limits for flameholders having different gutter widths (same afterburners that provided data of figures 210(a) and (c) are shown in figure 211. Although the minimum pressure limits are not clearly defined, it is evident from the consistent trends of lean and rich blow-out limits that the minimum pressure for combustion is higher for the narrower gutters. The magnitude of the increase in minimum pressure limit as gutter width decreases from 2 inches to $3/4$ inch is probably of the order of 100 pounds per square foot. Effects of number of gutters on blow-out limits for the afterburners investigated in references 30 and 31 were negligible.

Number of gutters. - Some data showing the effects of the number of flameholder gutters or rings on combustion efficiency are presented in figure 212. In this figure, a $1\frac{1}{2}$ -inch-wide, three-ring flameholder is compared with a $3/4$ -inch-wide, three-ring flameholder and a $1\frac{1}{2}$ -inch-wide, two-ring flameholder. As discussed previously in connection with the effects of gutter width, the lower efficiency of the $3/4$ -inch-wide, three-ring flameholder at low pressures relative to the $1\frac{1}{2}$ -inch-wide, three-ring flameholder is attributed to partial blow-out (a gutter-width effect) of the narrower gutters. The three-ring, $3/4$ -inch-wide flameholder and the two-ring, $1\frac{1}{2}$ -inch-wide flameholder both had a blockage of 29 percent. The three-ring,

$\frac{1}{2}$ -inch-wide flameholder had a blockage of 48 percent. Comparison of these three flameholders shows that except in the region of partial blow-out for the $\frac{3}{4}$ -inch gutters, there is an improvement of about 5 percentage points in combustion efficiency, if three rather than two flameholder rings are used. It is, of course, not possible to separate completely the effects of blockage from the effects of number of rings. Comparison of the three curves at an inlet pressure of 1000 pounds per square foot (above the region of partial blow-out for the $\frac{3}{4}$ -inch gutters) indicates that blockage in the range from 29 to 48 percent has no separate effect on combustion efficiency. At lower pressures, the effects of number of gutters and blockage on combustion efficiency are not separable, but as is shown subsequently, it is probable that blockage effects are small.

The observed effects of number of gutters, as pointed out in reference 31, are probably due to the increased average burning time obtained by using three rings (six flame fronts or $\frac{1}{2}$ - or 2-inch spacing between gutters), rather than two rings (four flame fronts or about 3-inch spacing between gutters). If the flame front always extends downstream from the gutter edges at approximately the same angle, it is obvious that the fuel particles will, on the average, encounter a flame front farther upstream in the case of the three-ring flameholder than in the case of the two-ring flameholder. Hence, the average burning time is greater for the larger number of flame fronts.

Although the available data are meager, it appears that, if the gutters are wide enough (approximately $\frac{1}{2}$ in.) to prevent partial blow-out at low pressures, gains in efficiency of 5 to 7 percent are possible at burner-inlet pressures between 500 and 1000 pounds per square foot, by using three rather than two flameholder rings. Data are not available to determine the magnitude of the effects at higher pressures. In view of the apparent insensitivity of combustion efficiency to flameholder design at high afterburner-inlet pressures, it is probable that an afterburner sufficiently long to operate efficiently at low inlet pressure would not be appreciably improved in performance at high pressure by using three flameholder rings instead of two.

Blockage. - Effects of blockage on afterburner combustion efficiency are shown in figure 213 for several afterburners at a high and a low pressure level. Data for this figure were obtained with six afterburners, of which three were fitted with different flameholders to vary the blockage. The number of flameholder gutters used is indicated by the symbols. Included among the tests are a wide variety of fuel-air-ratio and velocity distributions at the burner inlet, average velocity level at the burner inlet, number of flameholder rings, and gutter widths. All the afterburners are similar, however, in that fuel was injected sufficiently far upstream to ensure adequate mixing and vaporization time and burner length was great enough to provide adequate burning time. Although the data at high pressures are few and no one afterburner was investigated over a range of blockages at this high pressure, it is evident that blockage effects at pressure levels near 3000 pounds per square foot are very small. These effects are confirmed by many results, such as those discussed in reference 32, which reports afterburners that operated with high efficiency at burner-inlet pressures of the order of 3000 pounds per square foot with blockages as low as 15 to 20 percent.

At lower pressures (fig. 213(b)), gains in efficiency by increasing blockage beyond 30 percent appear to be negligible. The data for the upper curve of figure 213(b) are representative of three of the best current afterburner designs (afterburners of refs. 6, 31, and 33) in approximately the same state of development.

The small effect of flameholder blockage on combustion efficiency for blockages greater than 30 percent is particularly apparent in these data.

For blockages less than 30 percent, the combustion efficiency decreases as blockage decreases. As indicated in the figure, however, the decrease in efficiency with blockage is greater when blockage is reduced by decreasing the number of flameholder gutters than when blockage is reduced by decreasing the width of the gutters and retaining the same number of gutters. The reduction in efficiency at the lowest blockage may, therefore, be due at least in part to the use of single-gutter flameholders. The lower curve of figure 213(b)(ref. 30), is for flameholders having two gutters, and it is evident that in this case the decrease in efficiency as blockage decreases below 30 percent is much less than for the other two curves. These results are further confirmation of the effects of number of flameholder gutters discussed previously in connection with figure 212.

Although the effects of blockage on operable fuel-air-ratio range and minimum pressure for stable combustion have not been well documented, isolated observations do not indicate any large or consistent trend with blockage.

All the results presented in figure 213 are for flameholders with four to six radial gutters interconnecting the annular gutters. Several experiments have shown that these interconnecting gutters have little effect on combustion efficiency, except at conditions near the minimum pressure limit. It has been shown that in some cases use of interconnecting gutters improves combustion efficiency and operating range of fuel-air ratio at very low inlet pressures without any appreciable penalty in flameholder pressure loss.

Summary. - The number, arrangement, and size of flameholders (of the V-gutter type) are important design considerations. For stable and efficient combustion at afterburner-inlet pressures down to 600 pounds per square foot, minimum gutter width appears to be about $1\frac{1}{2}$ inches. At very high burner-inlet pressures, both two- and three-ring flameholders have about the same combustion efficiency; at intermediate and low pressures, three-ring flameholders are superior. At burner-inlet pressures around 3000 pounds per square foot, change in flameholder blockage over the range from approximately 25 to 40 percent has negligible effect on combustion efficiency. At low pressures (800 lb/sq ft or less), in order to provide a sufficient number of flameholder rings of adequate width, blockages of 30 percent or more must be used for maximum combustion efficiency. Gutter width has a first-order effect on minimum pressure for stable combustion and on fuel-air-ratio range of afterburners; radial gutters interconnecting the annular flameholder rings have a favorable effect on low-pressure limits.

Effect of Flameholder Blockage on Pressure Drop

The pressure drop in the afterburner is due to losses in the diffuser or cooling liners, to the aerodynamic drag of the flameholders, and to the momentum changes associated with combustion of fuel. Numerous approximate methods of calculation of these pressure drops have been published (e.g., refs. 34, 35, and chapter II ref. 14). Some measurements of pressure loss in an afterburner (ref. 31) without burning are shown in figures 214 and 215. The flameholders used were simple nonstaggered V-gutters; the various blockages and sizes are indicated in the keys at the top of the figures. A comparison (fig. 214) of the pressure drops observed with flameholders of the same blockage (29 percent), but having different numbers and sizes of gutters, indicates that number and size have no separate effects on the cold-burner pressure losses. It is evident that velocity has a very large effect on pressure loss and

that, in general, there is a value of velocity at which the rate of change of pressure loss with velocity increases very rapidly.

A cross plot of the data of figure 214 is given in figure 215. At each inlet Mach number, pressure losses increase appreciably only after blocked area is increased above about 30 percent. For a blocked area of 35 percent, the pressure loss increases from about 0.007 to 0.024 of the inlet total pressure as burner-inlet Mach number increases from 0.2 (400 ft/sec) to 0.3 (600 ft/sec). It appears that blockages as high as 30 percent may be used at an inlet Mach number of 0.3, or as high as 37 percent at an inlet Mach number of 0.2, with a cold pressure loss of only 1 percent. Pressure losses at a burner-inlet Mach number of 0.306 computed by a method similar to that of reference 35 are shown by the dashed line. The method used in reference 35 employs an analytic solution for the flow conditions at the downstream, or exit, plane of the flameholder and application of empirically determined coefficients to compute the pressure drop. The agreement between the calculations and the experimental data is good for pressure losses of 0.04 or less. It has been previously shown that blockages of 35 percent are adequate for good performance at high altitudes; it is thus apparent that the "cold-pressure" losses introduced by such a flameholder in an afterburner amount to only 1 or 2 percent.

In figure 216(a), the combined pressure losses due to drag of the flameholder and cooling liner and to combustion of fuel are shown. The pressure loss is shown as a function of temperature ratio across the burner for several flameholder blockages. It is apparent that a change in blockage over the range between 22 and 31 percent has little effect on pressure losses during burning. Although the absolute values of the pressure loss shown in figure 216(a) are high because of an unusual cooling liner that was used, the relative effects of flameholder blockage are valid.

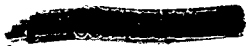
In figure 216(b), a comparison is made between the measured pressure loss and the pressure loss computed by the method of reference 34. Good agreement between the measured and calculated values indicates that, in the absence of cooling liners or other extraneous devices, the method of reference 34 is adequate for the prediction of internal afterburner pressure losses during burning.

COMBUSTION SPACE

The combustion efficiency and maximum obtainable temperature rise in an afterburner are, of course, functions of the space available for combustion. As length is reduced, the time available for the completion of combustion (residence time) is reduced and, in addition, the distance available for the spread of flame across the burner from the flameholders is decreased. Inasmuch as burner-inlet conditions influence these combustion processes, it would be expected that the effects of the combustion space on performance would be different for different pressure, temperature, and velocity levels. The arrangement of the flameholders across the burner cross-section and the amount of wall taper would also be expected to influence the combustion space requirements. Some of these effects for two different classes of afterburners are discussed in the following paragraphs.

Effects of Afterburner Length

Take-off afterburner. - In some afterburner installations, such as in subsonic bombers, it may be desirable to obtain a moderate amount of thrust augmentation at take-off and to carry the afterburner inoperative at altitude conditions. In these applications, minimum afterburner size is required in order to reduce weight and drag penalties to a minimum; internal pressure losses, with their attendant penalties on engine fuel consumption, are also of greater relative importance than the combustion efficiency.



An afterburner designed for take-off application is shown in figure 217. The diffuser, flameholder, fuel system, and perforated liner were designed for minimum pressure loss, as discussed in reference 4, and in part, elsewhere herein. Flameholder blockage amounted to about 14 percent of the burner cross-sectional area. The length of the burner from the flameholder to the exhaust-nozzle outlet was varied from 20 to 62 inches by adding or removing spool sections in the 31-inch-diameter section of the burner. The burner-inlet pressure for the tests was 3800 pounds per square foot absolute, and the burner-inlet velocity (at the flameholder location) was 350 feet per second.

The effect of the afterburner length on the combustion efficiency is shown in figure 218(a). As the length was reduced from 62 to 20 inches, the combustion efficiency decreased from over 90 percent to less than 60 percent. Although the efficiency decreased rather rapidly as the length was reduced below 3 feet, such a change may not be important for a take-off application because the afterburner operates for only a short time. Of greater importance is the thrust augmentation obtainable with different burner lengths shown in figure 218(b). For the reduction in length from 62 to 20 inches, the thrust augmentation ratio (ratio of augmented thrust to normal thrust with the standard tail pipe) decreased from about 1.50 to 1.36. It is evident, therefore, that for an afterburner designed for take-off use only, where the burner-inlet pressures are relatively high and combustor efficiency is not of primary importance, a length of 20 to 30 inches may be adequate.

The total-pressure losses across this afterburner were relatively low. For non-afterburning operation, the loss in total pressure from turbine outlet to exhaust-nozzle outlet was about 5 percent for the burner lengths investigated. This loss is slightly less than the total-pressure loss that usually occurs in a standard, nonafterburning tail pipe.

Altitude afterburner. - Some effects of afterburner length on performance for a limited range of conditions are reported in reference 36; more recent and previously unpublished data over a wide range of conditions and with an afterburner designed to have good performance at high-altitude conditions are discussed herein. A sketch of the afterburner used is shown in figure 219. A two-ring V-gutter flameholder of 29.5-percent blockage was installed. Fuel was injected from 24 fuel-spray bars located 32 inches upstream of the flameholder. The afterburner was cylindrical and its length was varied in four equal steps from 30 to 66 inches. With each burner length investigated, burner-inlet total pressure, total temperature, and velocity were varied over a wide range.

The variation of combustion efficiency with burner length is summarized in figure 220 for the range of burner-inlet conditions investigated. Although reducing inlet pressure and temperature, or raising inlet velocity lowered the general level of combustion efficiency, all the data showed the same general trend of increased combustion efficiency with burner length. Increasing burner length from 30 to 66 inches raised the combustion efficiency by 25 to 35 percentage points over the range of conditions investigated. The major portion of this efficiency variation occurred between burner lengths of 30 and 42 inches.

As a result of the sizeable drop in combustion efficiency at reduced burner-inlet pressures, it follows that a substantial increase in burner length is required to obtain a given efficiency as burner-inlet pressure is lowered. For example, maximum combustion efficiency at a burner-inlet pressure of 750 pounds per square foot was obtained with a burner length of about 66 inches. However, the same efficiency required a burner length of only about 42 inches at a burner-inlet pressure of 1800 pounds per square foot. In addition, the data of figure 218 indicate the same efficiency was attainable with a burner length of only about 32 inches at a burner-inlet pressure of 3800 pounds per square foot.

The data of figures 220(c) and (d) also illustrate the possible trades between burner length and burner-inlet velocity or temperature for operation at constant combustion efficiency. With relatively short burners, an increase in length of only a few inches is required to offset the efficiency reduction accompanying a 200° F drop in inlet temperature or a 100-foot-per-second increase in inlet velocity. However, for burners longer than about 42 inches the added length required to offset efficiency losses resulting from such changes in inlet conditions becomes very large. In fact, if the burner is already relatively long, further additions in length will fail to restore efficiency losses resulting from increased velocity or reduced temperature.

The pressure loss across this afterburner increased with inlet velocity in the manner indicated in figure 214. As might be expected, there was a negligible effect of burner length on pressure loss. For a burner temperature ratio of 2.0 and a burner-inlet temperature of 1200° F, the pressure loss increased from 0.04 to 0.11 of the burner-inlet total pressure as inlet velocity was increased from 400 to 600 feet per second.

Effect of Flameholder Gutter Diameter

Variations in flameholder gutter diameter have been observed to significantly influence the combustion efficiency of an afterburner operating at high altitudes. To demonstrate these effects, a brief investigation was conducted using the afterburner of figure 219 as the reference configuration. Data indicating the effect of flameholder gutter diameter were obtained by using a flameholder with gutter diameters slightly smaller than the one used in the reference configuration. A comparison of these two flameholders is shown in figure 221. The advantage of moving the gutters farther away from the burner wall is that it eases the problem of shell cooling, as is discussed in a later section.

The combustion efficiency obtained with the modified flameholder and that for the reference configuration (fig. 220) are compared in figure 222. The modified flameholder was tested with burner lengths of 42 and 66 inches, and the data for these configurations are shown by the solid symbols. Comparison is made with the performance of the reference flameholder over a range of lengths previously presented in figure 220. Moving the outer gutter away from the burner wall requires added length for the flame front to reach the wall, and thus, as shown here, lowers the combustion efficiency by 5 to 10 percent with a 66-inch burner length and as much as about 30 percent with the 42-inch burner length. This means that moving the flameholder gutters inward to ease shell cooling is equivalent to reducing afterburner length. For the cases investigated, the net effect of the flameholder modification was to reduce the combustion efficiency by about the same amount as would a 15- to 20-inch reduction in length of the reference configuration.

Effect of Afterburner-Shell Taper

To demonstrate the effect of burner-shell taper on performance, the afterburner described in figure 219 was operated with a tapered burner section having a length of 42 inches. A sketch of this configuration is shown in figure 223.

The combustion efficiencies obtained with the 42-inch-large tapered afterburner are compared with those for the cylindrical reference afterburner in figure 224. The data of figure 224(a) indicate that a drop in combustion efficiency of 13 to 18

percent resulted from tapering the burner. The primary reason for this drop in combustion efficiency is reduced residence time, inasmuch as the volume of the tapered burner was only 78 percent of that for the cylindrical burner of equal length. To illustrate this point, the combustion efficiencies of the two afterburners are compared in figure 224(b) on the basis of afterburner volume instead of length. For the single point of comparison (and for two pressure levels), the efficiency is the same for a given afterburner volume, independent of the taper of the outer shell. Such agreement indicates that the secondary factors associated with tapering the burner are relatively unimportant.

Because combustion efficiency is relatively insensitive to length variations for burners about 60 inches long, it might be expected that tapering burners of this length would result in a smaller efficiency reduction than was observed with the 42-inch burner. Unfortunately, data for longer afterburners of sufficiently similar design and operating conditions for inclusion on figure 224 are not available. However, some slightly tapered afterburners about 60 inches in length have been found to operate with combustion efficiencies of about 90 percent at burner-inlet total pressures down to about 1000 pounds per square foot. These observations, therefore, offer some substantiation to the premise that tapering of afterburners having a length greater than about 60 inches will have a relatively minor effect on combustion efficiency.

EFFECTS OF OPERATING VARIABLES ON PERFORMANCE OF A TYPICAL AFTERBURNER

Performance of an afterburner of fixed design is affected by inlet values of velocity, pressure, temperature, and by fuel-air ratio. The effects of inlet conditions on afterburner performance are illustrated to some degree in numerous reports. Reference 2, for example, discusses effects of inlet pressure and velocity in detail. Because most turbojet engines operate at about the same turbine-outlet (afterburner-inlet) temperature, data have not been obtained to show the effect of afterburner-inlet temperature on afterburner performance. Although the quantitative effect of these inlet variables on combustion efficiency differs with afterburner design, as is illustrated elsewhere in this report, the general trends of efficiency with changes in inlet conditions are similar for all burners. With this generality in mind, only a brief summary of the principal trends is given here.

The afterburner selected for the discussion is illustrated in figure 225. The burner is 53 inches long and $25\frac{3}{4}$ inches in diameter. A two-ring V-gutter with a gutter width of $1\frac{1}{2}$ inches and a blocked area of 29 percent was used. Fuel was injected through radial spray bars located approximately 30 inches upstream of the flameholder. Particular attention was given in the design to achieving reasonably uniform fuel-air-ratio distribution at the afterburner inlet. The afterburner had an inlet-velocity distribution (fig. 226) typical of current afterburners.

In figure 227, the effects of inlet velocity and inlet pressure on the combustion efficiency of the burner are illustrated. As shown in figure 227(a), combustion efficiency decreases as burner-inlet pressure decreases. At an inlet velocity of 450 feet per second, the efficiency decreases about 5 percentage points as pressure decreases from 1000 to 570 pounds per square foot. At higher velocities, however, the effects of pressure are greater; at an inlet velocity of 600 feet per second, the efficiency falls off about 13 percentage points for this decrease in pressure. As shown in figure 227(b), this divergence continues for velocities up to 700 feet per second. A loss in efficiency of about 18 percentage points results from decreasing pressure from 1060 to 566 pounds per square foot at an inlet velocity of 650 feet per second.

Although these results are for a fuel-air ratio of 0.047, similar trends are obtained at other fuel-air ratios. Because of the manner in which the particular burner under consideration was operated, individual effects of fuel-air ratio at constant values of pressure and velocity were not obtained. Fuel-air-ratio effects are illustrated, however, for several burners in the section on fuel-injection systems.

The effect of inlet velocity on the blow-out limits is illustrated in figure 228. The minimum pressure for stable combustion at a given fuel-air ratio increases slightly as burner-inlet velocity increases. The minimum pressure at any fuel-air ratio, which occurs at a fuel-air ratio of about 0.060, increases from about 350 pounds per square foot at an inlet velocity of 500 feet per second to 400 pounds per square foot at a velocity of 600 feet per second.

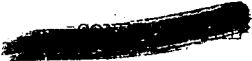
It may be concluded that the effects of inlet velocity on blow-out limits are small but that the inlet velocity and pressure greatly affect the combustion efficiency, even in an afterburner of good design. Although changes in inlet velocity and inlet pressure affect the performance of various burners to different degrees, the trends shown by these data are general and are probably representative of many current afterburner designs.

COMBUSTION INSTABILITY (SCREECH)

The phenomenon commonly known as "screech" in afterburners is a combustion instability characterized by high-frequency, high-amplitude pressure oscillations. Combustion-chamber pressure has been observed to oscillate in various afterburners at frequencies between 800 and 4000 cycles per second and with amplitudes between one-third and one-half the burner-inlet pressure. The oscillations are usually accompanied by increased burner-shell temperature and improved combustion efficiency. The combination of high burner-shell temperature and high-frequency pressure variations frequently leads to structural failure. Numerous failures have been encountered in the afterburner shells, flameholders, and fuel-system components after only a few minutes of operation with screeching combustion. A photograph of a typical failure due to screeching combustion is shown in figure 229. Other oscillations of lower frequency, often referred to as buzz or rumble, sometimes occur in afterburners, but screech is the only type of instability that has become a severe operational problem. Some fundamental considerations of various types of combustion instability, including screech, are discussed in chapter VIII of reference 14.

The afterburner-inlet conditions at which screech occurs differ widely for various afterburner designs. The occurrence of screech has been shown, however, to be consistently related to fuel-air ratio and afterburner-inlet pressure. In general, screeching combustion is observed to occur over a wider range of fuel-air ratios as inlet pressure is increased in the range between 500 and 4000 pounds per square foot. Recent unpublished data indicate that at pressures above 4000 pounds per square foot the range of fuel-air ratio for screech may be reduced. The effects of afterburner-inlet velocity on screech have not been defined completely.

Because of the destructive nature of screeching combustion, considerable effort has been expended in attempts to find methods of suppressing or preventing the occurrence of screech. The principal results of these investigations are summarized in references 37 and 38; they are repeated, in part, in the following discussion. Early experiments, conducted before special transient pressure and flame-front detection instrumentation was available, consisted of determining the effects on screech limits (screech limits are defined as the fuel-air ratio and pressure conditions at which screech starts or stops) of various systematic changes in the de-



sign features of afterburners. Later experiments with both small-scale burners and full-scale afterburners, utilizing special transient instrumentation, were made to identify the mode of oscillation and to develop special devices for preventing screech.

Effect of Afterburner Design on Screech Limits

In the early experiments on effects of afterburner design on screech limits, variations in nearly all afterburner components were investigated. Included in these tests were variations in radial distribution of fuel-air ratio, in distance between fuel injectors and flameholder, in shape of the inlet-diffuser centerbody, in radial velocity distribution at the flameholder, in radial location of the gutters, in flameholder cross-sectional shape, and in gutter width. Results of these tests showed that the centerbody shape, the distance between flameholders, and the distance between the flameholder and the outer wall had no consistent effect on screech limits.

In contrast to these results, the velocity distribution at the flameholder influenced the screech limits to a considerable degree in one afterburner. A high degree of whirl originally existed at the turbine outlet in the particular afterburner investigated. This large whirl resulted in the velocity distribution at the burner inlet (diffuser outlet) shown by the circled points in figure 230. With this velocity distribution, screech was encountered over a fairly wide range of fuel-air ratio, as shown in figure 230(b). The addition of antiwhirl vanes (diamond symbols) eliminated the whirl and also eliminated the low-velocity region at the inner diffuser wall. With the improved velocity profile, screech was not encountered. To determine whether removal of the whirl or of the low-velocity region had eliminated screech, the flow was tripped off the diffuser inner cone by an obstruction. The resultant velocity profile at the burner inlet was very close to the original profile, but no whirl was present. With this configuration, screech again occurred at approximately the same conditions as with the original configuration. It was concluded that the change in velocity profile rather than the change in whirl was responsible for the improved screech limits. It is evident, therefore, that at least in this case the occurrence of screech was dependent upon the velocity profile at the flameholder.

An effect of the radial distribution of fuel-air ratio on screech limits has been observed in several experiments. The results have, however, been erratic and inconclusive. In some cases, a change of as little as 1/8 inch in the immersion of fuel-spray bars eliminated screech at a particular operating condition. In other cases, larger variations in radial fuel distribution have been ineffective in altering the screech limits. Reducing the mixing distance between the fuel injectors and the flameholder has also successfully eliminated screech, but the required reduction in mixing distance has always been so great that altitude performance was sacrificed. Although further research into these effects may reveal some useful design criteria for avoiding screech, it seems unlikely at the present time that alteration in fuel distribution will yield significant benefits in screech suppression without some performance sacrifice.

As illustrated in figure 231, the flameholder gutter width may influence the screech limits. In this figure, the number of times various flameholders of different gutter widths were tested in a particular afterburner is shown; the solid bars represent configurations that screeched, and the open bars those that did not screech. It is then apparent that the wider the gutter, the greater the probability that screech will occur. No screech was encountered in the particular afterburner

investigated if gutters of $1\frac{1}{2}$ inches or less in width were used. This result is not general; other burners using gutters as narrow as $1/2$ inch have produced screech, although of lower severity. The general trend of lower screech tendency with narrower gutters has, however, been confirmed in several other investigations. The blockage areas of the flameholders used in these tests were substantially the same. Separate blocked-area effects have not been determined.

A few experiments conducted with various radial locations of the flameholder revealed no effects on screech limits. Similarly, effects of changing the cross-sectional shape from a "V" to a "U" were negligible. However, the addition of an aft splitter plate (such as those shown schematically in fig. 232) to annular V-gutters had appreciable effect on screech limits. As shown in figure 232, a 9-inch splitter was effective in eliminating screech at some conditions. Other experiments have shown that longer splitter plates are even more effective in preventing screech. Although the 9-inch splitter plate was not adversely affected by the surrounding hot gases, the necessity for cooling longer splitters may make them impractical. The effects of splitter plates on combustion efficiency are not known.

These experiments show that the conditions under which an afterburner will screech may be controlled at least partially by proper design of the diffuser, the fuel system, and the flameholder. Proper selection of these components may enable many afterburners to operate over the required range of inlet conditions without encountering screech. In addition, it appears from the large effects of flameholder design and velocity distribution on screech limits that the origin or mechanism of sustenance of screech is associated with the aerodynamics of the flow upstream of the combustion region as well as with the combustion process itself. This relation of the aerodynamic and combustion processes in screech has been appreciated by many investigators, although several different theories to explain the nature of the driving force or "feedback" mechanism have been advanced. It is suggested in reference 39, for example, that vortex shedding from the flameholders may account for the relation between screeching combustion and aerodynamic phenomena. Reference 40 goes farther by stating that the screech oscillations are driven by vortex-induced variations in the flame area with time. Satisfactory verification of either of these hypotheses has not been obtained, however.

Identification of Mode of Oscillation

The tests to determine the effect of burner configuration on screech limits were ineffective in revealing the origin or nature of the pressure oscillations encountered during screech. To identify the mode of oscillation, additional tests were conducted on two afterburners in which transient pressure instrumentation was used to measure temporal variations in pressure and to determine the phase relation between components of the pressure oscillations at various stations around the burner circumference and along the burner length.

A typical oscilloscope record from one of these tests is shown in figure 233. A cross-sectional sketch of the burner used showing the relative positions of the pressure pickups around the circumference and the flameholder location is shown at the bottom of the figure. The oscilloscope record shows that the variation of pressure with time is small at stations 1 and 3 and large at stations 2 and 4. It is evident that the pressure pulses at stations 2 and 4 are 180° out of phase. Similar phase relations were measured for other types of flameholders and for burners of different size. Analysis of the possible modes of oscillation (refs. 14 or 38) shows that the indicated phase relation can occur only in the mode of pressure oscillation called the first transverse mode.

A diagram schematically illustrating the first transverse mode (fig. 234) indicates that the particle paths are curved transverse lines. For the first transverse mode, two nodes exist; for higher-order transverse modes, additional nodes exist, with appropriate increases in frequency. Phase and frequency measurements indicate, as shown in figure 235, that for small afterburners (about 6 in. in diam.) without inlet-diffuser centerbodies, the first mode most frequently exists. Modes up to the fourth apparently occur in larger afterburners (up to 36 in. in diam.) with diffuser centerbodies. The shaded areas of figure 235 indicate the ranges of frequencies that are encompassed by the first and fourth modes of oscillation over the range of gas temperature (speed of sound) in the burner. Similar areas, which would lie between the two shown, can be computed for the second and the third modes; they are omitted in figure 235 for clarity.

Oscillation Damping by Perforated Walls


After it was established that screeching combustion is associated with a transverse oscillation, attempts were made to prevent or suppress screech by dampening the oscillation with various devices arranged inside the burner shell. Experiments were made with an afterburner having fins attached to the wall of the burner that extended the entire length of the combustion chamber. The fins were radial and had various heights and circumferential spacings. The fins altered the screech limits and the oscillation frequency, but did not eliminate screech at all operating conditions. Other investigations of the use of fins are reported in reference 41. The results were generally similar to the NACA experience, in that the fins prevented screech in some, but not all, of the configurations investigated. The use of burner-shell taper is also reported in reference 41 to have successfully prevented screech. This result is, however, not supported by similar NACA tests, in which it was found that shell taper of reasonable amounts would not prevent screech. The difference between the results of reference 41 and of the NACA investigation is probably due to differences in flameholder design, fuel-injection systems, and burner-inlet conditions. It may be concluded that the use of fins or shell taper, while beneficial in some cases, will not prevent screech in all burners or under all conditions of operation.

In another attempt to dampen the pressure oscillations, a perforated liner was installed in an afterburner, as shown in figure 236. The liner, spaced concentrically $3/4$ inch from the burner wall, had $3/16$ -inch-diameter holes throughout, spaced on $1/2$ -inch centers. The liner extended from a few inches upstream of the flameholder to the end of the 24-inch-long combustion chamber. The use of this liner completely prevented screech with several flameholders at burner-inlet pressures up to approximately 3000 pounds per square foot, which was the maximum pressure investigated.

Many additional tests with similar perforated liners in other afterburners have demonstrated that these liners are effective in eliminating screech over the full operable range of fuel-air ratio and for burner-inlet pressures up to 6500 pounds per square foot absolute. The combustion-chamber length of these afterburners was about 5 feet; liner lengths of 3 feet were sufficient to eliminate screech at all conditions investigated. Corrugated, louvered liners have appeared to be more effective than plain cylindrical, perforated liners.

Summary

It is evident that the design of the flameholder, the fuel system, and the inlet diffuser have an appreciable influence on the screech limits (conditions of inlet pressure and fuel-air ratio) of afterburners. These facts indicate that the



aerodynamics of the flow approaching the burner are linked with the screech mechanism. By proper selection of flameholder, fuel system, and diffuser, many burners may be designed to be screech-free over their required range of operation. Phase and frequency measurements of pressure oscillations in several afterburners have led to identification of the modes of oscillation. The oscillations are transverse and occur in the first to fourth mode in most afterburners investigated. Perforated combustion-chamber liners have prevented screeching combustion in every afterburner investigated over a wide range of fuel-air ratio and pressure conditions.

EFFECT OF DILUENTS ON PERFORMANCE

The combination injection of refrigerants into the compressor or combustion chamber of a turbojet engine with afterburning may, as discussed in reference 42, result in higher thrust augmentation than can be achieved by either injection or afterburning alone. The jet-thrust ratio ideally obtainable with the combined systems is, in fact, approximately the product of the thrust ratios obtainable from the individual systems. Experimental investigation of combined refrigerant injection and afterburning are reported in references 43 and 44. In these experiments, afterburning was combined with injection of ammonia or a water-alcohol mixture. Alcohol is normally added to the water because it depresses the freezing point of the mixture and because it serves as a convenient source of the additional heat needed to vaporize the water. Because a water-alcohol mixture provides appreciable gains in thrust only at moderately high inlet-air temperatures, tests with these fluids were confined to sea-level, zero-ram conditions. Ammonia injection, on the other hand, provides useful thrust gains at low ambient temperatures and, consequently, tests with ammonia injection were conducted at conditions simulating flight above the tropopause at a Mach number of approximately 1.0.

In reference 43, augmentation ratios as high as 1.7 were obtained by combined water-alcohol injection and afterburning as compared to about 1.5 for afterburning alone and 1.22 for injection alone. In reference 44, appreciable thrust increases with combined ammonia injection and afterburning over that obtainable with either system alone were demonstrated. The thrust increases obtainable by the combined augmentation systems depend, however, upon the coolant used, the characteristics of the engine, and the gas-temperature limitations in the afterburner. Because of this dependence of thrust output on factors other than afterburner performance, the effect of the presence of the injected coolants (diluent) on the performance of the afterburner is discussed in this section with regard to operating limits and combustion efficiency of the afterburner rather than with regard to thrust augmentation obtainable.

The afterburners used in the experiments (figs. 237 and 238) were representative of the best current design practices as discussed in other sections of this report. The afterburners were over 5 feet long and had two- or three-ring V-gutter flameholders with blockages of about 35 percent. The fuel-injection systems were located to provide adequate mixing length.

Effect of Water-Alcohol Injection

In figure 239 are shown the effects of the presence of water and alcohol on the combustion efficiency and outlet-gas temperature of the afterburner. The mixture used was 30 percent alcohol and 70 percent water by volume; the alcohol was a blend of 50 percent ethyl and 50 percent methyl alcohol. The value of fuel-air ratio presented in the figure is the weight ratio of fuel flowing to the afterburner (including alcohol not consumed in the engine combustors) to unburned air flowing

to the afterburner. Values of equivalence ratio presented are based on total flow of all fuels (engine fuel, afterburner fuel, and alcohol) and total air flow. At each fuel-air ratio, or equivalence ratio, increasing the flow of coolant decreases the combustion efficiency. These effects are particularly pronounced at the higher equivalence ratios. With an equivalence ratio of 0.93, the efficiency decreases more than 35 percent as the coolant-to-air ratio increases from zero to 0.072. The effects of water-alcohol injection on gas temperature are shown in figure 239(b). Outlet temperature decreases 17 percent over the same range of coolant-to-air ratios. The temperature could not be increased by raising the equivalence ratio beyond the value of 0.93 because the decrease in combustion efficiency offset the increase in fuel flow. The large reduction in combustion efficiency as water-alcohol flow is increased is probably due to a reduction in reaction rate, as discussed in reference 45.

The maximum equivalence ratios that could be used in the engine were limited by afterburner screech. The limits of stable combustion are shown in figure 240. The afterburner fuel-air ratio at which screech occurred was approximately constant over most of the coolant flow range and occurred at a value greater than the fuel-air ratio for maximum temperature. The over-all equivalence ratio was also nearly constant over the range of injected flows.

Although afterburner blow-out was not encountered in the full-scale work of reference 43, some small-scale combustor work reported in reference 46 indicates that for some burner designs, blow-out limits may be affected by water injection. Results of blow-out tests on a 6-inch-diameter V-gutter-type combustor (ref. 48) are shown in figure 241. Afterburner equivalence ratio is plotted against the injected water-air ratio. With the burner operating with JP-3 fuel, the possible range of operation decreases as water-air ratio increases, and operation was not possible at water-air ratios above 0.07.

Also shown in figure 241 are operating points for a slurry fuel of 60 percent magnesium (approximately 3-micron particle size) and 40 percent JP-3 fuel. As indicated by the stable operation obtained at equivalence ratios over 1.0 at water-air ratios as high as 0.15 (limited only by water-pumping capacity), the effect of water injection on blow-out limits is eliminated in the practical range of water injection rates by the use of the slurry fuel.

The small-scale burner results with the slurry fuel have been partially confirmed in a full-scale afterburner. Unpublished full-scale afterburner tests with a slurry of 50 percent magnesium and JP-4 fuel have shown that stable screech-free operation is possible with a water-air ratio of about 0.10 at stoichiometric fuel-air ratio in the afterburner.

Effect of Ammonia Injection

The effect on combustion efficiency and outlet-gas temperature of ammonia injection in the afterburner of figure 238 is shown in figure 242. In this afterburner, maximum combustion efficiency and highest gas temperature over the range of equivalence ratios covered occurred at an over-all equivalence ratio of 1.0 for all ammonia flows. Increasing the ammonia-air ratio decreased both the combustion efficiency and the maximum gas temperature. This effect, while quite small at an equivalence ratio of 1.0, became much greater as the equivalence ratio was decreased.

Although screech was not encountered during these tests, the effect of ammonia injection on blow-out limits shown in figure 243 was observed. At the higher ammonia-injection rates, the afterburner was operable over only a very narrow range

of equivalence ratios. At ammonia-air ratios above 0.05, afterburner operation was not possible at any equivalence ratio at these inlet conditions. A similar, though less pronounced, trend of decreasing limits of flame propagation with increases in ammonia-air ratio above 0.02 is noted in reference 47.

The relative effects of water and ammonia on afterburner combustion efficiency cannot be determined by direct comparison of the results because the tests were run on different afterburners with somewhat different inlet conditions. It is probable that the superior performance of the afterburner of figure 238 with ammonia injection as compared to the afterburner in figure 237 with water injection is due, at least in part, to its greater length.

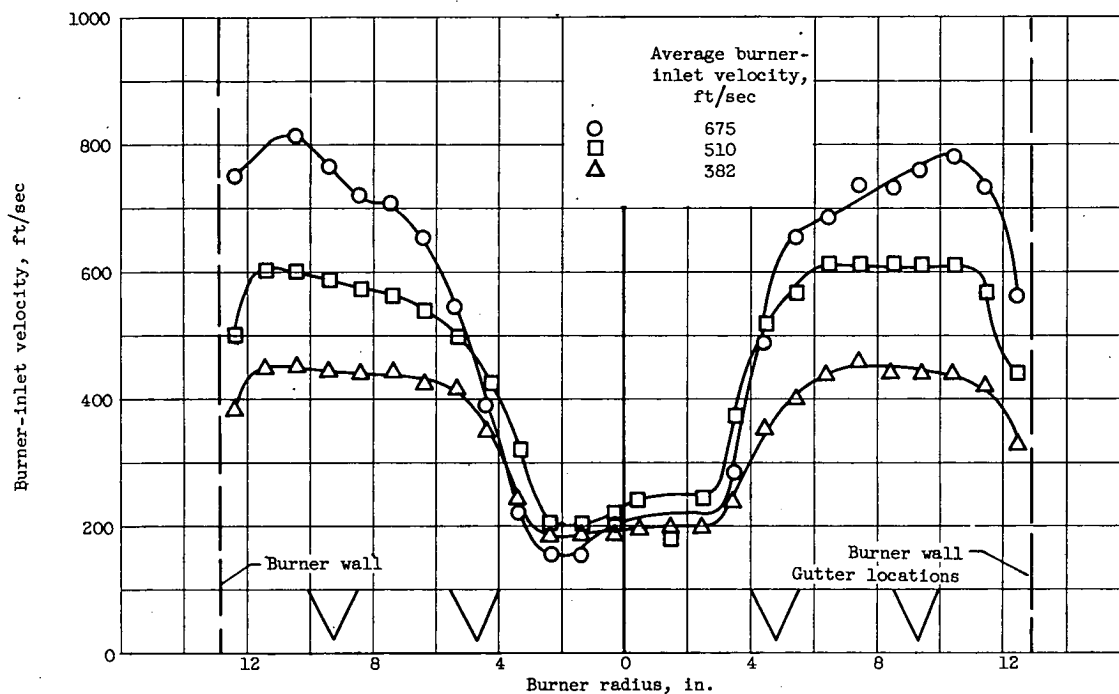
REFERENCES

1. Nakanishi, S., Velie, W. W., and Bryant, L.: An Investigation of Effects of Flame-Holder Gutter Shape on Afterburner Performance. NACA RM E53J14, 1954.
2. Schulze, F. W., Bloomer, H. E., and Miller, R. R.: Altitude-Wind-Tunnel Investigation of Several Afterburner Configurations Having Moderately High Burner-Inlet Velocities. NACA RM E54G22, 1954.
3. Wood, Charles C., and Higgenbotham, James T.: Effects of Diffuser and Center-Body Length on Performance of Annular Diffusers with Constant-Diameter Outer Walls and with Vortex-Generator Flow Controls. NACA RM L54G21, 1954.
4. Ciepluch, Carl C., Velie, Wallace W., and Burley, Richard R.: A Low-Pressure-Loss Short Afterburner for Sea-Level Thrust Augmentation. NACA RM E55D26, 1955.
5. Wood, Charles C.: Preliminary Investigation of the Effects of Rectangular Vortex Generators on the Performance of a Short 1.9:1 Straight-Wall Annular Diffuser. NACA RM L51G09, 1951.
6. Conrad, E. William, Schulze, Frederick W., and Usow, Karl H.: Effect of Diffuser Design, Diffuser-Exit Velocity Profile, and Fuel Distribution on Altitude Performance of Several Afterburner Configurations. NACA RM E53A30, 1953.
7. Conrad, E. William, and Campbell, Carl E.: Altitude Wind Tunnel Investigation of High-Temperature Afterburners. NACA RM E51I07, 1952.
8. Patterson, G. N.: Modern Diffuser Design. Aircraft Eng., vol. X, no. 115, Sept. 1938, pp. 267-673.
9. Mallett, William E., and Harp, James L., Jr.: Performance Characteristics of Several Short Annular Diffusers for Turbojet Engine Afterburners. NACA RM E54B09, 1954.
10. Braithwaite, Willis M., Walker, Curtis L., and Sivo, Joseph N.: Altitude Evaluation of Several Afterburner Design Variables on a J47-GE-17 Turbojet Engine. NACA RM E53F10, 1953.
11. Renas, P. E., Harvey, R. W., Sr., and Jansen, E. T.: Altitude Starting Characteristics of an Afterburner with Autoignition and Hot-Streak Ignition. NACA RM E53B02, 1953.

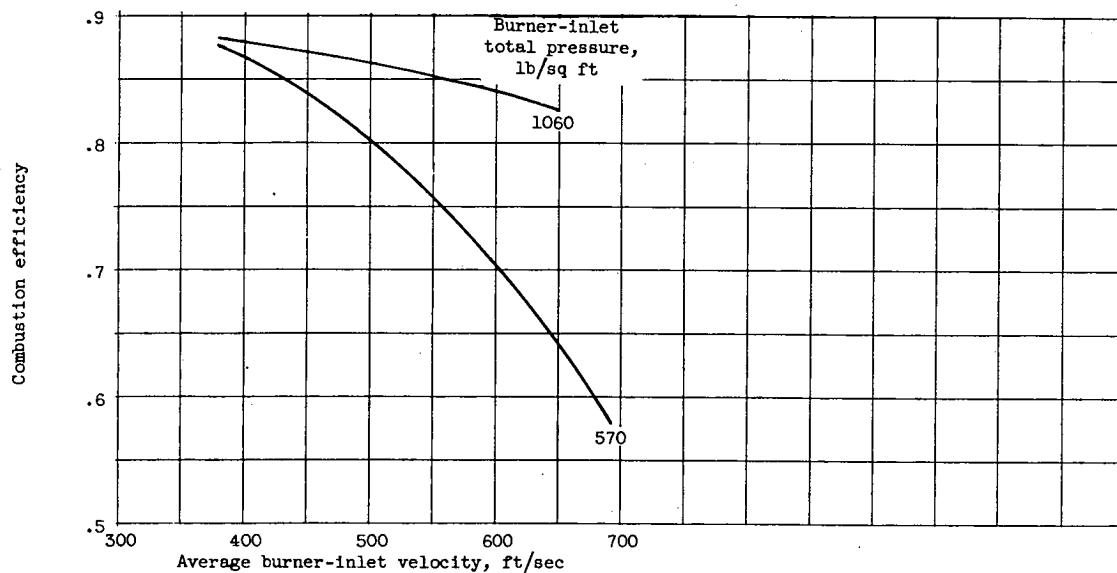
11. Renas, P. E., Harvey, R. W., Sr., and Jansen, E. T.: Altitude Starting Characteristics of an Afterburner with Autoignition and Hot-Streak Ignition. NACA RM E53B02, 1953.
12. Fleming, W. A., Conrad, E. William, and Young, A. W.: Experimental Investigation of Tail-Pipe-Burner Design Variables. NACA RM E50K22, 1951.
13. Thorman, H. Carl, and Campbell, Carl E.: Altitude-Wind-Tunnel Investigation of Tail-Pipe Burner with Converging Conical Burner Section on J35-A-5 Turbo-Jet Engine. NACA RM E9I16, 1950.
14. Fuels and Combustion Research Division: Adaptation of Combustion Principles to Aircraft Propulsion. Vol. I - Basic Considerations in the Combustion of Hydrocarbon Fuels with Air. NACA RM E54I07, 1955.
15. Conrad, E. William, Bloomer, Harry E., and Sobolewski, Adam E.: Altitude Operational Characteristics of a Prototype Model of the J47D (RX1-1 and RX1-3) Turbojet Engines with Integrated Electronic Control. NACA RM E51E08, 1952.
16. Gerrish, Harold C., Meem, J. Lawrence, Jr., Scadron, Marvin D., and Colnar, Anthony: The NACA Mixture Analyzer and Its Application to Mixture-Distribution Measurement in Flight. NACA TN 1238, 1947.
17. Jansen, Emmert T., Velie, Wallace W., and Wilsted, H. Dean: Experimental Investigation of the Effect of Fuel-Injection-System Design Variables on Afterburner Performance. NACA RM E53K16, 1954.
18. Longwell, John P., and Weiss, Malcolm A.: Mixing and Distribution of Liquids in High-Velocity Air Streams. Ind. and Eng. Chem., vol. 45, no. 3, Mar. 1953, pp. 667-677.
19. Johnson, LaVern A., and Meyer, Carl L.: Altitude Performance Characteristics of Turbojet-Engine Tail-Pipe Burner with Variable-Area Exhaust Nozzle Using Several Fuel Systems and Flame Holders. NACA RM E50F28, 1950.
20. Trout, Arthur M., and Wentworth, Carl B.: Altitude Investigation of a 20-Inch Ram-Jet Combustor with a Rich Inner Zone of Combustion for Improved Low-Temperature-Ratio Operation. NACA RM E52L26, 1953.
21. Henzel, James G., Jr., and Wentworth, Carl B.: Free-Jet Investigation of 20-Inch Ram-Jet Combustor Utilizing High-Heat-Release Pilot Burner. NACA RM E53H14, 1953.
22. Dangle, E. E., Friedman, Robert, and Cervenka, A. J.: Analytical and Experimental Studies of a Divided-Flow Ram-Jet Combustor. NACA RM E53K04, 1954.
23. Huntley, S. C., Auble, Carmon M., and Useller, James W.: Altitude Performance Investigation of a High-Temperature Afterburner. NACA RM E53D22, 1953.
24. Chelko, Louis J.: Penetration of Liquid Jets into a High-Velocity Air Stream. NACA RM E50F21, 1950.
25. Callaghan, Edmund E., and Ruggeri, Robert S.: Investigation of the Penetration of an Air Jet Directed Perpendicularly to an Air Stream. NACA TN 1615, 1948.

26. Huntley, S. C., and Wilsted, H. D.: Altitude Performance Investigation of Two Flame-Holder and Fuel-System Configurations in Short Afterburner. NACA RM E52B25, 1952.
27. Nickolson, H. M., and Field, J. P.: Some Experimental Techniques for the Investigation of the Mechanism of Flame Stabilization in the Wakes of Bluff Bodies. Third Symposium on Combustion and Flame and Explosion Phenomena, The Williams & Wilkins Co. (Baltimore), 1949, pp. 44-68.
28. Williams, Glenn C.: Basic Studies on Flame Stabilization. Jour. Aero. Sci., vol. 16, no. 12, Dec. 1949, pp. 714-722.
29. Younger, George G., Gabriel, David S., and Mickelsen, William R.: Experimental Study of Isothermal Wake-Flow Characteristics of Various Flame-Holder Shapes. NACA RM E51KO7, 1952.
30. Renas, Paul E., and Jansen, Emmert T.: Effect of Flame-Holder Design on Altitude Performance of Louvered-Liner Afterburner. NACA RM E53H15, 1953.
31. Henzel, James G., Jr., and Bryant, Lively: Investigation of Effect of Number and Width of Annular Flame-Holder Gutters on Afterburner Performance. NACA RM E54C30, 1954.
32. Lundin, Bruce T., Dowman, Harry W., and Gabriel, David S.: Experimental Investigation of Thrust Augmentation of a Turbojet Engine at Zero Ram by Means of Tail-Pipe Burning. NACA RM E6J21, 1947.
33. Braithwaite, Willis M., Renas, Paul E., and Jansen, Emmert T.: Altitude Investigation of Three Flame-Holder and Fuel-Systems Configurations in a Short Converging Afterburner on a Turbojet Engine. NACA RM E52G29, 1952.
34. Hawthorne, W. R., and Cohen, H.: Pressure Losses and Velocity Changes Due to Heat Release and Mixing in Frictionless, Compressible Flow. Rep. No. E.3997, British R.A.E., Jan. 1944.
35. Sterbentz, William H.: Analysis and Experimental Observation of Pressure Losses in Ram-Jet Combustion Chambers. NACA RM E9H19, 1949.
36. Useller, James W., Braithwaite, Willis M., and Rudey, Carl J.: Influence of Combustion-Chamber Length on Afterburner Performance. NACA RM E54E06, 1954.
37. Harp, James L., Jr., Velie, Wallace W., and Bryant, Lively: Investigation of Combustion Screech and a Method of Its Control. NACA RM E53L24b, 1954.
38. Lewis Laboratory Staff: A Summary of Preliminary Investigations into the Characteristics of Combustion Screech in Ducted Burners. NACA RM E54B02, 1954.
39. Bragdon, Thomas A., Lewis, George D., and King, Charles H.: Interim Report on Experimental Investigation of High Frequency Oscillations in Ramjet Combustion Chambers. M.I.T. Meteor Rep. UAC-53, Res. Dept., United Aircraft Corp., Oct. 1951. (BuOrd Contract NOrd 9845.)
40. Kaskan, W. E., and Noreen, A. E.: High-Frequency Oscillations of a Flame Held by a Bluff Body. A.S.M.E. Trans., vol. 77, no. 6, Aug. 1955, pp. 855-891; discussion, pp. 891-895.

41. Newton, R. T., and Truman, J. C.: An Approach to the Problem of Screech in Ducted Burners. General Eng. Lab., General Electric Co., Schenectady (N.Y.), Mar. 12, 1954.
42. Hall, Eldon W., and Wilcox, E. Clinton: Theoretical Comparison of Several Methods of Thrust Augmentation for Turbojet Engines. NACA Rep. 992, 1950. (Supersedes NACA RM E8H11.)
43. Useller, James W., and Povolny, John H.: Experimental Investigation of Turbojet-Engine Thrust Augmentation by Combined Compressor Coolant Injection and Tail-Pipe Burning. NACA RM E51H16, 1951.
44. Useller, James W., Harp, James L., Jr., and Fenn, David B.: Turbojet-Engine Thrust Augmentation at Altitudes by Combined Ammonia Injection into the Compressor Inlet and Afterburning. NACA RM E52L19, 1953.
45. Kapp, N. M., Snow, B., and Wohl, K.: The Effect of Water Vapor on the Normal Burning Velocity and on the Stability of Butane-Air Flames Burning above Tubes in Free Air. Meteor Rep. UAC-30, United Aircraft Corp., Nov. 1948. (U. S. Navy, BuOrd Contract NOrd-9845 with M.I.T.)
46. Tower, Leonard K.: Effect of Water Vapor on Combustion of Magnesium-Hydrocarbon Slurry Fuels in Small-Scale Afterburner. NACA RM E52H25, 1952.
47. O'Neal, Cleveland, Jr.: Effect of Ammonia Addition on Limits of Flame Propagation for Isooctane-Air Mixtures at Reduced Pressures and Elevated Temperatures. NACA TN 3446, 1955.



(a) Velocity profiles.



(b) Combustion efficiency at fuel-air ratio of 0.047.

Figure 158. - Effect of velocity in region of flameholders on afterburner performance.

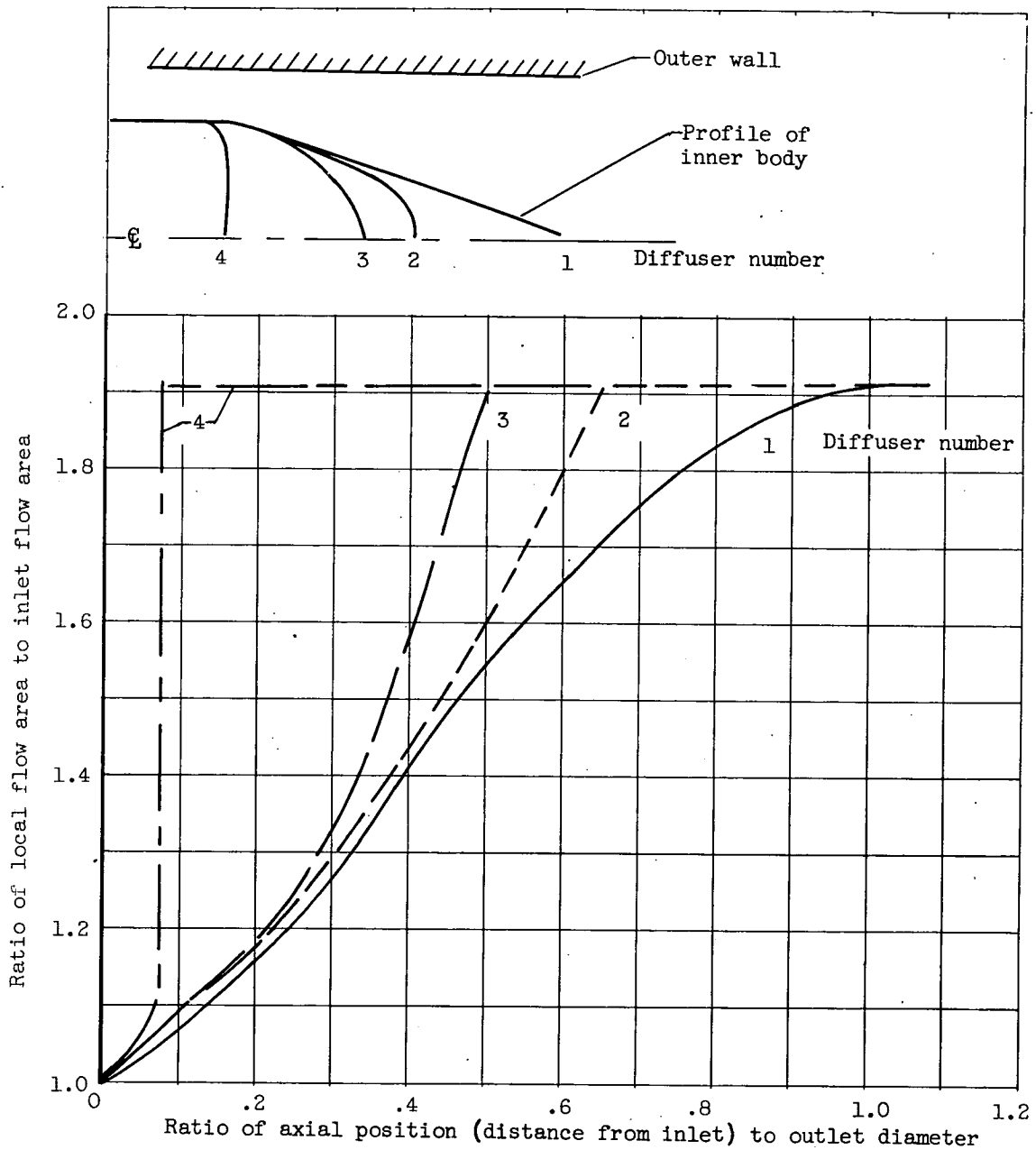
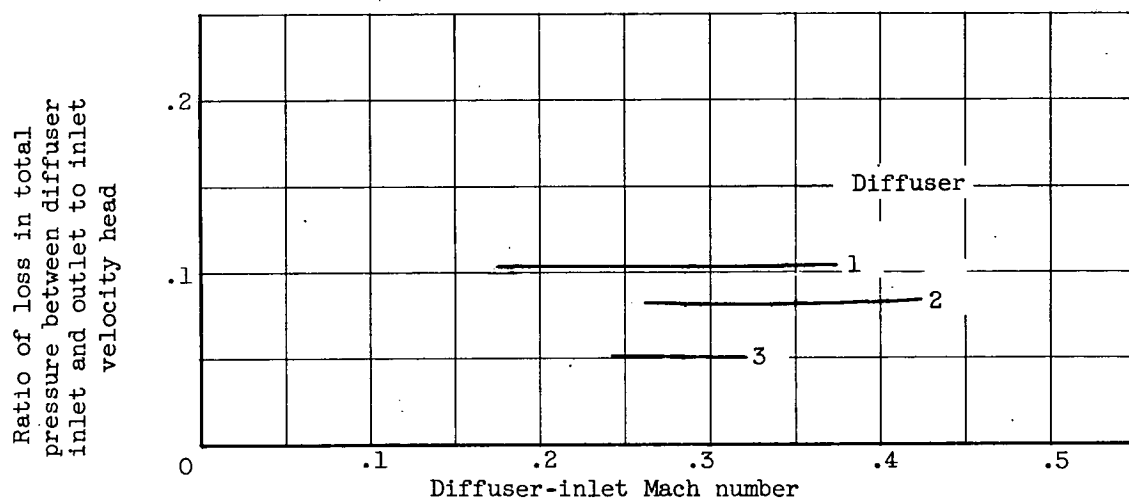
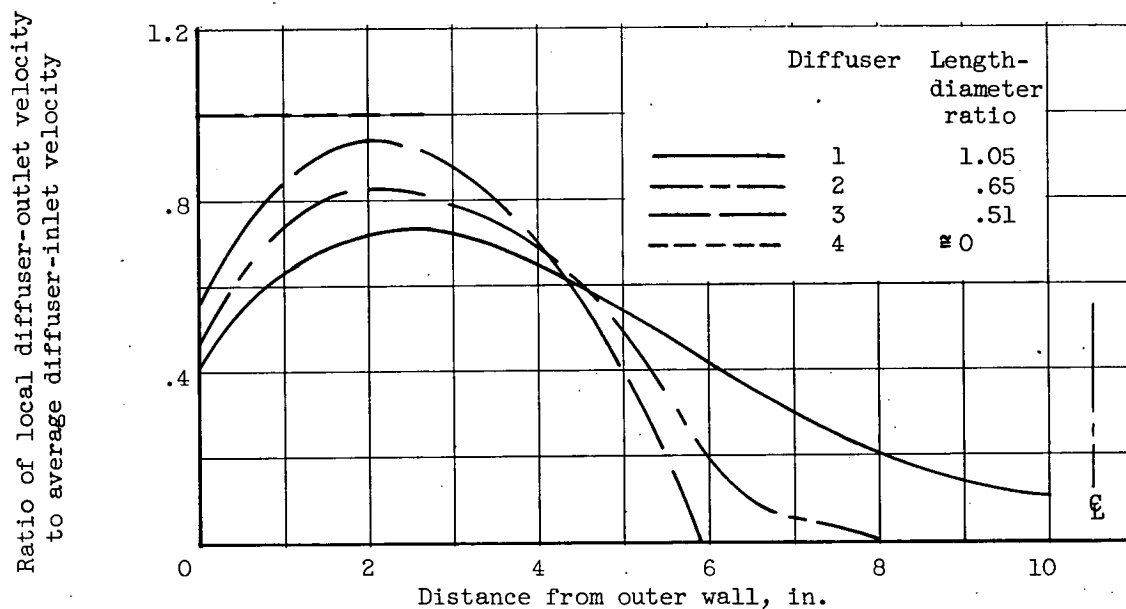


Figure 159. - Geometric relations of diffusers investigated to determine length effects.



(a) Pressure loss.



(b) Velocity profile.

Figure 160. - Performance of four diffusers of different length.

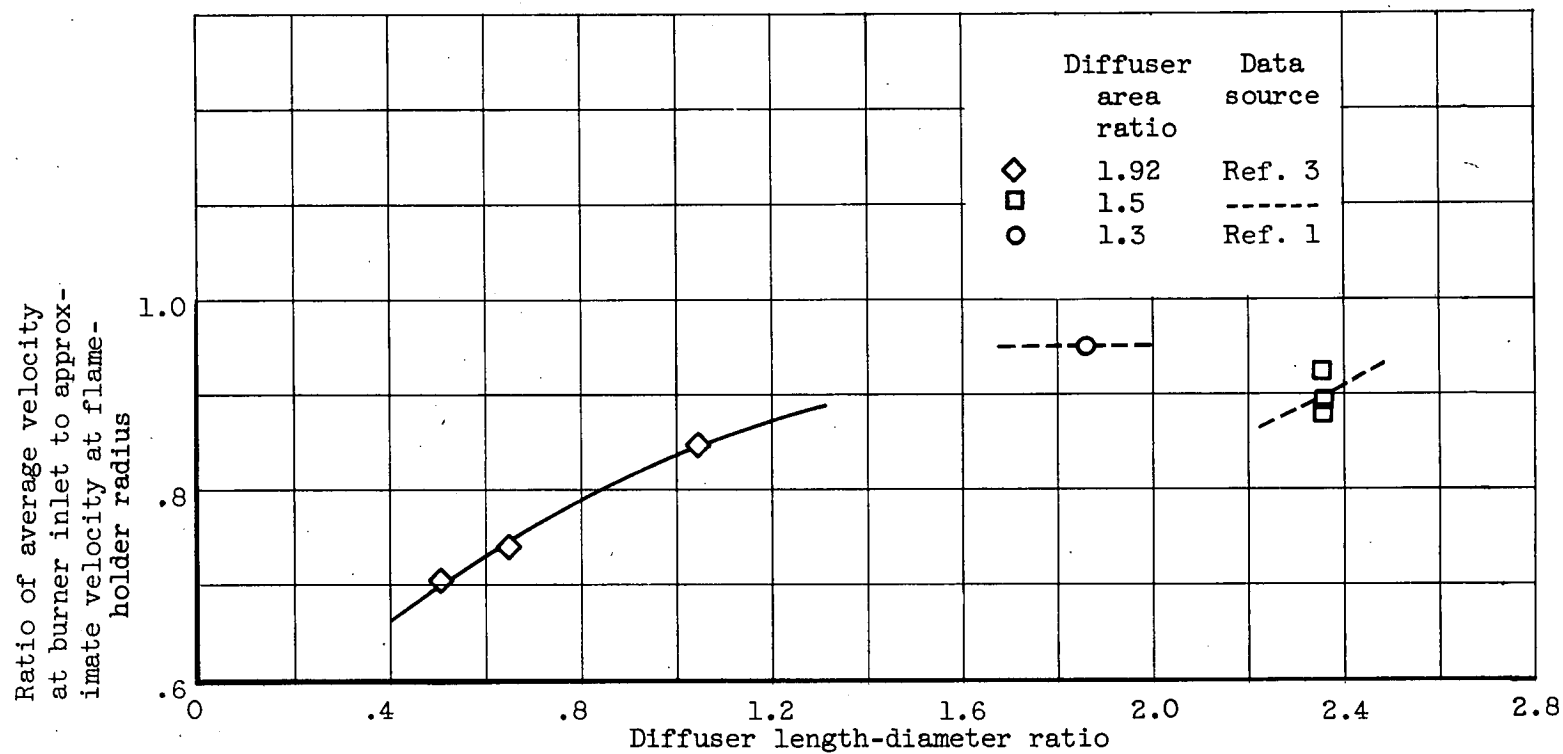
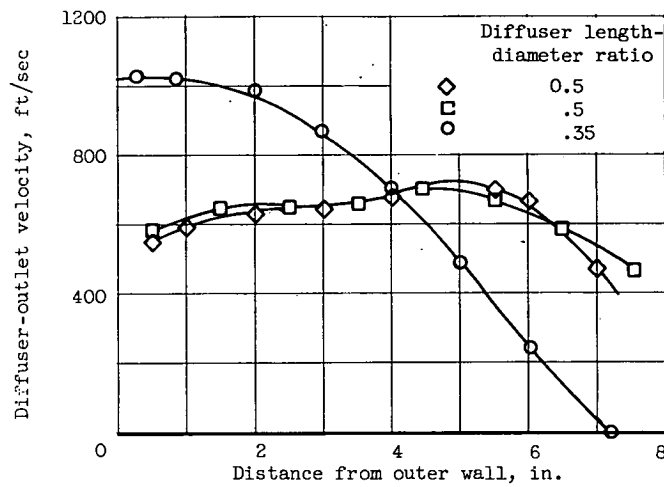
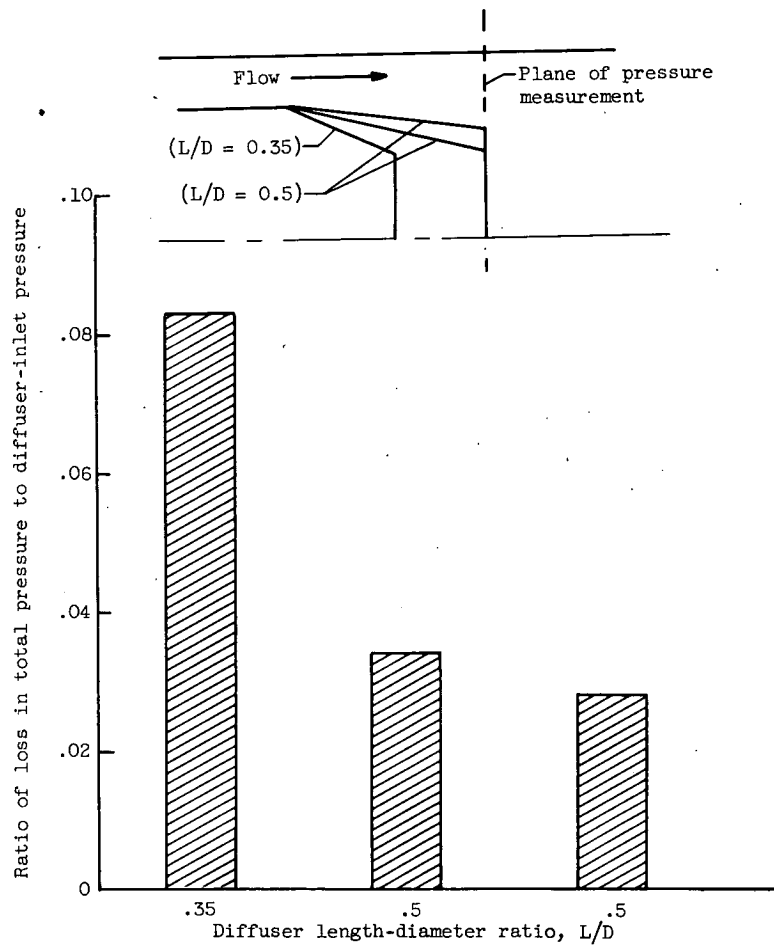


Figure 161. - Effect of diffuser length-diameter ratio on velocity near flameholder.

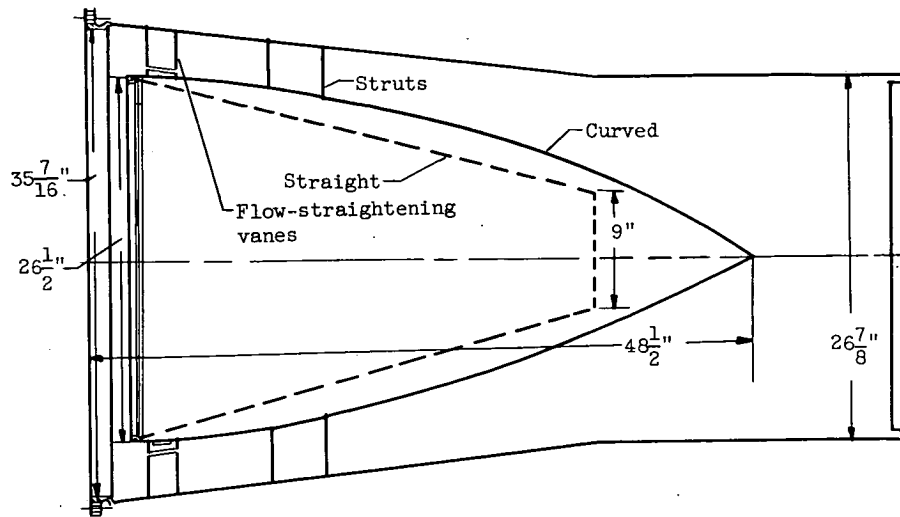


(a) Velocity profiles.

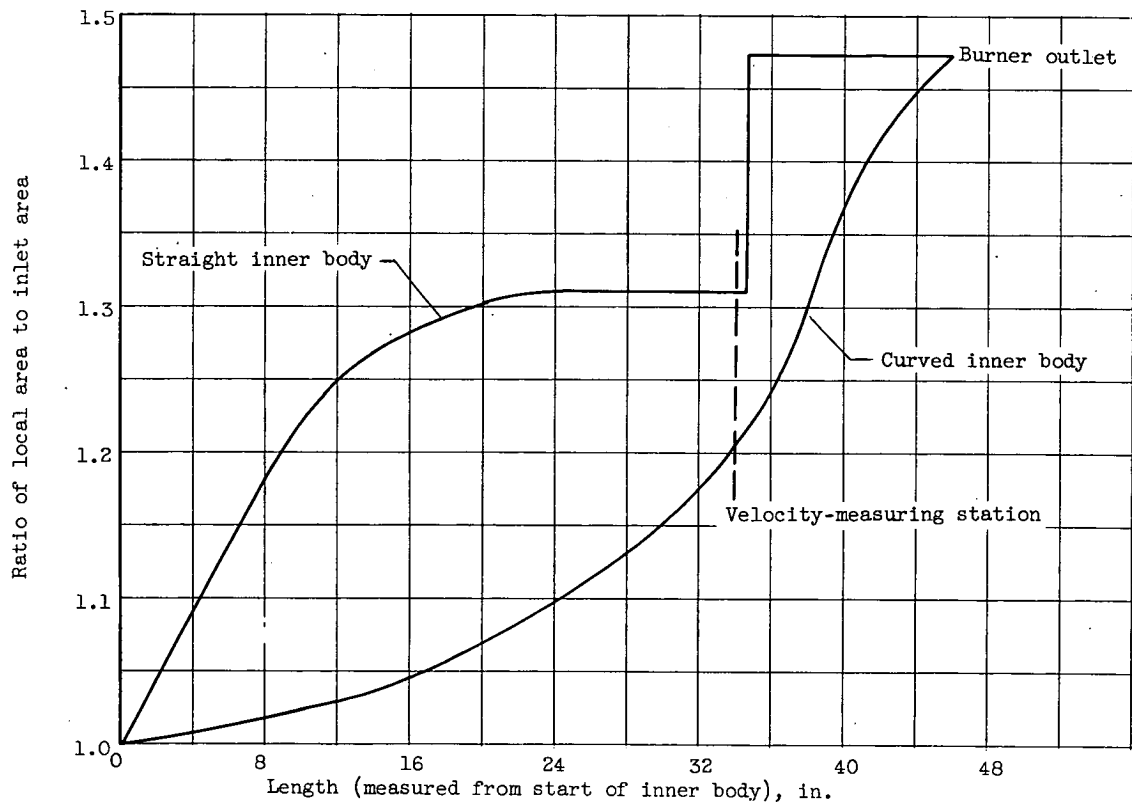


(b) Pressure loss.

Figure 162. - Effect of length on diffuser performance.



(a) Diffuser configurations.



(b) Diffuser area variation.

Figure 163. - Diffusers used in investigation of inner-body shape.

Ratio of local velocity to maximum velocity

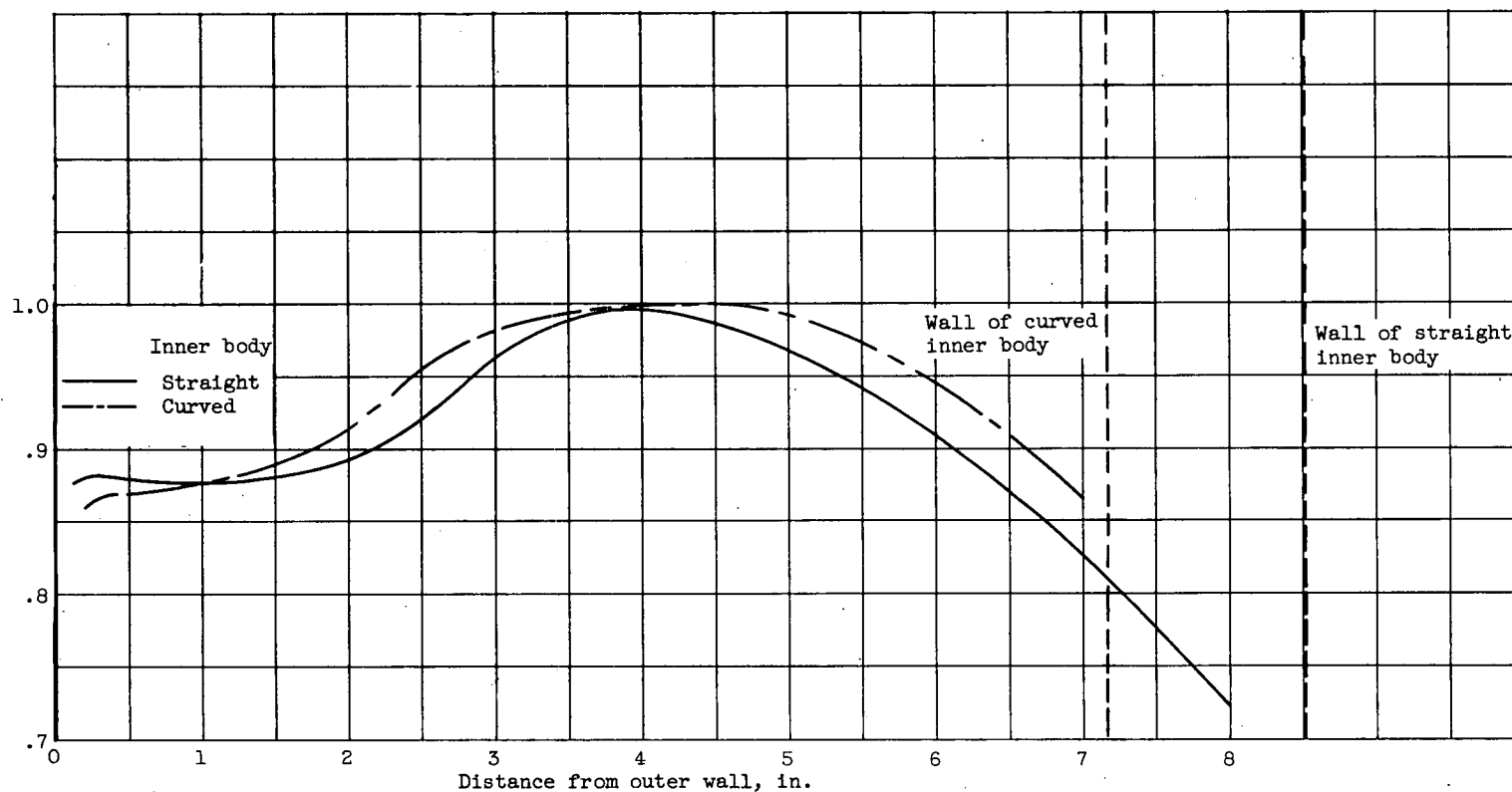
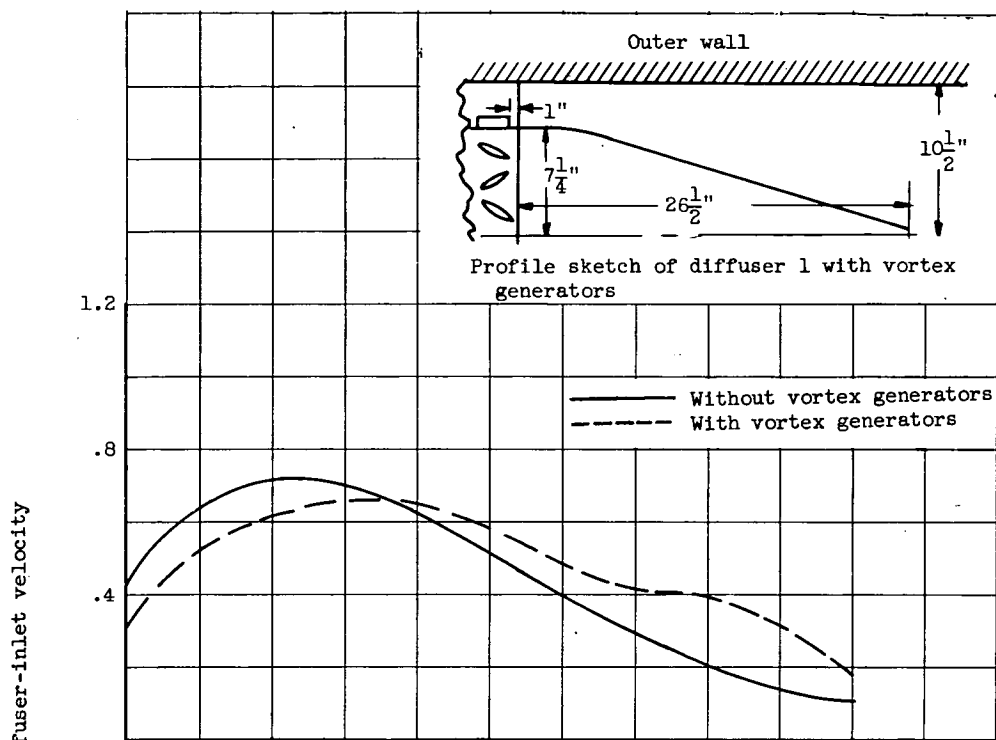


Figure 164. - Radial velocity profiles 34 inches from diffuser inlet with two inner-body shapes.

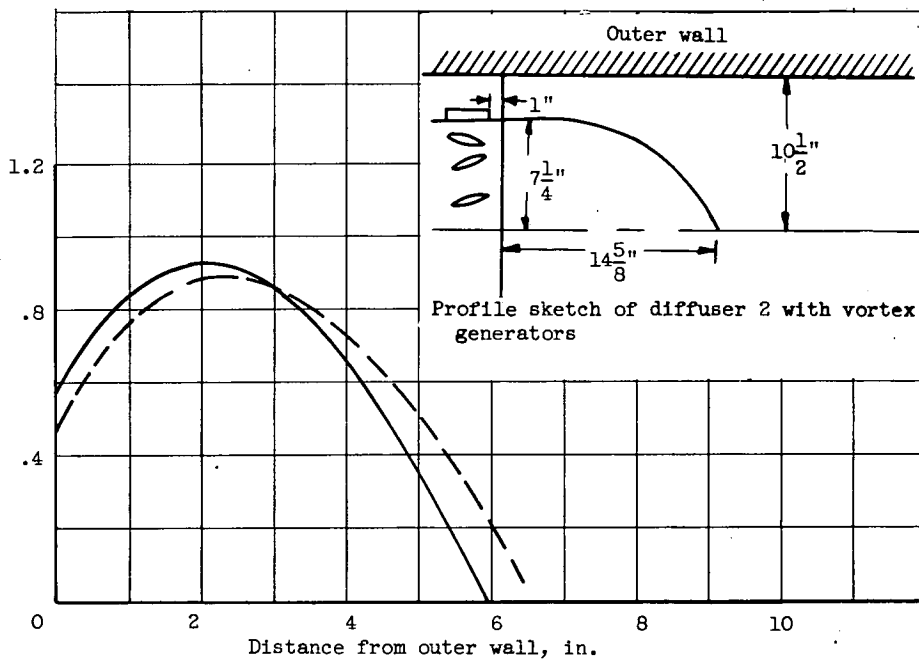
350

CONFIDENTIAL

NACA RM E55G28



(a) Diffuser 1.



(b) Diffuser 2.

Figure 165. - Effect of vortex generators on diffuser-outlet velocity profiles.

CONFIDENTIAL

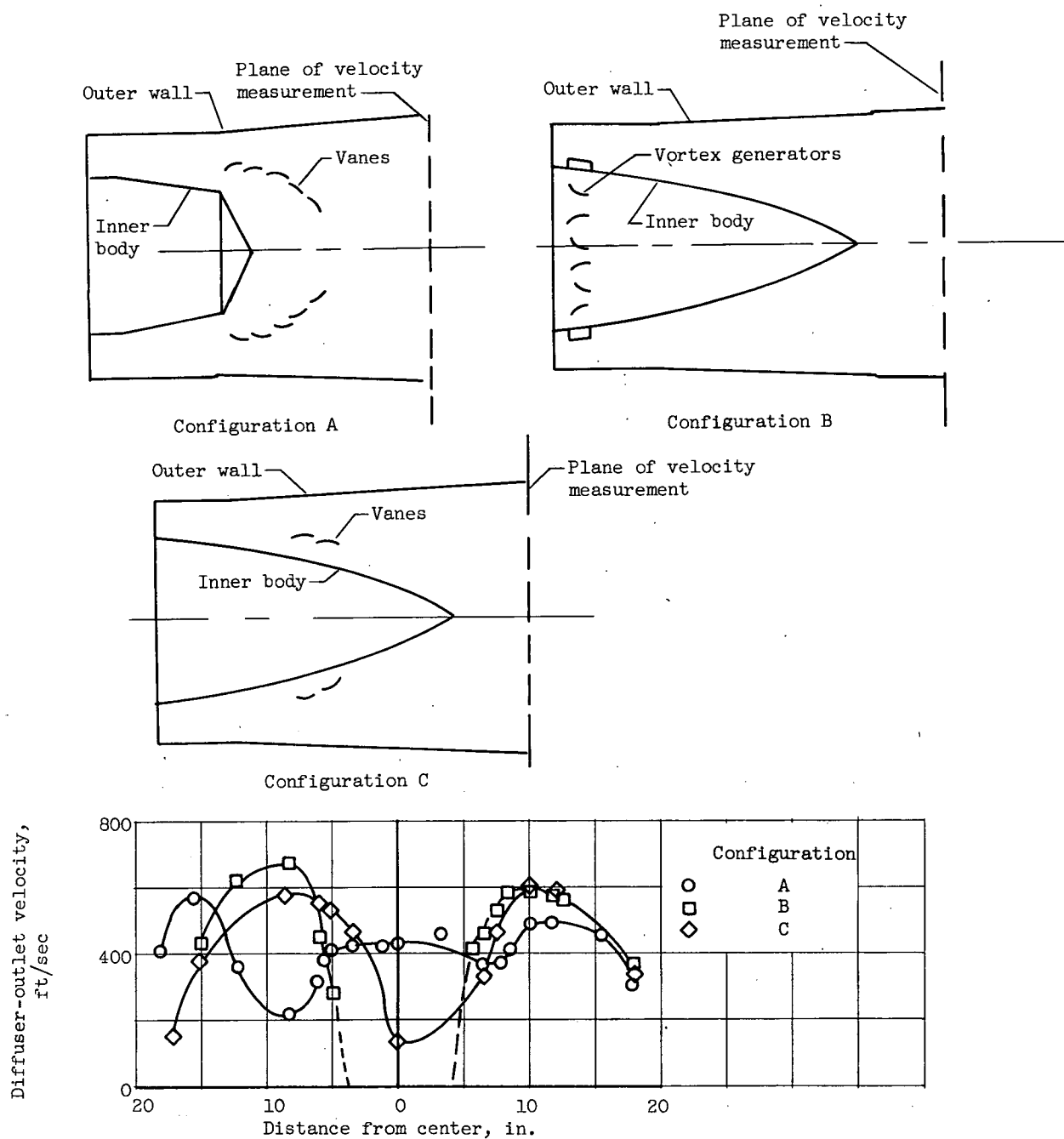


Figure 166. - Effect of annular vanes on diffuser-outlet velocity profiles.

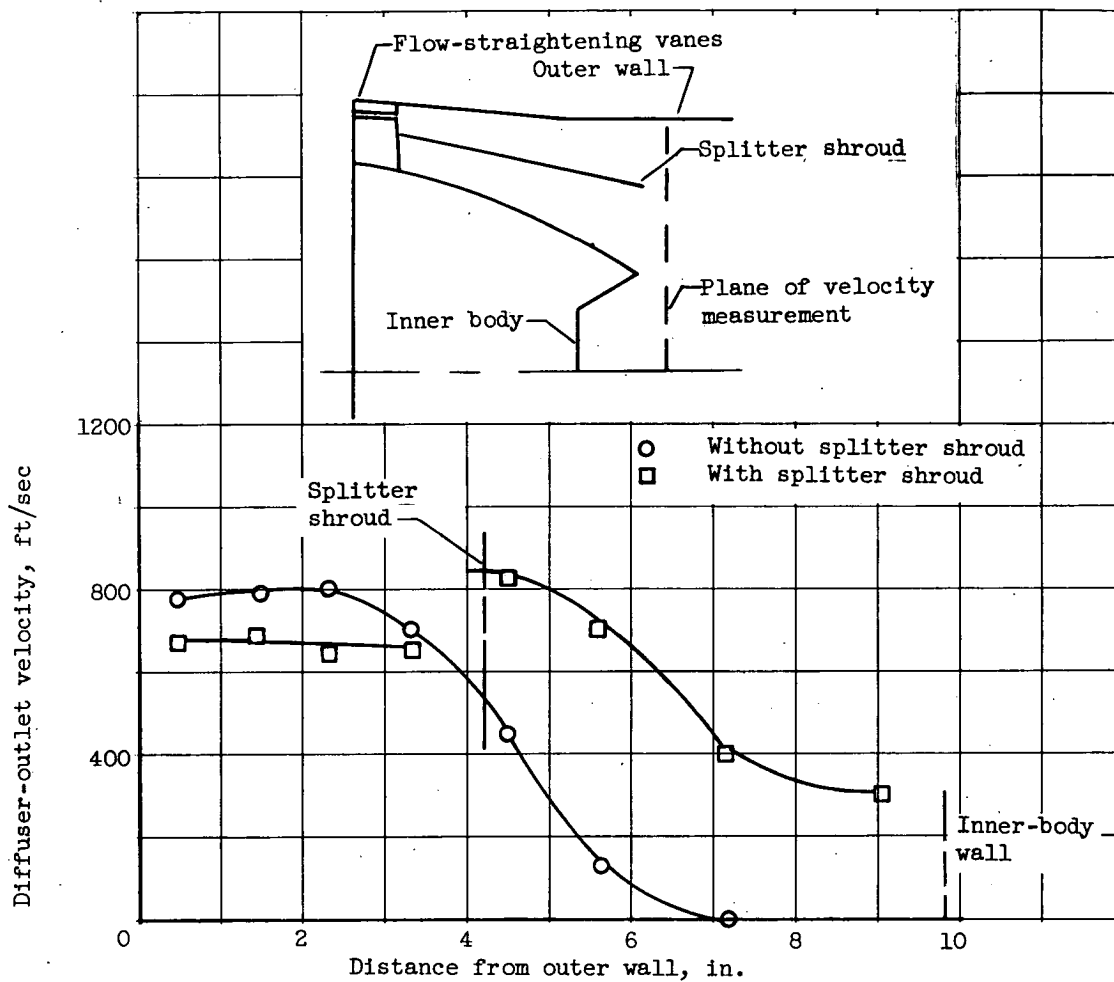
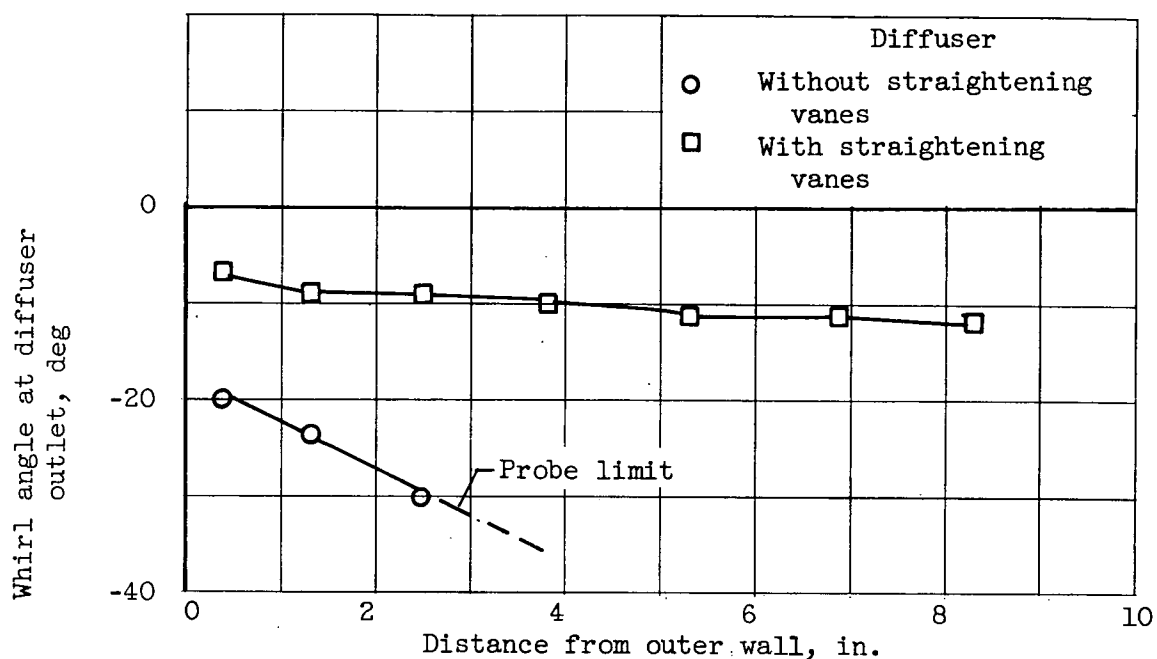
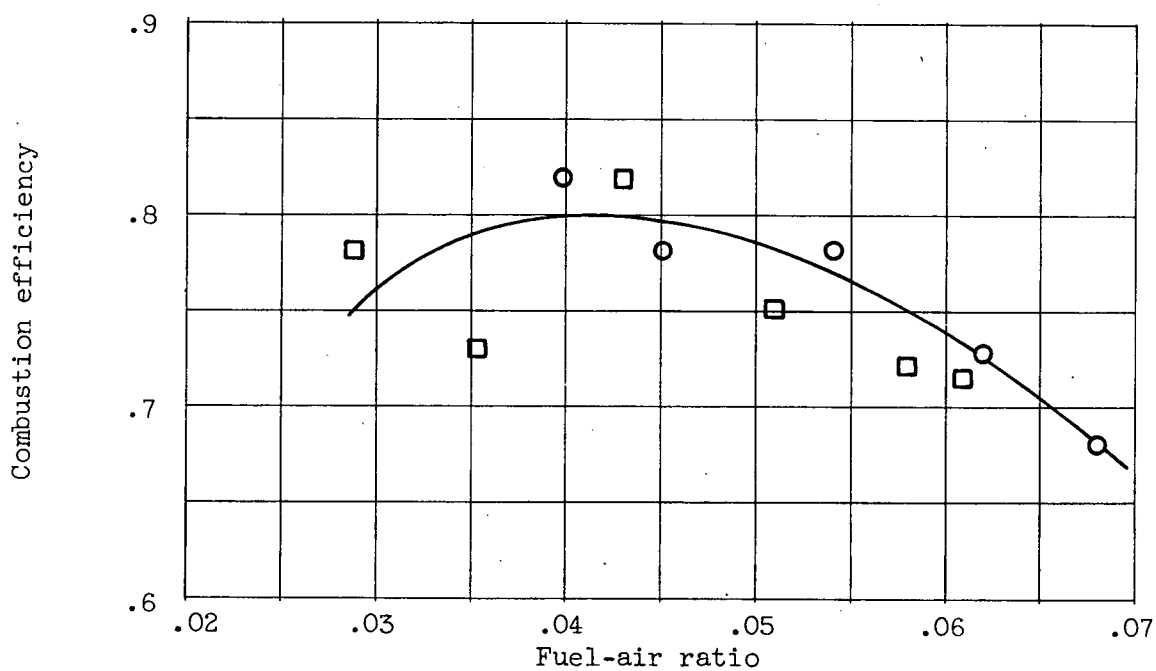


Figure 167. - Effect of splitter shroud on diffuser-outlet velocity profile.



(a) Representative diffuser-outlet whirl angles.



(b) Effect of diffuser-outlet whirl on combustion efficiency at altitude.

Figure 168. - Effect of diffuser-outlet whirl on afterburner performance.

REF ID: A55713

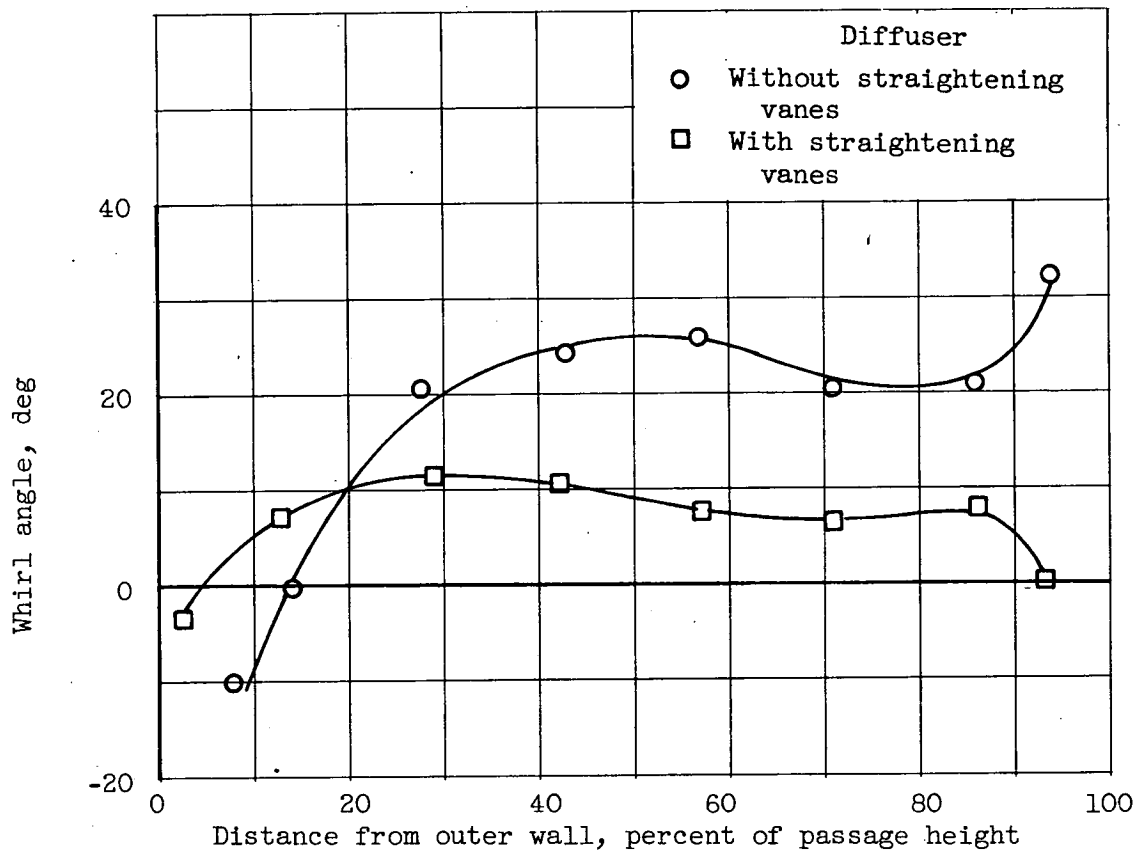


Figure 169. - Effect of straightening vanes on whirl angles near diffuser inlet.

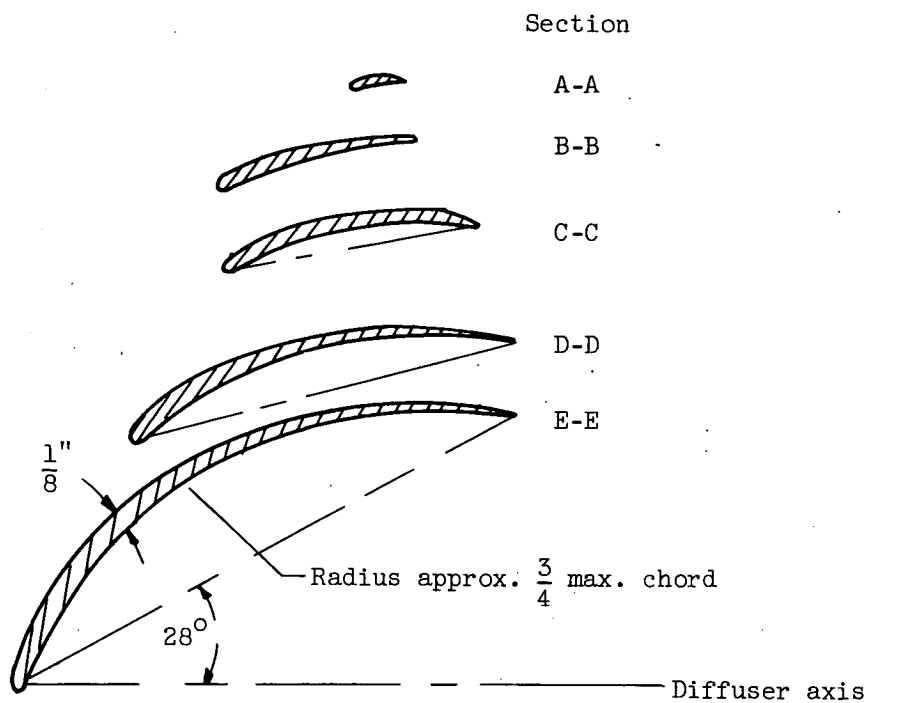


Figure 170: - Typical flow-straightening vane at turbine outlet.

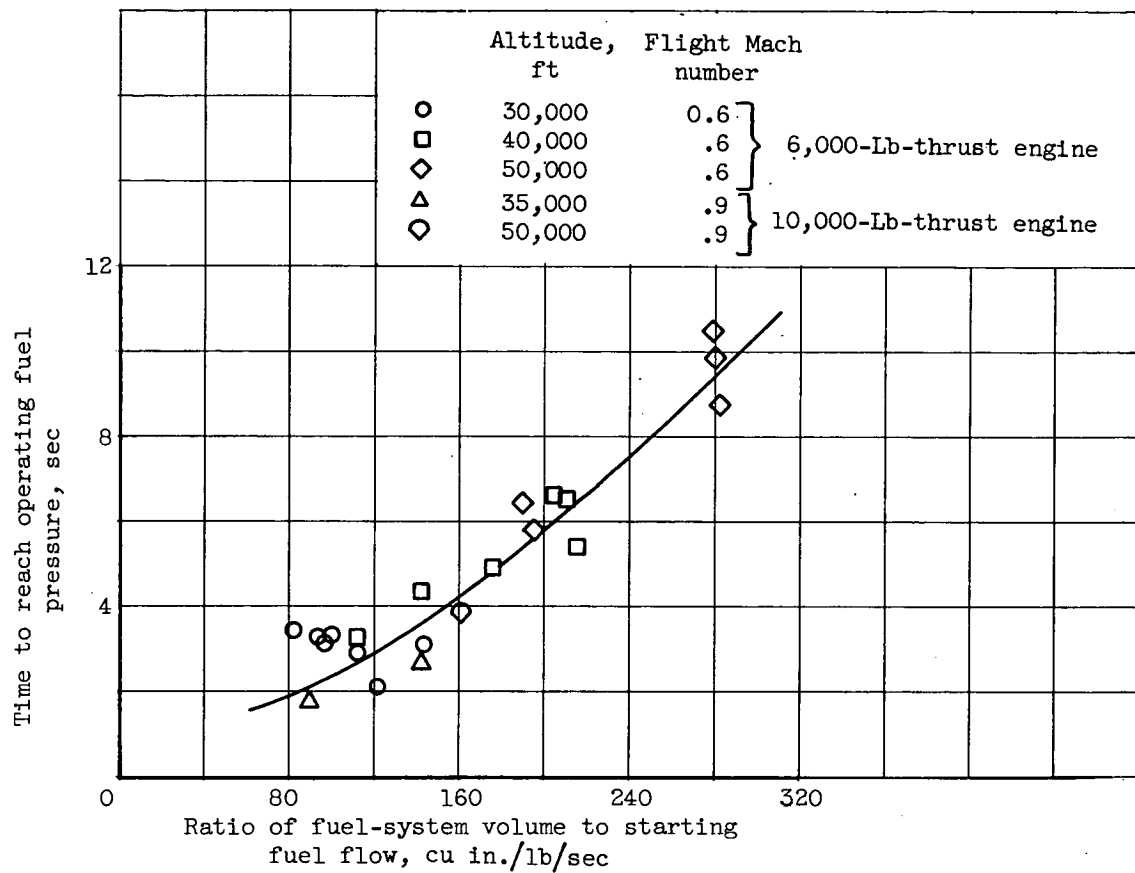


Figure 171. - Time required to reach operating fuel-manifold pressure for an afterburner start.

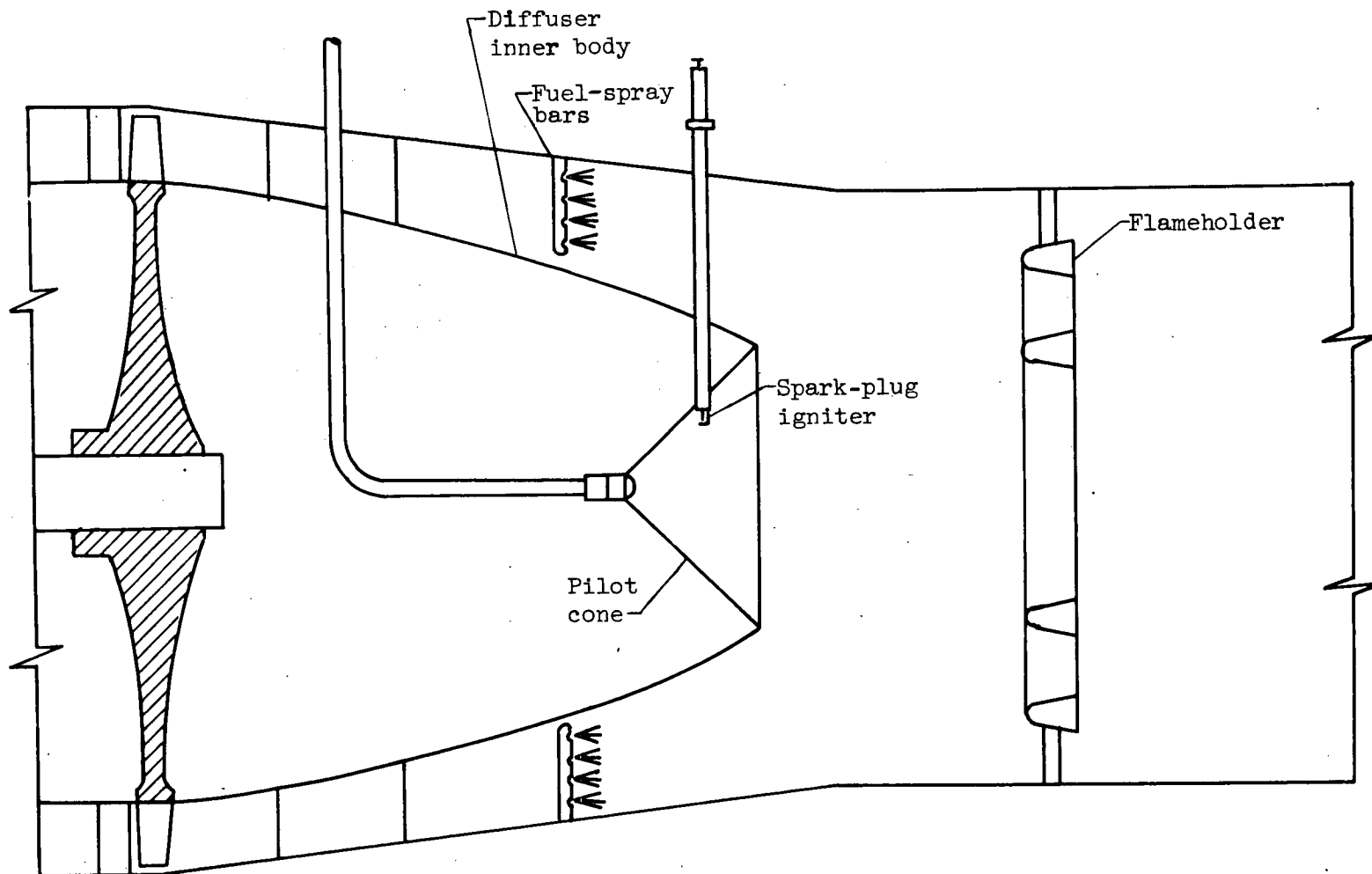


Figure 172. - Typical spark-plug igniter installation in afterburner.

358
CONFIDENTIAL

NACA RM E55G28

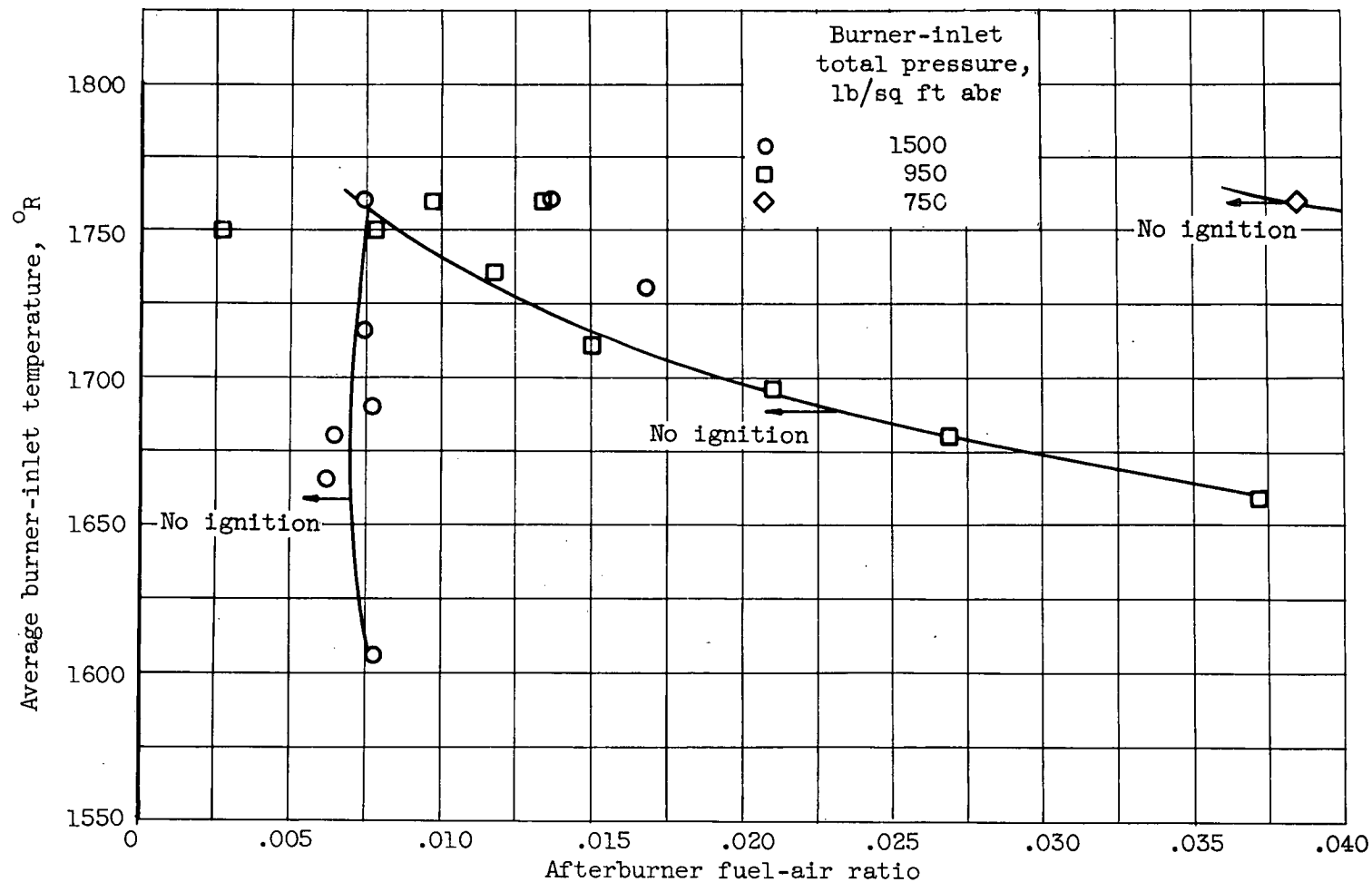


Figure 173. - Effect of afterburner-inlet pressure and temperature on limits of spontaneous ignition. Fuel, MIL-F-5624, grade JP-3, with Reid vapor pressure of 7 pounds per square inch.

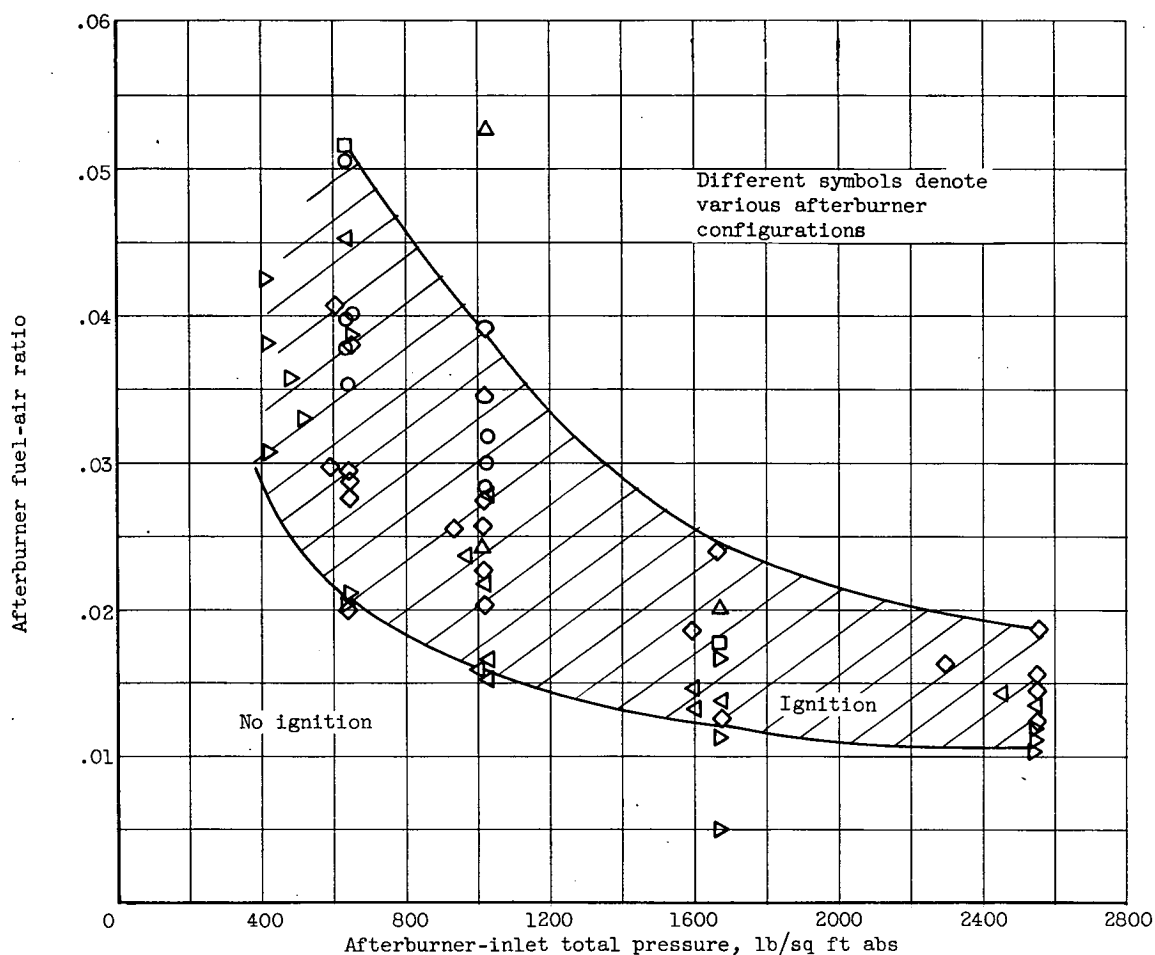


Figure 174. - Minimum afterburner fuel-air ratios at which autoignition occurred with several afterburner configurations. Fuel, MIL-F-5624, grade JP-3; burner-inlet temperature, 1710° to 1760° R.

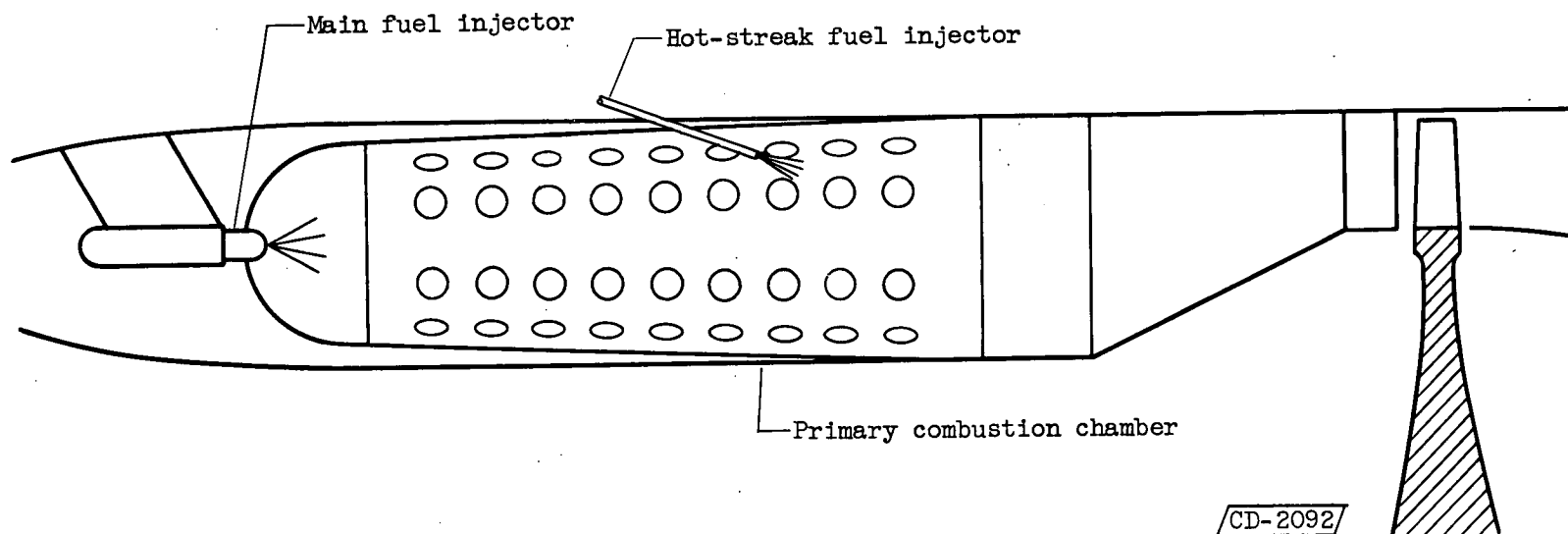
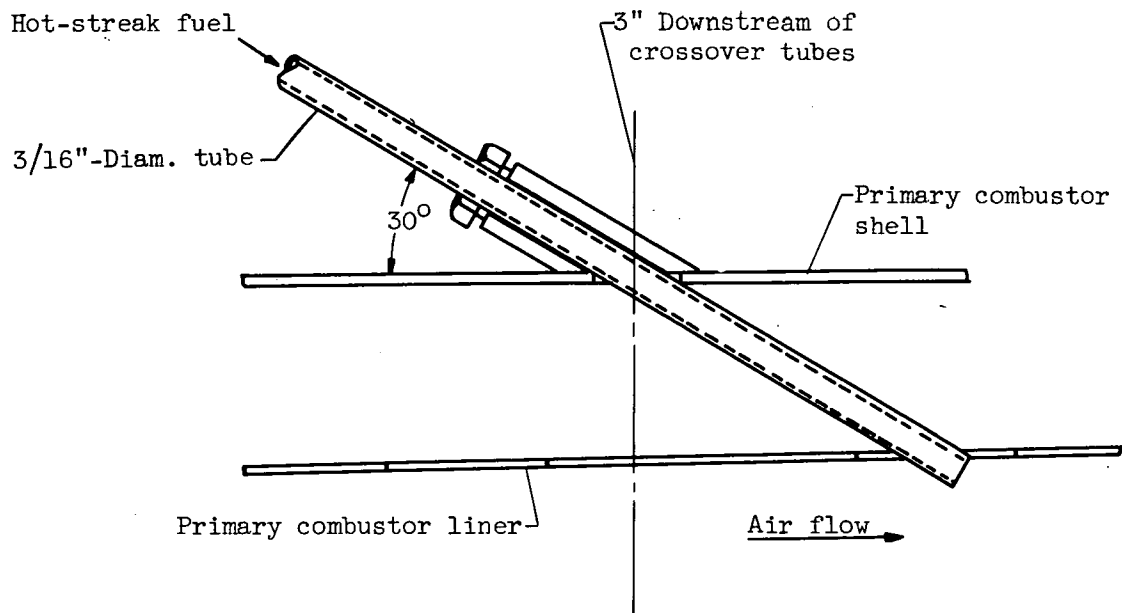
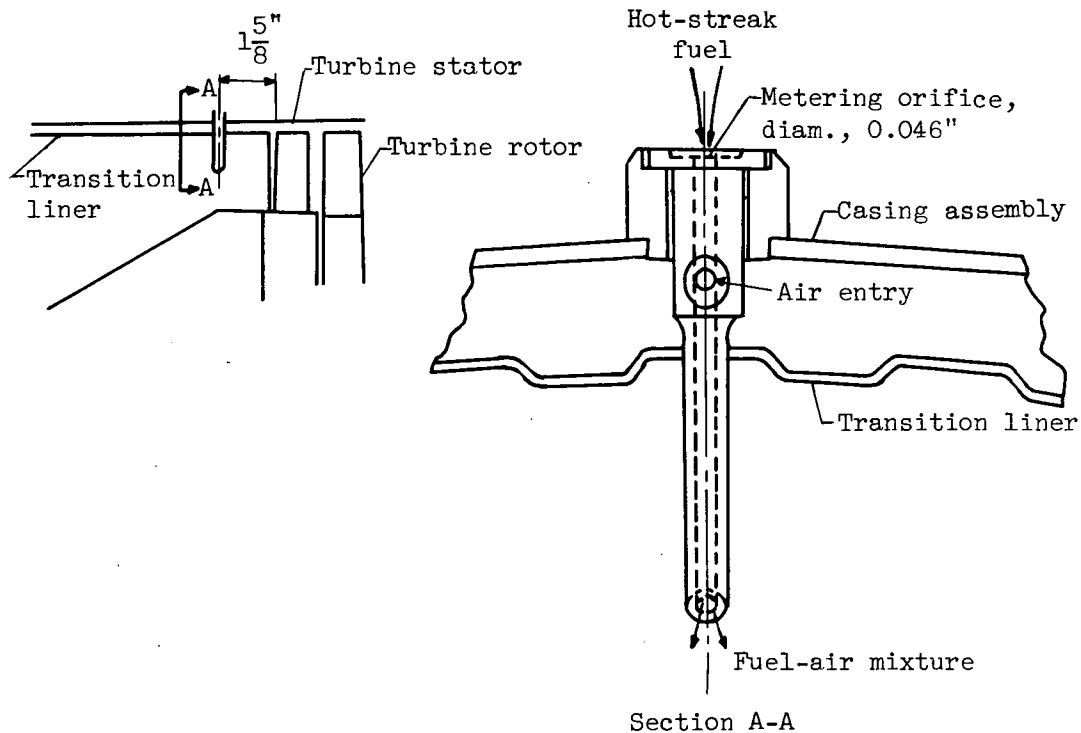


Figure 175. - Schematic diagram of hot-streak ignition system.

CONFIDENTIAL



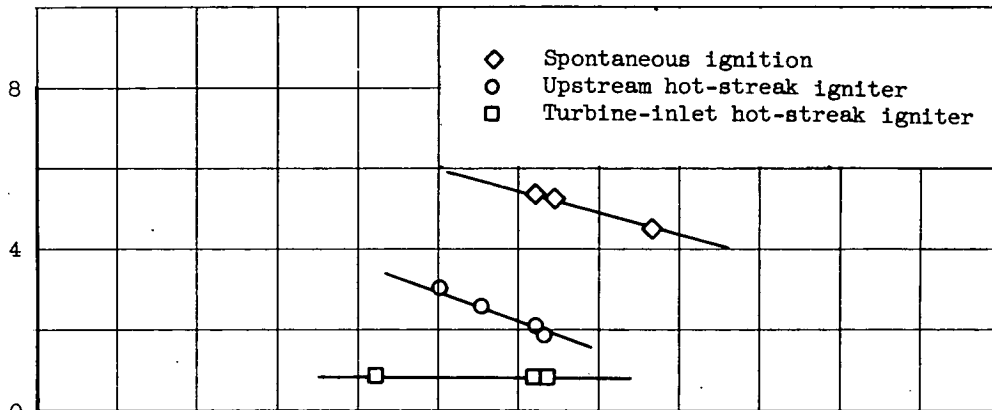
(a) Igniter A.



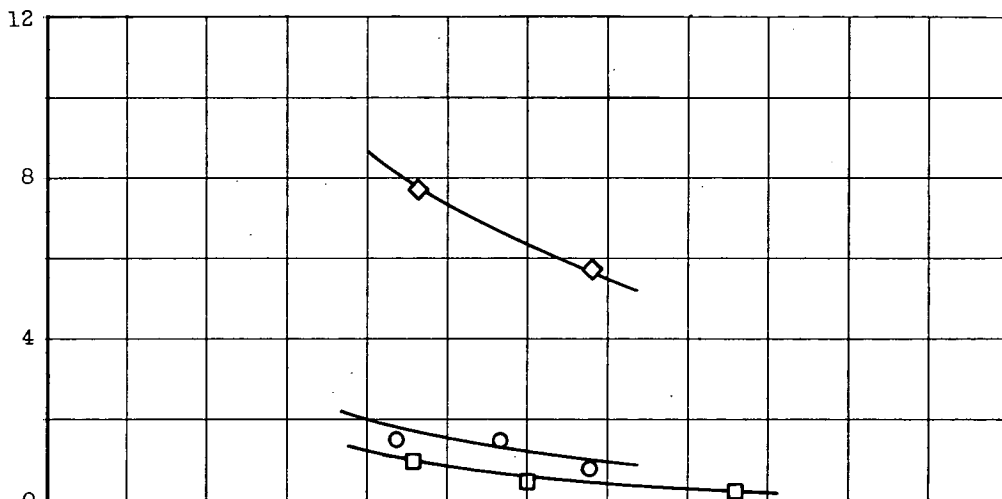
(b) Igniter B.

Figure 176. - Details of two hot-streak igniters.

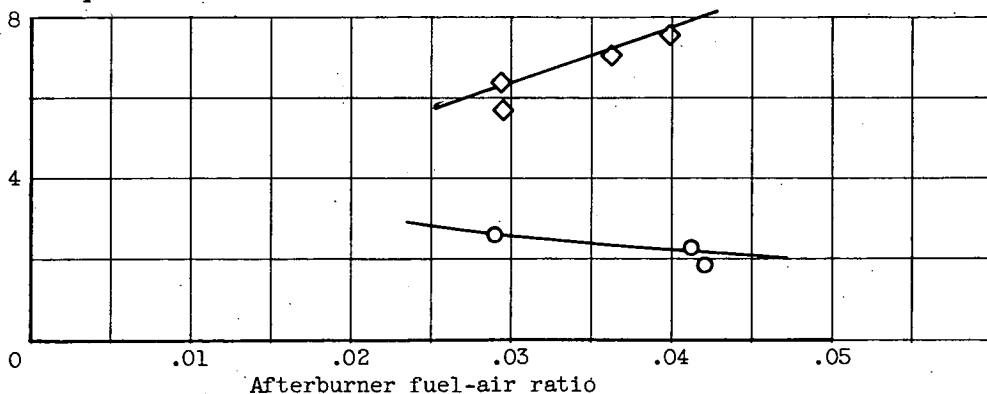
Time for ignition after obtaining set manifold pressure, sec



(a) Altitude, 30,000 feet; burner-inlet total pressure, 1720 pounds per square foot absolute.



(b) Altitude, 40,000 feet; burner-inlet total pressure 1090 pounds per square foot absolute.



(c) Altitude, 50,000 feet; burner-inlet total pressure, 660 pounds per square foot absolute.

Figure 177. - Effect of altitude on time for afterburner ignition. Flight Mach number, 0.6.

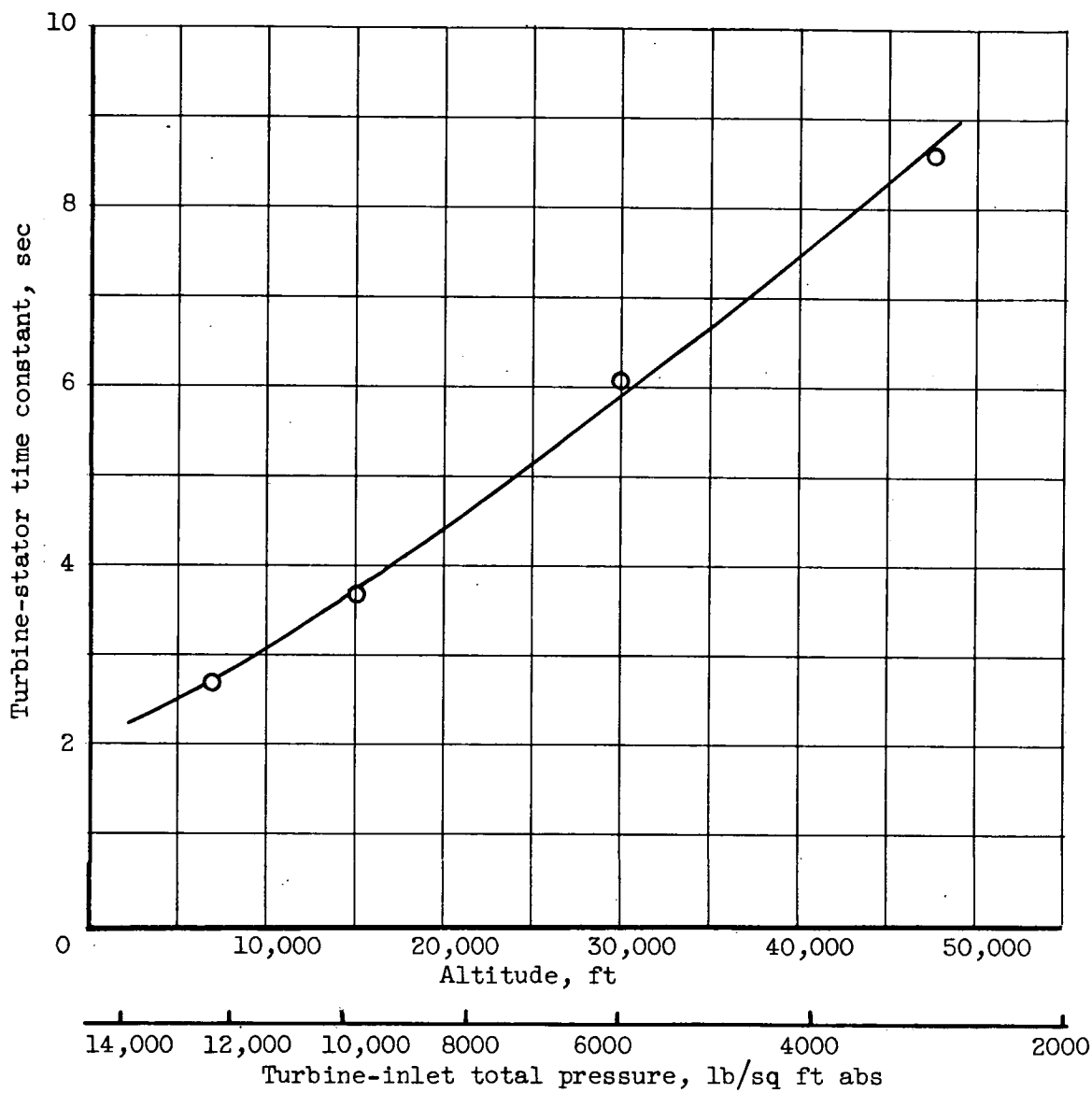


Figure 178. - Variation of turbine-stator time constant with altitude.
Flight Mach number, 0.8.

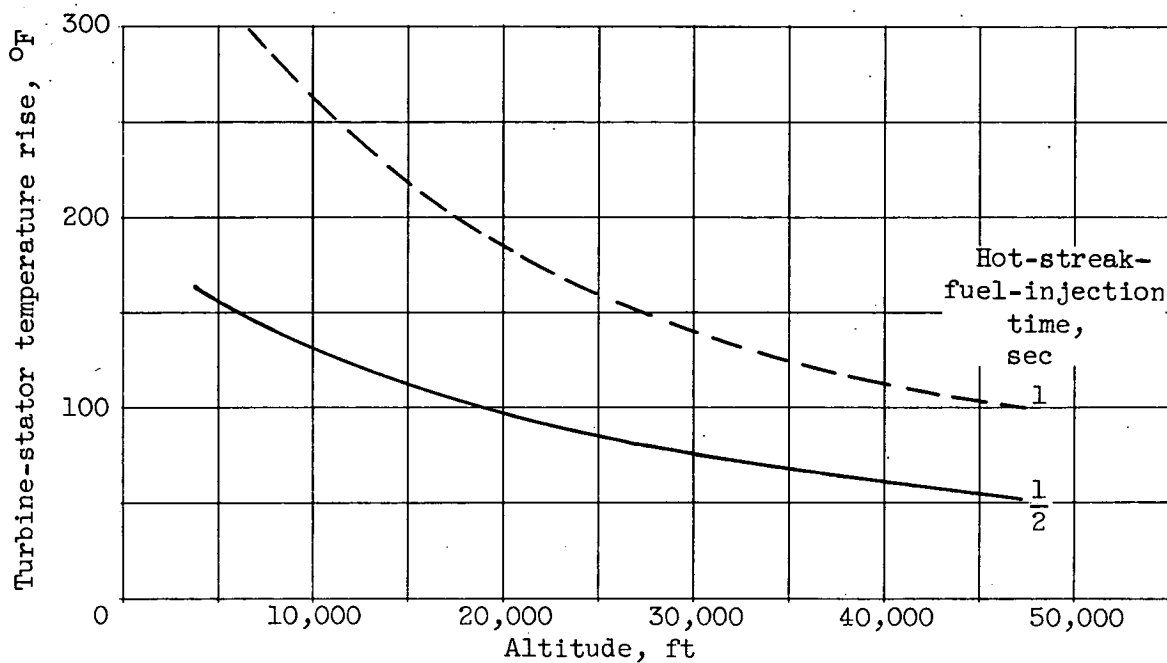
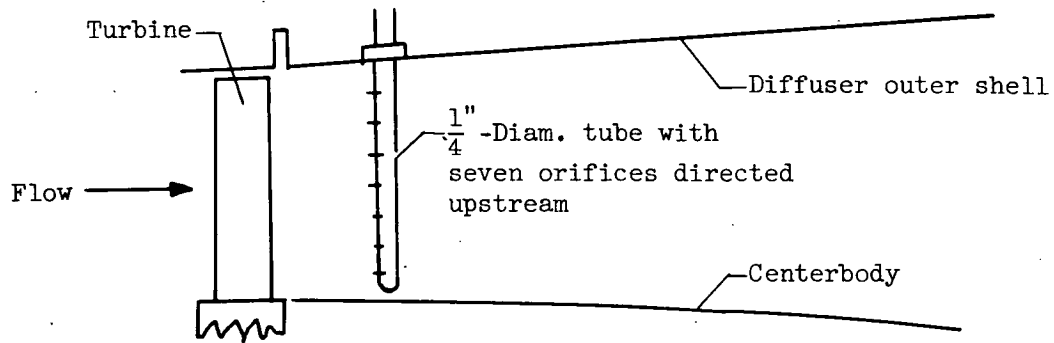
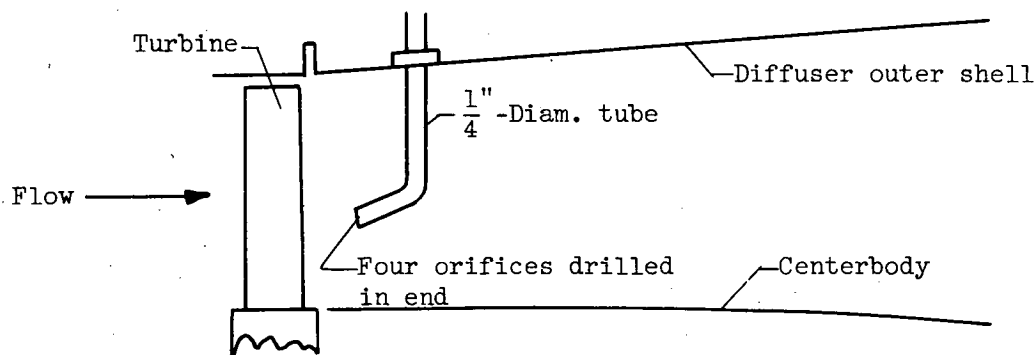


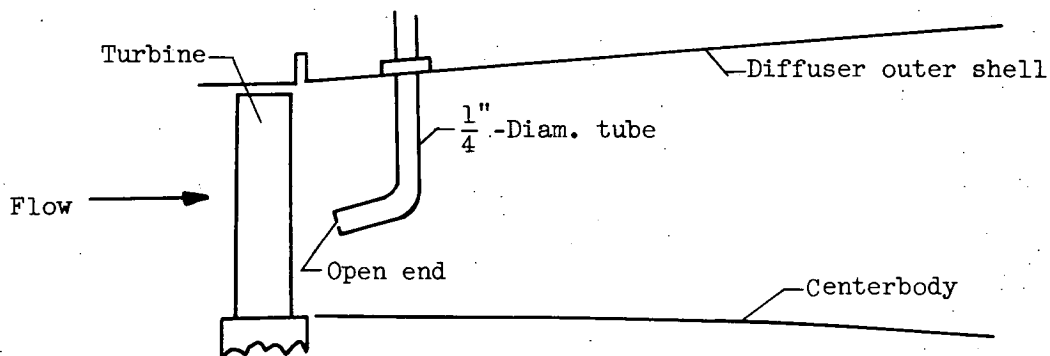
Figure 179. - Effect of hot-streak-fuel-injection time on variation of turbine-stator-blade temperature rise with altitude. Initial gas temperature, 2000°R ; local gas temperature, 3000°R ; equilibrium blade temperature equal to 0.93 gas temperature; flight Mach number, 0.8.



(a) Configuration A, multiorifice bar.

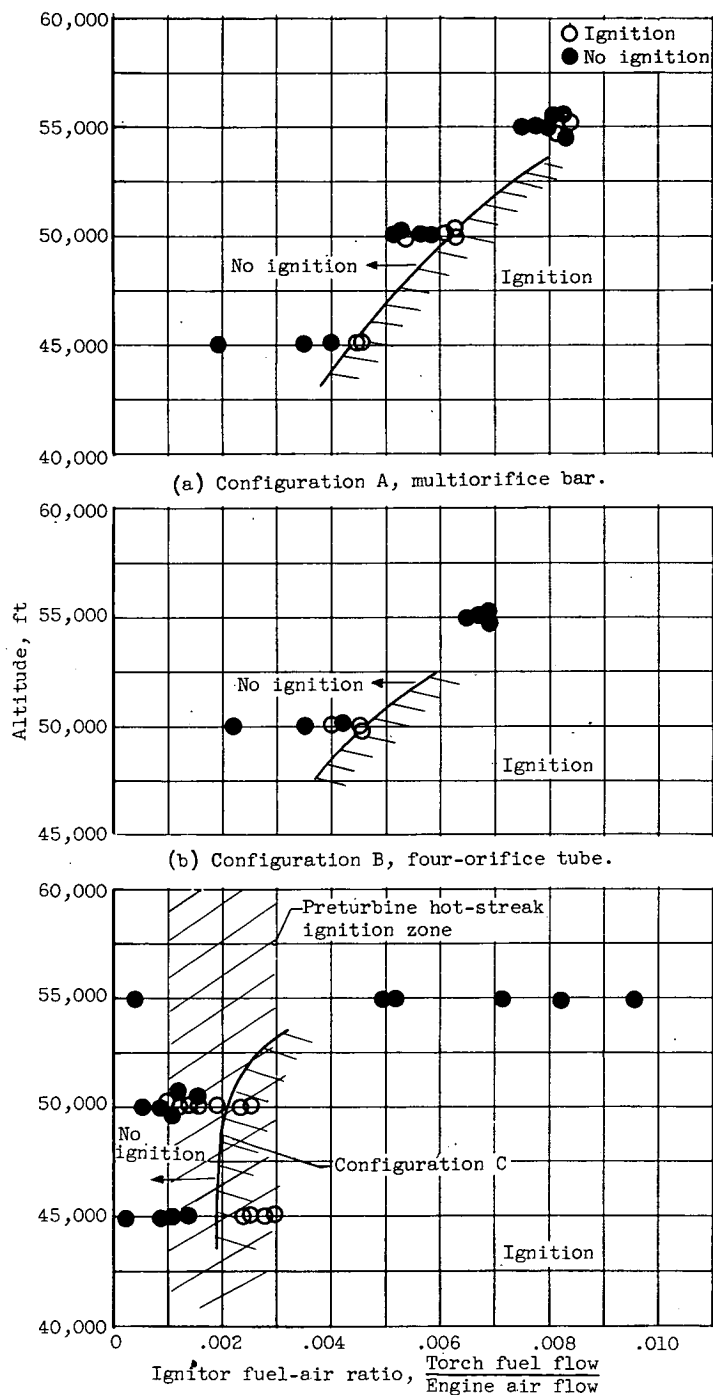


(b) Configuration B, four-orifice bar.



(c) Configuration C, open-end tube.

Figure 180. - Turbine-outlet hot-streak systems evaluated.



(c) Configuration C, open-end tube, compared with typical preturbine hot-streak configuration.

Figure 181. - Ignition limits of turbine-outlet hot-streak systems in comparison with typical preturbine hot streak. Turbine-outlet temperature, 1710° R.

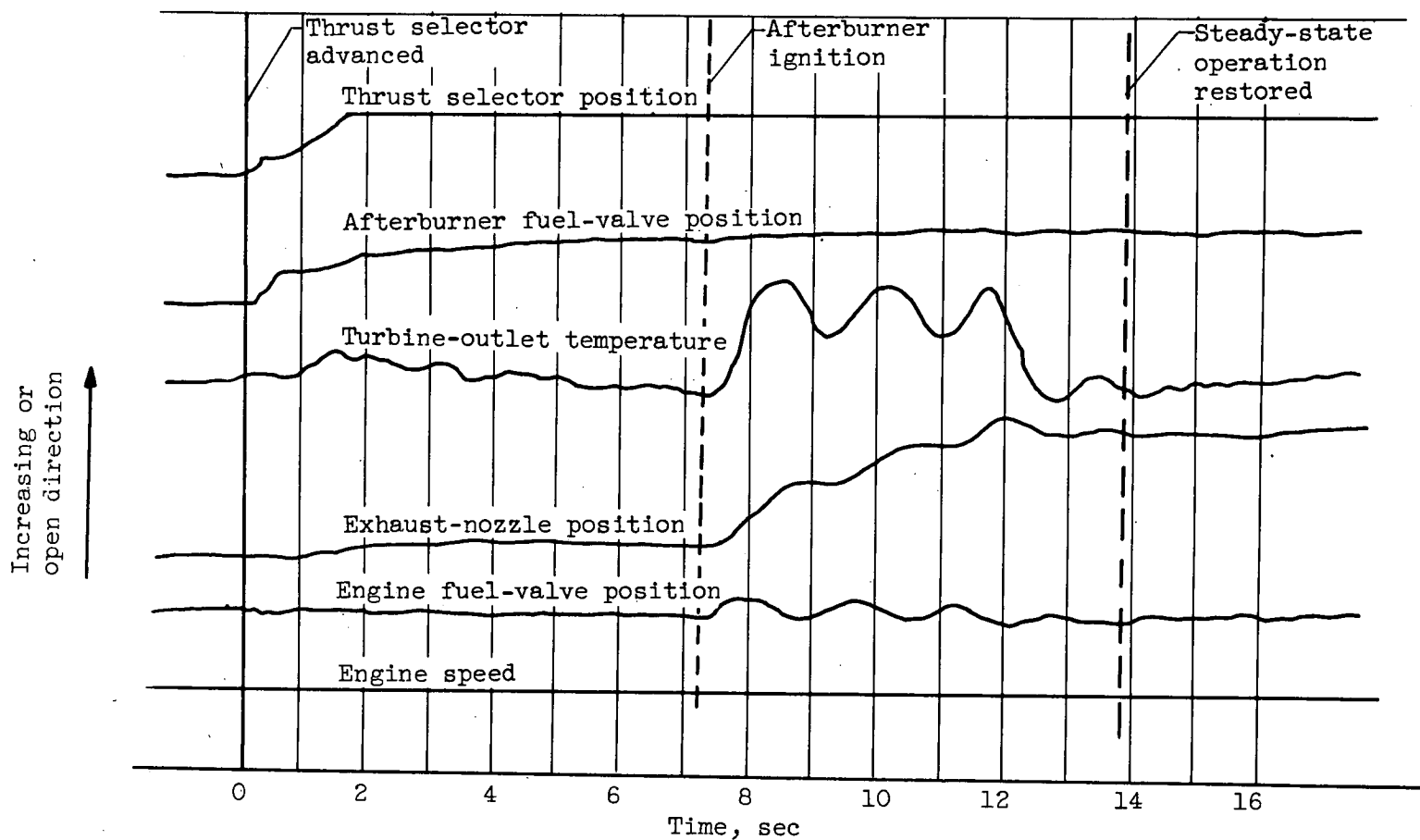


Figure 182. - Oscillograph indications of control-parameter variations during afterburner ignition and transient to steady-state operation. Altitude 30,000 feet; flight Mach number, 0.6.

368

CONFIDENTIAL

NACA RM E55G28

RECEIVED

569

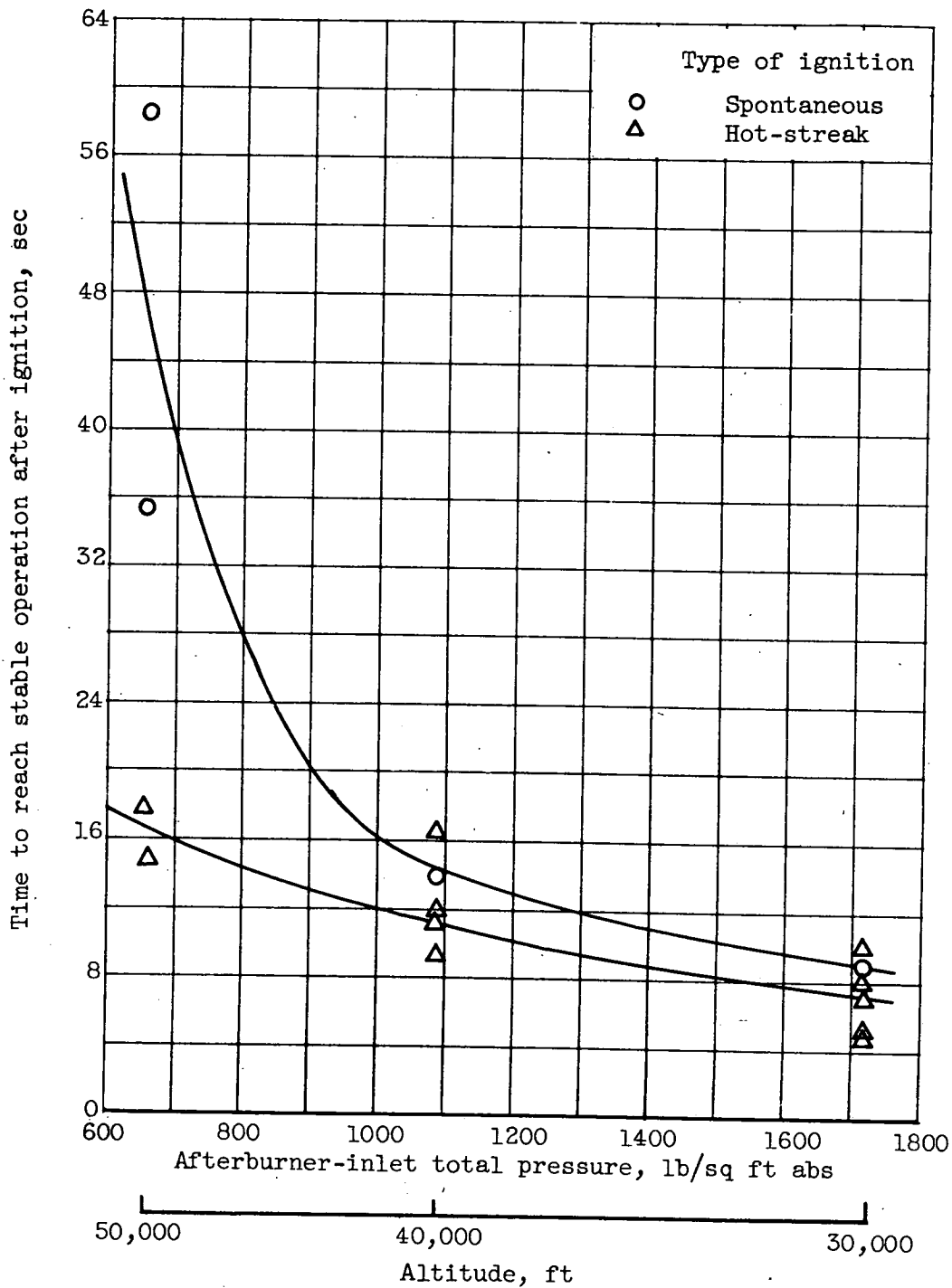


Figure 183. - Effect of afterburner-inlet total pressure on time to reach stable operation after ignition. Flight Mach number, 0.60.

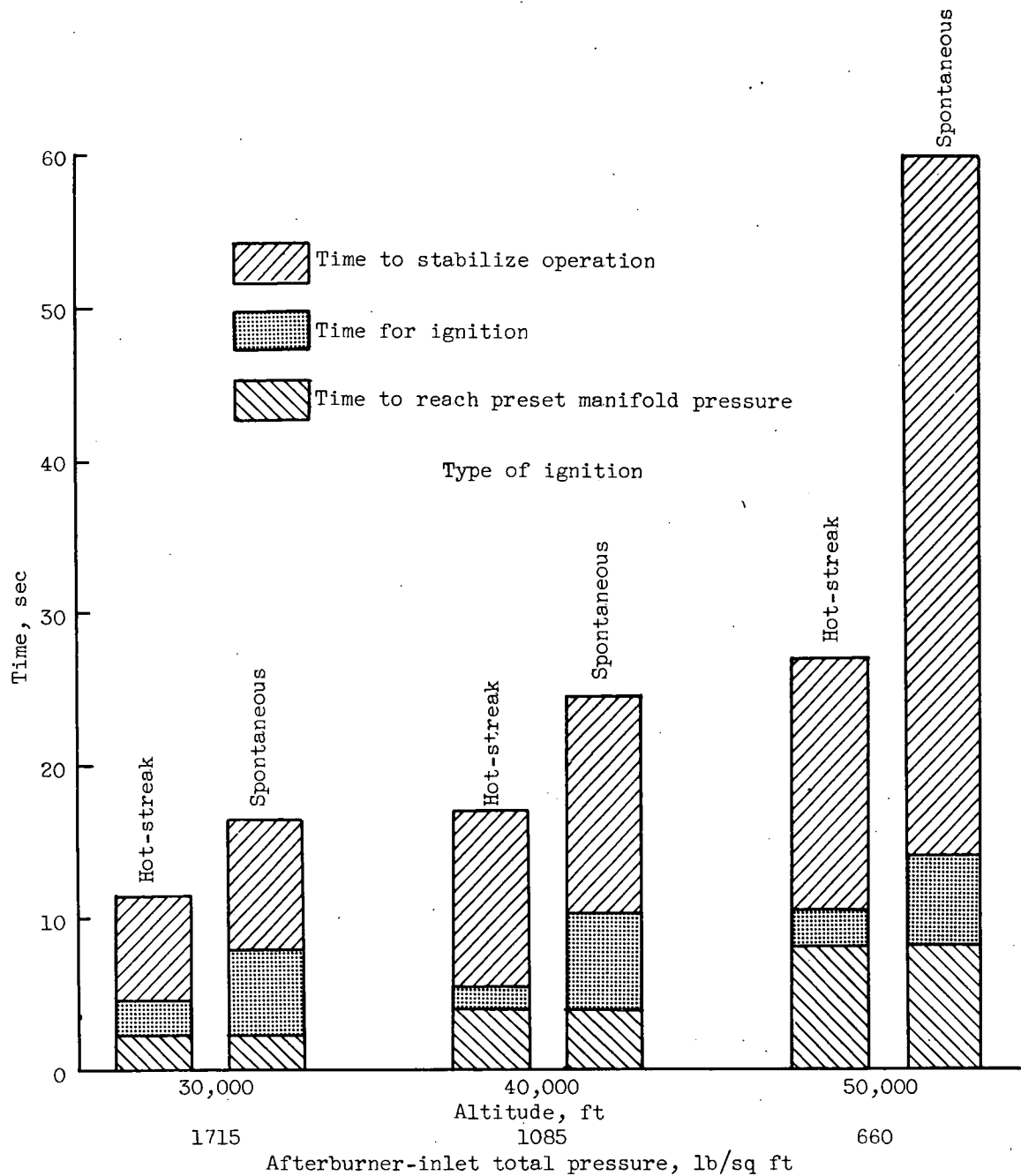


Figure 184. - Effect of altitude on over-all time required for afterburner starting. Preset fuel-air ratio, 0.03; flight Mach number, 0.6.

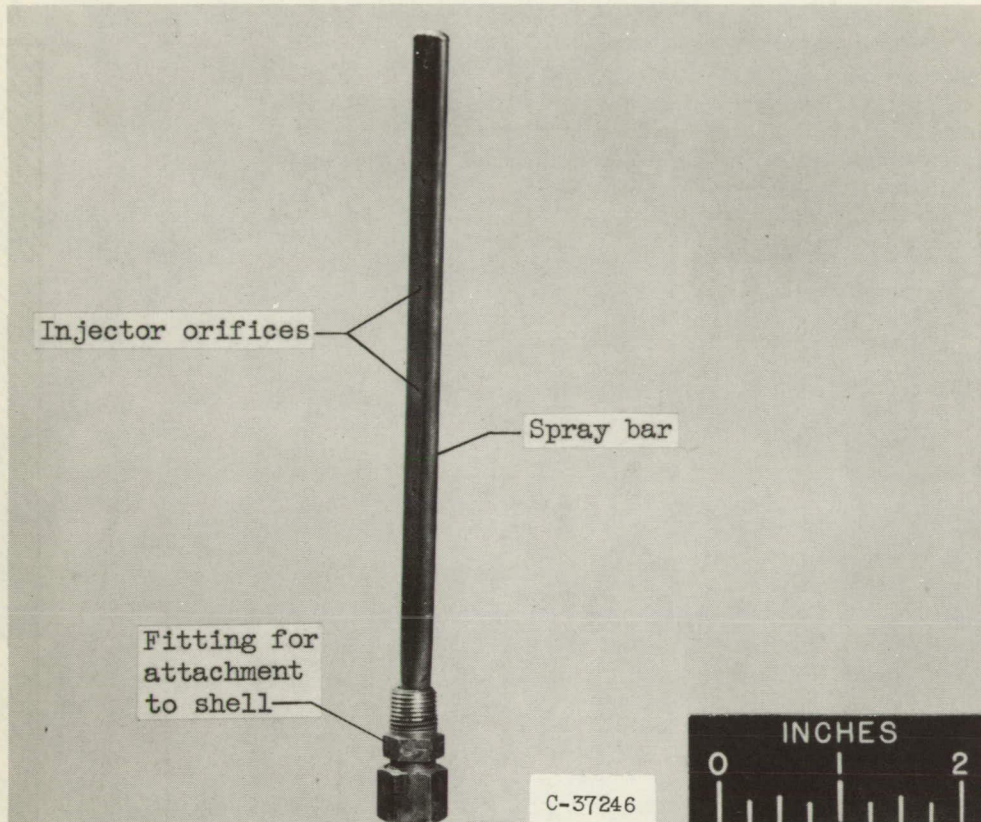
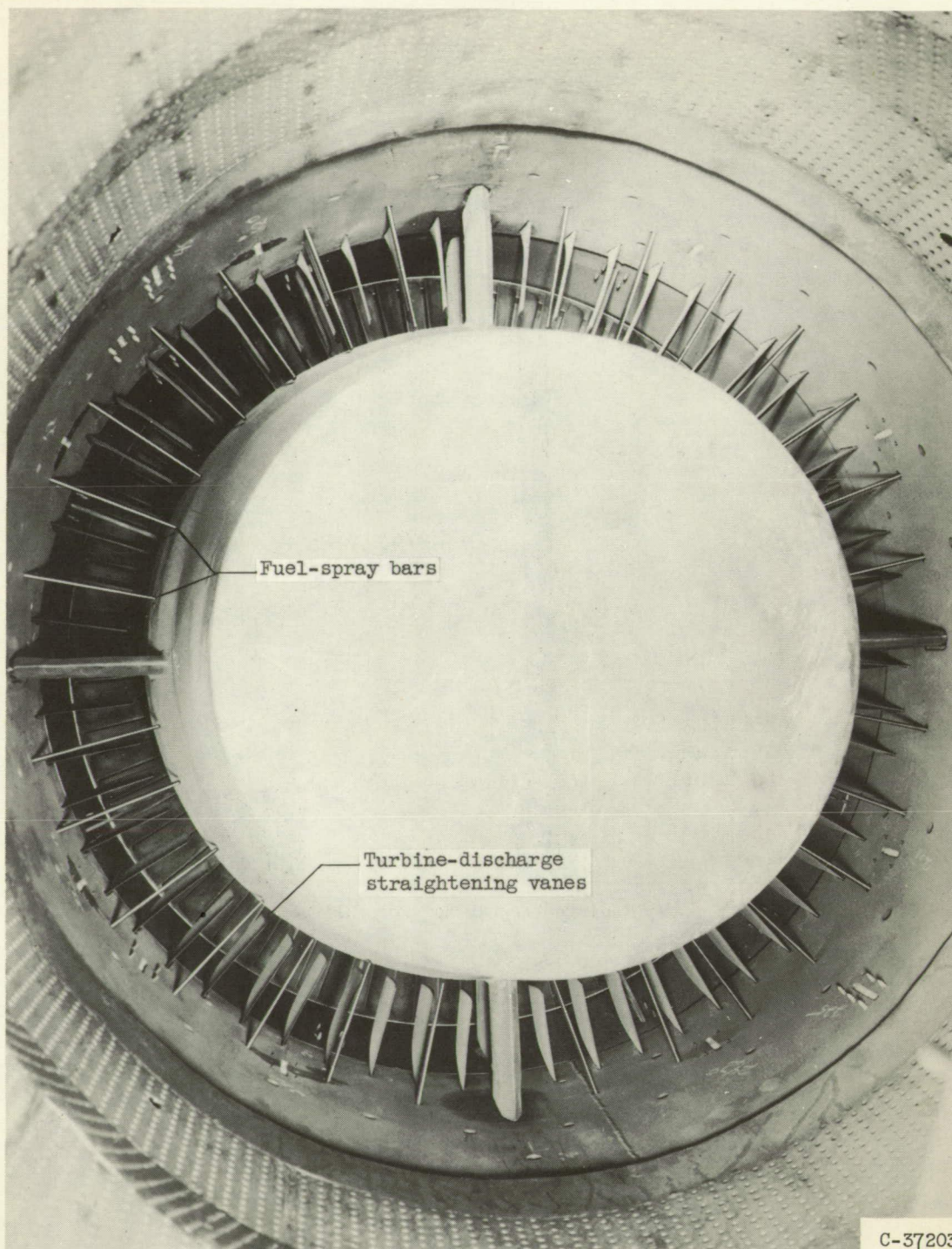


Figure 185. - Typical fuel-spray bar for full-scale afterburner.



C-37203

Figure 186. - View looking upstream into full-scale afterburner diffuser showing typical installation of fuel-spray bars at turbine discharge.

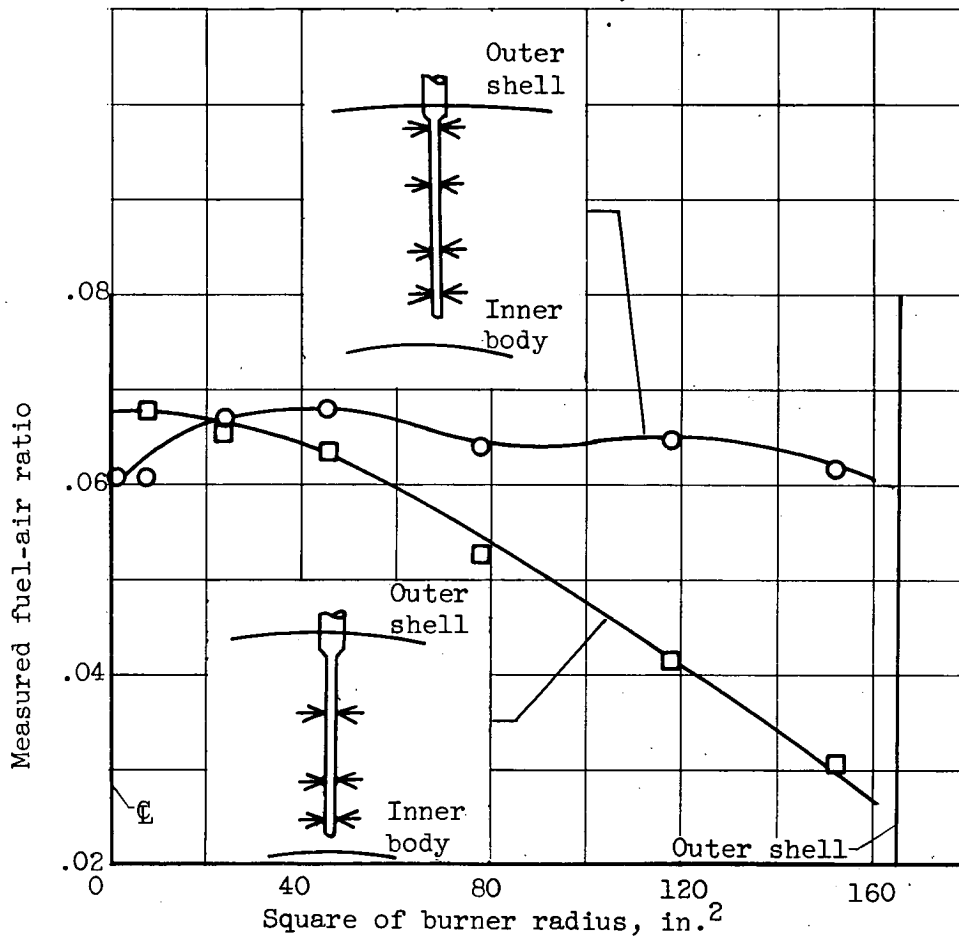


Figure 187. - Effect of spray-bay design on fuel-air-ratio distribution 22.5 inches downstream of spray bars. Transverse injection from 24 spray bars having 0.030-inch-diameter orifices.

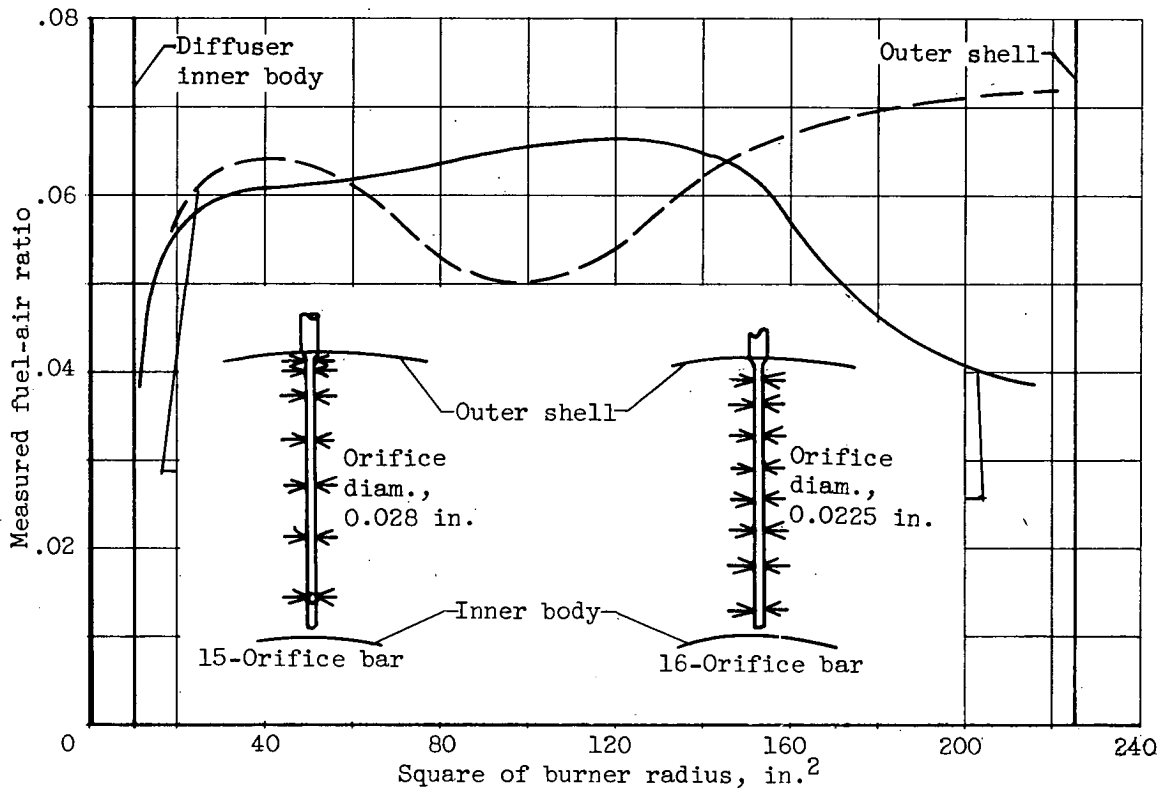


Figure 188. - Effect of radial location of fuel orifices on fuel-air-ratio distribution 15 inches downstream of spray bars. Transverse injection from 20 spray bars.

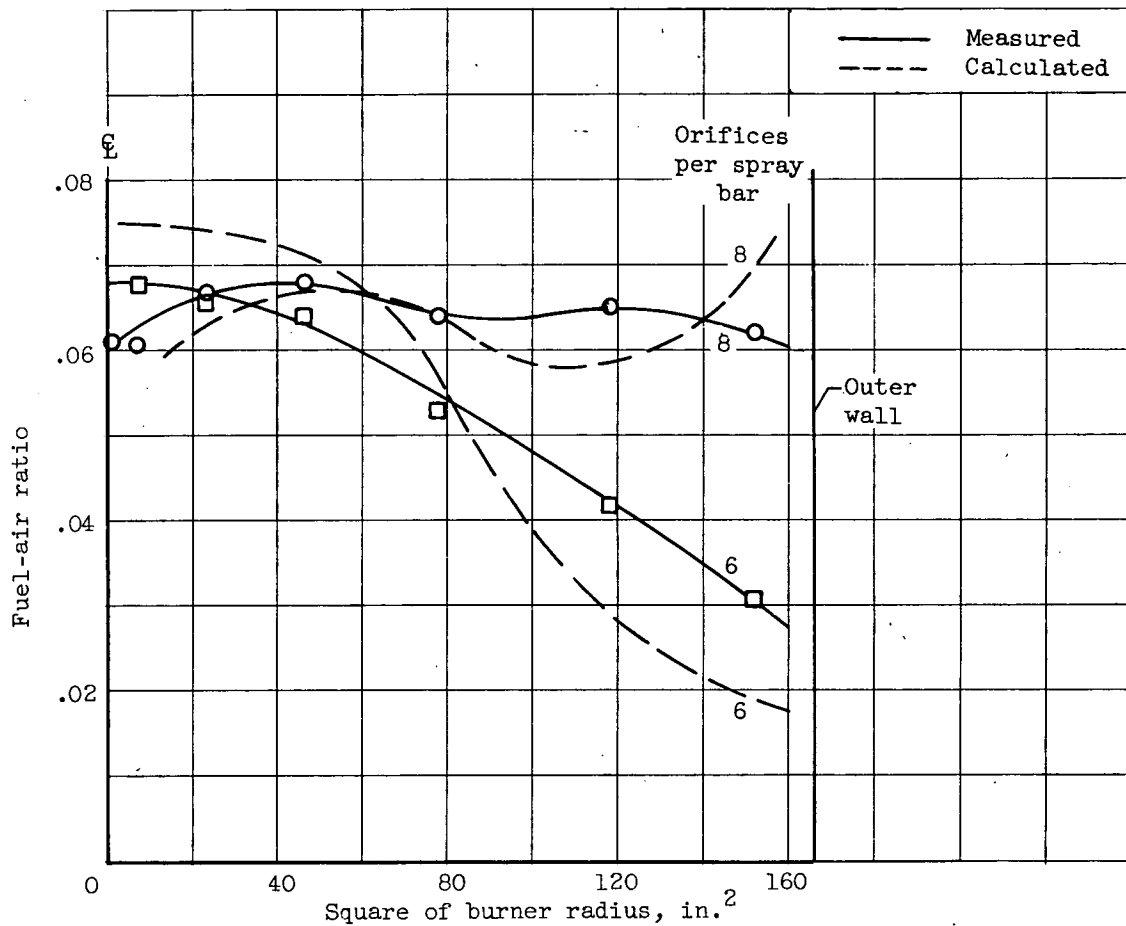


Figure 189. - Comparison of calculated fuel-air-ratio distribution with measured values from figure 187. Fuel mixing distance, 22.5 inches.

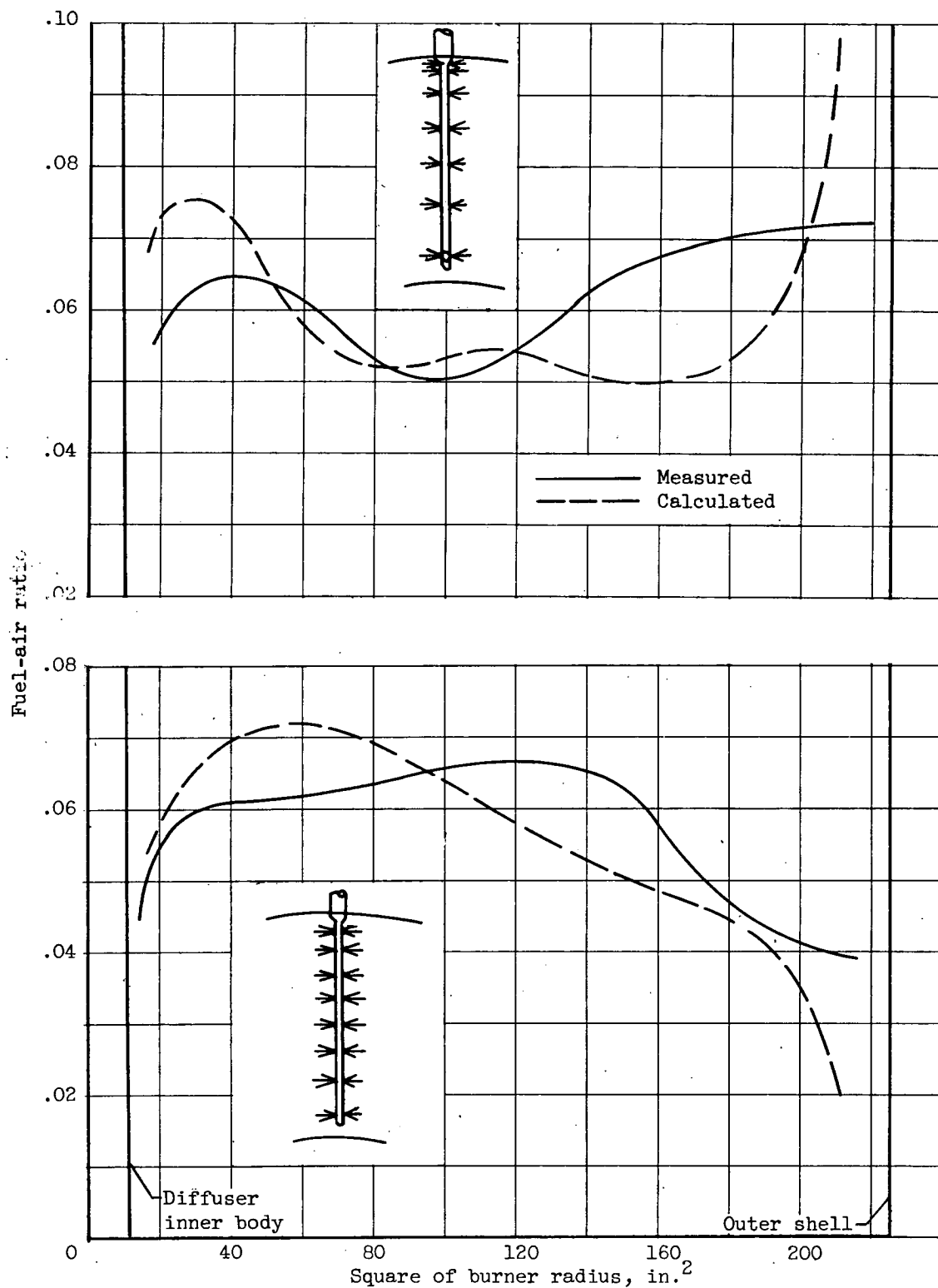


Figure 190. - Comparison of calculated fuel-air-ratio distribution with measured values of figure 188. Fuel mixing distance, 15 inches.

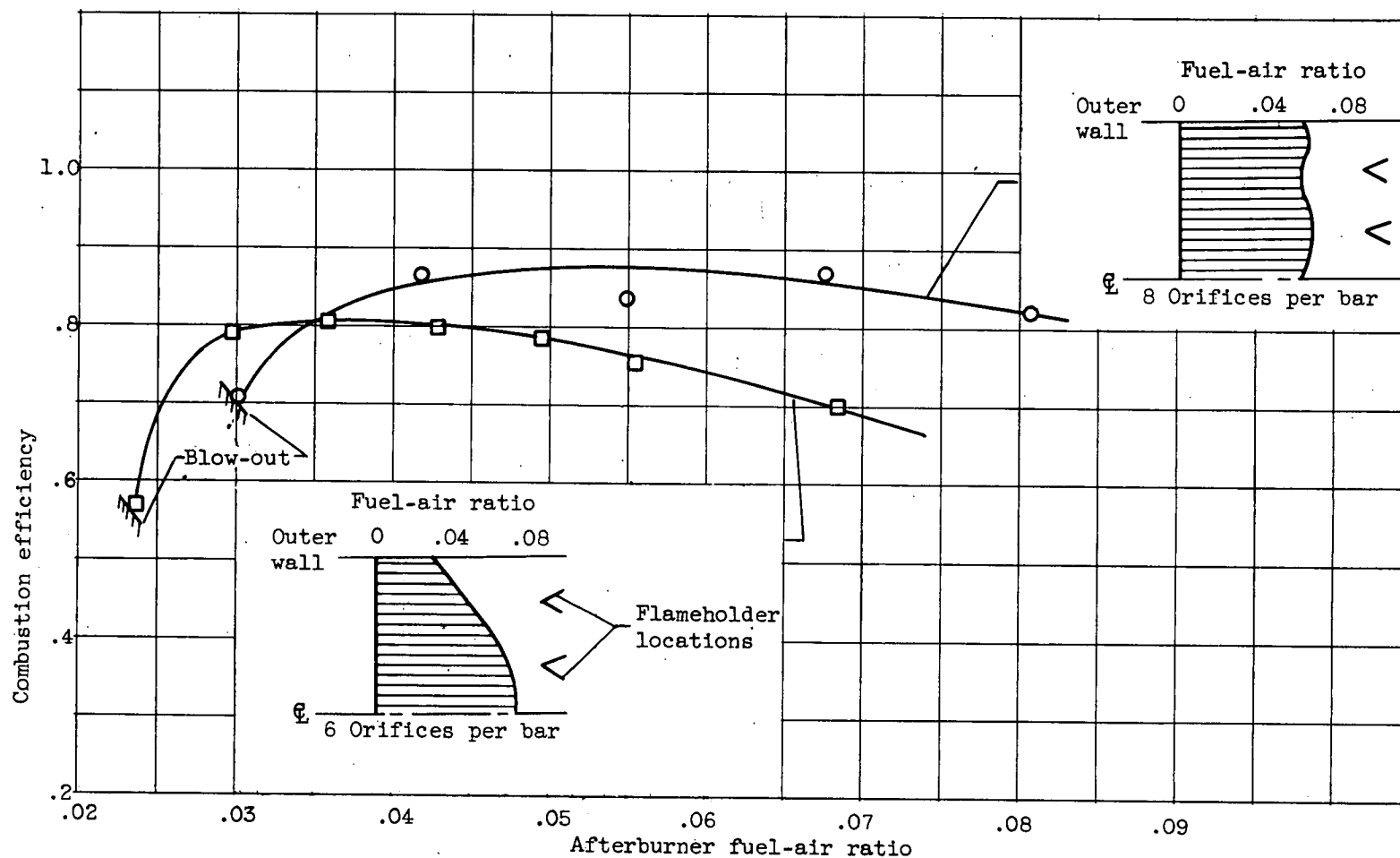


Figure 191. - Effect of radial fuel-air-ratio distribution on combustion efficiency.

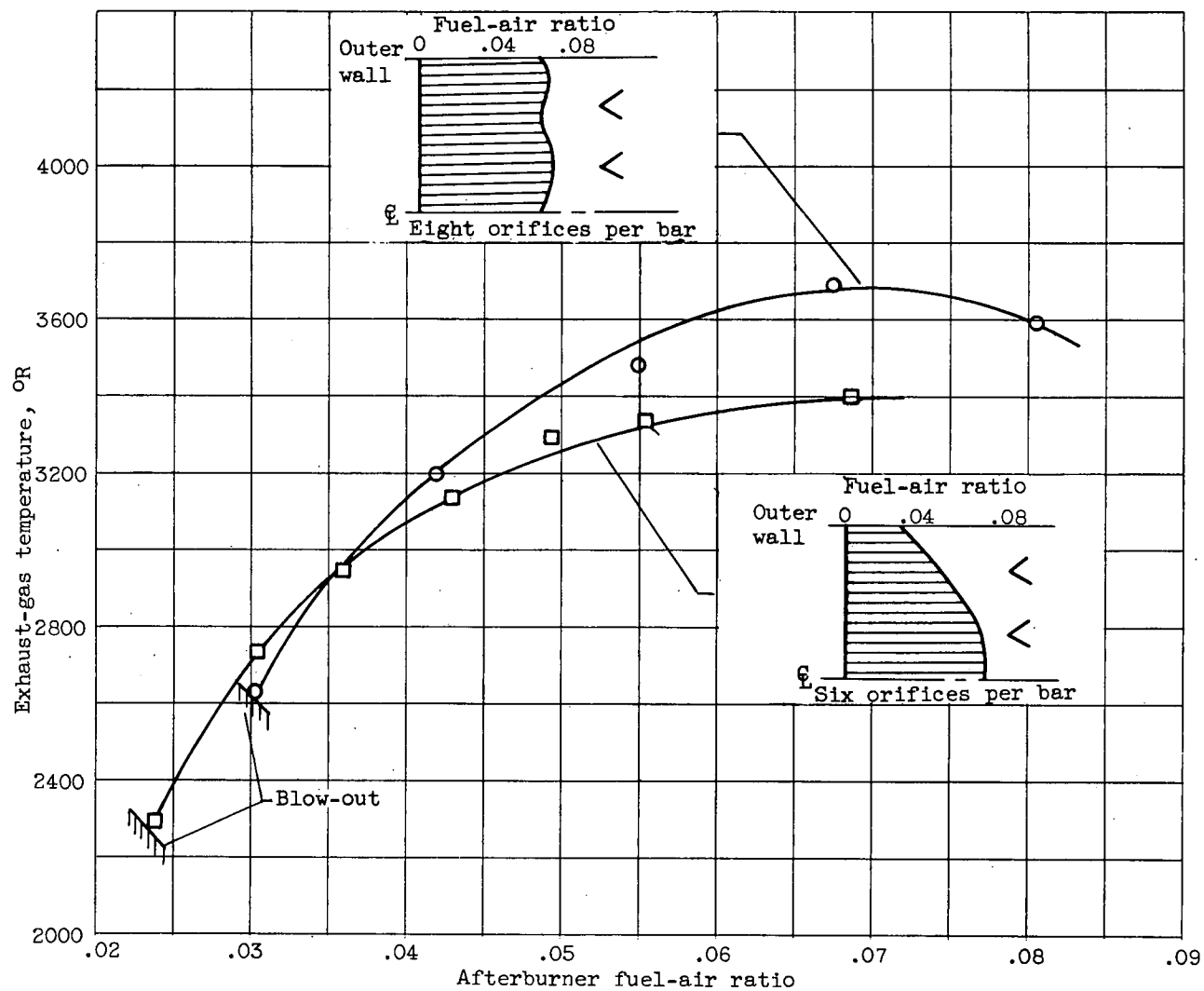


Figure 192. - Effect of radial fuel-air-ratio distribution on exhaust-gas temperature.

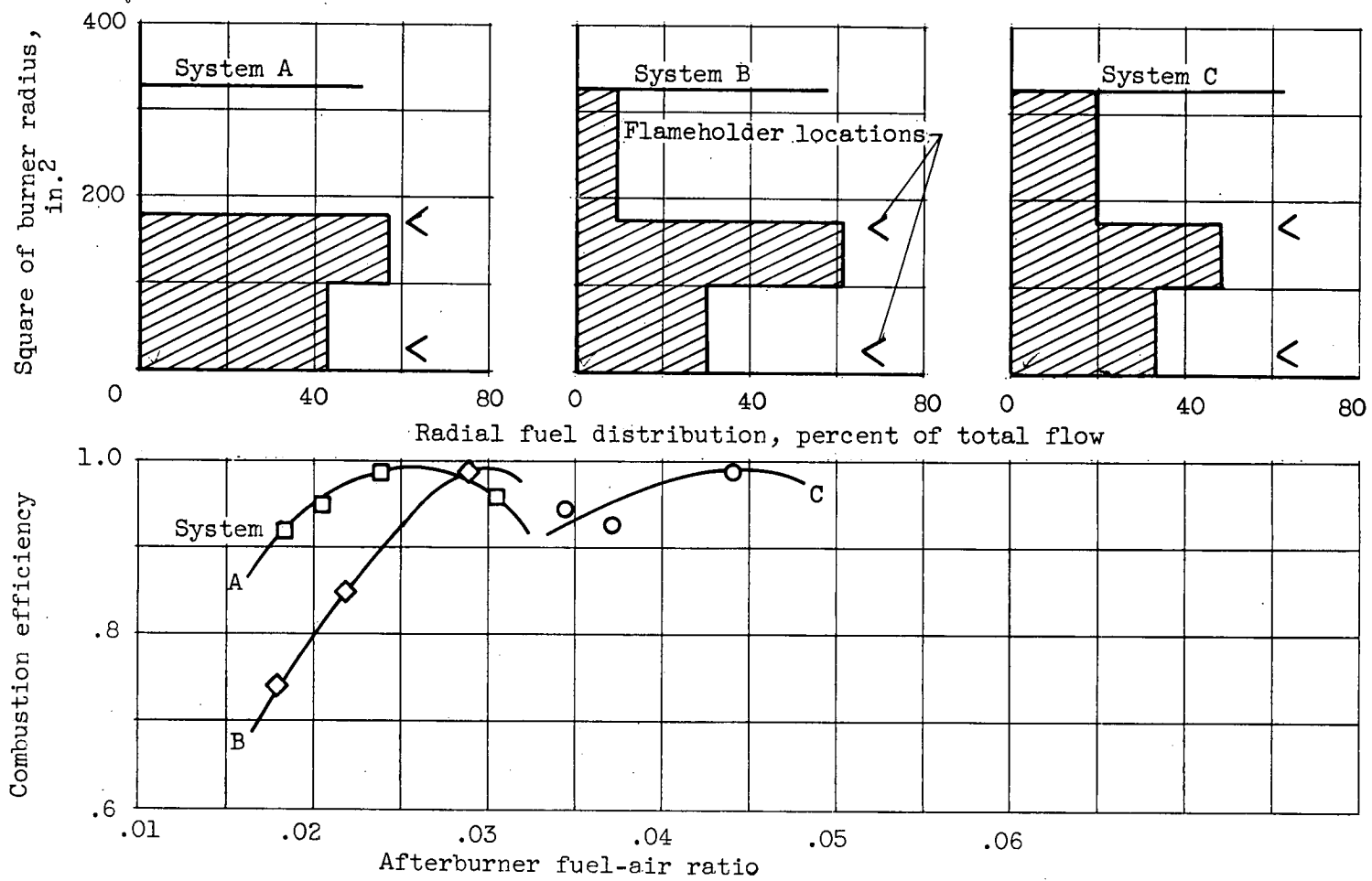
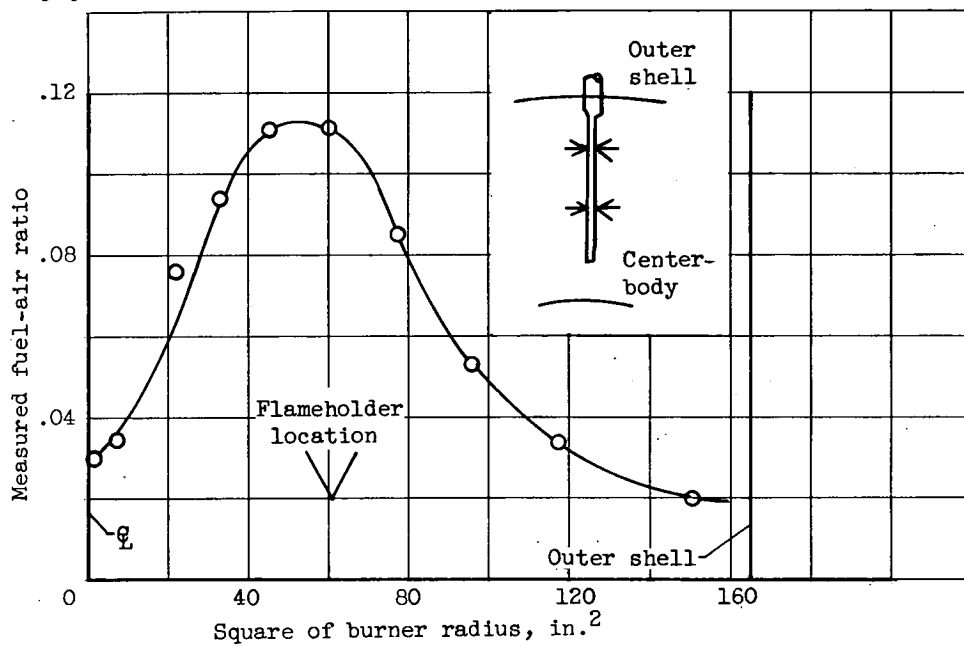
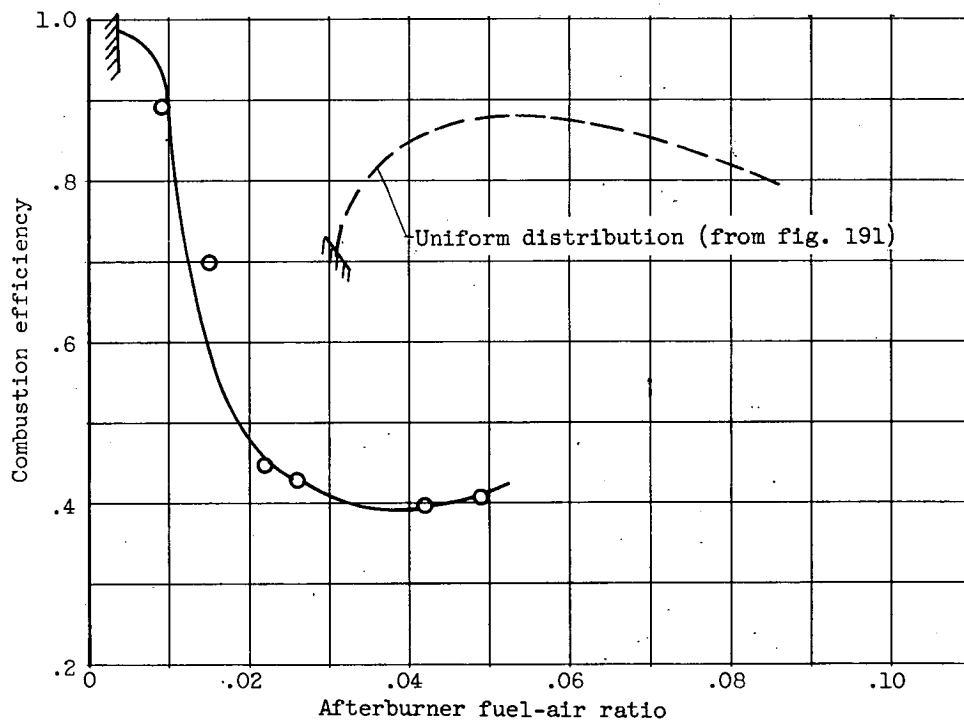


Figure 193. - Effect on combustion efficiency of varying radial distribution of fuel.



(a) Fuel-air-ratio distribution. Average fuel-air ratio, 0.055.



(b) Combustion efficiency.

Figure 194. - Combustion performance of afterburner with locally rich fuel injection. Transverse fuel injection from 12 bars having four 0.030-inch-diameter orifices.

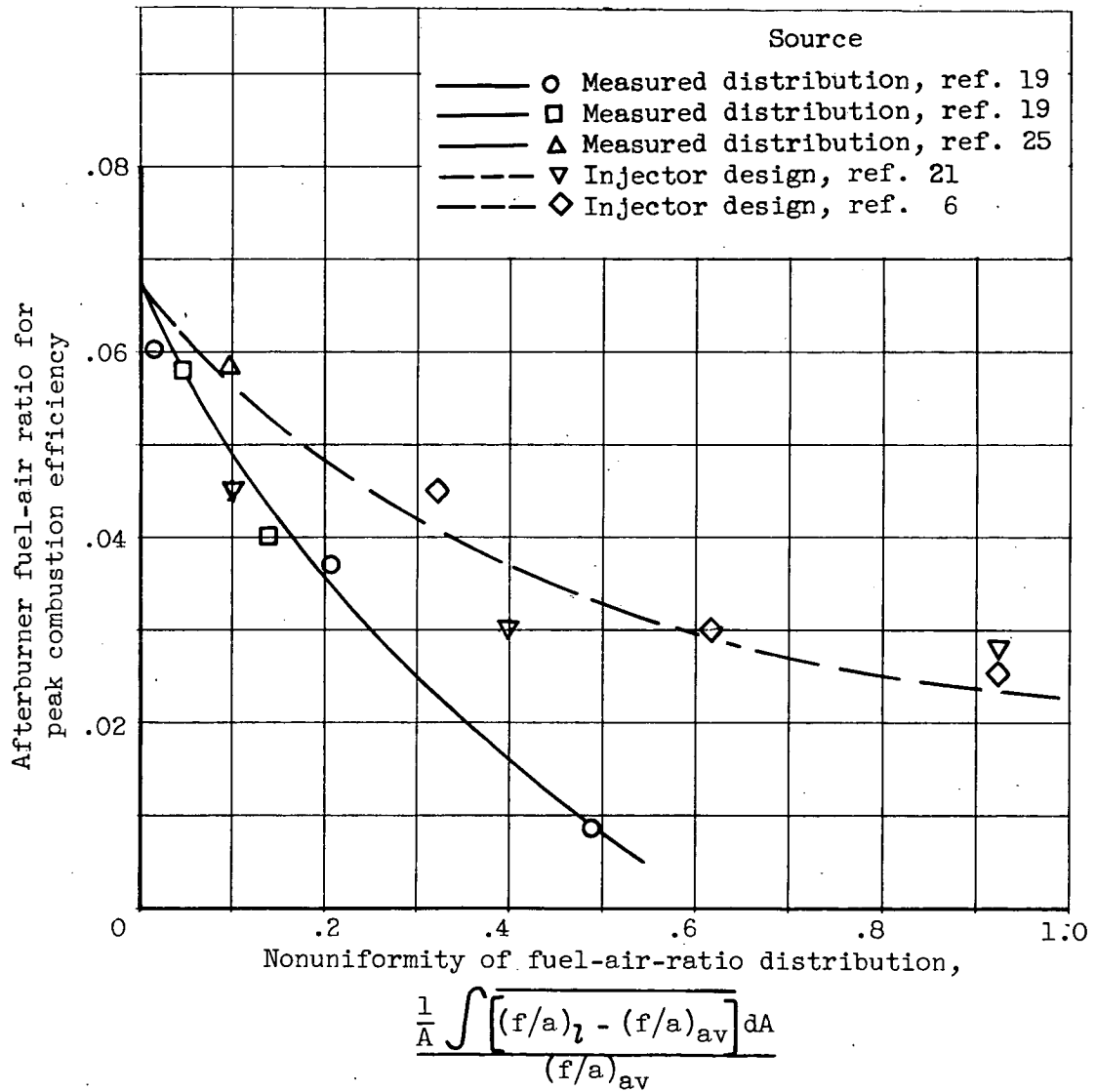


Figure 195. - Variation of fuel-air ratio at which peak combustion efficiency occurs with uniformity of fuel-air ratio distribution.

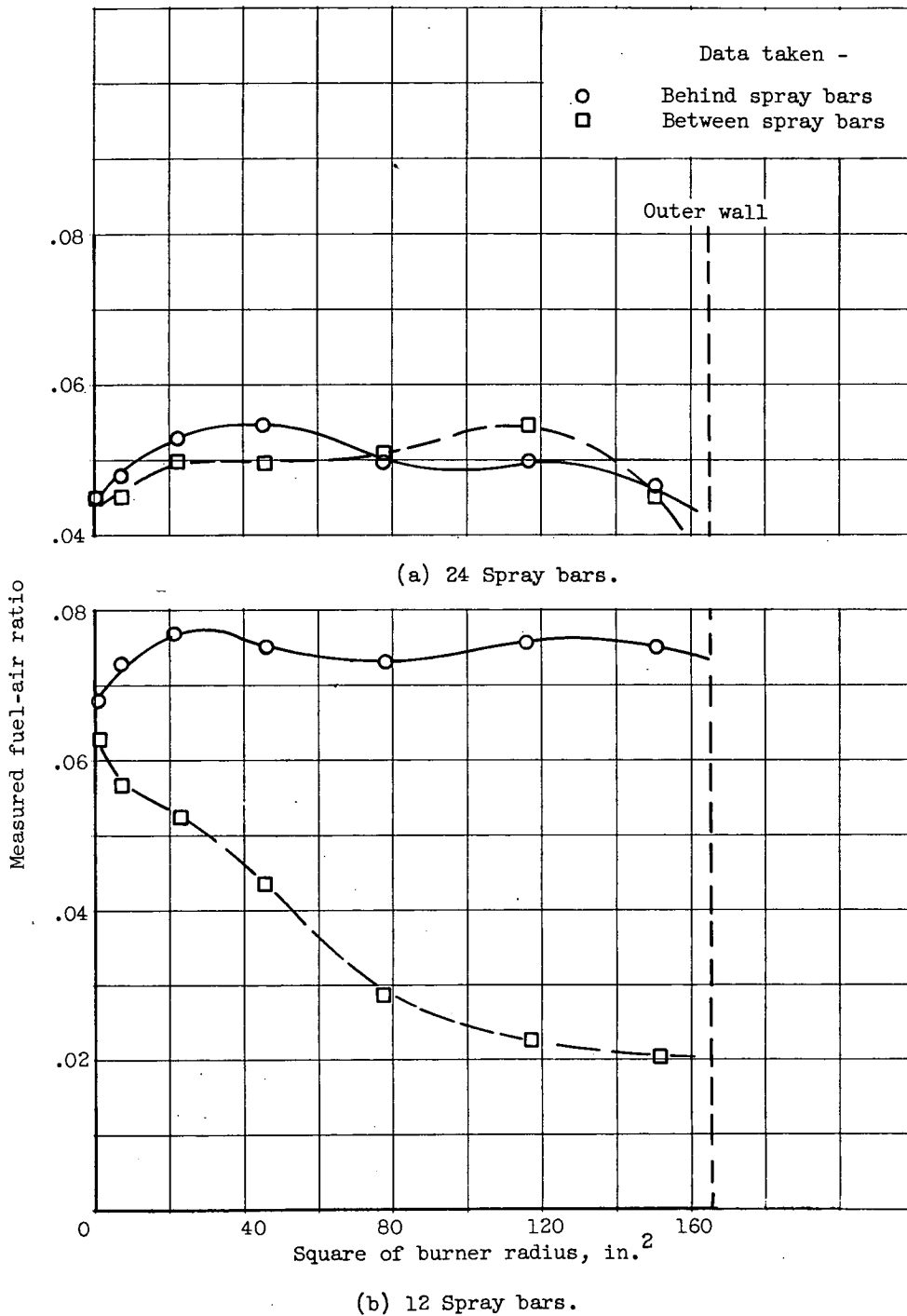


Figure 196. - Effect of number of spray bars on circumferential fuel-air-ratio distribution. Transverse injection from eight 0.030-inch-diameter orifices in each bar. Gas velocity, 500 to 600 feet per second; burner diameter, 26 inches.

DECLASSIFIED

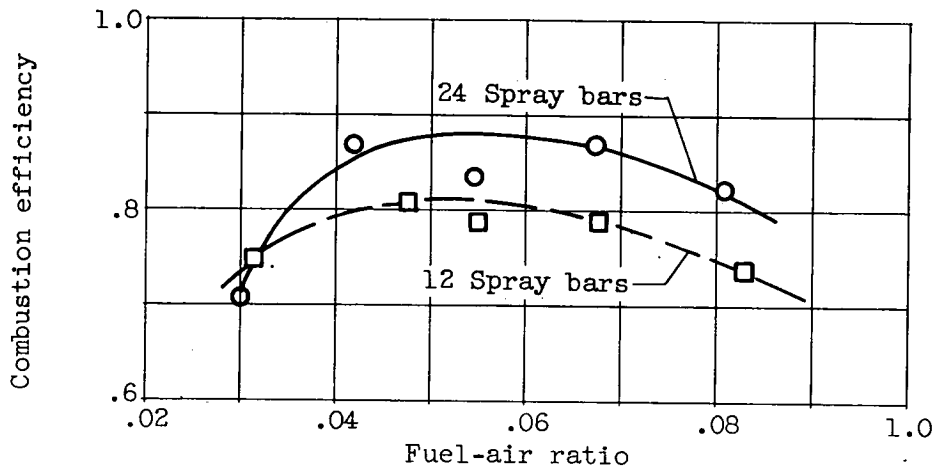


Figure 197. - Effect of number of spray bars on combustion efficiency. Transverse injection. Eight 0.030-inch-diameter orifices per spray bar; gas velocity, 500 to 600 feet per second.

03710201030

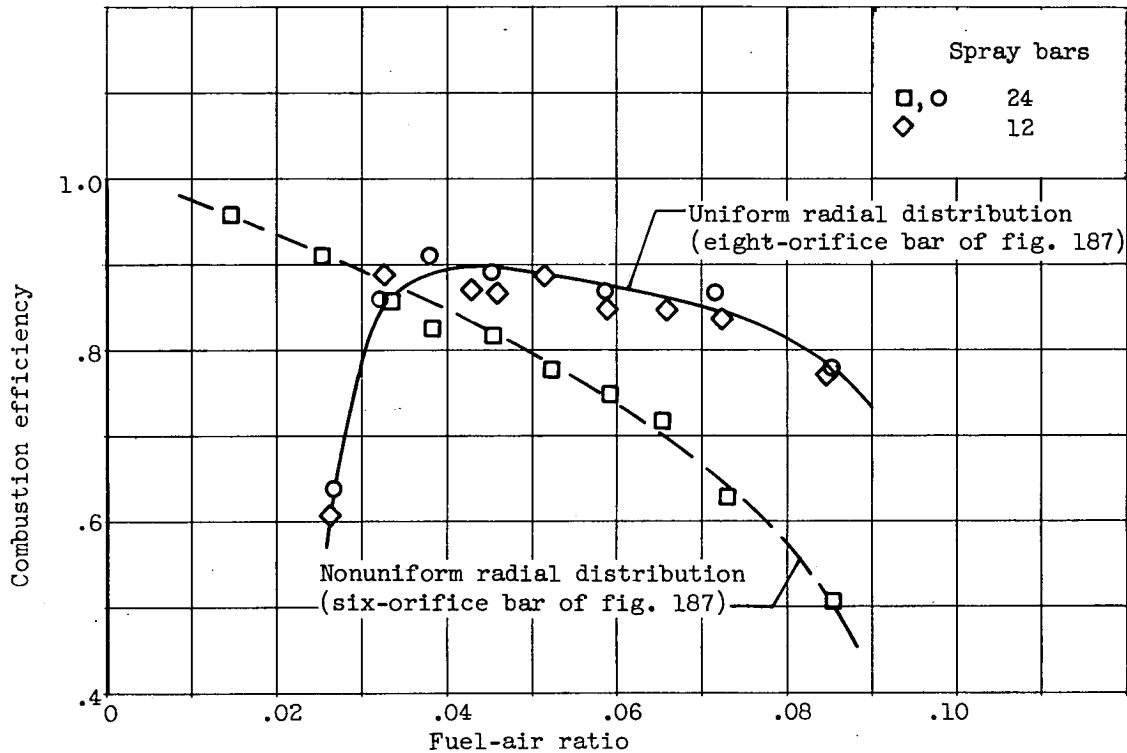


Figure 198. - Effect of radial and circumferential fuel-air-ratio distribution on combustion efficiency. Orifice diameter, 0.030 inch; burner-inlet velocity, 380 to 480 feet per second.

DECLASSIFIED

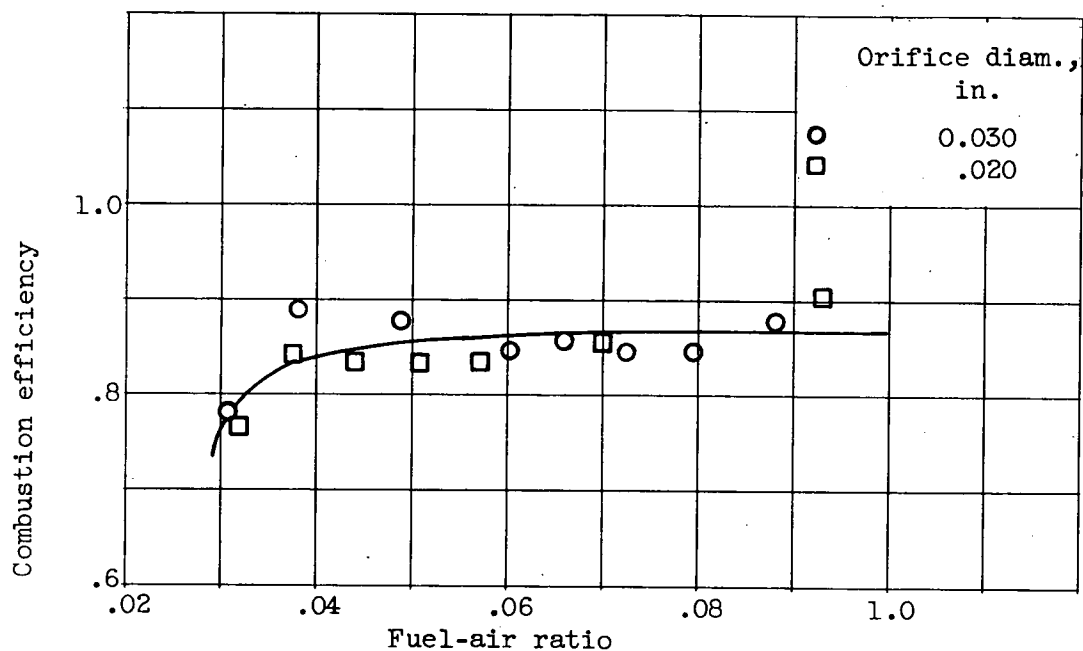
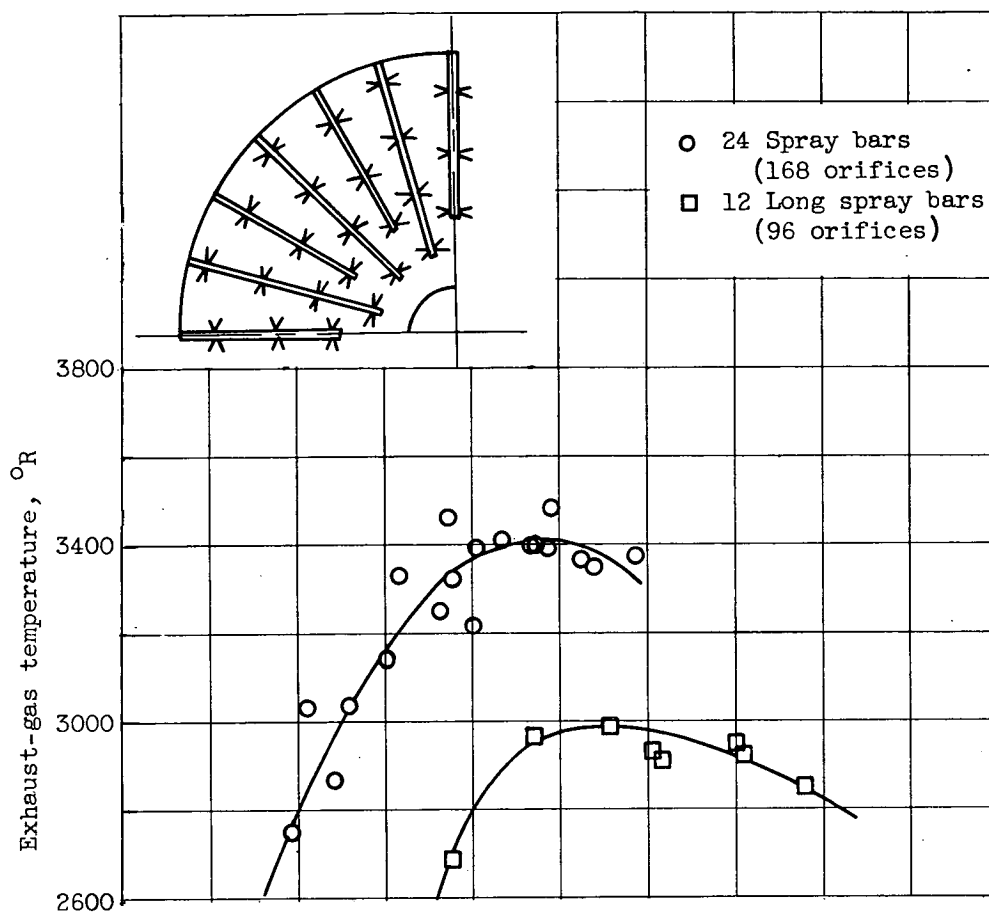
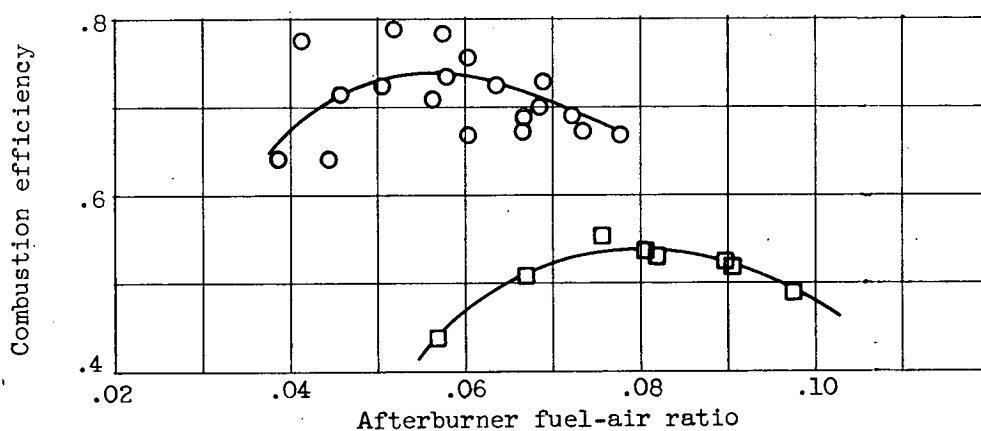


Figure 199. - Effect of spray-bar-orifice size on combustion efficiency. Transverse injection from 24 spray bars, each having eight orifices. Gas velocity, 500 to 600 feet per second; burner diameter, 26 inches.



(a) Exhaust-gas temperature.



(b) Combustion efficiency.

Figure 200. - Effect of number of fuel-spray bars on combustion efficiency and exhaust-gas temperature. Burner-inlet velocity, approximately 400 feet per second; diameter of transverse injection orifice, 0.020 inch.

DECLASSIFIED

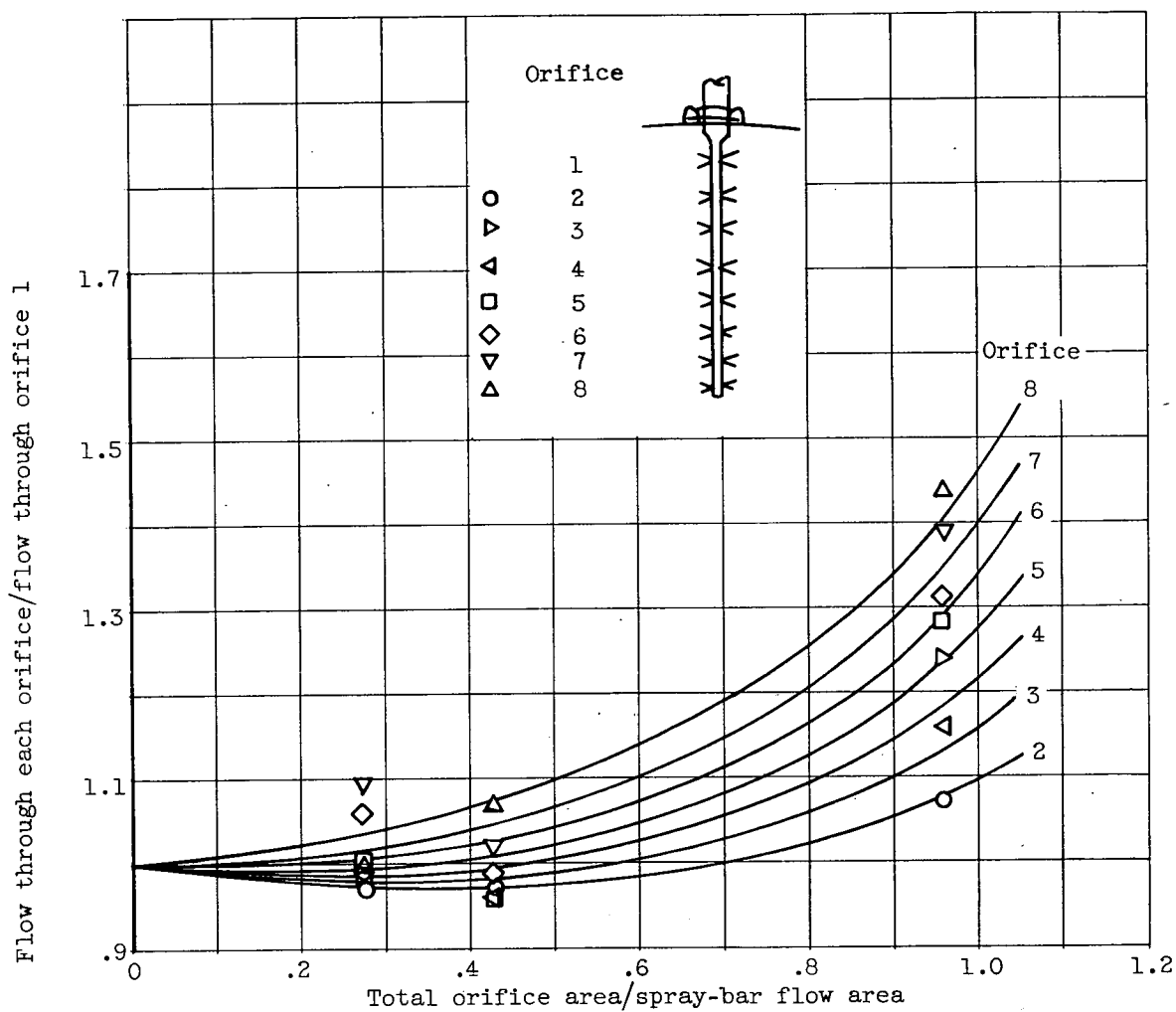


Figure 201. - Flow distribution among orifices of spray bars having various ratios of total orifice area to spray-bar flow area.

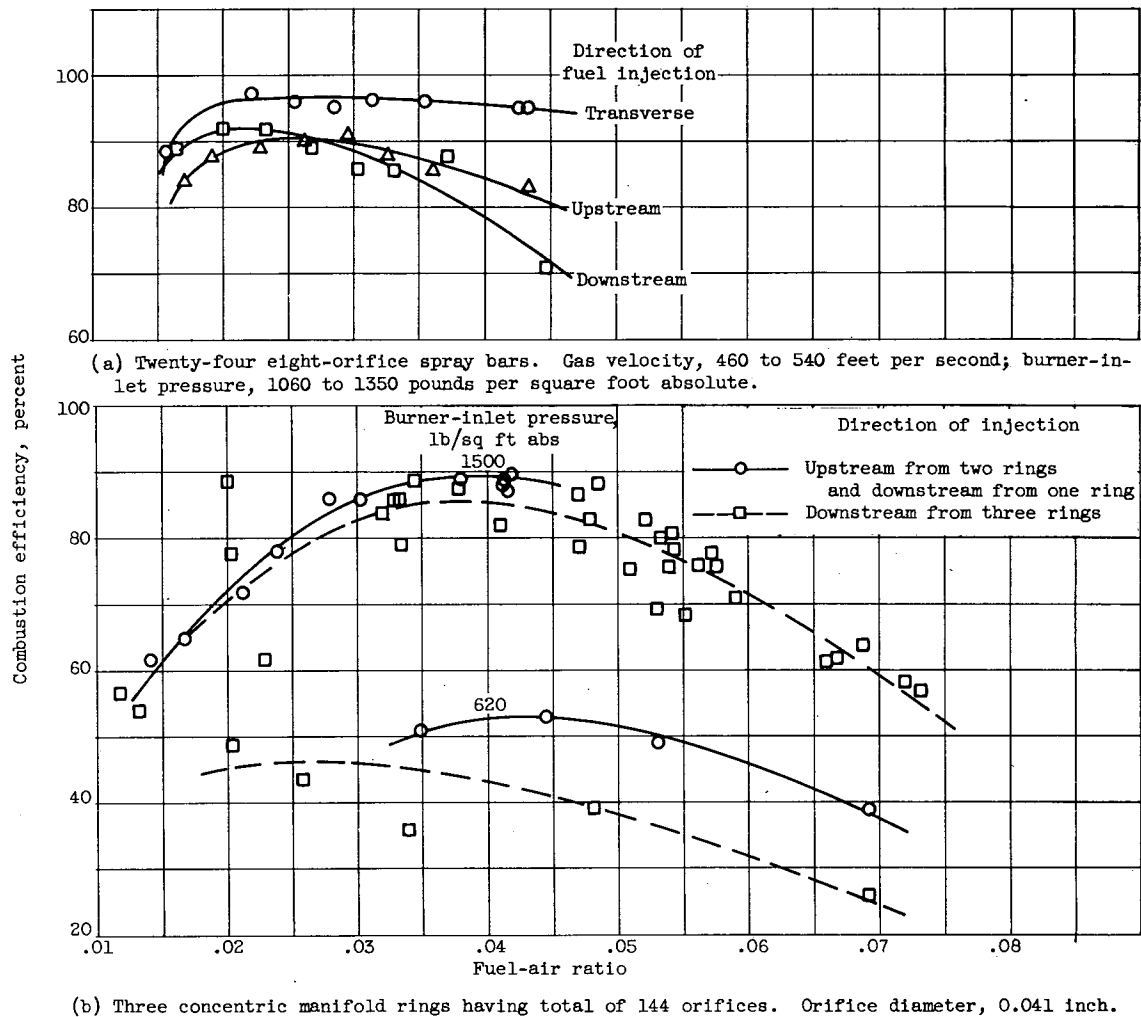


Figure 202. - Effect of direction of fuel injection on combustion efficiency.

DECLASSIFIED

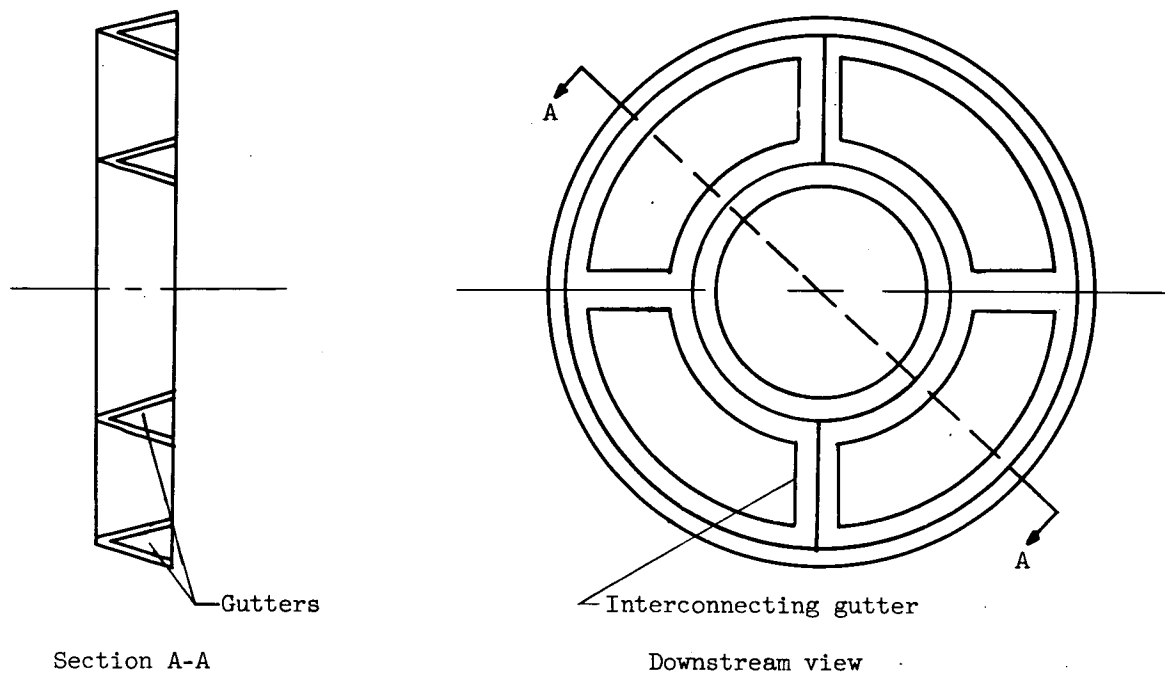


Figure 203. - Typical two-ring V-gutter flameholder.

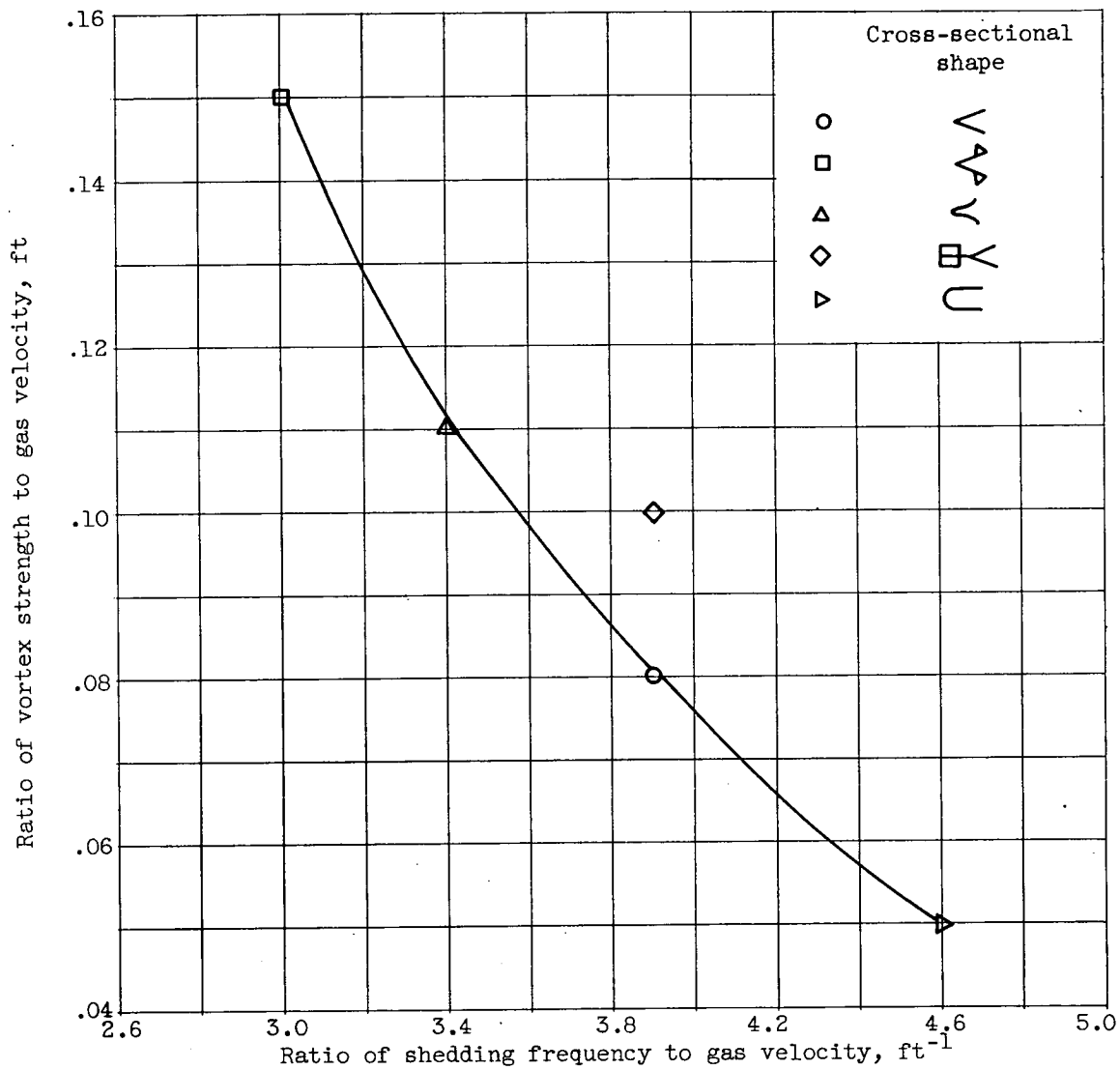


Figure 204. - Effect of cross-sectional shape on isothermal wake characteristics. Gutter width, $3/4$ inch.

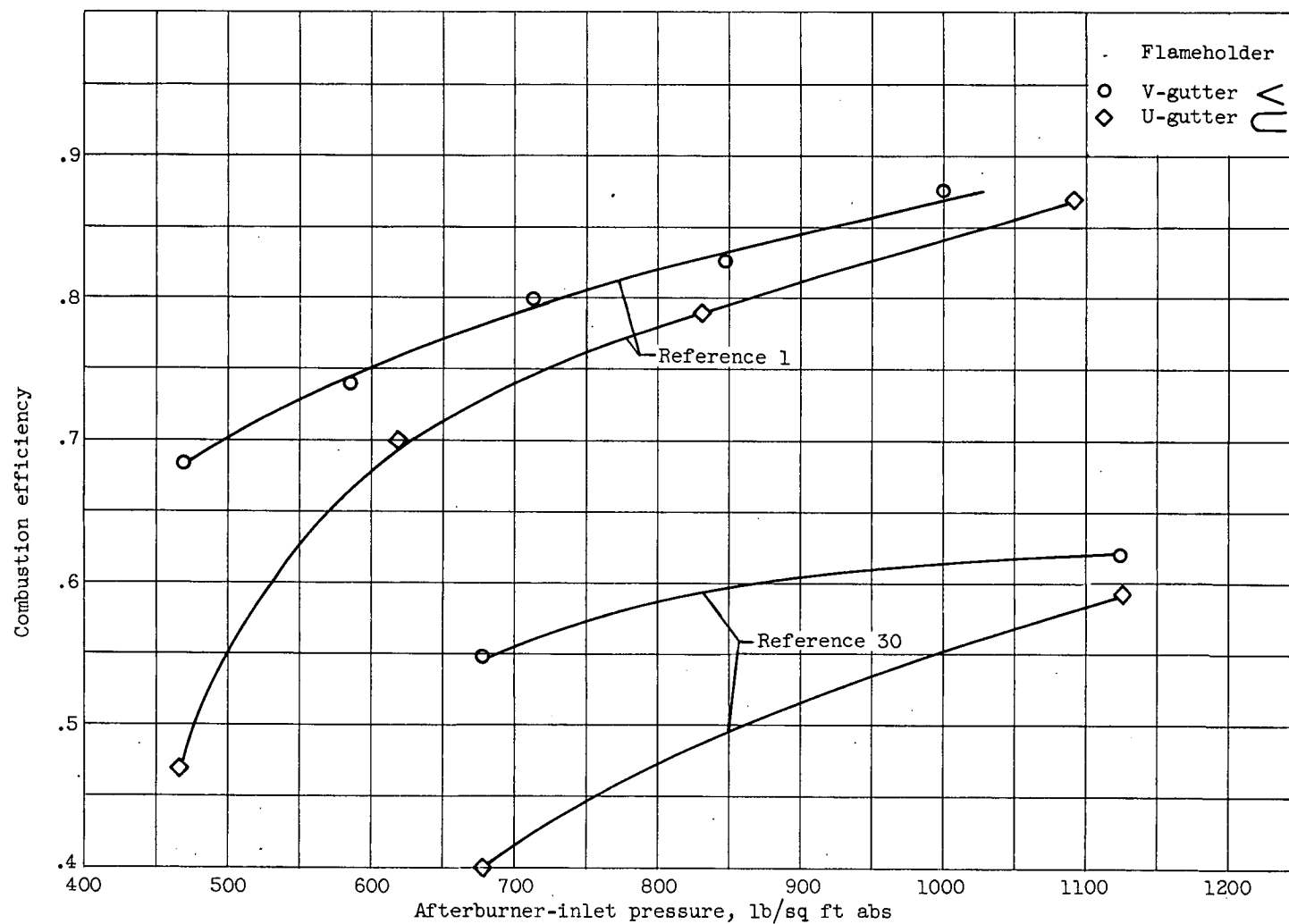
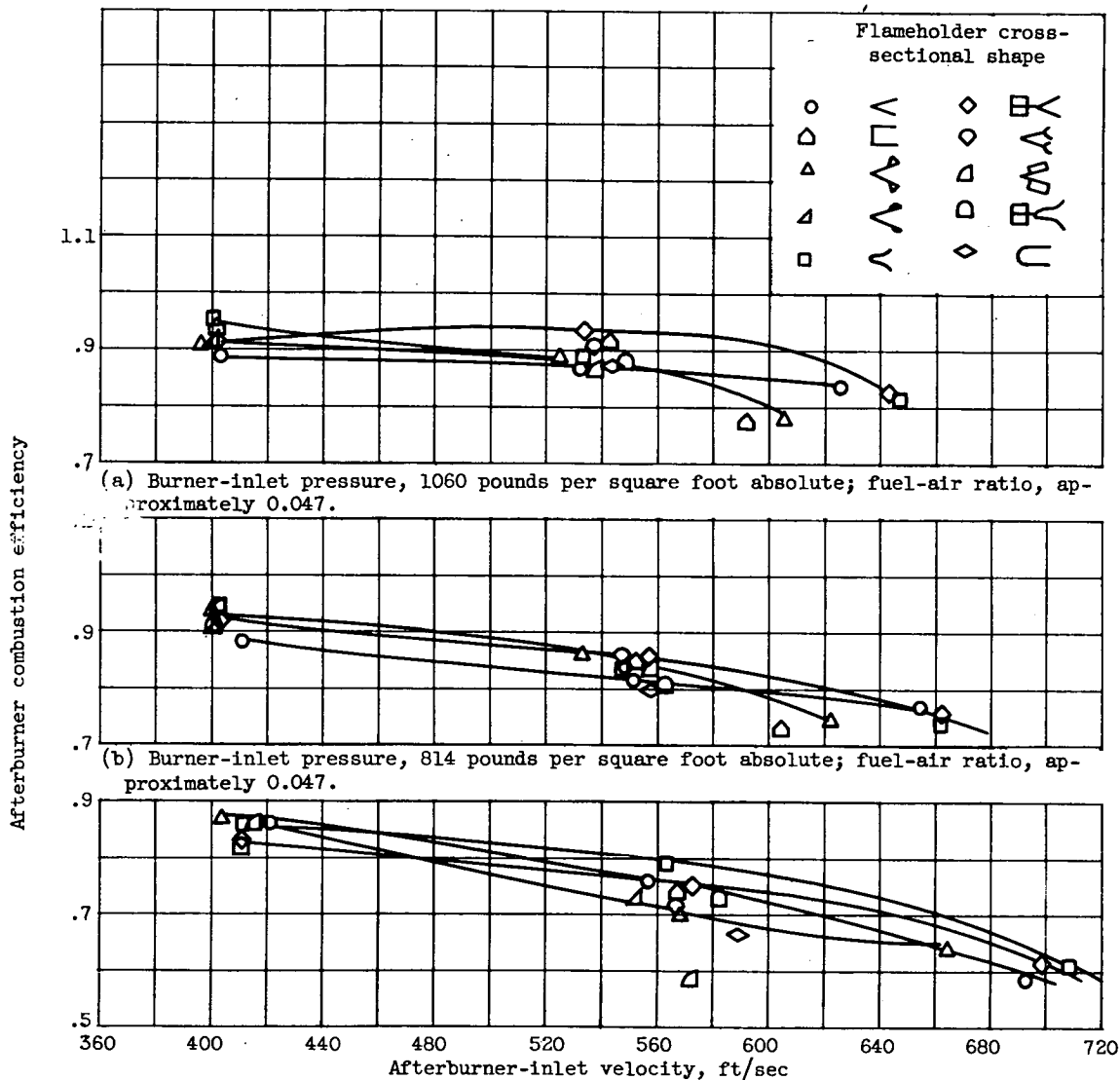


Figure 205. - Effect of flameholder cross-sectional shape on afterburner combustion efficiency as function of afterburner-inlet pressure. Afterburner fuel-air ratio, approximately 0.045.

CONFIDENTIAL

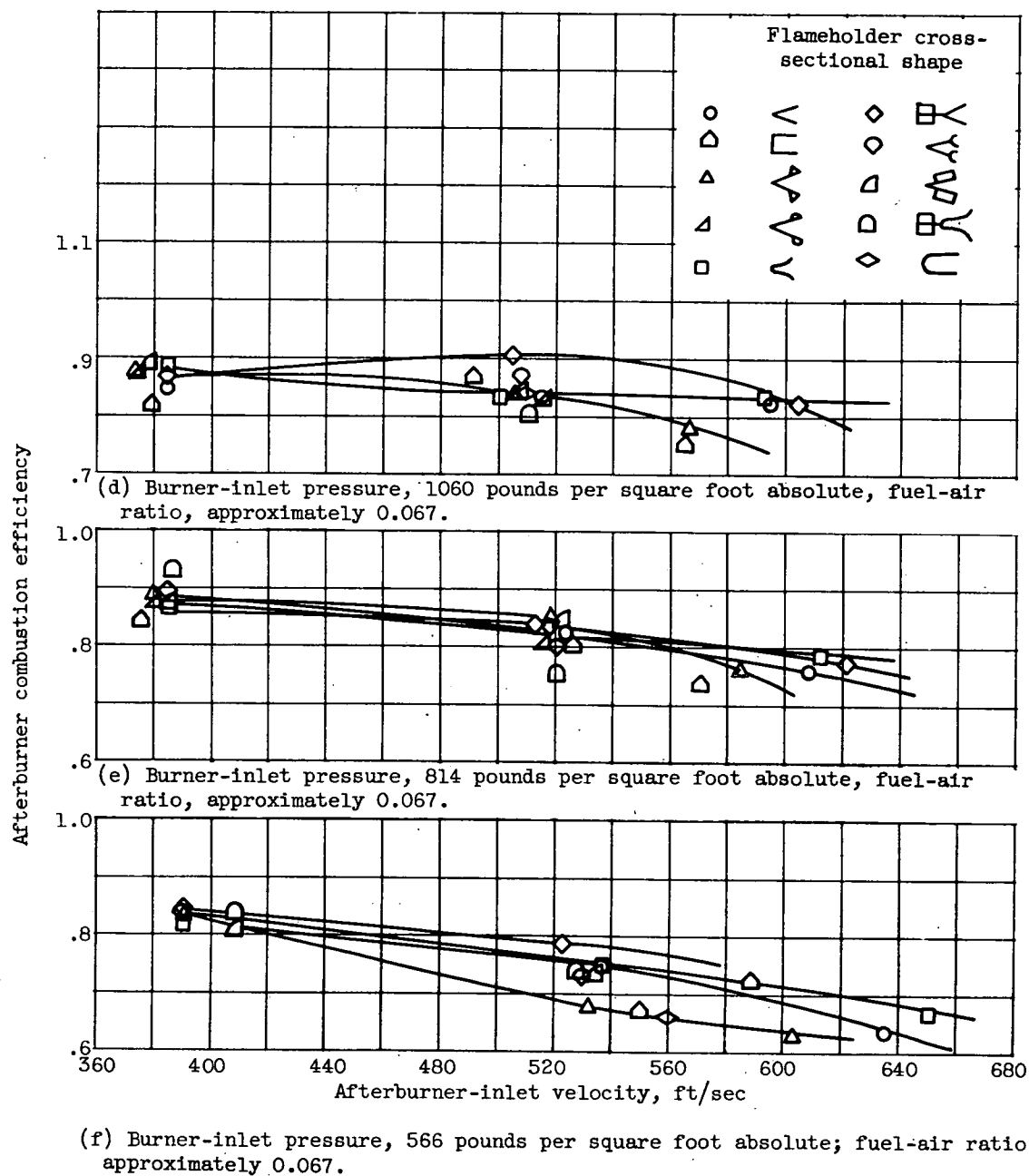


(c) Burner-inlet pressure, 566 pounds per square foot absolute; fuel-air ratio, approximately, 0.047.

Figure 206. - Effect of flameholder cross-sectional shape on afterburner as function of afterburner-inlet velocity.

~~CONFIDENTIAL~~

393



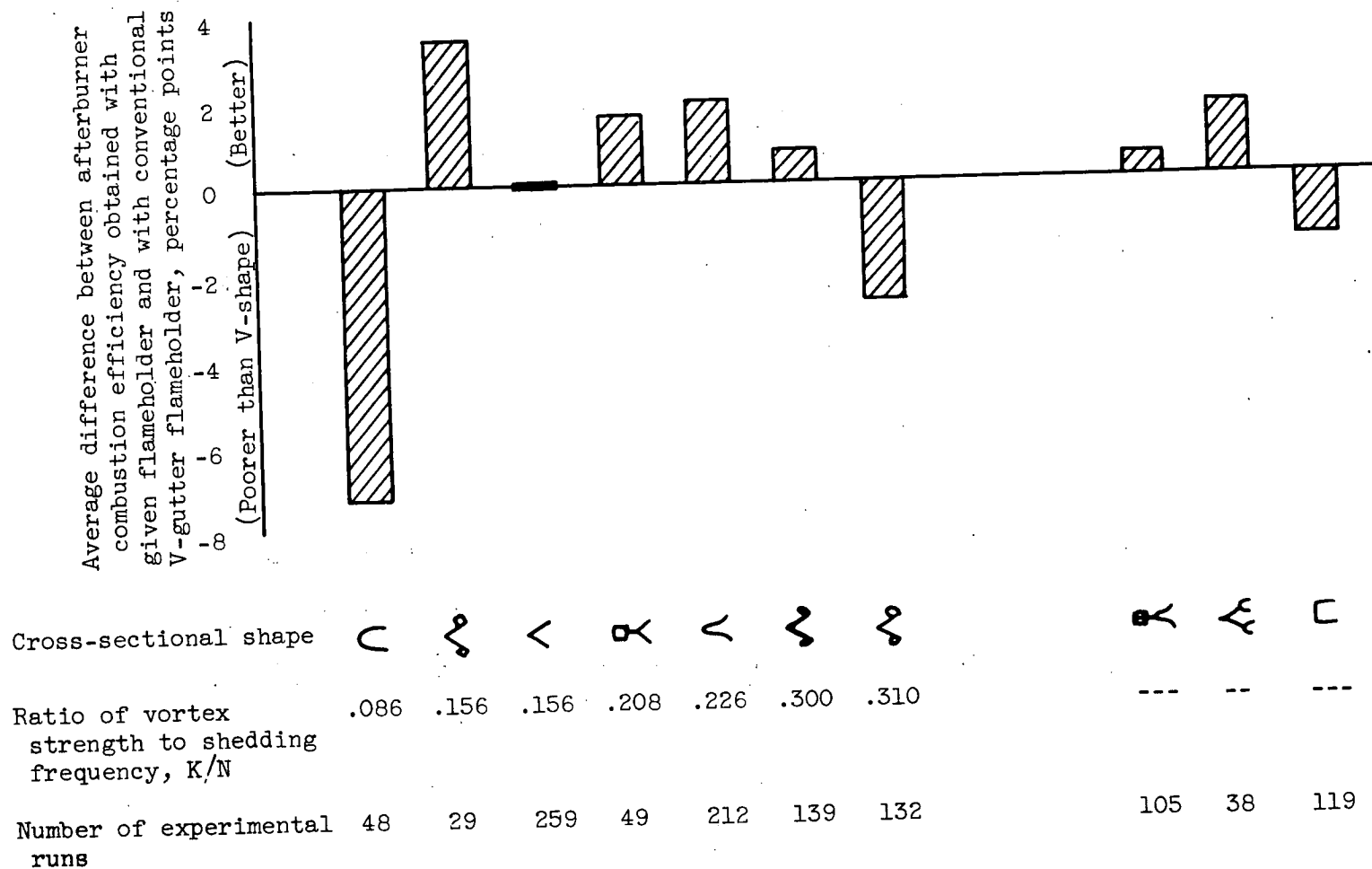


Figure 207. - Average difference in afterburner combustion efficiency obtained with various flameholder shapes.

394
CONFIDENTIAL

NACA RM E55G28

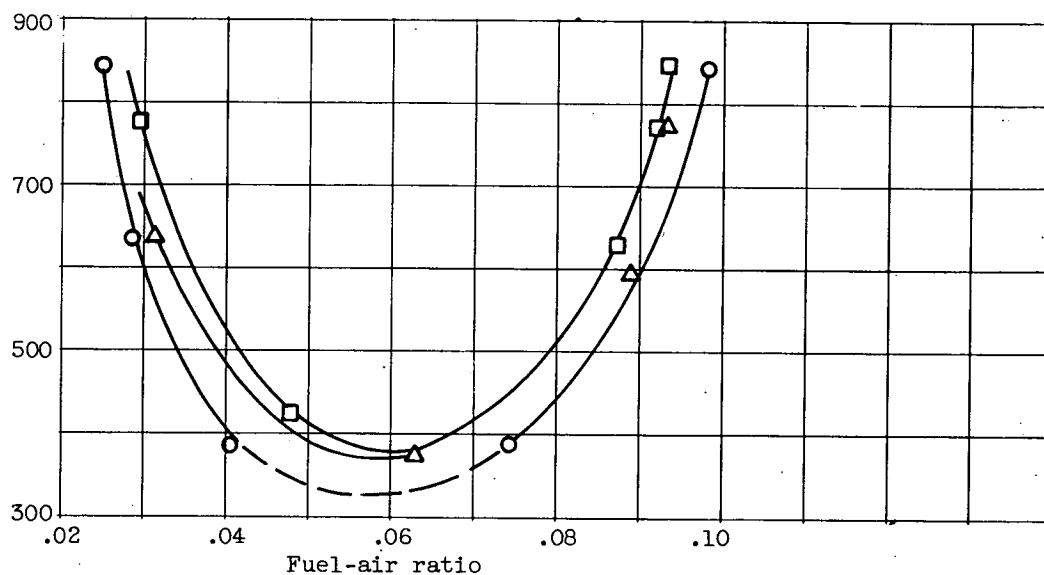
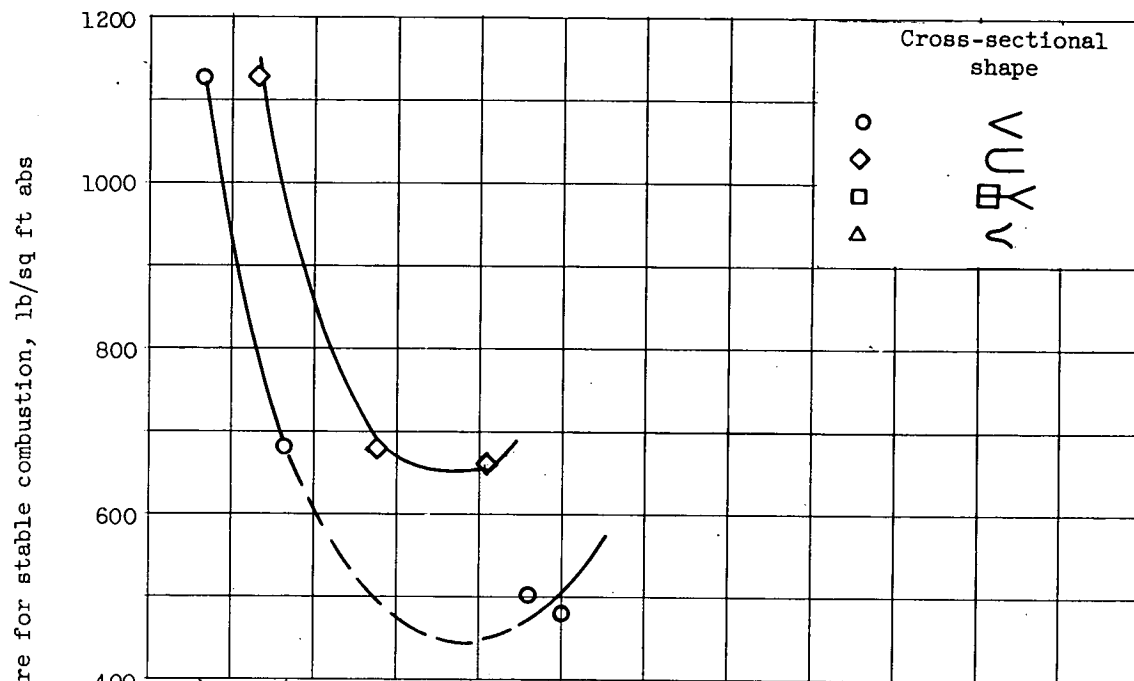
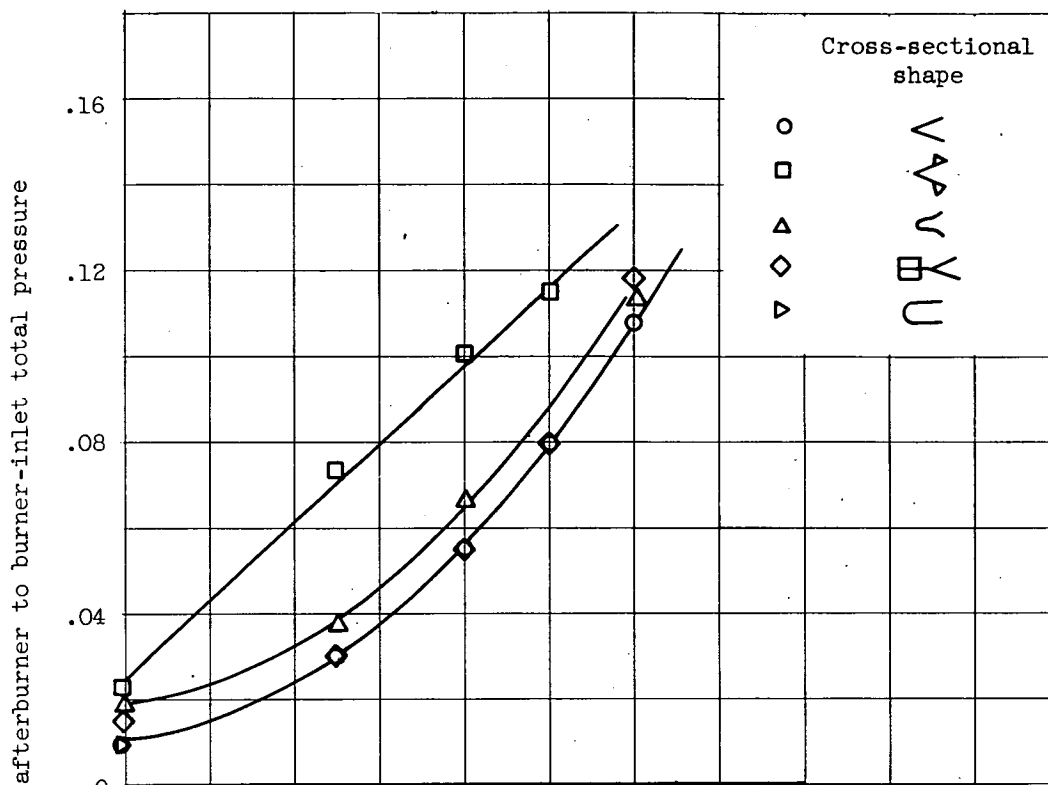
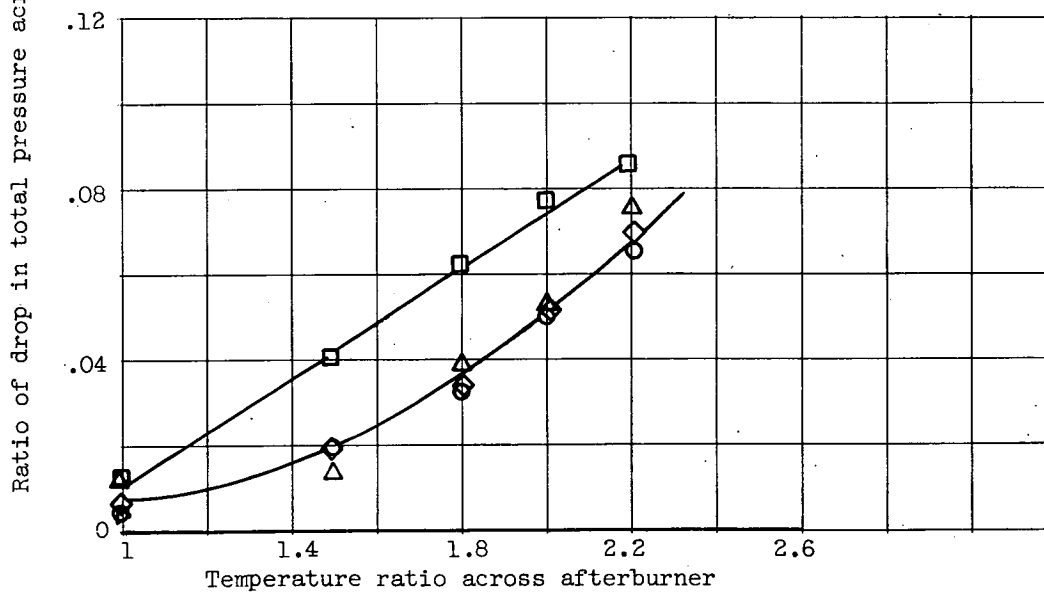


Figure 208. - Effect of flameholder cross-sectional shape on blow-out limits.



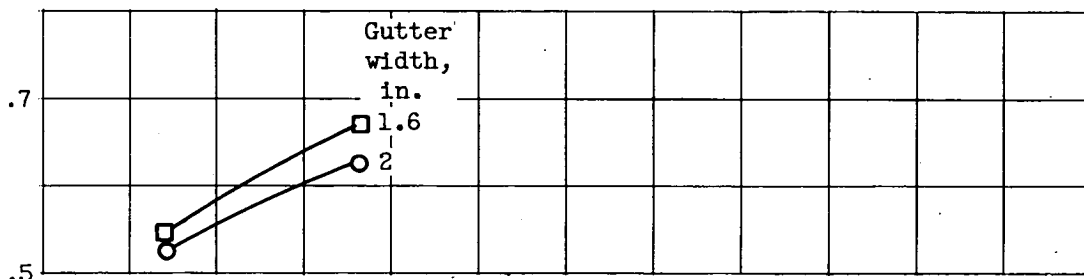
(a) Burner-inlet velocity, 600 feet per second.



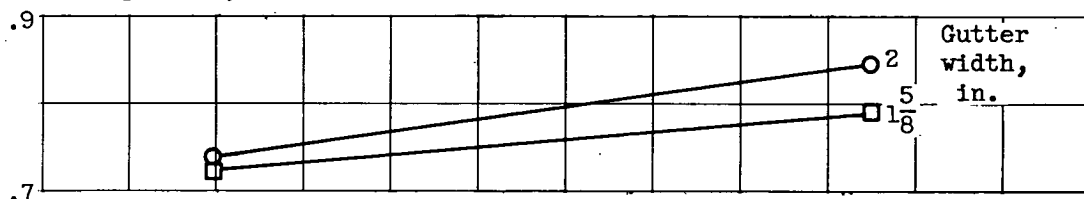
(b) Burner-inlet velocity, 500 feet per second.

Figure 209. - Effect of flameholder cross-sectional shape on afterburner pressure loss. Blockage, 29 percent.

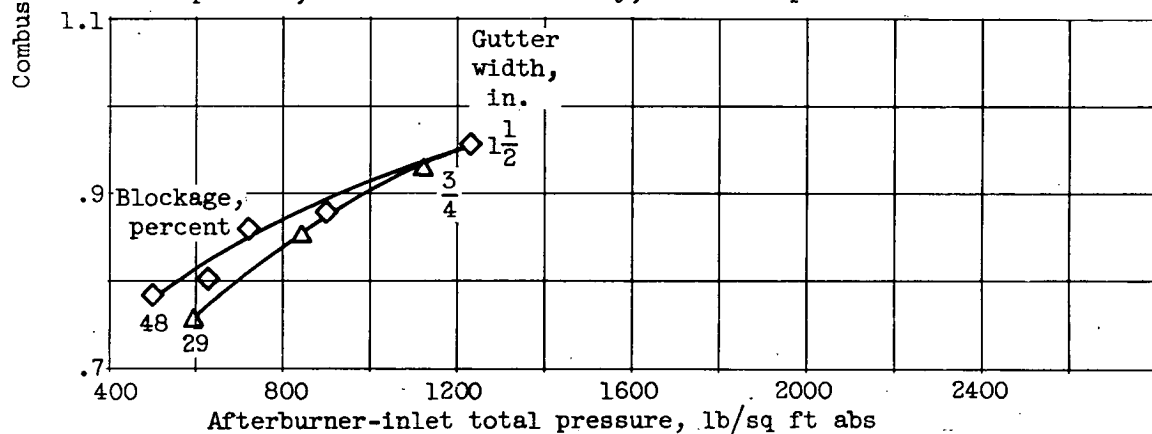
CONFIDENTIAL



(a) Fuel-area ratio, 0.04; two-ring flameholder; blockage, 27 percent; burner-inlet velocity, 450 feet per second.



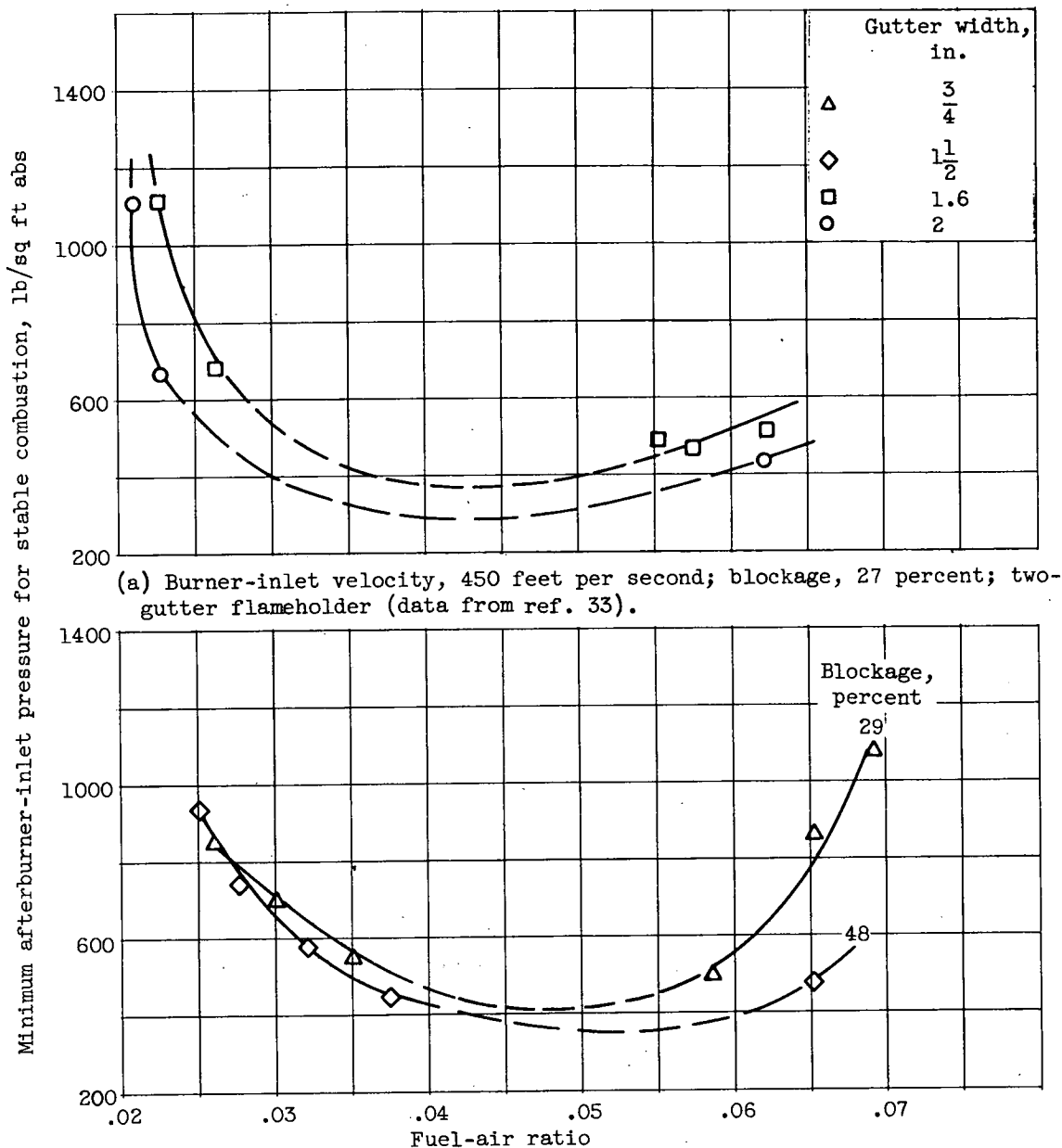
(b) Fuel-area ratio, 0.04; two-ring flameholder; blockage, 35 percent; burner-inlet velocity, 620 feet per second.



(c) Fuel-air ratio, 0.05; three-ring flameholder; burner-inlet, velocity, 520 feet per second.

Figure 210. - Effect of flameholder V-gutter width on afterburner combustion efficiency.

CONFIDENTIAL



(b) Burner-inlet velocity, 520 feet per second; three-gutter flameholder (data from ref. 32).

Figure 211. - Effects of flameholder gutter width on afterburner blow-out limits.

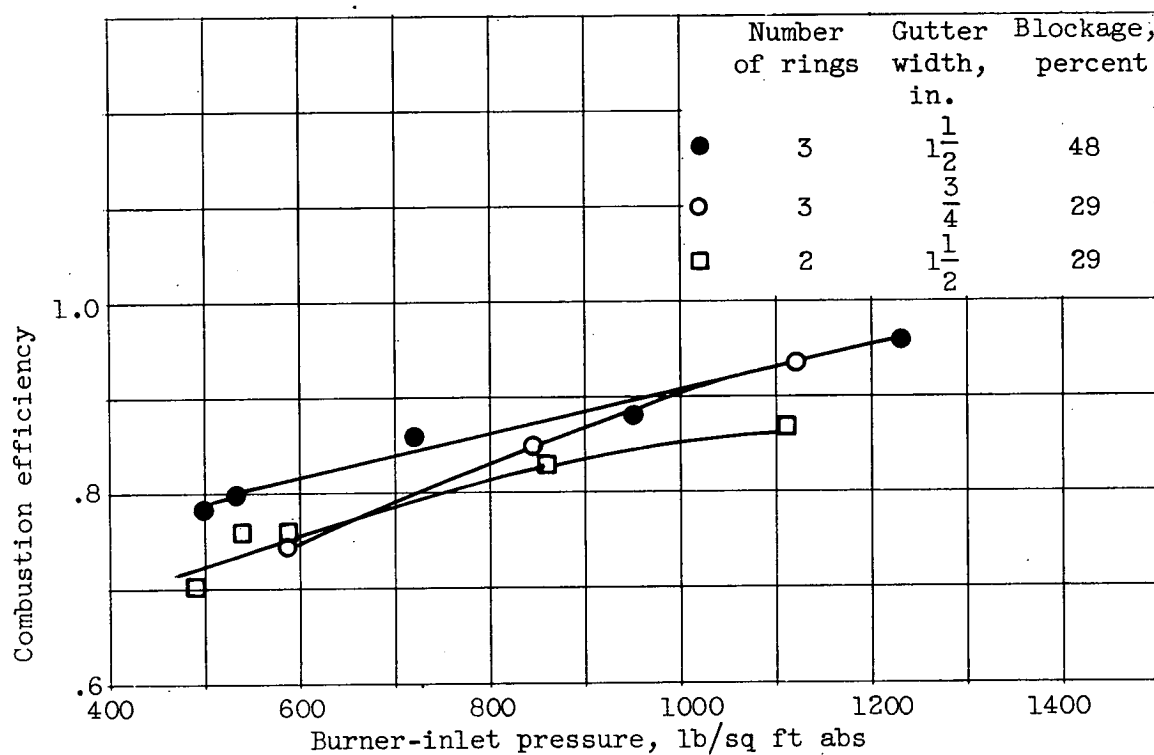


Figure 212. - Effect of number of gutters on afterburner combustion efficiency. Afterburner-inlet velocity, 520 feet per second; fuel-air ratio, 0.05.

CONFIDENTIAL

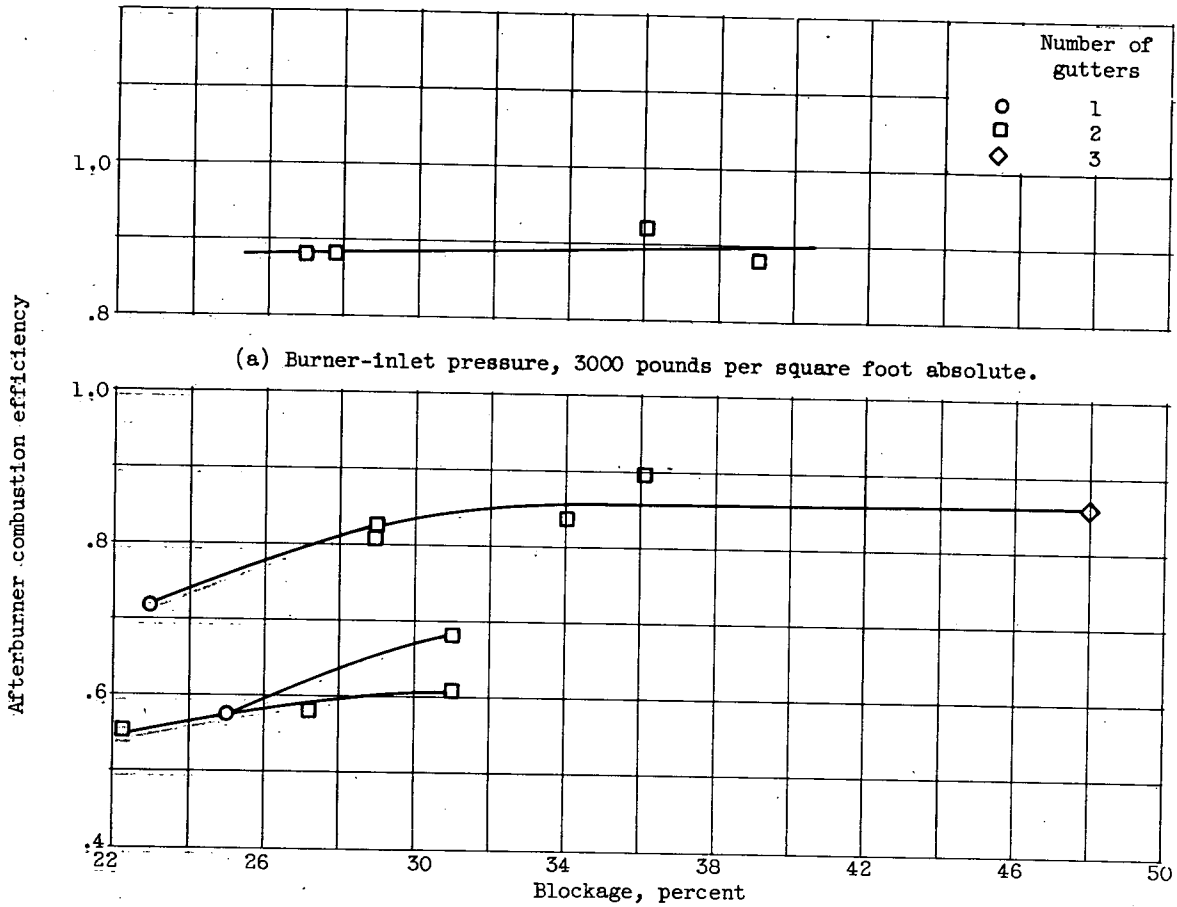


Figure 213. - Effect of blockage on afterburner combustion efficiency. Fuel-air ratio, between 0.04 and 0.05.

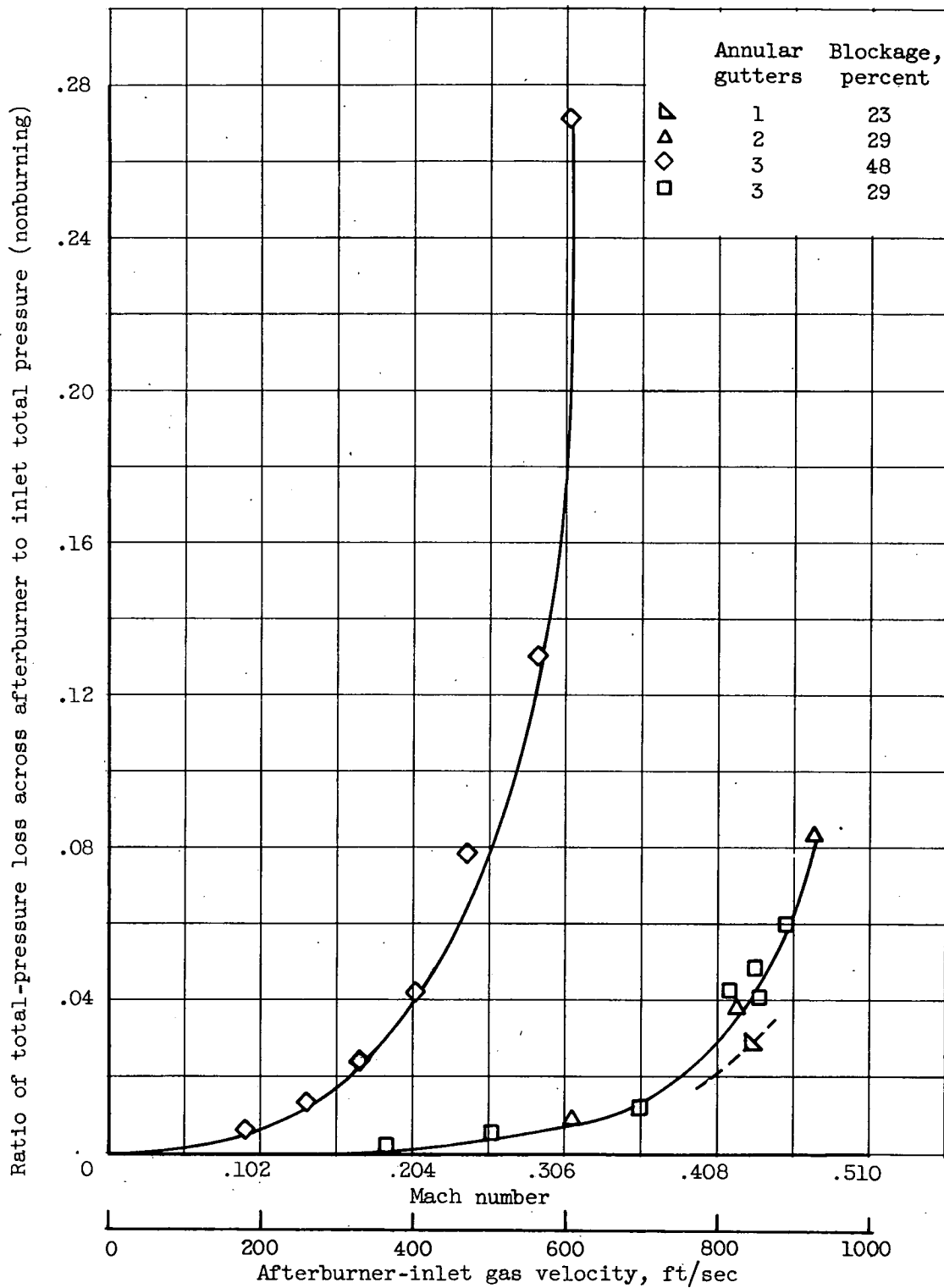


Figure 214. - Effect of afterburner-inlet gas velocity on nonburning total-pressure loss.

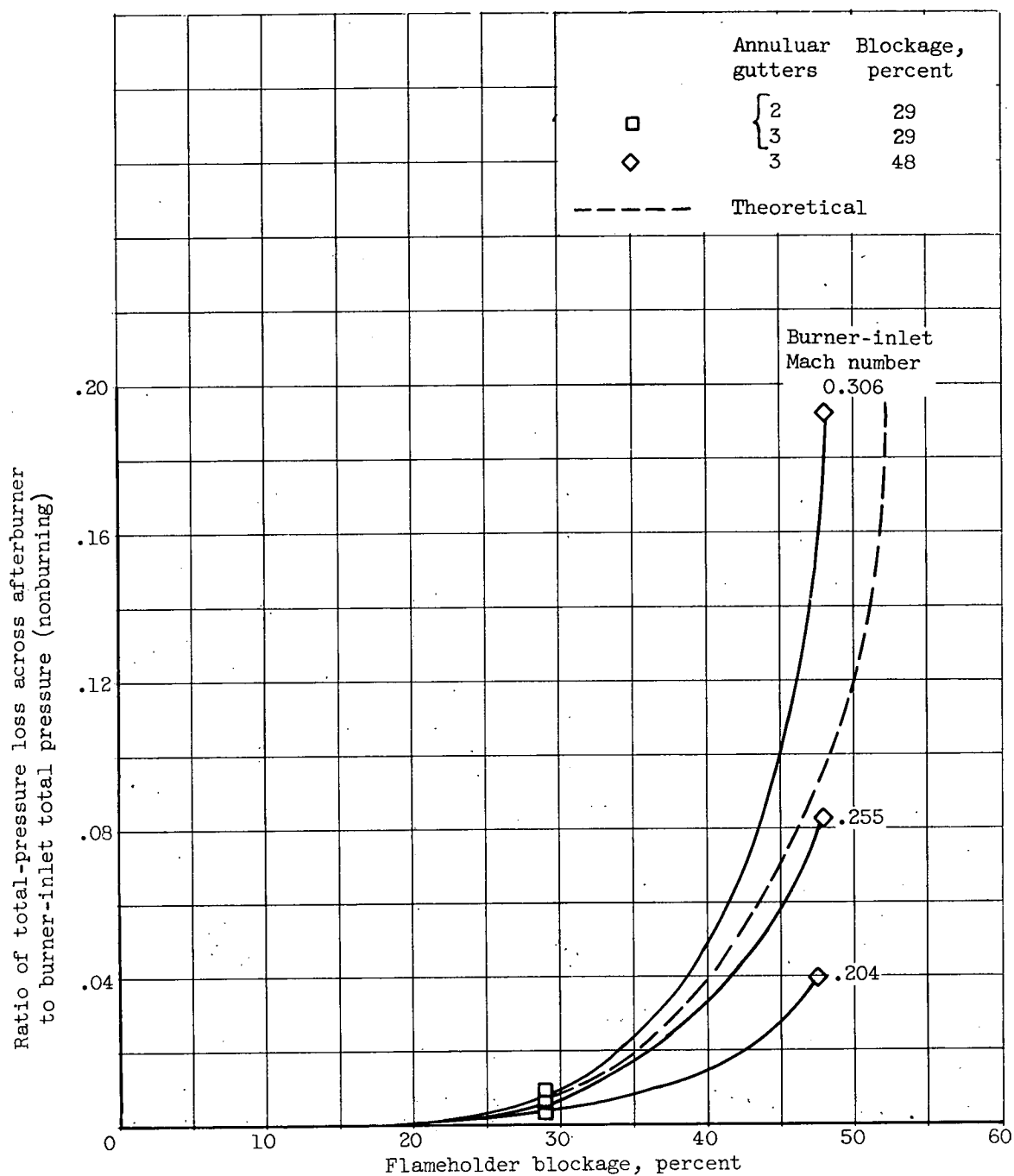
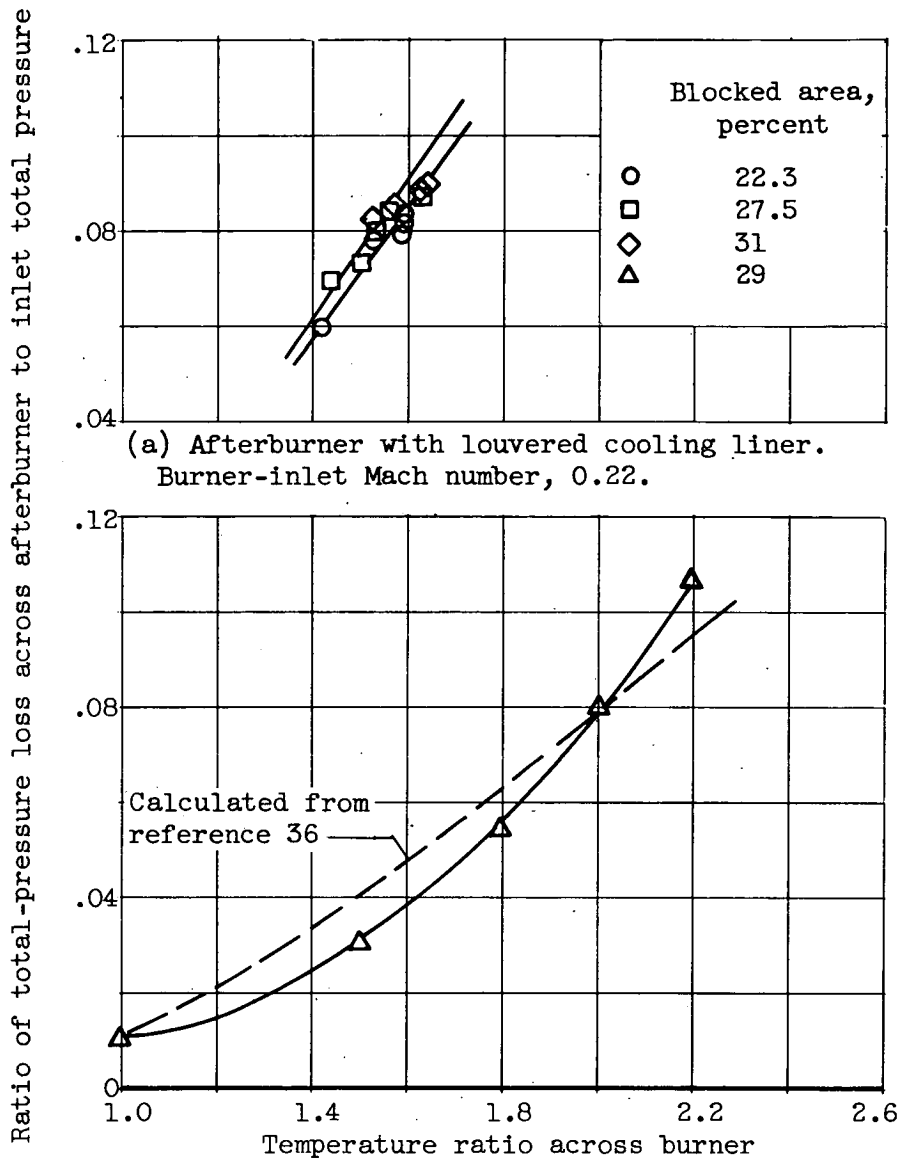


Figure 215. - Effect of flameholder blockage on nonburning total-pressure loss.



(b) Afterburner without cooling liner. Burner-inlet Mach number, approximately 0.30.

Figure 216. - Effect of temperature ratio and blocked area on pressure losses, with burning.

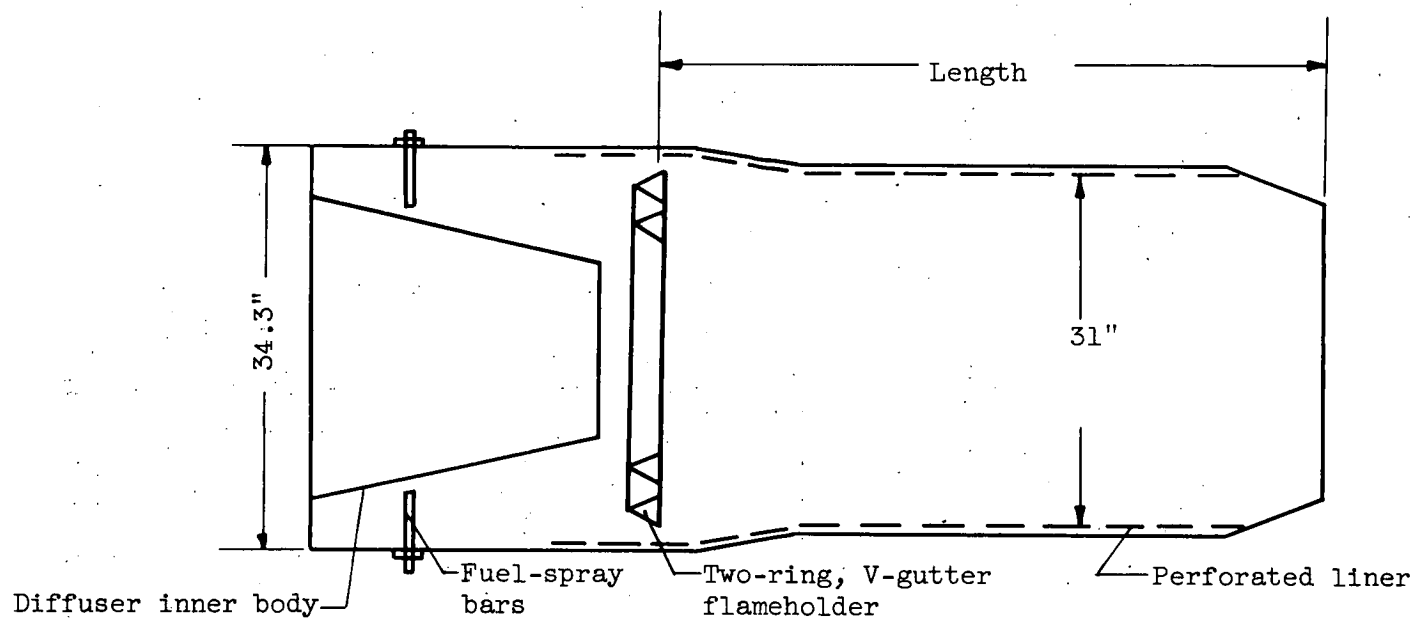
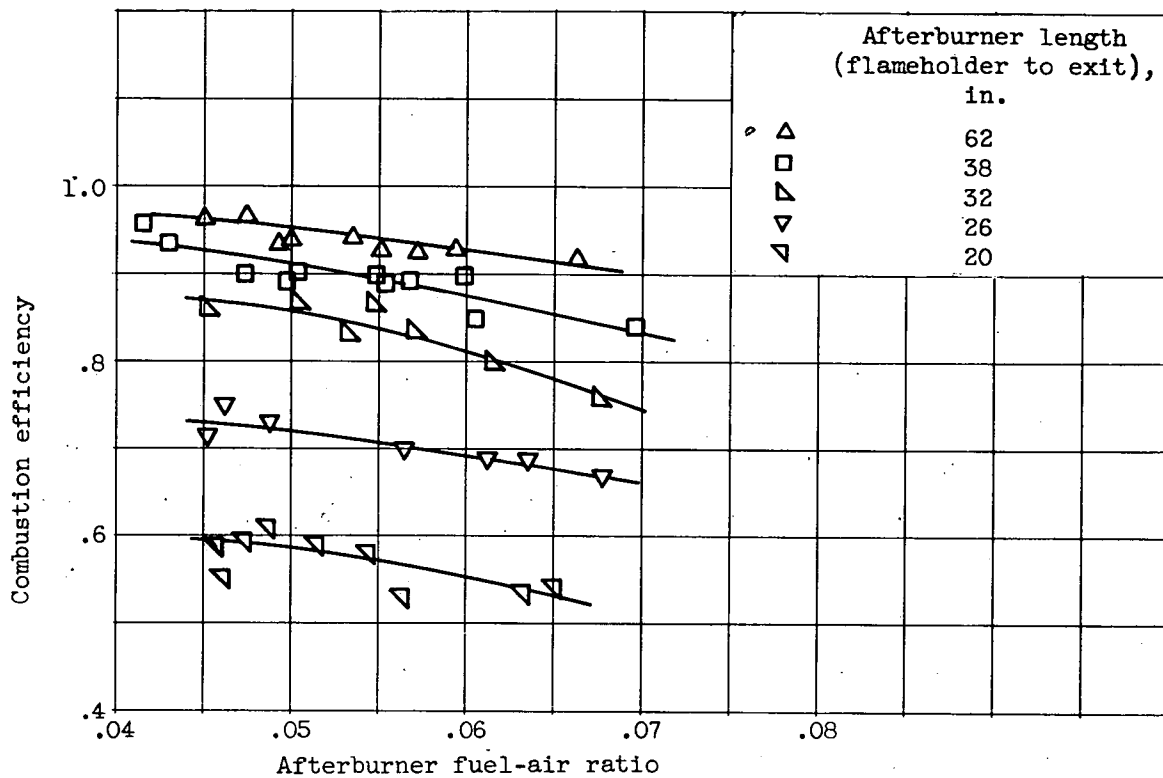


Figure 217. - Afterburner designed for take-off application.

404
CONFIDENTIAL

MACA RM E55G28

CONFIDENTIAL

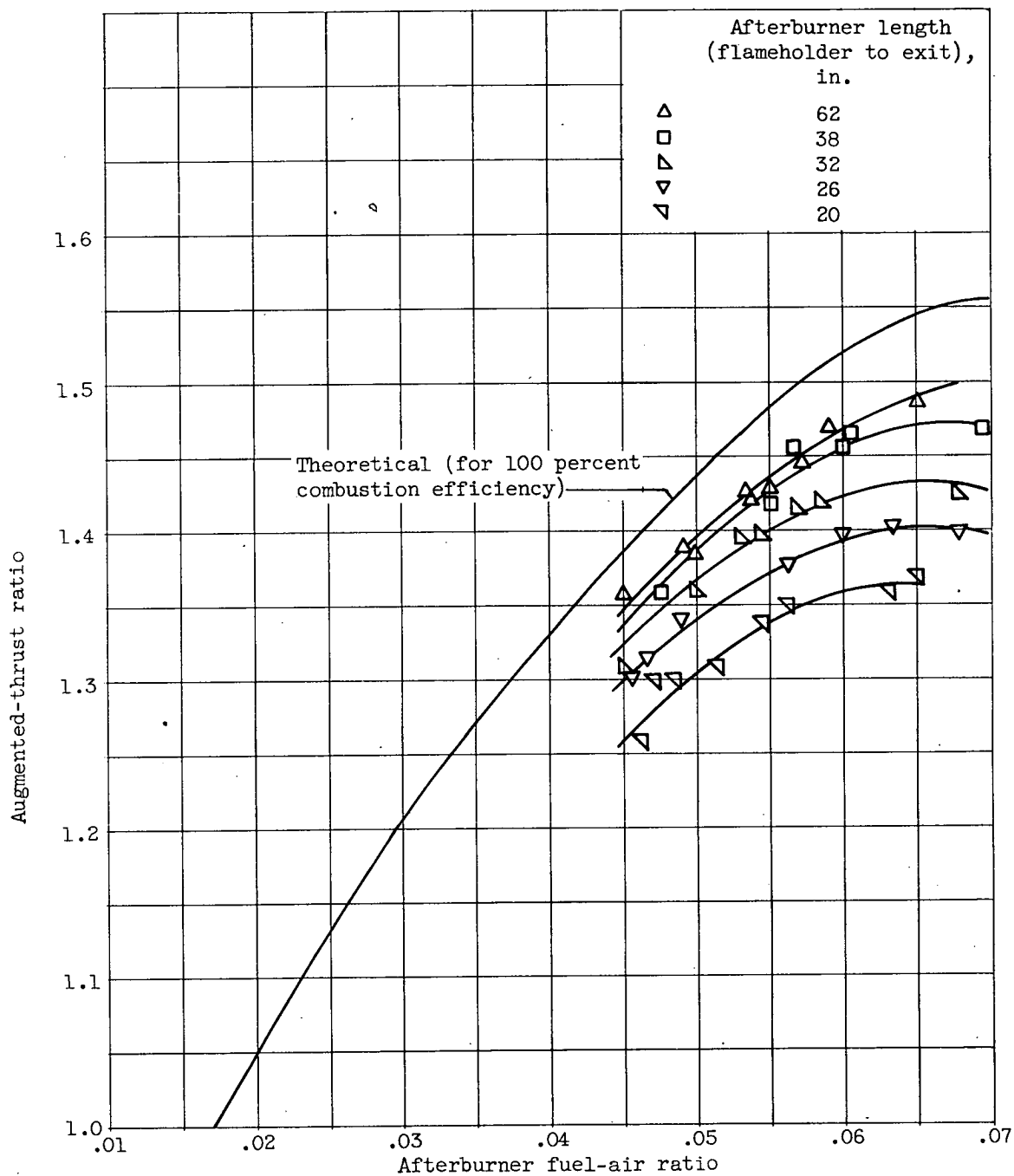


(a) Combustion efficiency.

Figure 218. - Effect of afterburner length on performance of take-off afterburner. Burner-inlet pressure, 3800 pounds per square foot absolute.

CONFIDENTIAL

CONFIDENTIAL



(b) Augmented-thrust ratio.

Figure 218. - Concluded. Effect of afterburner length on performance of take-off afterburner. Burner-inlet pressure, 3800 pounds per square foot absolute.

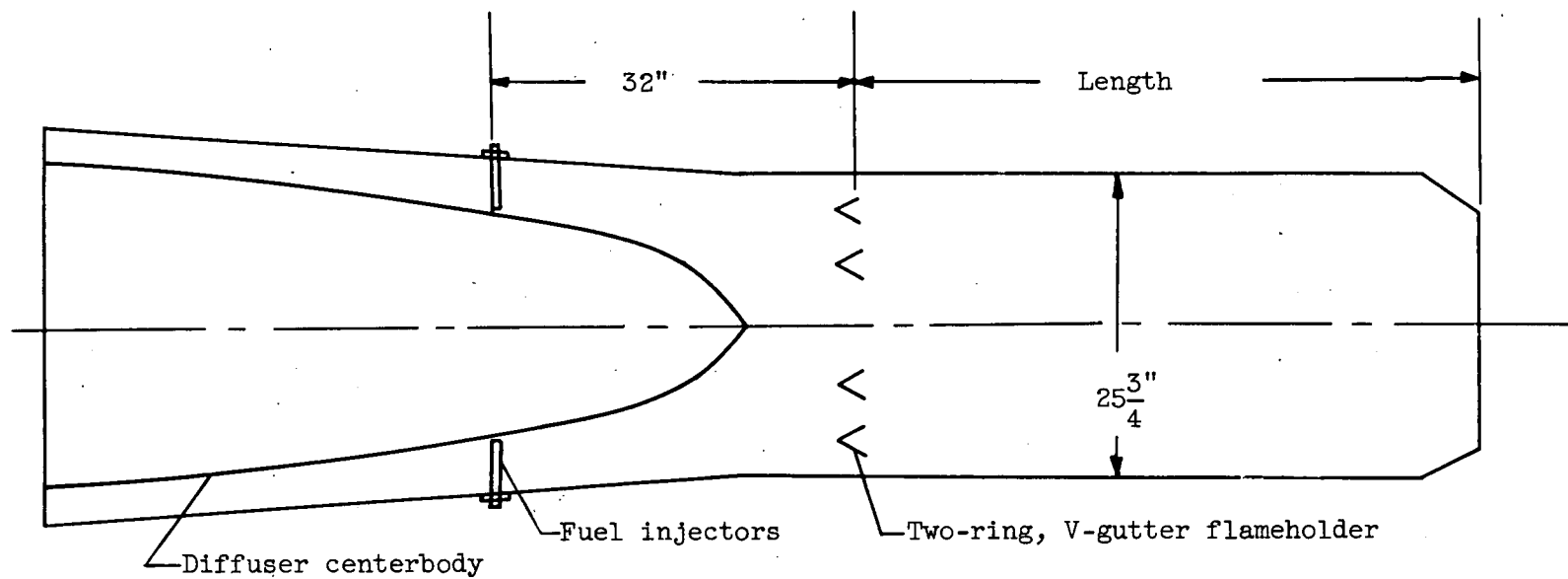
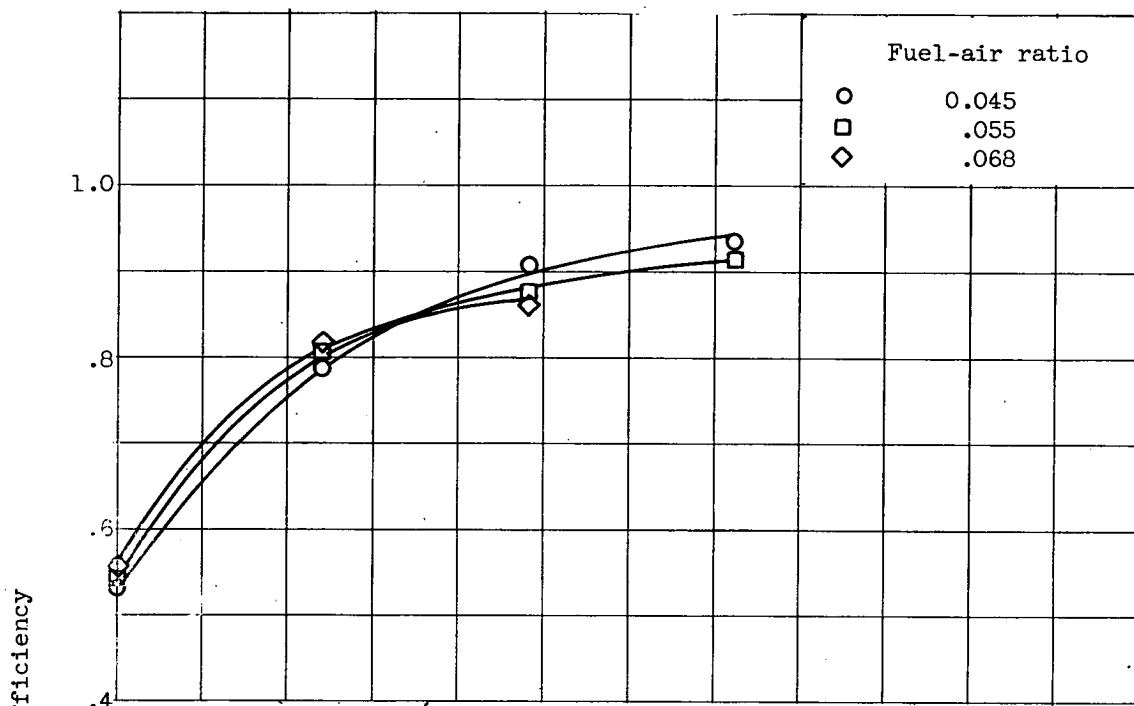
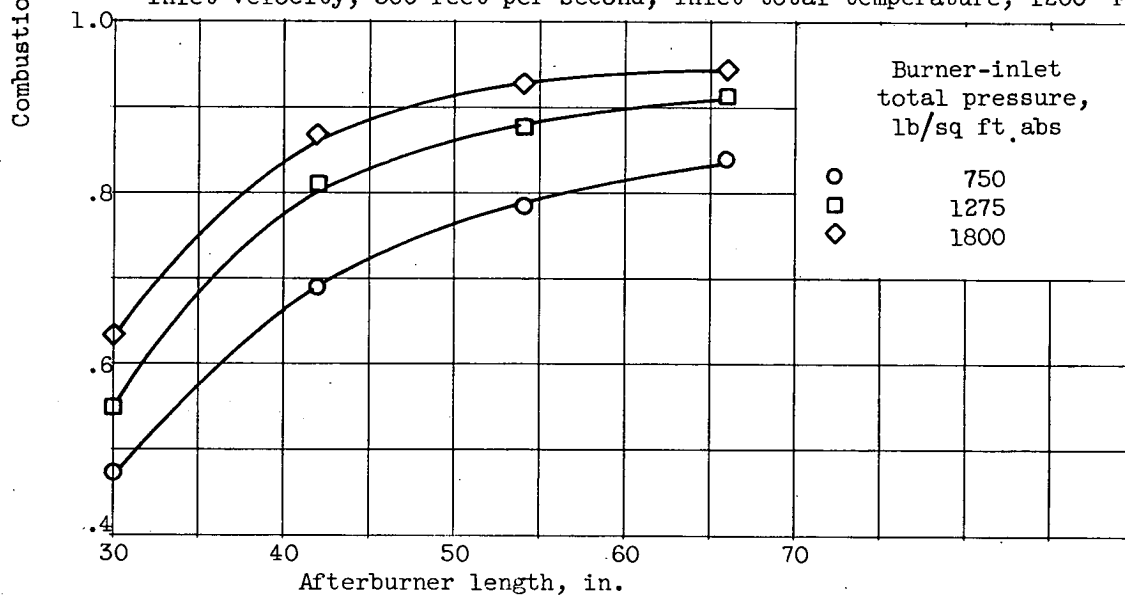


Figure 219. - Afterburner designed for high-altitude conditions.

CONFIDENTIAL



(a) Burner-inlet total pressure, 1275 pounds per square foot absolute; inlet velocity, 500 feet per second; inlet total temperature, 1200° F.

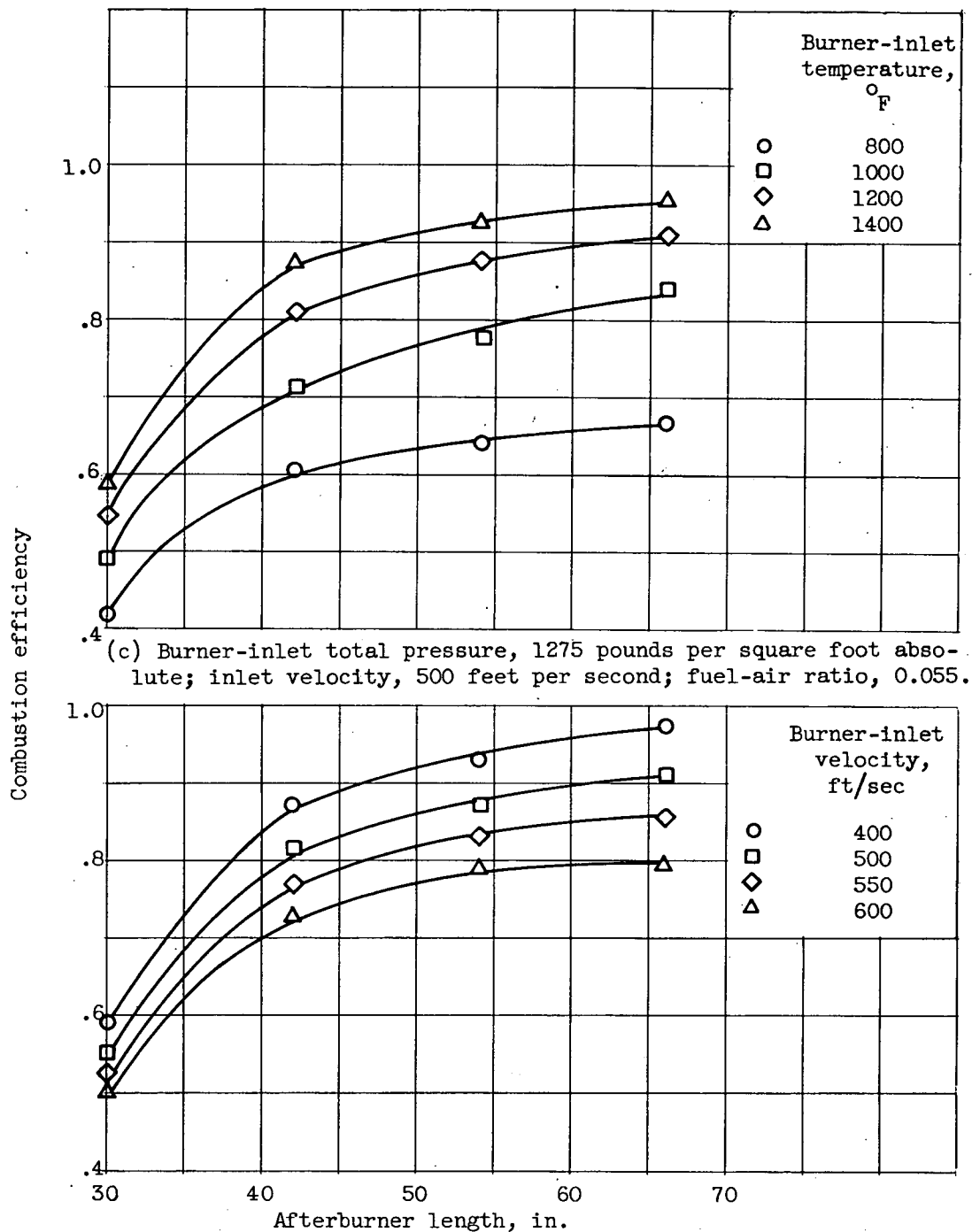


(b) Burner-inlet velocity, 500 feet per second; inlet temperature, 1200° F; fuel-air ratio, 0.055.

Figure 220. - Effect of afterburner length on performance of high-altitude afterburner.

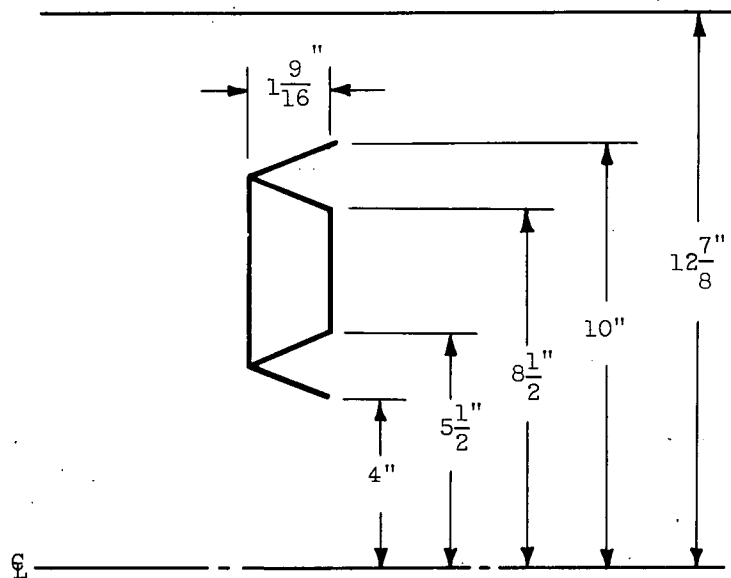
CONFIDENTIAL

409

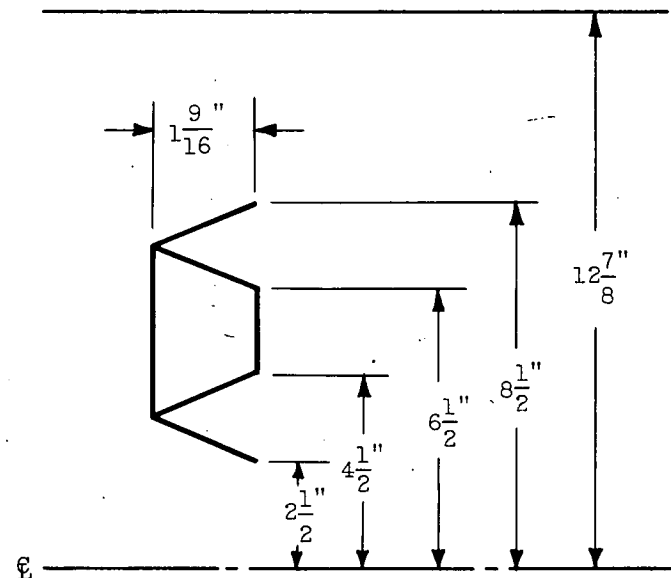


(d) Burner-inlet total pressure, 1275 pounds per square foot absolute; inlet temperature, 1200° F; fuel-air ratio, 0.055.

Figure 220. - Concluded. Effect of afterburner length on performance of high-altitude afterburner.



(a) Original flameholder with optimum gutter diameters.



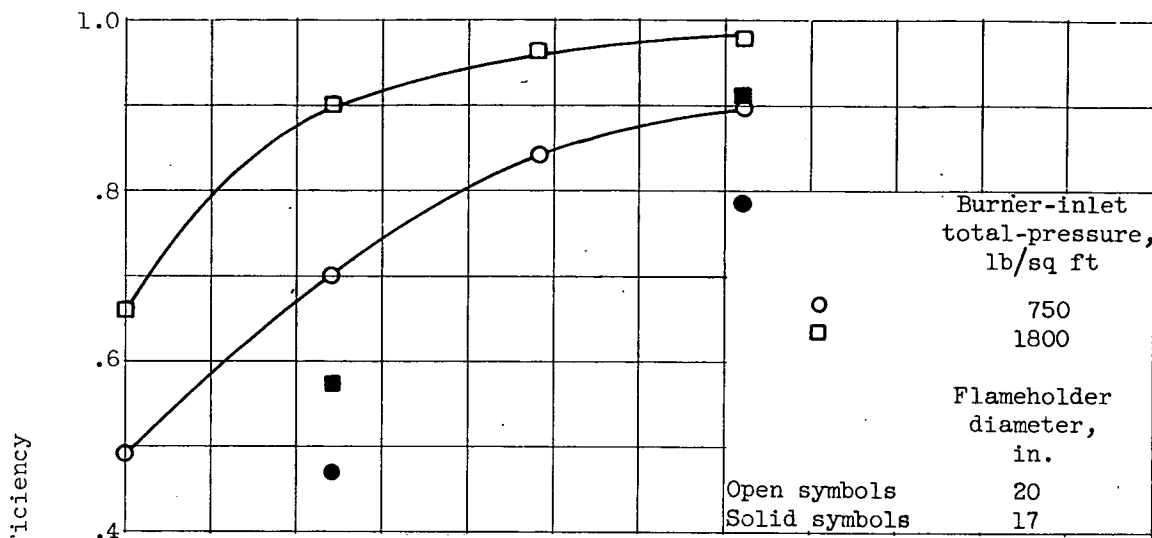
(b) Modified flameholder with reduced gutter diameters.

Figure 221. - Comparison of flameholders with optimum and reduced gutter diameters.

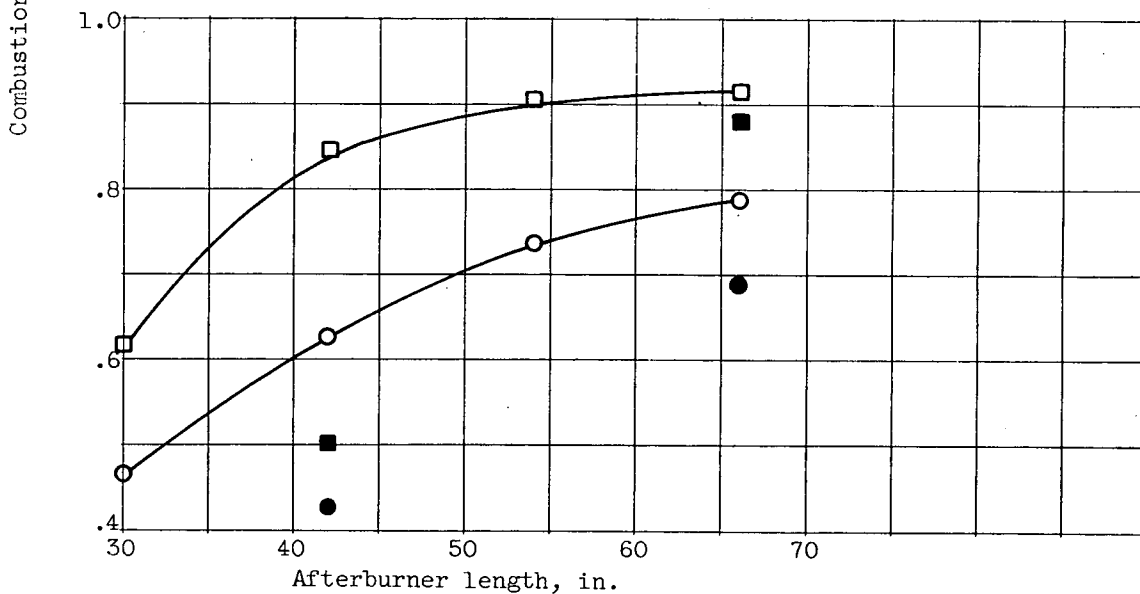
410
CONFIDENTIAL

NACA RM E55G28

DECLASSIFIED



(a) Burner-inlet velocity, 400 feet per second.



(b) Burner-inlet velocity, 550 feet per second.

Figure 222. - Effect of reduced flameholder-gutter diameter on combustion efficiency. Burner-inlet total temperature, 1200° F; fuel-air ratio, 0.055.

CONFIDENTIAL

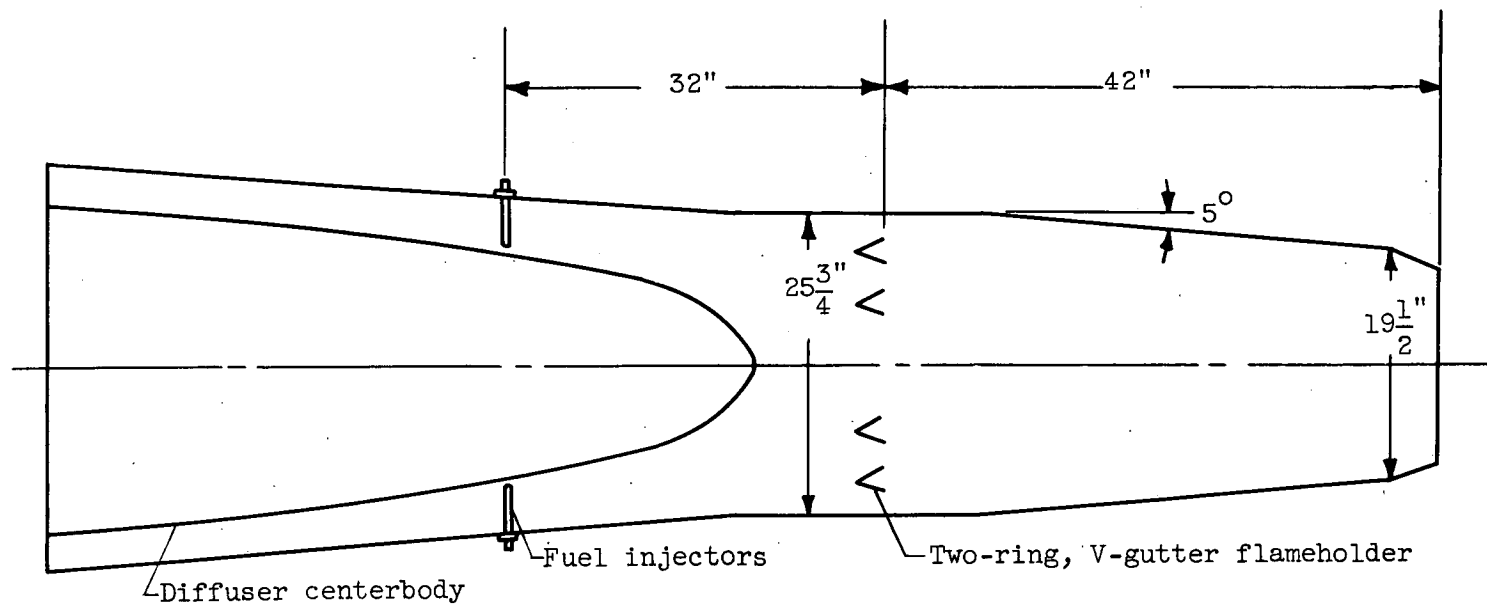
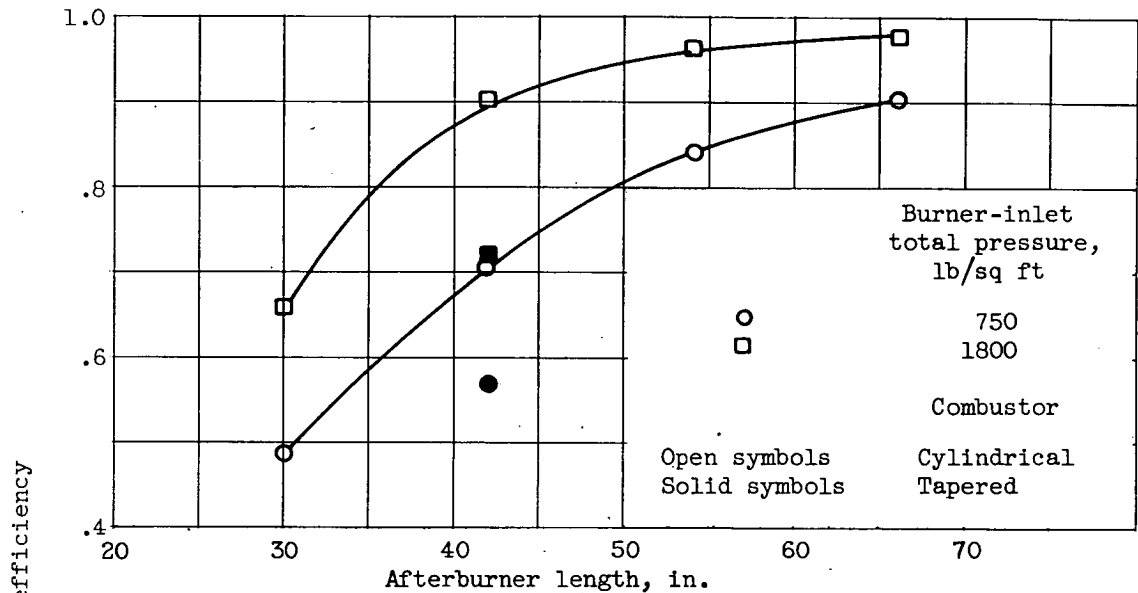
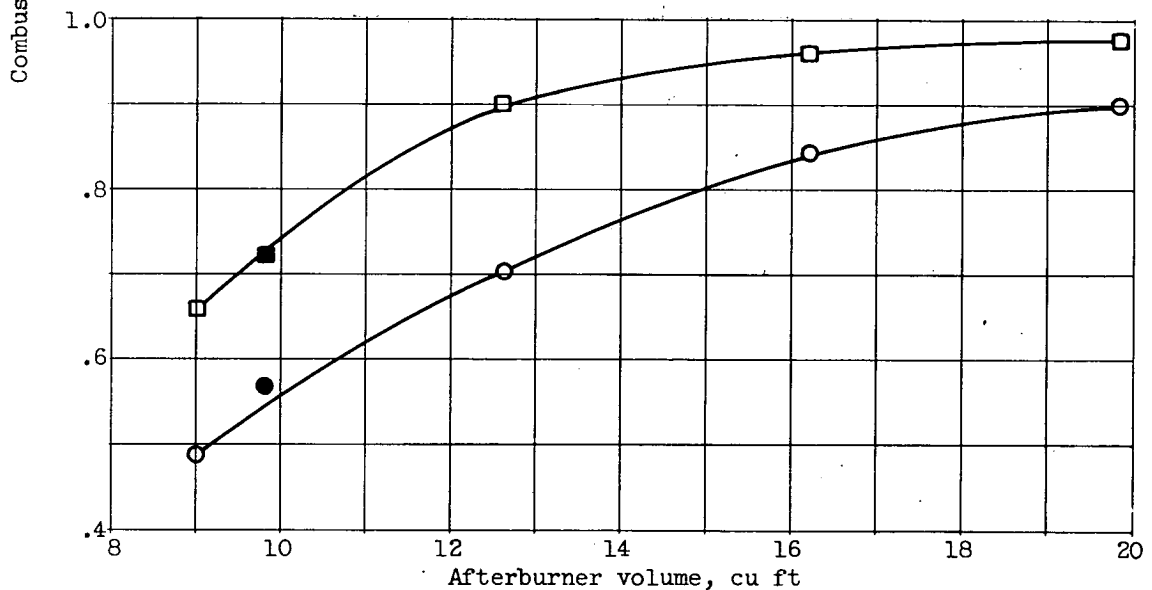


Figure 223. - Tapered afterburner designed for high-altitude operation.

CONFIDENTIAL



(a) Variation of efficiency with afterburner length.



(b) Variation of efficiency with afterburner volume.

Figure 224. - Effect of afterburner-shell taper on combustion efficiency.
 Burner-inlet velocity, 400 feet per second; inlet total temperature,
 1200° F; fuel-air ratio, 0.055.

CONFIDENTIAL

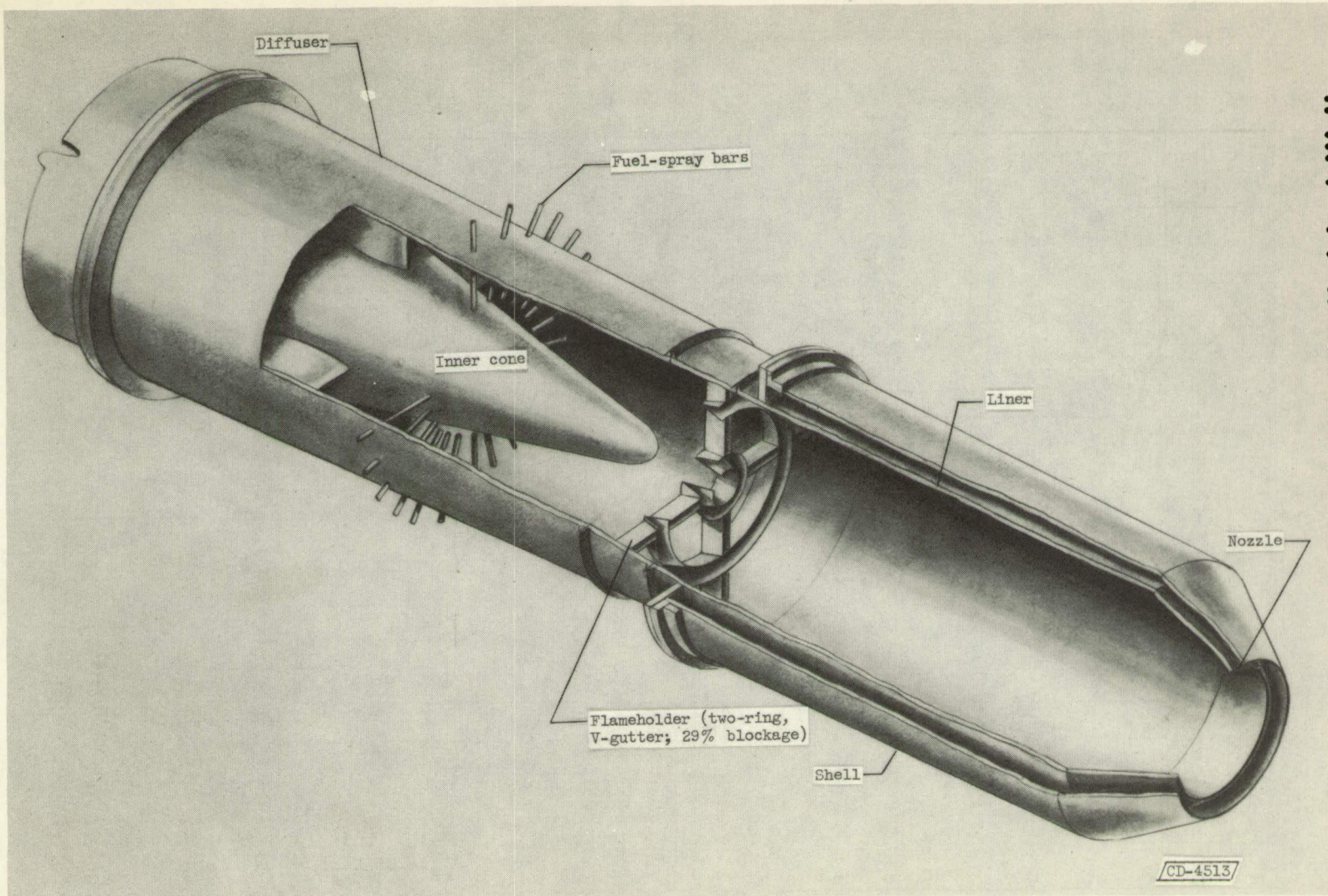


Figure 225. - Cutaway view of afterburner.

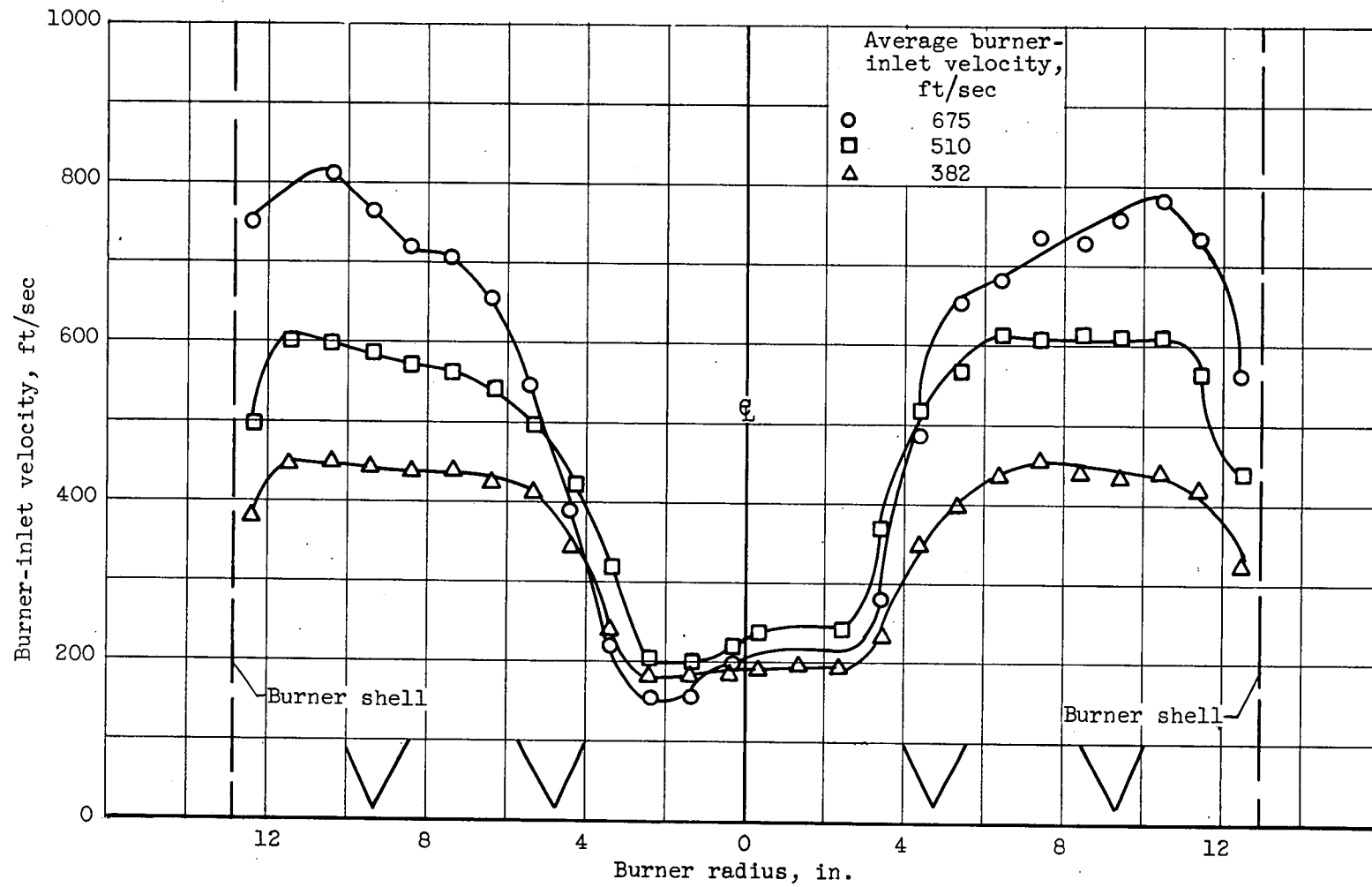
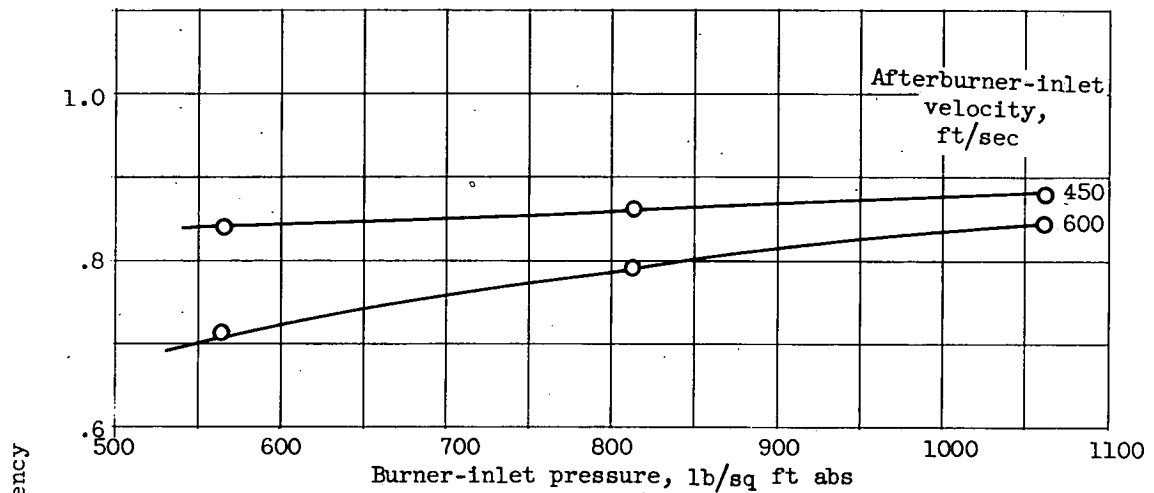
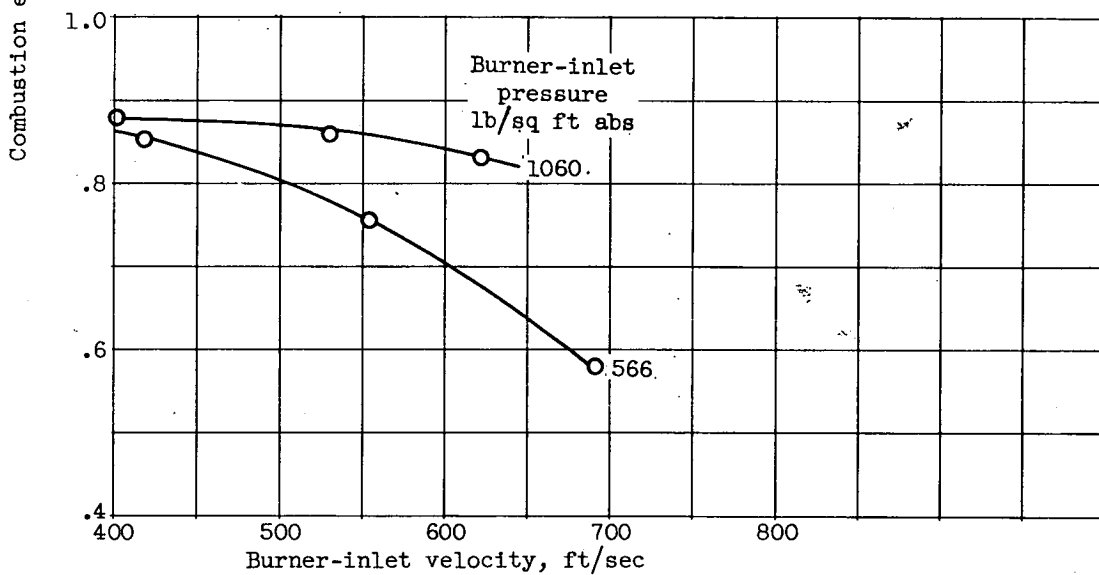


Figure 226. - Velocity profile at burner inlet showing relative location of flameholder gutters.

0371020000



(a) Effect of burner-inlet pressure.



(b) Effect of burner-inlet velocity.

Figure 227. - Effect of inlet pressure and inlet velocity on combustion efficiency of afterburner. Blockage, 30 percent; V-gutter flameholder; fuel-air ratio, 0.047.

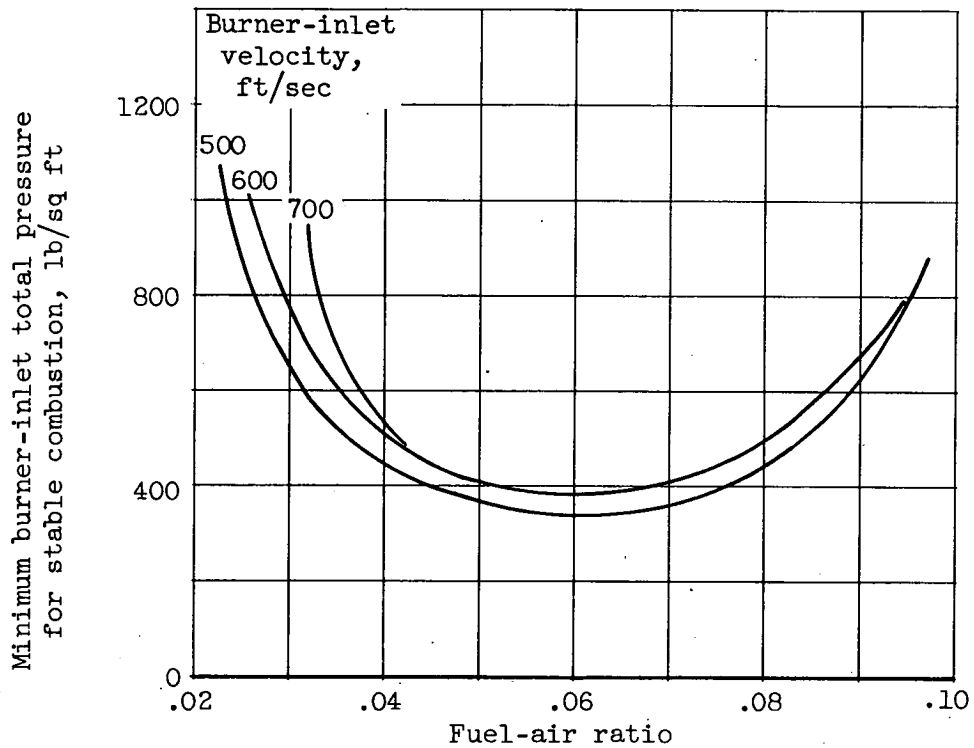


Figure 228. - Effect of velocity on stable operating range of afterburner with 30-percent-blocked-area V-gutter flameholder.

CONFIDENTIAL

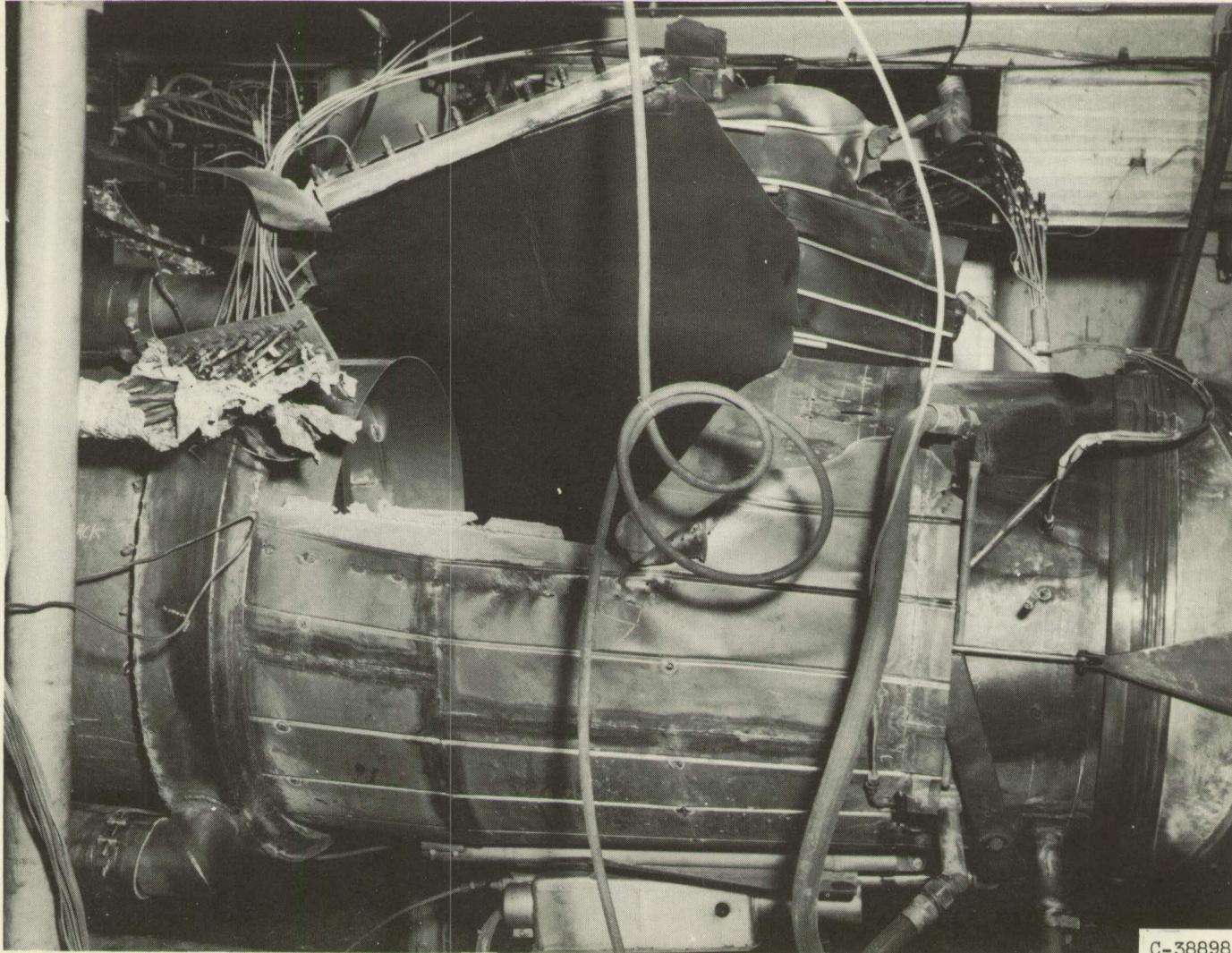
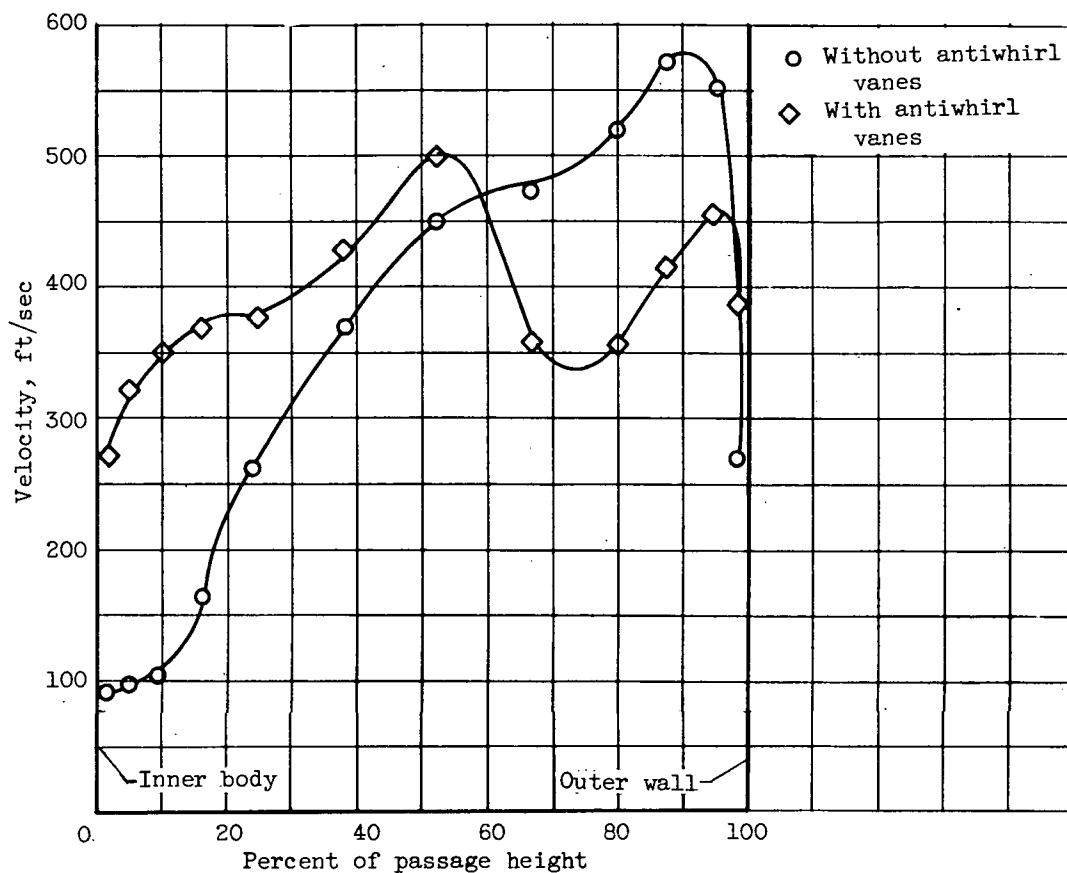


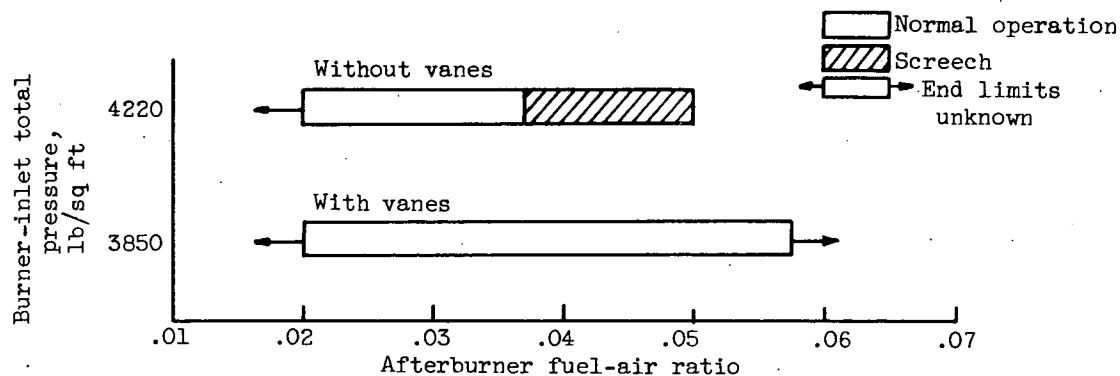
Figure 229. - Burner damaged by screech.

CONFIDENTIAL

DECLASSIFIED



(a) Diffuser-exit velocity profile.



(b) Screech limits.

Figure 230. - Effect of radial distribution of velocity at afterburner inlet on screech limits.

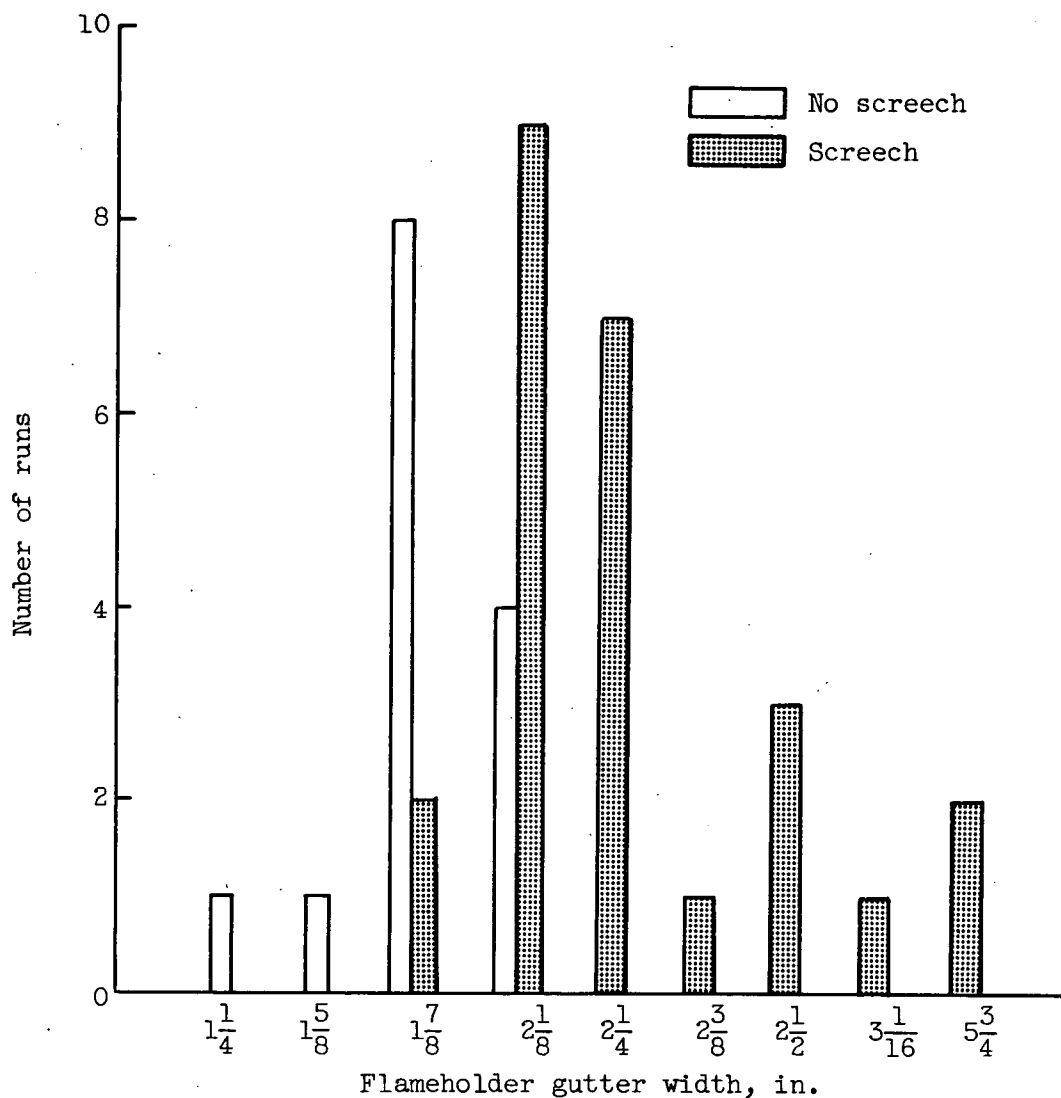
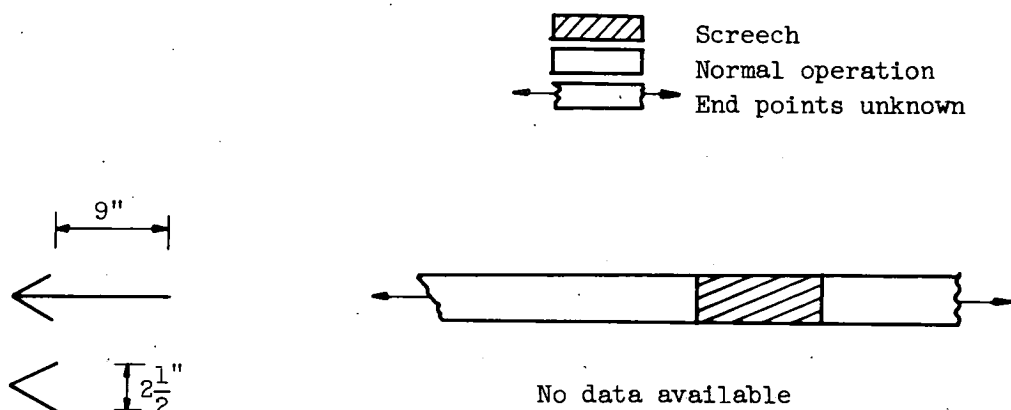


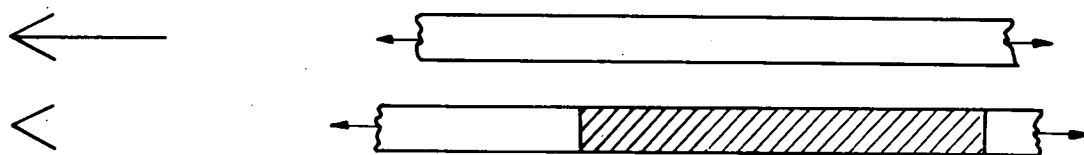
Figure 231. - Influence of flameholder gutter width on occurrence of screech. Burner-inlet total pressure, 3850 to 4220 pounds per square foot absolute; flameholder blockage, 32 to 40 percent of flow area.

CONFIDENTIAL
DECLASSIFIED

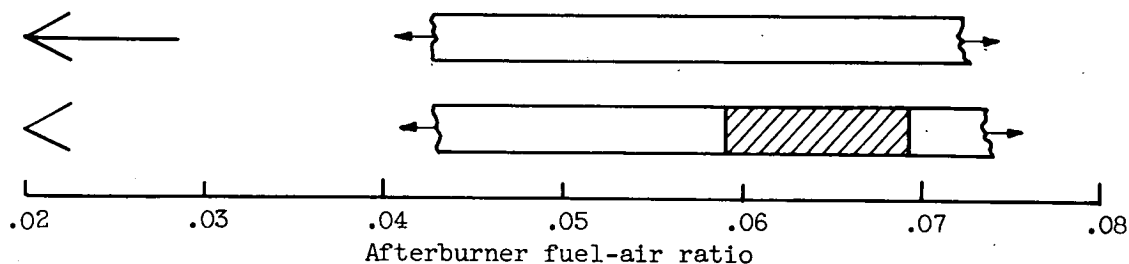
3925



(a) Burner-inlet pressure, 1080 pounds per square foot.



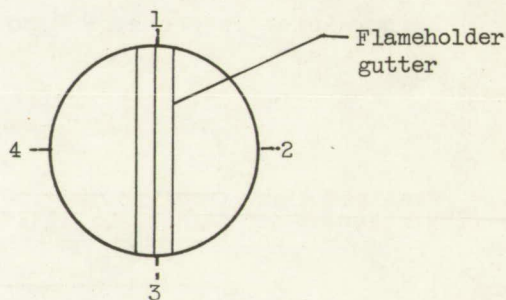
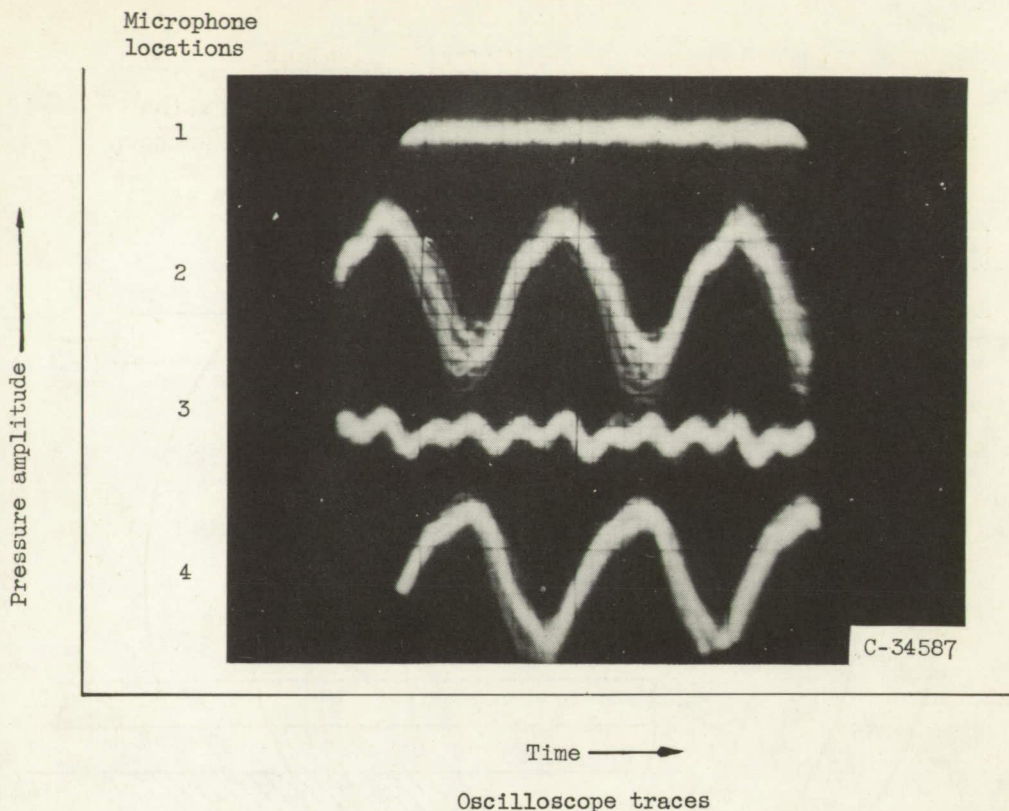
(b) Burner-inlet pressure, 990 pounds per square foot.



(c) Burner-inlet pressure, 870 pounds per square foot.

Figure 232. - Effect of flameholder splitter on screech limits.

CONFIDENTIAL



Microphone locations;
downstream view.

Figure 233. - Phase relations of screech oscillations in 26-inch-diameter afterburner with diametrical V-gutter flameholder. Microphones equally spaced; location of microphone taps, 1.0 inch downstream of flameholder; flameholder width, 8 inches; screech frequency, 650 cycles per second.

CONFIDENTIAL

CONFIDENTIAL

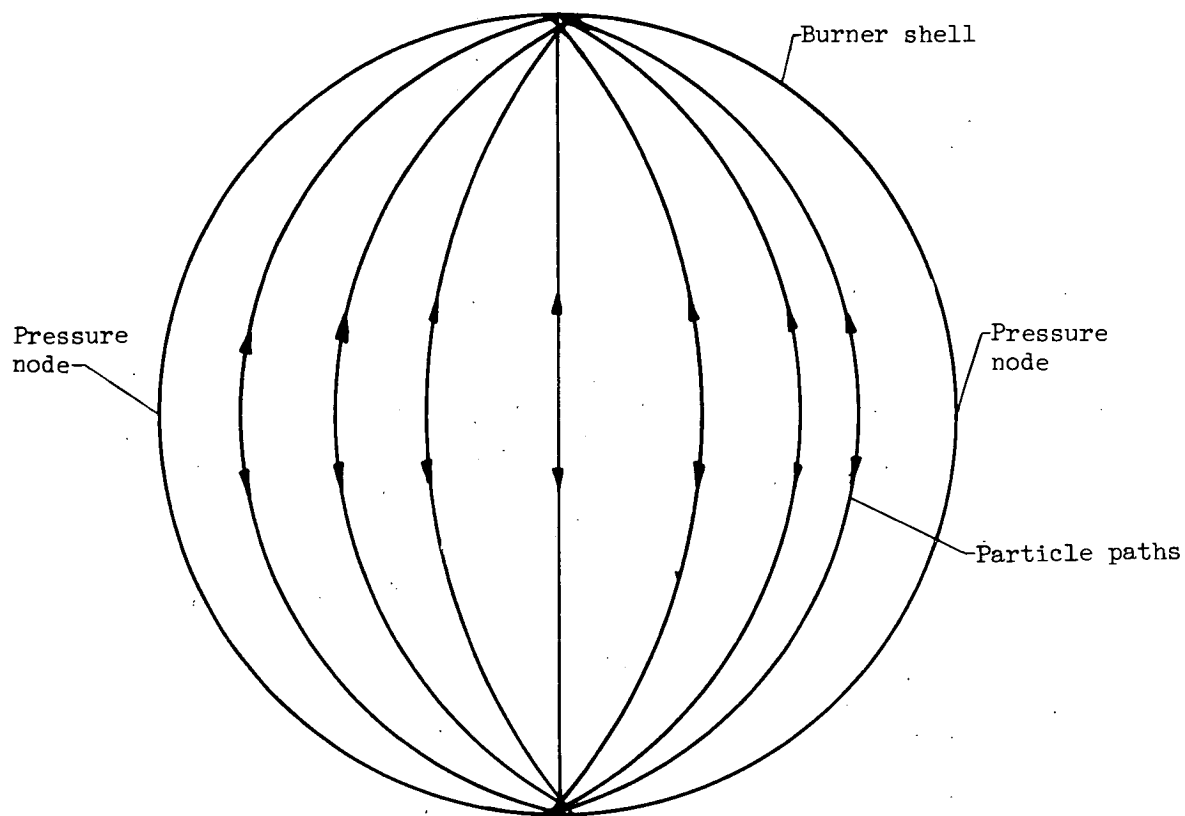


Figure 234. - Idealized cross section of afterburner, showing loci of wave-front paths for first transverse mode of oscillation.

CONFIDENTIAL

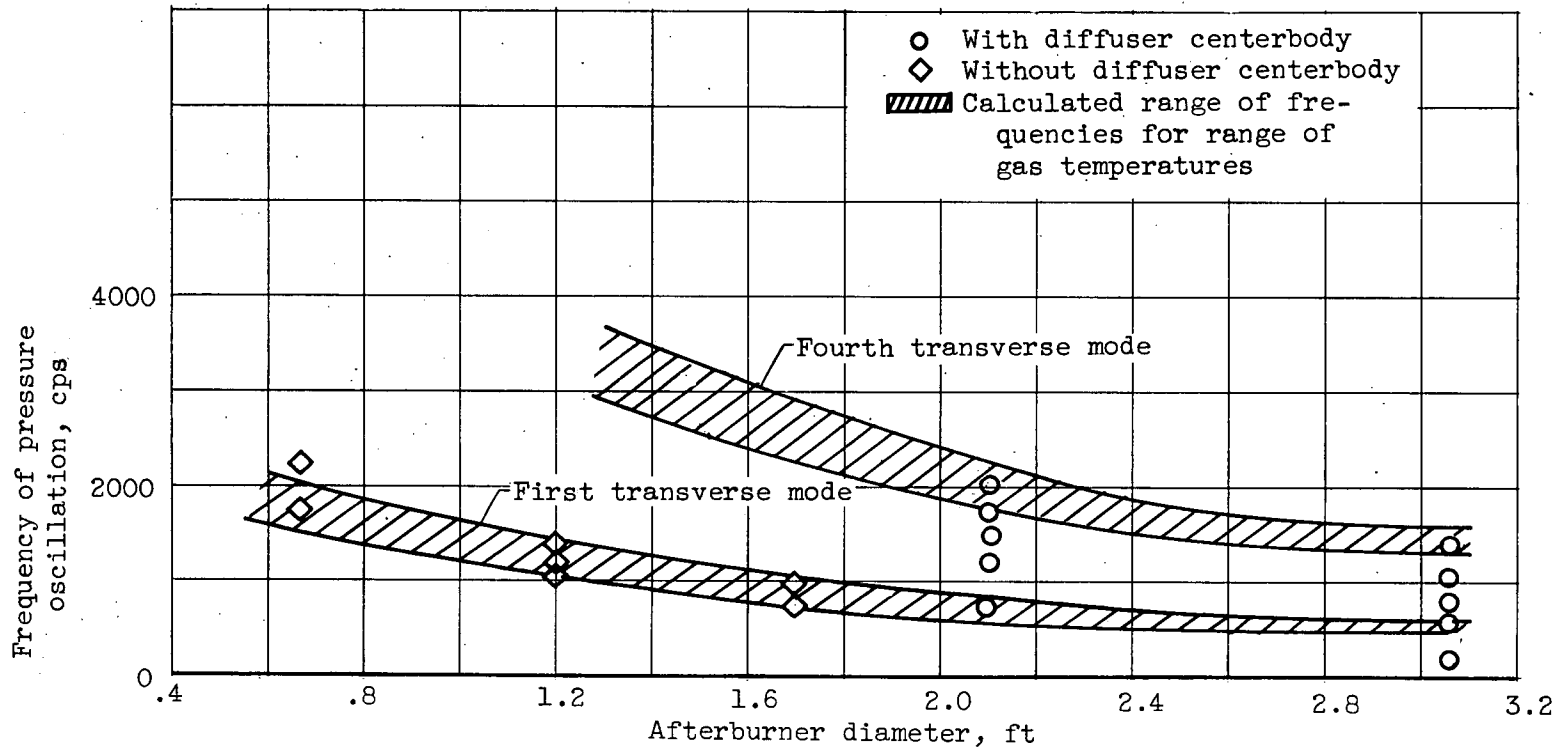
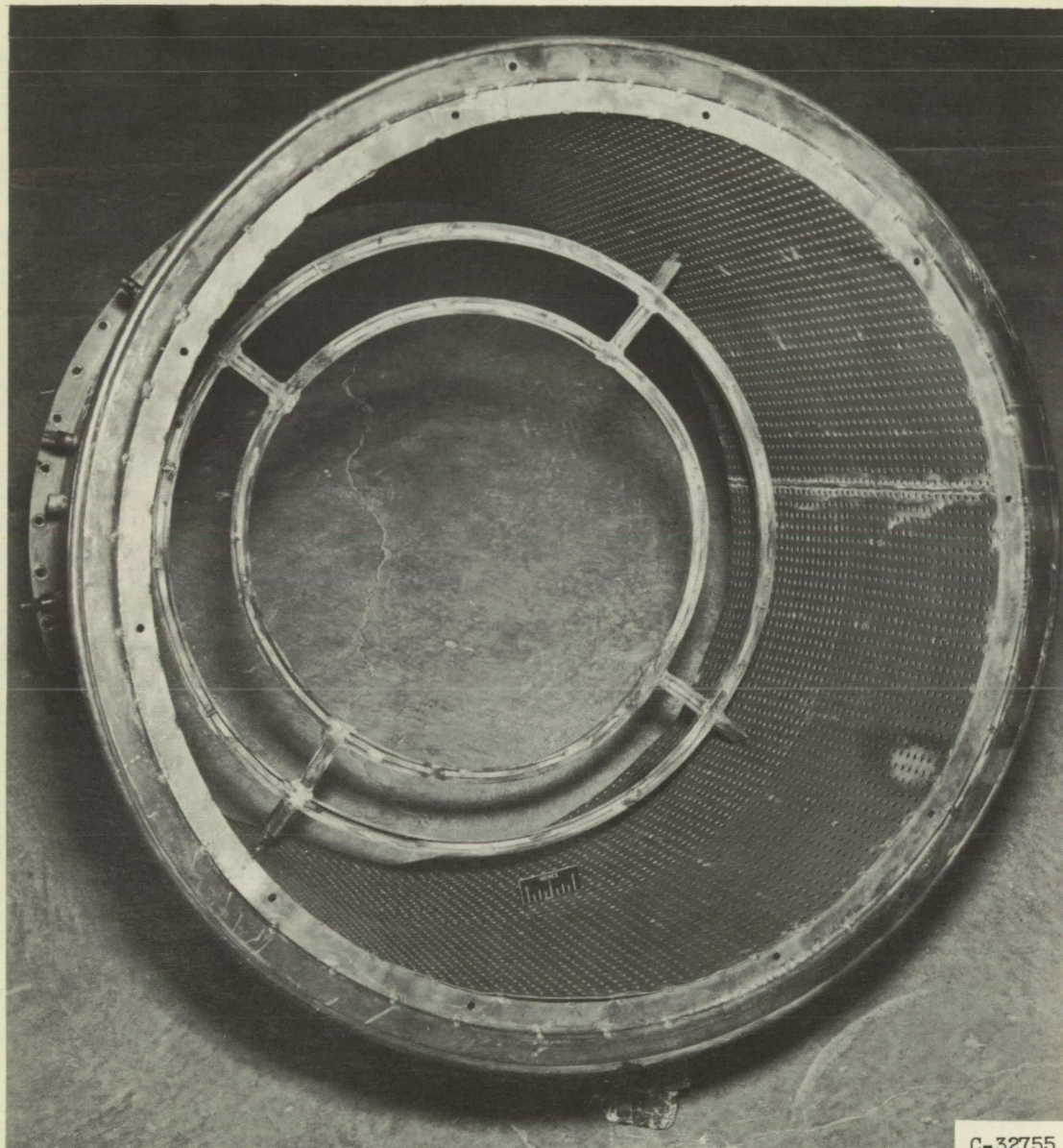


Figure 235. - Screech frequencies of afterburners of various diameters.

CONFIDENTIAL



C-32755

Figure 236. - Perforated liner installed in 32-inch-diameter afterburner for suppression of screech.

CONFIDENTIAL

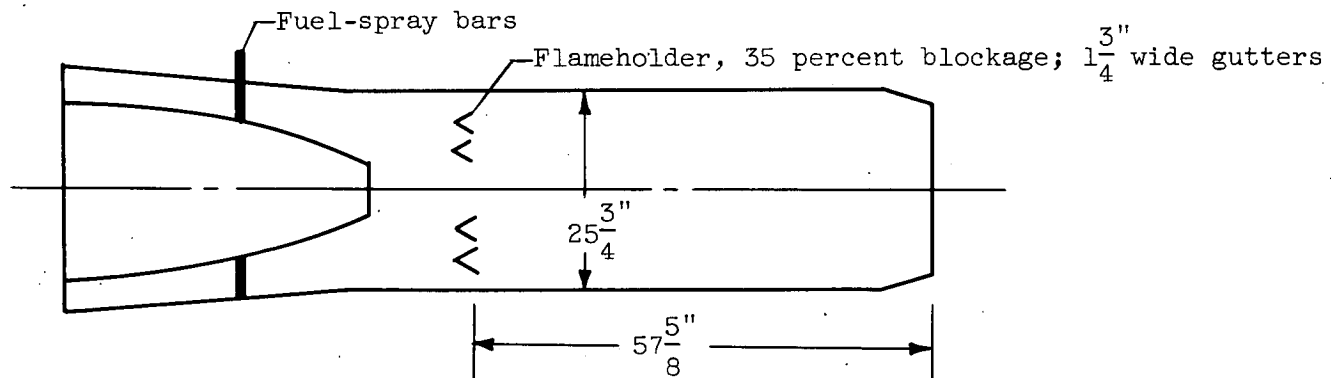


Figure 237. - Afterburner used with water-alcohol injection. Inlet velocity, 350 feet per second.

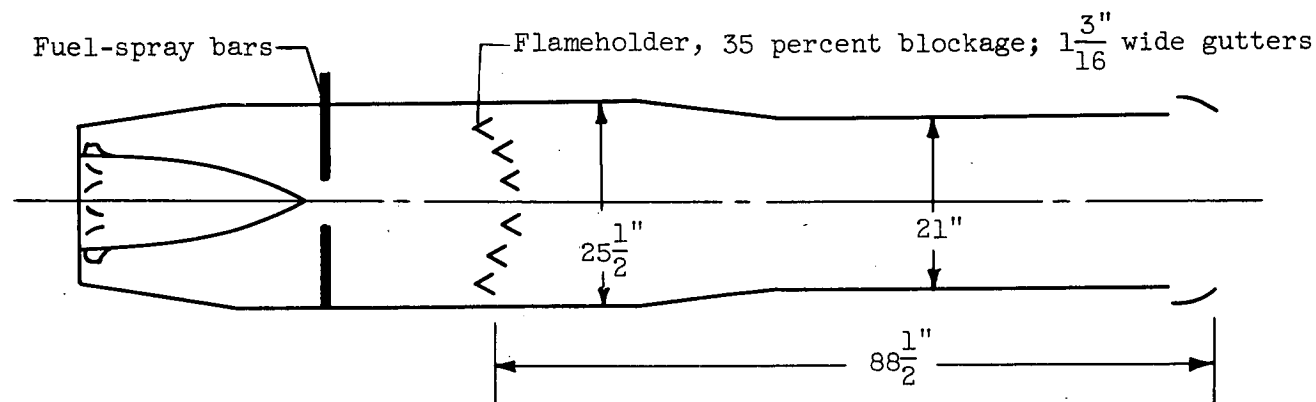
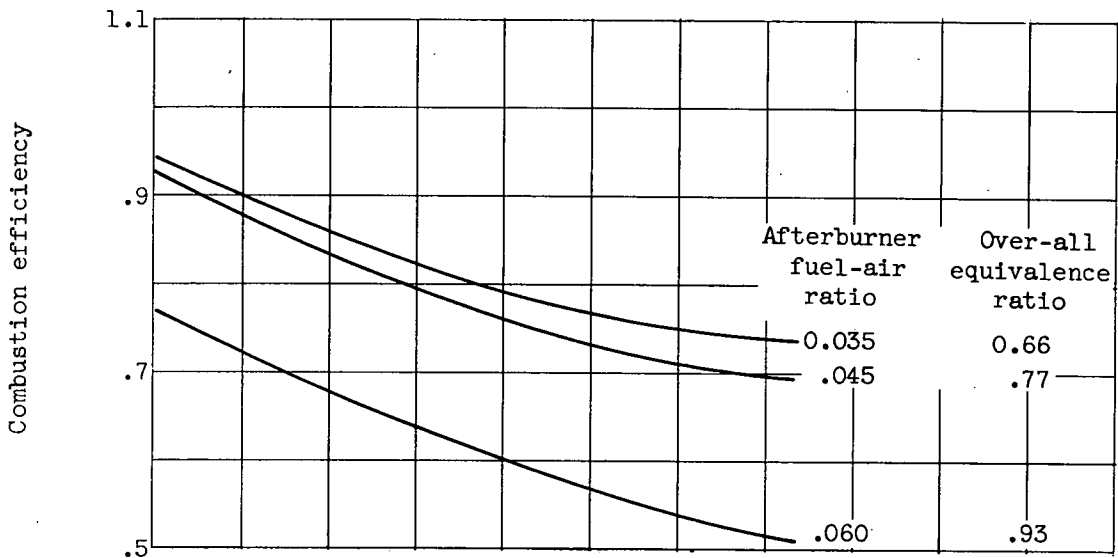


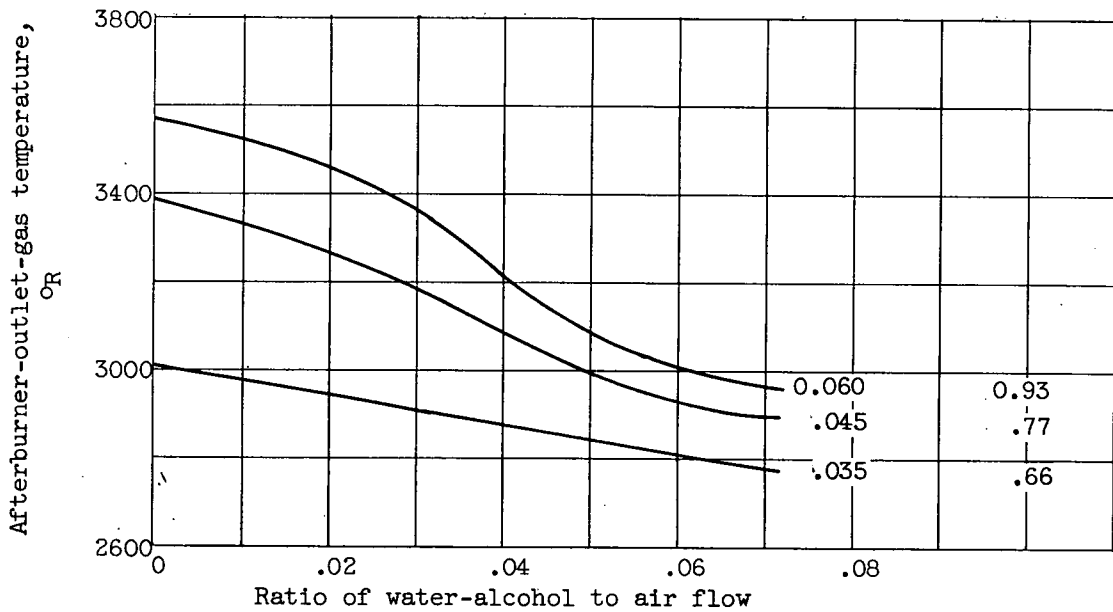
Figure 238. - Afterburner used with ammonia injection. Inlet velocity, 391 feet per second.

CONFIDENTIAL

CONFIDENTIAL



(a) Combustion efficiency.



(b) Afterburner-outlet-gas temperature.

Figure 239. - Effect of water-alcohol injection on afterburner performance. Afterburner-inlet pressure, approximately 3800 pounds per square foot absolute.

CONFIDENTIAL

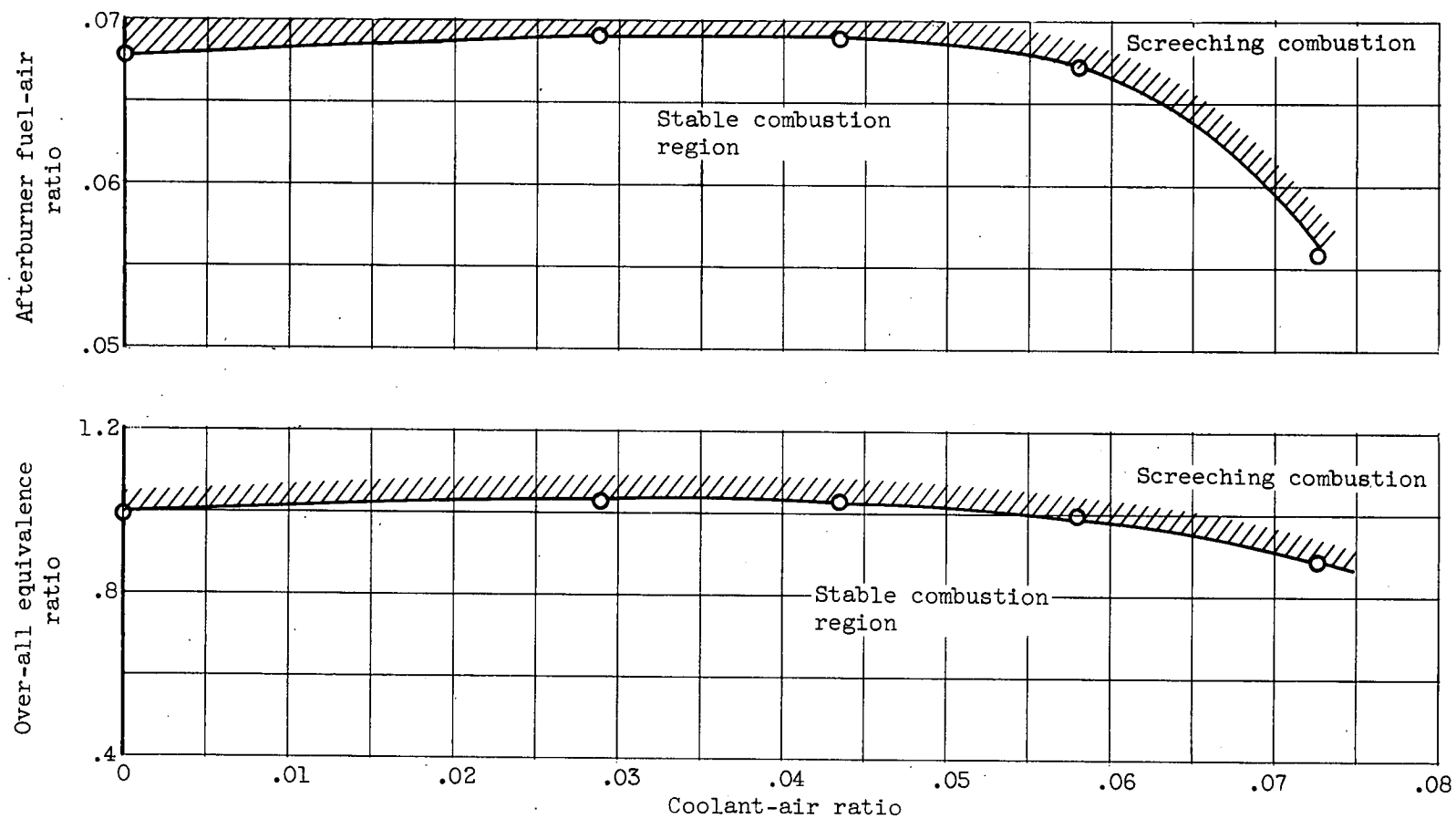


Figure 240. - Afterburner combustion stability limits with water-alcohol injection in compressor.

CONFIDENTIAL

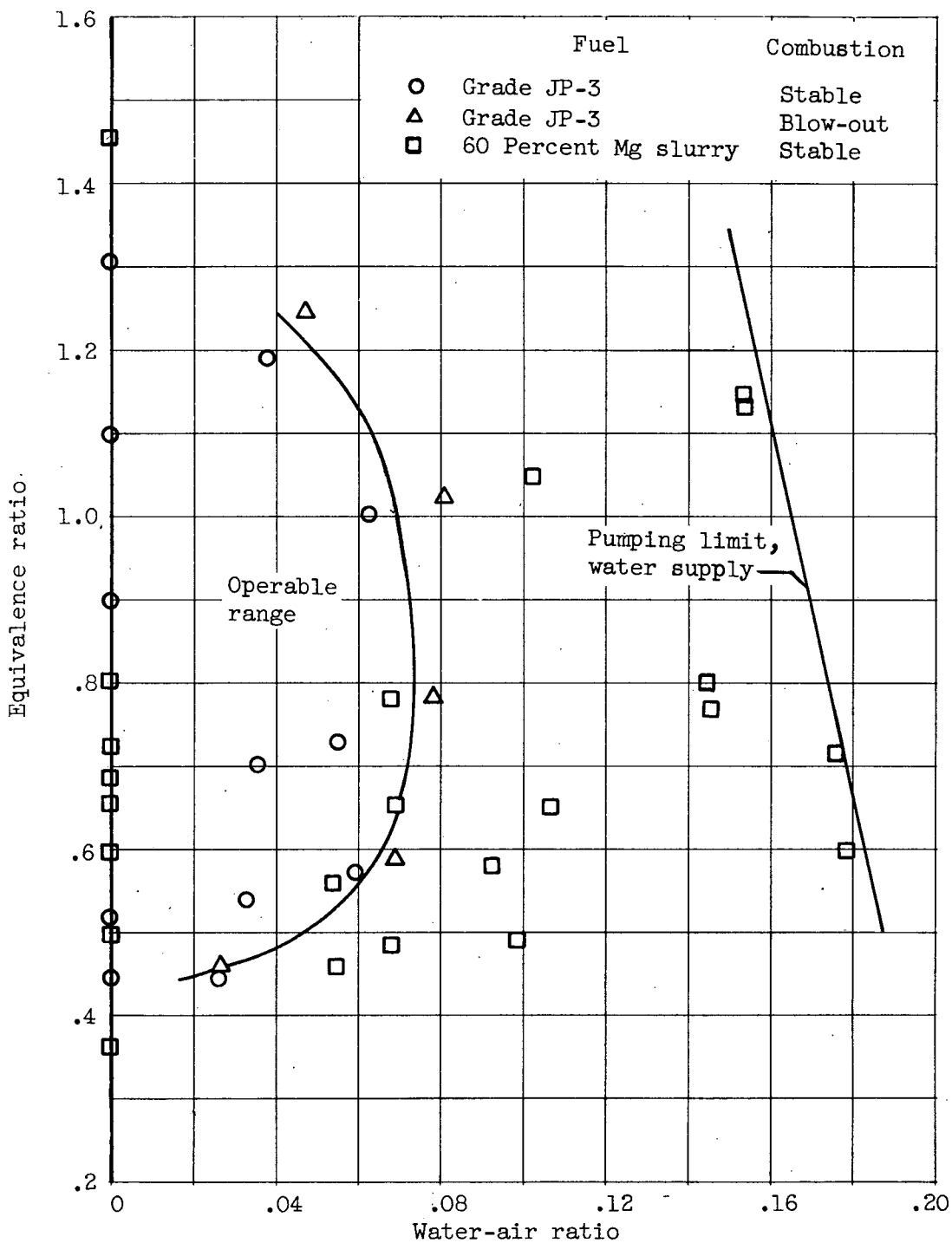
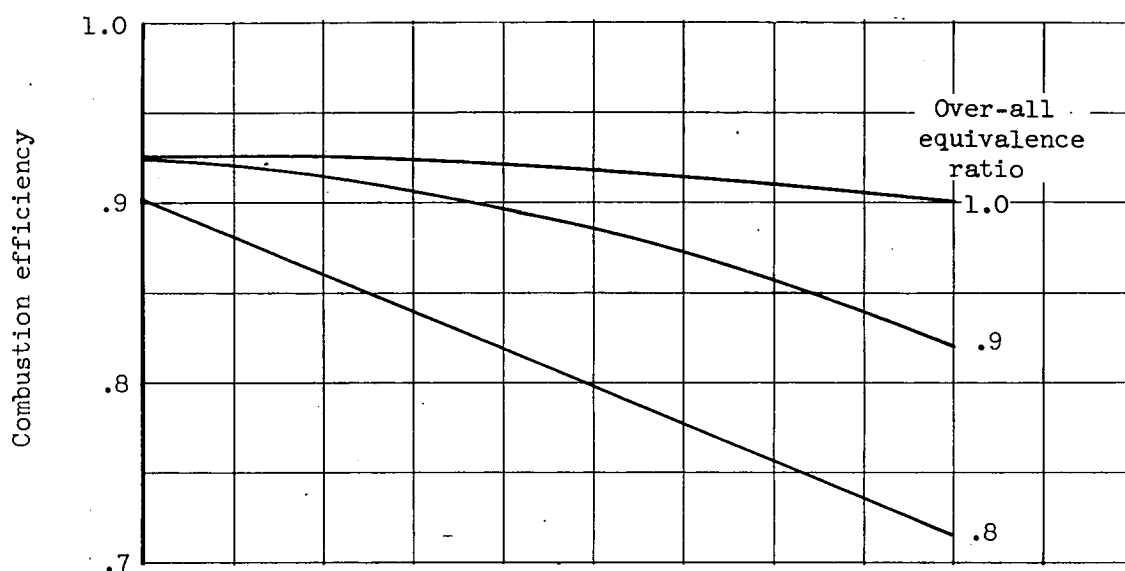
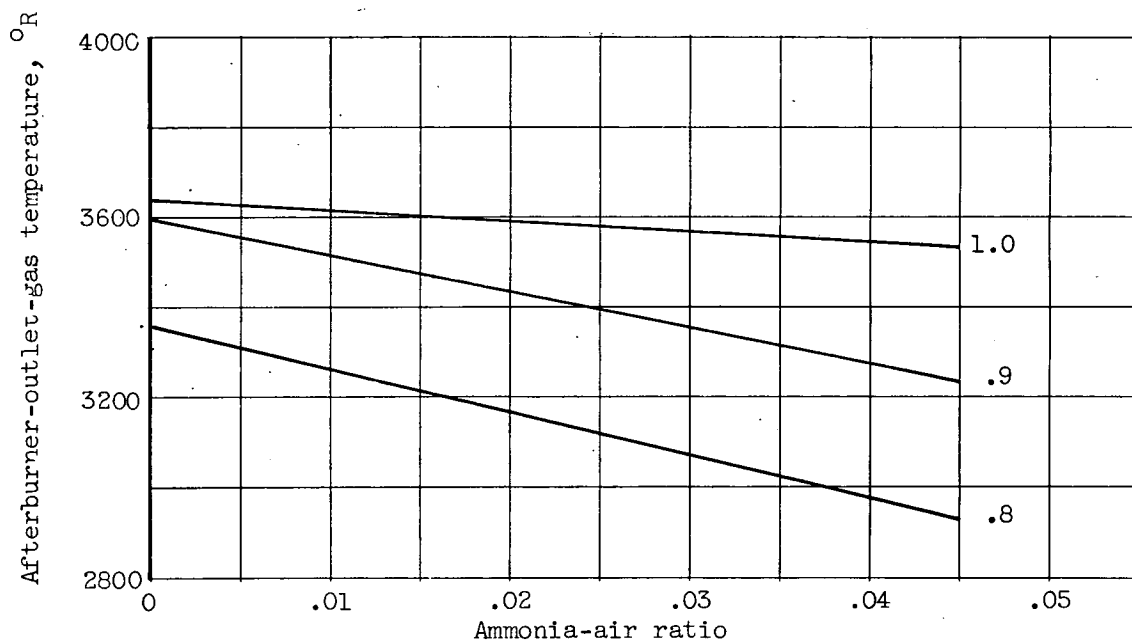


Figure 241. - Blow-out limits for JP-3 fuel and 60-percent magnesium slurry fuel in 6-inch burner. Burner-inlet velocity, 300 to 450 feet per second; burner-inlet pressure, 1100 to 1700 pounds per square foot absolute.

CONFIDENTIAL



(a) Combustion efficiency.



(b) Afterburner-outlet-gas temperature.

Figure 242. - Effect of ammonia injection on afterburner performance..
Afterburner-inlet pressure, 1780 pounds per square foot absolute.

CONFIDENTIAL

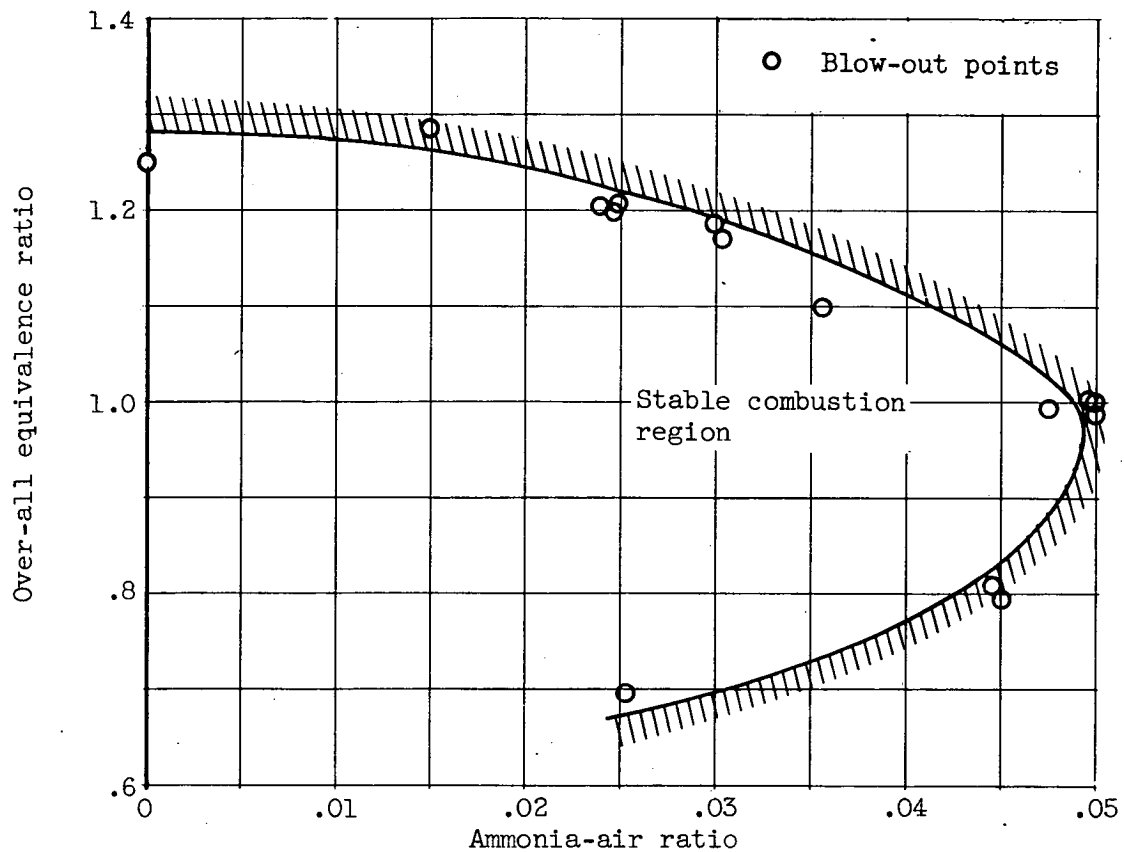


Figure 243. - Effect of ammonia-air ratio on blow-out limits.
Afterburner-inlet pressure, 1780 pounds per square foot
absolute.